FACTORS IN GLUTAMATE EXCITOTOXICITY, INFLAMMATION, AND EPILEPSY

by

Shanshan Zhu

B.Sc., Peking University, P. R. China, 2003

A THESIS SUBMITTED IN PARTIAL FULFILLMENT OF

THE REQUIREMENTS FOR THE DEGREE OF

DOCTOR OF PHILOSOPHY

in

THE FACULTY OF GRADUATE STUDIES

(Neuroscience)

THE UNIVERSITY OF BRITISH COLUMBIA

(Vancouver)

December, 2011

ABSTRACT

Studying the mechanisms underlying glutamate excitotoxicity and inflammatory responses provides hints to the pathology of neurological diseases such as epilepsy. In this dissertation I investigated the expression and function of Krüppel-like factor 4 (KLF4) in glutamate excitotoxicity. I also studied the distribution and the role of progranulin (PGRN) in inflammatory stimulation, in epilepsy and in astrocytes subjected to glutamate excitotoxicity.

First, I studied the role of KLF4 and found that NMDA induced KLF4 expression in cultured neurons and in brain slices. Overexpression of KLF4 upregulated cyclin D1 and downregulated $p21^{Waf1/Cip1}$, suggesting the neuron's progression into cell cycle. KLF4 expression also induced the cleavage of caspase-3 under conditions of a subtoxic dose of NMDA. Thus our work suggests that KLF4 might play a role in NMDA-induced apoptosis.

Second, I studied the function of PGRN and observed that PGRN was enhanced in activated microglia after pilocarpine-induced epilepsy. In mixed cultures, lipopolysaccharide (LPS) also induced PGRN expression. Recombinant PGRN protein promoted microglial activation in the dentate gyrus after epilepsy and in purified microglial cell culture. PGRN was also required for LPS-induced microglial migration. Our work suggests that PGRN may contribute to microglial activation after epileptic and inflammatory insults.

Third, I performed a preliminary study on the role of PGRN in purified culture of astrocytes. I found that our cultured astrocytes express PGRN, and PGRN was required

for glutamate-induced lactate release. PGRN was also involved in glutamate-induced glucose uptake and participated in the regulation of monocarboxylate transporter 1 (MCT1) expression in excitotoxic conditions. Our findings suggest that PGRN may be involved in glutamate-evoked increase of glycolysis in cultured astrocytes.

In conclusion, our findings provide insights into factors involved in glutamate excitotoxicity, inflammation, and epilepsy.

PREFACE

The work in the Chapter Two has been published (Zhu, S., Tai, C., MacVicar, B.A., Jia, W., Cynader, M.S., 2009. Glutamatergic stimulation triggers rapid Krupple-like factor 4 expression in neurons and the overexpression of KLF4 sensitizes neurons to NMDA-induced caspase-3 activity. Brain Res. 1250**,** 49-62). Under the supervision of Dr Max Cynader and Dr William Jia, I designed and conducted all the experiments and analyzed all of the results in this publication, except that Dr. Chao Tai in Dr Brian MacVicar's lab conducted the brain slice experiment in the Fig. 2.3.

For chapters three and four, I designed and conducted all the experiments and analyzed all of the results except stated as follows: (1) Dr. Zhifang Dong and Dr. Chao Tai contributed to preparing the pilocarpine epilepsy models used in the Fig. 3.1, Fig. 3.2, Fig. 3.3 and Fig. 3.4; (2) Ms. Terri L. Petkau and Dr. Blair Leavitt provided progranulin knockout mice used in the Fig. 3.14, Fig. 3.15, and Fig. 3.16; (3) Dr. Chengyong Liao performed the expression, purification and verification of recombinant human progranulin protein as shown in Fig. 3.17; (4) Ms. Aobo Guo prepared the lentiviral vectors used in Fig. 5.1.

In regards to the preparation of this dissertation, I wrote the entire manuscript which was edited by Dr. Max Cynader. Dr. William Jia and Dr. Ljubomir Z. Kojic also contributed to the edition of the manuscript in the Chapter Two.

The seizure studies conducted in this dissertation have been approved by the Animal Care Committee of the University of British Columbia (Protocol A09-0949; Certificates RBH-680-09, RA-373-09, RSHX-285-09, 0333).

TABLE OF CONTENTS

LIST OF TABLES

LIST OF FIGURES

LIST OF ABBREVIATIONS

[^{3}H]2DG, deoxy-d-glucose 2-[1,2–3H(N)]

AD, Alzheimer's disease

ALS, amyotrophic lateral sclerosis

AMPA, 2-amino-3-(5-methyl-3-oxo-1,2- oxazol-4-yl)propanoic acid

ANLSH, astrocyte-neuronal lactate shuttle hypothesis

ANOVA, analysis of variance between groups

AP-1, activator protein 1

ATP, adenosine triphosphate

BBB, blood brain barrier

BDNF, brain-derived neurotrophic factor

bFGF, basic fibroblast growth factor

CA1, cornu ammonis region superior

CA3, cornu ammonis regio inferior

CaMK-II, calmodulin-dependent protein kinase-II

cAMP, cyclic adenosine monophosphate

CD11b, complement receptor type 3

Cdk, cyclin-dependent kinase

ChemR23, chemokine-like receptor 1

CNS, central nervous system

CRE, cAMP response elements

CtBP, carboxy-terminal binding protein

DG, dentate gyrus

DMEM, Dulbecco's modified eagle medium

DNase I, deoxyribonuclease I

DIV, days in vitro

EGFP, enhanced green fluorescent protein

ELISA, enzyme-linked immunosorbent assay

EP, e-prostanoid

ERK, extracellular signal-regulated kinase

FAK, focal adhesion kinase

FBS, fetal bovine serum

Flt-1, vascular endothelial growth factor receptor-1

FTLD, frontal temporal lobe dementia

FTLD-U, frontotemporal lobe dementia with ubiquitinated inclusions

GAG, general antigen gene

GFP, green fluorescent protein

GLAST, glutamate aspartate transporter

GLT1, glutamate transporter 1

GPCR, G-protein coupled receptor

HPLC, high performance liquid chromatography

IEG, immediate early gene

IL-1, interleukin-1

IL-1RA, IL-1 receptor antagonist

IL-6, interleukin-6

IL-10, interleukin-10

IgG, immunoglobulin G

i.p., intraperitoneal

JNK, c-jun N-terminal kinase

KLF, Krüppel-like Factor

LPS, lipopolysaccharide

MAP2, microtubule-associated protein 2

MAPK, mitogen-activated protein kinase

MCP-1, monocyte chemotactic protein-1

MCT, monocarboxylate transporter

mEPSC, miniature excitatory postsynaptic current

MOI, multiplicity of Infection

NCXs, Na+/Ca2+ exchangers

NF-kappa B, nuclear factor kappa-light-chain-enhancer of activated B cells

NGF, nerve growth factor

NMDA, N-methyl-D-aspartate

NSAIDs, nonsteroidal anti-inflammatory drugs

NT, neurotensin

PBS, phosphate buffered saline

PD, Parkinson's disease

PFA, paraformaldehyde

PGE2, prostaglandin E2

PGRN, progranulin

PI_3K, the phosphatidylinositol 3-kinase

PKA, protein kinase A

PKB/Akt, protein kinase B

PMCA, plasma membrane Ca^{2+} pump

PTK, protein tyrosine kinase

RT-PCR, real time polymerase chain reaction

SDS, sodium dodecyl sulfate

SE, status epilepticus

SG, the stratum granulosum layer

SLPI, secretary leukocyte protease inhibitor

SM, stratum molecular layer

SRS, spontaneous recurrent seizure.

TLE, temporal lobe epilepsy

VSCC, voltage-sensitive calcium channel.

VEGF, vascular endothelial growth factor

TDP-43, TAR DNA binding protein 43

TNF, tumor necrosis factor

TNFR, tumor necrosis factor-alpha receptors

TPA, 12-O-tetradecanoylphorbol-13-acetate

TRE, TPA response elements

TrkB, tyrosine kinase B

TUNEL, terminal deoxynucleotidyl-transferase mediated dUTP nick-end labeling

VEGF, vascular endothelial growth factor

ACKNOWLEDGEMENTS

I would like to express my sincere gratefulness to my supervisor, Dr. Max Cynader for his exceptional supervision, insight, guidance and encouragement, not only on my research but also on my life throughout the course of this dissertation. I also thank Dr. William Jia for his encouragement and his valuable advice and assistance for my research.

I sincerely appreciate my supervisory committee members, Dr. Yu Tian Wang, Dr. Ann Marie Craig, and Dr. Tim Murphy for their great advice and support for this dissertation.

I would like to thank Dr. Julia A. Segre for her gift of KLF4 antibody and Dr. Nasreen Khalil for providing the $p21^{Waf1/Cip1}$ antibody. I also thank Dr. Hyun Choi and Dr. James Mclarnon for their advice on microglial culture, transwell migration assay and lactate assay.

I also thank all of the past and present members of the Cynader lab and the Jia lab, for assistance and friendship throughout the course of this PhD studies. I would particularly like to thank Ms. Wendy Wen for her supply of neuronal and astroglial cultures all these years. I sincerely appreciate the advice, help and friendships from Dr. Guang Yang, Dr. Cleo Lee, Dr. Dong Qiang, Dr. Chengyong Liao, Dr. Ljubomir Kojic, Dr. Li Pang, Dr. Shiv Prasad, Ms. May Cui, Ms. Rui Liu, Ms. Aobo Guo, Ms. Mianwei Wang, Ms. Guoyu Liu., Ms. Qing Chang, Ms. Swarni Sunner, Ms. Stephanie Thomason, Ms. Melanie Bertrand, Mr. Ainsley Coquinco, Mr. Alan Huang, and Mr. Lin Tian.

I also thank all of my beloved family members and friends who accompanied me during these precious years in my graduate school.

Last but not least, I would like to thank Canadian Institutes of Health Research (CIHR), the Natural Sciences and Engineering Research Council of Canada (NSERC), Savoy Foundation and the University of British Columbia for financial support during my PhD studies.

DEDICATION

To my parents,

and my beloved husband, Chao Tai,

for their support and love all these years.

CHAPTER ONE: INTRODUCTION

1.1 Temporal lobe epilepsy

1.1.1 Introduction of temporal lobe epilepsy

Epilepsy is characterized by various forms of seizures, and affects 1% of the population in the North America. To date, the available medication can only control but can't cure epilepsy, and many types of epilepsies are medication-resistant (Berg, 2011; Morimoto et al., 2004). Depending on the location in the brain from which epileptic discharges originate, epileptic seizures are classified as focal (seizure discharges localized in specific brain regions) and generalized (seizure discharges widely spread) seizures. Focal seizures can develop into generalized ones. Temporal lobe epilepsy (TLE) is the most common type of drug-resistant focal epilepsy in adults, with epileptic discharges originating in mesial temporal brain structures such as hippocampus and/or amygdala. Pathological studies of TLE patients shows chronic atrophy of hippocampus with gliosis and neuronal cell death, and circuit reorganization in hippocampus associated with synaptogenesis and axonal sprouting (Morimoto et al., 2004; Pitkanen and Lukasiuk, 2011). The causal etiology of TLE can be either idiopathic and/or symptomatic (Bhalla et al., 2011): the former type has genetic mutations which have been recently identified mainly at ion channel loci, while the latter type is epilepsy induced following other diseases such as birth accident, traumatic brain injury, infection, stroke, or neurodegeneration. Although TLE may have numerous causes, a common history of most TLE patients is a sustained period of seizure attacks.

1.1.2 Animal models for temporal lobe epilepsy

Experimental epilepsy studies in rodents provide valuable information about the underlying mechanisms involved in epileptogenesis, hippocampal sclerosis, and neural circuit reorganization (Loscher, 2011; Louis et al., 1987). These studies also demonstrate similar epileptic discharge patterns and behavioral and pathological changes as in human TLE. The most typical non-transgenic experimental models used are the status epilepticus (SE) model and the kindling model.

1.1.2.1 Status epilepticus model

Status epilepticus (SE) is characterized by a prolonged period of seizure. SE causes severe brain damage and neurological deficits, including memory impairment, learning disabilities, and behavioral and psychiatric problems (Morimoto et al., 2004). Such manipulation leads to a delayed chronic phase in which seizure spontaneously recurs. The behavioral symptoms and pathological changes in hippocampus during the chronic phase are very similar to those found in TLE patients.

The common way to induce SE is by systemic injection of a convulsant such as pilocarpine (a muscarinic receptor agonist) or kainic acid (a glutamate receptor agonist) (Loscher, 2011). Intra-cerebral deliveries of these drugs are also used to induce epilepsy, but these procedures often produce notable brain damage. In our study we used the systemic injection of pilocarpine to induce SE. Three stages are noted after pilocarpine-induced SE (Cavalheiro, 1995; Curia et al., 2008): the acute phase with 6-24 h of continual SE; a silent phase that can last 4-44 days with no overt convulsions; the chronic phase when animals develop spontaneous recurrent seizures (SRSs) with a frequency of 2-3 times per week. Neuronal loss and gliosis in hippocampus starts from the acute phase,

and mossy fiber sprouting and synaptogenesis in dentate gyrus are evident during the chronic phase (Cavalheiro, 1995; Curia et al., 2008).

1.1.2.2 Kindling model

The Kindling model was first developed by Goddard in 1967 (Goddard, 1967). To develop SRSs, the generation of over-kindled model is more laborious than the SE model and usually involves three steps (Goddard, 1967; Morimoto et al., 2004; Racine, 1972b): First, progressively increasing electrical currents are applied in focal brain regions such as piriform cortex or amygdala until stage 5 seizures are reached, and the highest used current is considered as threshold current; on following days seizures are evoked many times, sometimes hundreds of times, by the threshold current in the first step ("over-kindled"); finally spontaneous seizures reoccur in animals. If the over-kindling step is omitted, the spontaneous seizures will not be completely induced in most studies. Hippocampal morphological changes, including neuronal loss and mossy fiber sprouting, can be observed in kindled animals, but are less intense than those seen in SE animals (Loscher, 2011; Louis et al., 1987).

1.1.3 Hippocampal circuit in TLE

The critical role of hippocampus in mesial TLE has drawn the attention of scientists since the early 20th century. From then on medical practitioners surgically resect atrophic limbic areas to ameliorate epilepsy in TLE patients (Li et al., 1999). One famous example is the case of H.M., whose epilepsy symptoms were successfully controlled after two-thirds of his hippocampus was removed (Corkin, 1968). In the kindling paradigm, animals with kindling developed from non-hippocampus sites, lesion or chemical inhibition of hippocampus can delay and reduce the duration of generalized seizures

induced by kindling (Dasheiff and McNamara, 1982; Mirnajafi-Zadeh et al., 2002; Savage et al., 1985). Thus the hippocampus functions either as a seizure generator, or as an essential component propagating seizure discharges. In both cases, intensive connection among hippocampus and other brain regions especially the limbic areas are critical for spreading of epileptiform firing to the whole brain to reach the full stale convulsive response.

1.1.3.1 Anatomy of hippocampal formation

The hippocampal formation contains four regions: the dentate gyrus (DG), cornu ammonis regio inferior (CA3), cornu ammonis region superior (CA1) and subiculum. The small zone connecting CA1 and CA3 is called CA2. Cajal RY (1911) first reported that the regions are connected by a simplified trisynaptic circuit (Cajal, 1911): layer II and III neurons in the entorhinal cortex project to the DG via the perforant path; the DG granule cells project to CA3 pyramidal cells via mossy fibers; the CA3 pyramidal cells send Schaffer collateral projections to CA1 pyramidal cells which in turn project to the subiculum; the subiculum cells send axons out of the hippocampal formation to all fields of adjacent cortices. As a hundred years passed by, our understanding of hippocampal formation and its role in mesial TLE is much more comprehensive.

1.1.3.1.1 Dentate gyrus in TLE

Dentate gyrus contains three layers: the stratum molecular layer (SM), the stratum granulosum layer (SG) and the polymorphic layer (Amaral et al., 2007). The stratum molecular layer, which is about 250 μm thick in rat, is composed of dendrites from the dentate granule cells and interneurons, perforant path fibers from EC, and other afferent input fibers to DG. The cells in the stratum granulosum layer are densely packed with

about 60 μm thick granule cells. Granule cells use glutamate for fast transmission, but also release GABA at early age of development and when hyperexcited in adult (Gutierrez, 2003; Gutierrez et al., 2003). Another common cell type in the SG is the dentate pyramidal basket cells, slightly larger in soma size (25-35 μm in diameter) than the granule cells (10-18 μm). Dentate pyramidal basket cells are GABAergic inhibitory interneurons located along the boundary of the SG adjacent to the polymorphic layer. The polymorphic layer, also called dentate hilus, is the area enclosed by the SG. There are many types of neurons and the most common type is the mossy cells (25-35 μM in diameter). Mossy cells receive inputs from granule cells and their dendrites even extend to the SM to receive the perforant path inputs (Scharfman, 1991). Mossy cells also provides a "feedback" modulation by projecting glutamatergic axon fibers to granule cells and other inhibitory interneurons (Scharfman, 1995). Such a type of projection has been called the associational/commissural projection.

Many epileptologists investigated the dentate gyrus in TLE. The granule cells are one of the few neurons that can be reborn in the adult brain, and the turn-over of granule cells and sprouting of their axons (mossy fibers) have been found in the epileptic brain (Parent and Lowenstein, 1997). Unlike most CA3/CA1 pyramidal neurons, most of the granule cells survive, but are dispersed and form a wider layer after epileptiform discharges (Houser, 1990; Young et al., 2009). The granule cells have a high threshold for excitation by maintaining a very negative resting potential. They are very hard to be excited to fire repetitively for long periods because they maintain a large after-hyperpolarization after the burst of action potentials. Therefore, the dentate gyrus is considered as the "gate" for the hippocampus. Hyperexcitation of granule cells could lead to failure of this gating

property, and cause propagation of seizure activity into other brain regions (Heinemann et al., 1992; Pallud et al., 2010; Stringer and Lothman, 1992; Young et al., 2009). In contrast to granule cells, mossy cells in the hilus maintain a low threshold for excitation (Scharfman and Schwartzkroin, 1988). Some mossy cells, those not expressing calcium binding proteins parvalbumin and calbindin, degenerate after prolonged stimulation of perforant afferents, probably due to their weak buffering of the huge calcium influx (Scharfman and Schwartzkroin, 1988; Scharfman, 1995). Other mossy cells, expressing calretinin, have better tolerance to seizure-induced death (Kotti et al., 1996). It has been hypothesized that the death of mossy cells during epilepsy could lead to disinhibition of granule cells by losing its excitation on hilar inhibitory interneurons that inhibit granule cells (Sloviter, 1987), and such disinhibition might trigger the mossy fiber sprouting from granule cells (Cavazos and Sutula, 1990). Similar to mossy cells, interneurons in dentate gyrus exhibit type-selective susceptibility to epileptic stimulations. Somatostatin and neuropeptide Y-immunoreactive interneurons are preferentially damaged in the hippocampus from epileptic samples (de Lanerolle et al., 1989; Kuruba et al., 2011). Interneurons expressing the calcium binding proteins such as calbindin-D28k and parvalbumin tend to survive in the epileptic brain (Sloviter, 1989; Sloviter et al., 1991).

1.1.3.1.2 CA3/CA2 in TLE

The CA3 and CA2 regions are considered as the “pacemaker” of hippocampus formation (Andersen, 2007; Engel and Pedley, 2008), and the performance of CA3/CA2 pyramidal neurons during epilepsy has been extensively studied. The CA3/CA2 pyramidal neurons form excitatory synapses with their neighbors, creating a highly excitable collateral network. Such intrinsic properties of CA3/CA2 pyramidal cells lead

to the generation of rhythmic synchronized bursting patterns, which are comparable to the interictal epileptiform activity that occurs between seizures (Engel and Pedley, 2008; Wittner et al., 2009). Moderate increase in extracellular potassium, which might occur during seizures, extends the interictal-like bursting to a more prolonged ictal-like discharges in CA3 region (Rutecki and Yang, 1998), but a bigger increase in extracellular potassium leads desynchronization of the interictal-like firing patterns, probably due to the hyperpolarization induced by prolonged activation of potassium channels (Rutecki and Yang, 1998). As brain regions generating interictal spikes do not necessarily overlap with ictal-onset areas (Morimoto et al., 2004), the interictal-like firing of CA3/CA2 may not be the solitary mechanism explaining the vulnerability of CA3 in epileptic models. Interestingly, the pyramidal neurons in the transitioning CA2 area, which differs from CA3 in that it does not receive mossy fiber input and does not fire in the epileptiform pattern, tend to survive after epilepsy (Nadler, 2003; Williamson and Spencer, 1994).

1.1.3.1.3 CA1 and subiculum in TLE

As the major "outputs" of hippocampus, CA1 and subiculum have different outcomes in epilepsy. CA1 pyramidal neurons have no collateral excitatory connections with neighbor cells, but a proportion of them are able to generate synchronized discharges in response to epileptic stimulation, while others keep a regular firing pattern (Andersen, 2007; Engel and Pedley, 2008; Rafiq et al., 1995; Sanabria et al., 2001). The burst firing pattern may be caused by synchronized input from CA3 neurons (Engel and Pedley, 2008). In addition, increasing extracellular K^+ concentrations can raise the proportion of burst firing neurons among total CA1 neurons (Jensen et al., 1994). Extracellular K^+

concentration is raised as epileptiform firings are discharged in epileptic brain slices (Avoli et al., 1996; Moody et al., 1974). Thus it has been proposed that the narrow extracellular spaces may lead to burst of extracellular current flow, and thus may also contribute to synchronized burst discharges and CA1 pyramidal neuronal death (Engel and Pedley, 2008). While most CA3 and CA1 neurons are absent as a result of seizure, the subiculum pyramidal neurons tend to survive and originate interictal-like spontaneous rhythmic discharges in TLE patient (Cohen et al., 2002; Wozny et al., 2005b), suggesting their critical role in epileptogenesis. Downregulation of the K^+/Cl^- cotransporter 2 could contribute to the hyperexcitability of subicular pyramidal neurons (de Guzman et al., 2006). While subiculum is the major output of hippocampus, it is possible that the connection between subiculum and entorhinal cortex facilitates epileptogenesis and propagation of ictal firing (Stafstrom, 2005). Disruption of the subiculum- entorhinal cortex connection on brain slices could weaken epileptiform firings originated from the subiculum (Panuccio et al., 2010; Wozny et al., 2005a).

The hippocampal formations are critical brain regions for epileptogenesis in TLE, since areas generating intensified ictal firings are vulnerable to subsequent cell death. To interpret epilepsy-induced changes to the brain, in the following chapters, we will discuss the biochemical and pathological changes observed in response to epileptic stimulations *in vivo* and *in vitro,* including secretion of growth factors and cytokines, activation of glial cells and glutamate excitotoxicity.

1.2 Modulation of growth factors and inflammatory factors on seizure-induced sequelae

Seizures alter the expression of many secretable factors including growth factors, cytokines and chemokines. These factors can be secreted from neurons, microglia or astrocytes. The loss of function and gain of function studies of these secretable factors suggest that they participate in seizure-induced neuronal cell death and axonal sprouting, and also regulate the development of spontaneous recurrent seizures.

1.2.1 Production of growth factors and inflammatory factors during epilepsy

The expression levels of many growth factors such as brain-derived neurotrophic factor (BDNF) and nerve growth factor (NGF) are induced in the hippocampal neurons from experimental epileptic models and in TLE patients (Jankowsky and Patterson, 2001). However, one recent study showed that the serum BDNF levels were decreased in patients with epileptic seizures (LaFrance et al., 2010). Seizures also increase the expression of several growth factors and cytokines in non-neural cells (Jankowsky and Patterson, 2001). For example, in response to epileptic stimulations, the strongest upregulation of interleukin-1 beta (IL-1beta) and the endogenous IL-1 receptor antagonist (IL-1RA) are found in microglial cells (Eriksson et al., 1998; Yabuuchi et al., 1993), while increased basic fibroblast growth factor (bFGF) and interleukin-6 (IL-6) are mainly expressed in astrocytes (de Bock et al., 1996; Humpel et al., 1993; Jankowsky and Patterson, 2001; Van Der Wal et al., 1994). Post-seizure elevation of bFGF reaches the peak within less than 24 hours and declines to normal level in a few days (Kondratyev et

al., 2002; Riva et al., 1994; Van Der Wal et al., 1994). When seizure activity is prolonged, the upregulation of bFGF can last as long as two weeks (Riva et al., 1994).

Interestingly, the upregulation of these factors and their receptors is not limited to one specific cell type. Upregulation of IL-6 following seizure is also found in astrocytes, blood vessels and meninges after pilocarpine-induced SE (Jankowsky and Patterson, 2001). IL-6 induction is also detected in the cerebrospinal fluid of patients with newly developed seizures (Peltola et al., 1998). While bFGF is induced in astrocyte and even in neurons after seizures (Gall et al., 1994; Humpel et al., 1993; Van Der Wal et al., 1994), the FGF receptor-1 is induced in neurons and astrocytes (Van Der Wal et al., 1994) and the FGF receptor-3 is highly expressed in astrocyte and microglia following KA-induced seizures (Ballabriga et al., 1997). Elevation of vascular endothelial growth factor (VEGF) expression has been found in both astrocytes and neurons in animal models of TLE and TLE patients (Nicoletti et al., 2008; Rigau et al., 2007). Receptors of VEGF have been found in microglia, astrocyte and vascular endothelium (Croll et al., 2004a). Since these factors can be secreted and their receptors are located in different cell types, they may act as cross-talk signals between neuron and glial cells and modulate seizure-induced sequelae.

1.2.2 The complex role of growth factors in regulating seizure-induced cell loss, neural circuit reorganization and SRS

The expression of growth factors and their receptors are changed in human TLE and experimental models of epilepsy including our pilocarpine model. Most growth factors and their receptors are upregulated by seizures including NGF, BDNF, bFGF and VEGF.

Experimental approaches to study their function in epilepsy include the intracerebral application of exogenous growth factors or their blocking peptide/antibodies, and the use of heterozygous or conditional knock out transgenic mice with deletion of the growth factor. Noteworthy, for most growth factors the homozygous knockout mice do not survive till adulthood due to the critical role of growth factors in development. Using these methods, researchers have found that growth factors play a complex role in modulating seizure-induced cell loss, neural circuit reorganization and SRS. We select NGF, BDNF, bFGF and VEGF as examples.

1.2.2.1 The role of NGF in epilepsy

Studies on the role of NGF in epilepsy have shown complicated results. It has been found that the administration of anti-NGF antibody can inhibit mossy fiber sprouting, delay the onset of SRS and increase the kindling threshold in kindling models (Rashid et al., 1995; Van der Zee et al., 1995), while intracerebral infusion of NGF results in the opposite effect (Adams et al., 1997). However, in the pilocarpine SE model NGF antibody exerts no effect on mossy fiber sprouting from dentate granule cells, but reduces the sprouting of axons from cholinergic neurons in the forebrain (Holtzman and Lowenstein, 1995). NGF also fails to induce axon sprouting in dissociated cultures of DG granule cells (Patel and McNamara, 1995). In addition, the influence of NGF on cell death can be protective or toxic, depending on the ratio between the activated receptors p75NTR and TrkA (Chao et al., 1998; Frade and Barde, 1998; Jankowsky and Patterson, 2001).

1.2.2.2 The role of BDNF in epilepsy

Investigations on the effect of administration of BDNF on epileptogenesis show ambiguous results, since the studies have been conducted with different periods and doses of BDNF in different experimental models of epilepsy. Some groups have shown that infusion of BDNF prevents the seizure development in kindling models (Larmet et al., 1995) and in kainic acid models (Kuramoto et al., 2011). Others have reported that intra-hippocampal infusion of BDNF induces behavioral seizures and increases susceptibility to pilocarpine (Scharfman et al., 2002), and that transgenic mice overexpressing BDNF are more vulnerable to kainic acid-induced epilepsy (Croll et al., 1999). Because continuous exposure to high levels of BDNF downregulates expression of its receptor tyrosine kinase B (TrkB) *in vitro* (Binder et al., 1999; Frank et al., 1996; Knusel et al., 1997) and *in vivo* (Xu et al., 2004), the paradox in these evidences may be due to different levels of TrkB. Loss-of-function studies suggest more consistent evidence for the contribution of BDNF and TrkB in epileptogenesis. Studies using intracerebroventricular infusion of TrkB antibody (Binder et al., 1999), TrkB conditional knockout (He et al., 2004) or mice overexpressing dominant negative TrkB (Lahteinen et al., 2002) indicate inhibition of epileptogenesis in kindling or kainate epilepsy models. However, the kindling-induced seizure stage in BDNF heterozygous mice (Kokaia et al., 1995) and BDNF conditional knockout mice (He et al., 2004) are only slightly suppressed, which can be explained by that TrkB can be activated by kindling in the mossy fiber pathway of hippocampus in these mice (He et al., 2004). In addition, treatment of anti-epileptic drug valproic acid decreases BDNF/TrkB expression in

microdissected hippocampus from TLE patients (Hou et al., 2010), further supporting the involvement of BDNF/TrkB in epileptogenesis.

Studies on the role of BDNF in epilepsy-induced mossy fiber sprouting and neuronal death also show conflicting results. Application of BDNF promotes axon growth from DG granule cells in dissociated primary cultures (Patel and McNamara, 1995) or in brain slice culture (Lowenstein and Arsenault, 1996). Intra-hippocampal infusion of BDNF also induces mossy fiber sprouting but does not affect neuronal death (Scharfman et al., 2002). However, another group reported that BDNF infusion exacerbates CA3 cell death in kainic acid model (Rudge et al., 1998). In addition, in BDNF heterozygous mice kindling-induced mossy fiber spouting is enhanced (Kokaia et al., 1995), but this might be due to the activation of TrkB in the mossy fiber pathway in BDNF heterozygous mice (He et al., 2004). Moreover, two types of administration of BDNF, a lower dose by multiple bolus infusions of BDNF which has no effect on TrkB receptor and accelerate the development of kindling, and a higher does by continuous infusion of BDNF which decreases the activity of TrkB receptor and inhibits kindling-induced seizures, both cause no alteration in kindling-induced mossy fiber sprouting (Xu et al., 2004). Mossy fiber sprouting observed in postnatal slice culture is also not affected by BDNF deficiency (Bender et al., 1998). The mossy fiber sprouting and DG hilar cell death induced in kainate SE models are not altered in mice overexpressing dominant negative TrkB (Lahteinen et al., 2002).

1.2.2.3 The role of bFGF and VEGF in epilepsy

The influence of bFGF in seizure susceptibility and epilepsy-induced cell damage and plasticity changes has also been studied. Acute application of high levels of bFGF (25-50

ng) immediately causes seizure (Liu and Holmes, 1997b), and another group has found that kainate induces faster and more severe SE in transgenic mice overexpressing bFGF (Zucchini et al., 2008). In contrast, chronic infusion of lower doses of bFGF (2.5 ng/h) for 7 days improves recovery from kainate-induced SE by reducing hippocampal cell damage and hence decreasing the frequency of spontaneous recurrent seizures (Liu and Holmes, 1997a). The bFGF transgenic mice are also protected from kainic acid-induced cell loss in hippocampus (Zucchini et al., 2008). In addition, exogenous bFGF enhances axon sprouting from cultured DG granule cells *in vitro* (Lowenstein and Arsenault, 1996; Patel and McNamara, 1995), but overexpressing bFGF in transgenic mice does not influence the DG neurogenesis and mossy fiber sprouting caused by kainate-induced SE (Zucchini et al., 2008).

VEGF also plays a critical but complicated role in epileptic seizures. Using infusion of VEGF or VEGF receptor-1 (Flt-1) antibody into hippocampus, Nicoletti et al. (2008) has shown that VEGF prevents hippocampal neuronal death in the pilocarpine SE model (Nicoletti et al., 2008). However, VEGF causes BBB break down and infiltration of monocytes, and thus induces inflammatory responses (Croll et al., 2004a; Croll et al., 2004b). Such destructive effects of VEGF may intermingle with its neuroprotective role during epilepsy.

Overall, it is still widely argued whether the secretion of growth factors following seizures contributes to the self-repairing mechanism in brain and prevents further spontaneous seizure attacks. In a highly complicated and delicate way, growth factors regulate seizure-induced cell damage, neural circuit rewiring, and SRSs.

1.2.3 The dichotomous role of inflammation in seizure

SE induces a rapid immune response by activating various cytokines, chemokines, the NF-kappa B (nuclear factor kappa-light-chain-enhancer of activated B cells) pathway, Toll-like receptors, the prostaglandin pathway and the complement system (Turrin and Rivest, 2004). Numerous inflammatory factors are released from activated microglial cells. The inflammatory responses exert a dichotomous role in seizure sequelae in neurons.

On the one hand, inflammation increases seizure susceptibility and inhibits adult neurogenesis. Infusion of proteins of the complement system into hippocampus of free-moving animals induces seizures (Xiong et al., 2003). Lipopolysaccharide (LPS) reduces seizure threshold in the pentylenetetrazol epileptic model (Sayyah et al., 2003). Systemic administration of LPS in postnatal rodents has a long-lasting effect on enhancing adult seizure susceptibility in the lithium-pilocarpine, kainic acid, and pentylenetetrazol models of epilepsy (Galic et al., 2008). Such role of LPS can be blocked by intracerebroventricular administration of antibody against tumor necrosis factor (TNF) alpha (Galic et al., 2008). Administration of LPS can also prevent adult neurogenesis in the dentate gyrus (Ekdahl et al., 2003; Monje et al., 2003). Systemic administration of minocycline which inhibits activation of microglia (Ekdahl et al., 2003), or anti-inflammation treatment with indomethacin (Monje et al., 2003), successfully re-establishes LPS-induced suppression of neurogenesis. Another example of a deleterious inflammatory factor is the IL1 beta. IL1 beta prolongs the duration of kainate-induced seizures (Vezzani et al., 1999), while IL-1RA is anticonvulsant (Vezzani et al., 2000). The pro-convulsant action of IL-1beta is probably mediated by its effects on enhancing

glutamatergic transmission (Viviani et al., 2003) and reducing GABAergic currents (Wang et al., 2000).

On the other hand, inflammation mediators promote brain repair by inducing production of growth factors. For example, administration of IL-1beta or TNFα increases NGF expression in neurons, microglia and astrocytes (Bandtlow et al., 1990; Friedman et al., 1990; Gadient et al., 1990; Heese et al., 1998). Inflammation also activates antioxidant pathways and alleviates brain damage. For example, following KA-induced seizures IL-6 deficient mice are subject to greater oxidative stress and cell death (Penkowa et al., 2001), and tumor necrosis factor-alpha receptor (TNFR) null mice also respond to epileptic and excitotoxic injuries with exacerbated neuronal damage, increased level of oxidative stress and microglial activation (Bruce et al., 1996; Lu et al., 2008).

Therefore, it is not surprising that treatments with nonsteroidal anti-inflammatory drugs (NSAIDs) act differently on brain injury and epileptogenesis. Of these drugs, mefenamic acid is anti-convulsant, ibuprofen is not effective, and sodium salicylate and phenylbutazone have a proconvulsant effect in the pilocarpine SE model (Ikonomidou-Turski et al., 1988). Application of another type of NSAID, the selective COX-2 inhibitor parecoxib, reduces SE-induced neuronal damage in the hippocampus and piriform cortex (Polascheck et al., 2010). Parecoxib decreases the severity of SRSs, but does not affect the frequency or duration of SRSs in the pilocarpine model (Polascheck et al., 2010). The final outcome of the effects of inflammation on recovery from seizures depends on the amounts and types of inflammation mediators, the timing of the production of inflammatory factors, and the balance between the deleterious and protective effects of inflammatory factors.

1.3 Activation of microglial cells and astrocytes by growth factors and inflammatory factors

Activation of glial cells is characterized by morphological changes and increased release of growth factors and inflammatory factors (Choi and Koh, 2008; Rodriguez et al., 2009). When resting microglial cells are activated, their resting ramified shape transforms into an amoeboid morphology. Increased proliferation, migration and phagocytosis are also signs of microglial activation. In addition, activated astrocytes become fibrillary and enlarged. The proliferation and expression levels of glial fibrillary acidic protein (GFAP) in activated astrocytes are increased. Near damaged areas in the brain, astrocytes and microglia form dense and hypertrophic "glial scar" to replace original tissue. At distal areas from lesion site, the morphological changes are milder.

Activation of microglial cells and astrocytes have been found in many neurological disease including TLE and neurodegenerative diseases (Borges et al., 2003; Choi and Koh, 2008; Martin et al., 2001; Rodriguez et al., 2009). Activation of glial cells have been detected at as soon as 4 h following seizure (Ravizza et al., 2005) and can persist for a few weeks (Borges et al., 2003; Ravizza et al., 2005; Yang et al., 2010). Activated microglia can clear away damaged neurons and hypertrophied astrocytes following seizures, and can be associated with neural circuit reorganization and epileptogenesis. Inhibition of microglial activation by minocycline inhibited SE-induced migration of newborn hilar cells in the lithium pilocarpine model (Yang et al., 2010). *In vivo* application of LPS or another compound 2,4,6-trinitrobenzene sulfonic acid, which induced inflammation and activated microglia, also enhanced seizure susceptibility (Galic

et al., 2008; Riazi et al., 2008). These evidences suggest that activations of microglia and astrocytes may be associated with generation and spreading of epileptic activity in a complicated way (Choi and Koh, 2008). Interestingly, development of reactive gliosis also accompanies the progression of many neurodegenerative diseases including Alzheimer's disease(AD) (Giulian, 1999; Rodriguez et al., 2009) and frontal-temporal lobe dementia(FTLD) (Baker et al., 2006; Martin et al., 2001). Therefore, when addressing the neuropathy of these diseases, it is important to ask how glial cells are activated by a variety of growth factors and inflammatory factors.

1.3.1 Growth factors and cytokines activate microglial cells and astrocytes

Many of the cytokines and growth factors produced by glial cells can affect proliferation, migration and morphological changes of glial cells with an autocrine and paracrine fashion. Examples of these factors include cytokines such as IL-1, IL-6, TNFalpha, and growth factors such as VEGF. Application of IL-1 induces astrogliosis (Giulian et al., 1994). IL-6-deficient mice have less activation of microglia and astrocyte when subjected to KA-induced seizures (Penkowa et al., 2001), while specifically overexpressing IL-6 in astrocytes leads to activation of astrocytes and microglia *in vivo* (Brett et al., 1995; Campbell et al., 1993). The microglial activation induced by epileptic seizures has been found to be abrogated in TNF receptor null mice (Bruce et al., 1996). The microglial-expressing Flt-1 also contributes to the microglial chemotactic response in the brains injected with amyloid beta (Ryu et al., 2009).

1.3.2 Introduction to chemokines

Chemokines are a family of 8-10kd cytokines that can be secreted from astrocytes and perivascular microglia during inflammatory responses (Moser et al., 2004). Chemokines are divided into four major subfamilies: two NH3-terminal Cys residues adjacent to each other (CC), split by one amino acid (CXC), or split by three amino acids (CX3C), and only one NH3-terminal Cys residue (C). There are at least 27 types of CC chemokines and 17 CXC chemokines, but only two C chemokines (XCL1 and XCL2) and one CX3C chemokine (CX3CL1). Chemokines can be expressed by neurons, microglia, astrocytes and leukocytes. They bind to their distinct G-protein coupled receptors (GRCRs) and modulate neuronal activity, inflammatory responses, and microglial migration.

1.3.3 Production and function of chemokines in neurological diseases

Chemokines can be induced by inflammatory insults during many neurological diseases including ischemia, neurodegenerative diseases and epilepsy. For instance, treatment with A beta or LPS in brain induces the release of the chemokine CCL2, also named monocyte chemotactic protein-1(MCP-1), *in vivo* (Szczepanik and Ringheim, 2003) and *in vitro* (Ryu et al., 2009). Induction of MCP-1 has been observed in patients with AD (Ishizuka et al., 1997) and in stroke patients (Losy and Zaremba, 2001). The upregulation of MCP-1 has also been found to evident in the hippocampus of human TLE patients (Lee et al., 2007) and in the experimental models of TLE such as pilocarpine (Foresti et al., 2009) and kainic acid models (Manley et al., 2007). Other chemokines such as CCL3, CCL4, CX3CL1, and chemokine receptors such as CCR3, CCR5 and CX3CR1 (Guzik-Kornacka et al., 2011; Louboutin et al., 2011; Xu et al., 2009; Yeo et al.,

2011) have also been shown to be enhanced in animal models of epilepsy. The increases in CCL3 and CCL4 have also been found in TLE patients (Lee et al., 2007; van Gassen et al., 2008). However, CCR7, CCR8, CCR9, and CCR10 have been shown to be downregulated in interneurons following pilocarpine-induced SE (Liu et al., 2007a).

1.3.4 The role of chemokines in migration of microglia/macrophages and in brain damage caused by ischemia and epilepsy

The binding of chemokines to their receptors is considered as one of the major driving forces for the migration of microglia cells and macrophages (Moser et al., 2004). Application of MCP-1 induces migration of microglia cells, but fails to do so in microglia cultures from CCR2 knockout mice (Tsirka and Yao, 2010). In brain injury models with breakdown of blood brain barrier (BBB), leukocytes may infiltrate from blood into the brain. The infiltration of leukocytes such as macrophage and monocytes is facilitated by the binding of CCR2 receptors on leukocytes to the MCP-1 secreted from glial cells (Babcock et al., 2003; Fabene et al., 2010). Blockade of MCP-1 or CCR2 with gene therapy or transgenic deletion reduces the release of inflammatory cytokines and decreases the activation of the number of microglia/macrophage around the infarcts (Dimitrijevic et al., 2007; Hughes et al., 2002; Kumai et al., 2004). In addition, chemokine CX3CL1 and its receptor CX3CR1 contribute to SE-induced microglial activation (Yeo et al., 2011). Interestingly, most of these studies cannot distinguish activated microglia from invading macrophages due to the similarity of their morphology or cellular markers. Recently using GFP-transgenic bone marrow to separate resident microglia from hematogenous macrophages, Schilling et al. have reported that the activation of resident microglia is not affected but the infiltration of GFP-positive

macrophages is attenuated by focal ischemia in CCR2-deficient mice (Schilling et al., 2009).

Chemokines could contribute to tissue damage in experimental models of epilepsy and stroke. The infarct induced by middle cerebral artery occlusion is reduced in MCP-1 deficient mice (Hughes et al., 2002), CCR2 null mice (Dimitrijevic et al., 2007) and in mice treated with gene therapy to knock down MCP-1 levels (Kumai et al., 2004). Administration of antibodies against CX3CL1 or its receptor CX3CR1 protects hippocampus from SE-induced neuronal loss in pilocarpine model (Yeo et al., 2011). Blocking CCR5 by specific siRNA alleviates neuronal damage and inflammatory responses in KA-induced SE (Louboutin et al., 2011).

In conclusion, chemokines and its receptors appear be involved in activation of microglia/macrophages, and neuronal damage in seizure models.

1.4 The role of PGRN

PGRN was first purified as a growth factor secreted from mouse teratoma PC cells (Zhou et al., 1993). PGRN was brought to the attention of neuroscientists since mutations of PGRN were detected in tau-negative frontal temporal lobe dementia (FTLD) families with linkage to chromosome 17 (Baker et al., 2006; Cruts et al., 2006). Most PGRN mutations cause mRNA decay, protein decay or the failure of secretion of PGRN, leading to decreased PGRN expression or even complete loss of PGRN function (Baker et al., 2006; Cruts et al., 2006; Mukherjee et al., 2008; Shankaran et al., 2008; van der Zee et al., 2007). In addition, the haploinsufficiency of PGRN mutations have also been found in some patients with AD (Brouwers et al., 2007; Cortini et al., 2008; Lee et al., 2011) or

Parkinson's disease (PD) (Rovelet-Lecrux et al., 2008). Chronic inflammation is indicated in the pathophysiology of neurodegenerative disorders including AD (Eikelenboom et al., 2006), PD (Li et al., 2011) and FTLD (Baker et al., 2006; Sjogren et al., 2004). PGRN expression has been found in activated microglia in the brain of pathologic FTLD and AD patients (Baker et al., 2006). Knocking down PGRN in cultured neuron increases the frequency of miniature excitatory postsynaptic current (mEPSC) and the amount of vesicles per synapse, but decreases the density of synapses (Tapia et al., 2011). This group's work suggests that PGRN could be involved in regulation of synaptic activity, which can be greatly changed during epileptiform firings. Therefore, it is worthwhile to study the function of PGRN in neuroinflammation and microglial activation, especially in the epileptic brain.

1.4.1 Introduction to PGRN

PGRN is also named acrogranin, epithelin/granulin precursor, proepithelin or PC-cell-derived growth factor. The PGRN gene is located on chromosome 17q21 in human and on chromosome 11 in the mouse genome (Bhandari and Bateman, 1992; Bucan et al., 1996; Mackenzie, 2007). In fish and many invertebrate organisms, multiple PGRN genes are found, whereas mammals possess only one member of the PGRN gene family, and it is still a mystery why only one family member is retained in mammals and other land vertebrates during evolution (Bateman and Bennett, 2009). Immature PGRN before glycosylation and secretion has a relatively lower molecular weight of about 68 KDa as calculated from the 583 amino acid residues in PGRN (Eriksen and Mackenzie, 2008). After glycosylation and secretion the molecular weight of PGRN is increased to 90 KDa (Eriksen and Mackenzie, 2008). Several clinical mutations of PGRN impair glycosylation

and secretion, causing PGRN to degrade in the cytoplasm (Shankaran et al., 2008). Interestingly, PGRN is composed of 7.5 sequential repeats of cysteine-rich motifs called epithelins or granulins (Mackenzie, 2007; Shoyab et al., 1990) (Fig. 1.1 A). Analysis of human granulin peptide sequence reveals a unique 12-cysteine motif consisting of four pairs of cysteines flanked by two single cysteines at the amino and carboxyl termini (Bateman and Bennett, 2009). All cysteines have been found to be fully crossed-linked to form six disulfide bridges (Bateman and Bennett, 2009). PGRN can be cleaved to several granulins by elastase-induced proteolysis, and secretary leukocyte protease inhibitor (SLPI) has been shown to block this cleavage action of elastase (Zhu et al., 2002) (Fig. 1.1A). Although both PGRN and granulin peptides have shown biological activities and function, most studies have focused on the larger PGRN protein (Bateman and Bennett, 2009).

1.4.1.1 The localization of PGRN

PGRN has been found to be expressed in many regions in mammals, such as epithelial cells of kidney, gastrointestinal tract, skin and lung (Daniel et al., 2000; Daniel et al., 2003). Interestingly, PGRN often shows high expression levels under conditions of tissue remodeling where cells are dividing or actively migrating (Bateman and Bennett, 2009; Eriksen and Mackenzie, 2008). Abundant PGRN protein levels are observed in regions that are rapidly turning-over, such as the intestinal deep crypt and epidermal keratinocytes (Daniel et al., 2000; Daniel et al., 2003). While in the regions with less mitotic activity, the expression of PGRN is at far lower levels. For example, the fibroblasts and endothelial cells are normally mitotically quiet and show very low levels of PGRN. When these cells display increased levels of proliferation and migration

following wounding, their expression of PGRN increases dramatically. Except those mitotically active cells, there are post-mitotic cells that neither proliferate nor migrate express PGRN strongly, and the most obvious being the neurons in the brain and spinal cord. Recent evidence suggests that PGRN might protect neurons from premature death (Gao et al., 2010; Ryan et al., 2009; Van Damme et al., 2008). Moreover, PGRN is found throughout the brain from early developmental stage to adulthood, although its expression levels decrease as animals aged (Matsuwaki et al., 2011). In adult brain, PGRN immunoreactivity is intense in neurons of the pyramidal cell layer and dentate gyrus of the hippocampus, cingulate and piriform cortices, striatum, amygdala, hypothalamus and cerebellum (Daniel et al., 2000; Matsuwaki et al., 2011; Petkau et al., 2010).

1.4.1.2 The PGRN receptor: sortilin-1 and TNF receptor

Despite the critical roles of PGRN in both health and disease, a fundamental and key question, the identity of the receptor(s) of PGRN, has remained a mystery for a long time. The receptor of PGRN has been estimated to have a size ranging from 120 to 179 KDa on epithelial cells and fibroblasts (Xia and Serrero, 1998), and has recently been identified as the sortilin-1 in neurons (Hu et al., 2010; Zheng et al., 2011). Hu et al. (2010) have made a key advance by identifying Sortilin as the major receptor for PGRN in the CNS (Hu et al., 2010). The authors use an unbiased expression cloning approach to identify binding partners for PGRN protein, and sortilin is the only high-affinity binding partner identified of the 225,000 clones screened, suggesting that sortilin is the major receptor of PGRN in the brain (Hu et al., 2010). Binding studies in neurons from sortilin knockout mice also demonstrate that sortilin is the major receptor for PGRN in cultured cortical

neurons (Hu et al., 2010). Sortilin is a member of a family of cellular VPS10p type 1 receptors expressed abundantly in neurons (Willnow et al., 2008) (Fig. 1.1B). A series of experiments have shown that PGRN binds only Sortilin and not other VPS10p proteins (Hu et al., 2010). PGRN is not the sole ligand of Sortilin. Sortinlin's ligands include the neuropeptide neurotensin (NT), and proNGF. Interestingly, NT and PGRN probably bind to Sortilin through a common site, while proNGF and PGRN may bind to different sites on the ectodomain of Sortilin (Hu et al., 2010; Lewis and Golde, 2010) (Fig. 1.1B).

Recently, another group independently reported that PGRN protein bound directly to tumor necrosis factor receptors (TNFRs) and disturbed the TNFα-TNFR interaction in chondrocytes, using a yeast two-hybrid screening system and the coimmunoprecipitation biochemical method (Tang et al., 2011). They also show that PGRN knockout mice display higher susceptibility to collagen-induced arthritis, and administration of PGRN protein reverses the inflammatory arthritis. PGRN protein can also prevent inflammation in multiple arthritis mouse models and can inhibit TNFα-activated intracellular signaling. These data indicate that PGRN is a ligand of TNFR and an antagonist of TNFα signaling, and that PGRN may play an essential role in the pathogenesis of inflammatory arthritis in mice (Tang et al., 2011). Taken together, the identities of the receptors of PGRN will help people understand normal PGRN function in the CNS of and pathology PGRN mutations in neurodegenerative diseases. It may also suggest potential novel therapeutic interventions for PGRN-related diseases.

1.4.1.3 The PGRN-induced signaling pathways

PGRN activates typical growth factor signal transduction pathways. For example, PGRN is reported to induce the phosphorylation of p44/42 mitogen-activated protein

kinase (MAPK) in the extracellular regulated kinase (ERK) cascades and the phosphorylation of protein kinase B (PKB/Akt) in the phosphatidylinositol 3-kinase (PI_3K) pathway (He et al., 2002). PGRN also promotes tyrosine phosphorylation of focal adhesion kinase (FAK), which is a cytoplasmic tyrosine kinase in the signaling pathways associated with clustered integrins (He et al., 2002; Schlaepfer et al., 1999). However, the majority of the signal transduction data of PGRN are achieved from cancer cells (Bateman and Bennett, 2009), and the upstream and downstream pathways of PGRN in the CNS are still largely unknown.

Interestingly, although extensive studies have shown that PGRN plays critical roles in cell division, survival, migration, and the development of early embryos (Bateman and Bennett, 2009), the knockout mice of PGRN are fertile, and do not exhibit any disorders in reproductive function (Kayasuga et al., 2007; Yin et al., 2010). PGRN deficient mice have similar litter size and survival rate as wildtype (Kayasuga et al., 2007). The mild knockout phenotypes suggest that PGRN may contribute to many physiological processes but may not be an absolutely irreplaceable factor for these processes (Bateman and Bennett, 2009). Recently, strategies to produce site-specific transgenic mice have also been applied to study the physiological roles of PGRN. For example, keratinocyte-specific over-expression of PGRN in mice leads to abnormal hair development, indicating a role for PGRN in regulating hair growth (Kato et al., 2009). In the following sections I will review certain function of PGRN in either physiological or pathophysiological conditions.

1.4.2 Progranulin and neurodegenerative diseases

The mammalian gene that encodes PGRN was identified as early as in 1993 (Zhou et al., 1993) , but the function of PGRN in the CNS had not been extensively studied until 2006, when mutations in *PGRN* were identified to be related with the frontotemporal lobar dementia with ubiquitin-positive inclusions (FTLD-U) (Baker et al., 2006; Cruts et al., 2006). FTLD-U is a familial neurodegenerative disease pathologically characterized by atrophy and neuronal loss in the frontal and temporal lobes of the brain, and is hallmarked by the intracellular accumulation of ubiquitinated inclusion of TDP-43, a TAR DNA binding protein (Kumar-Singh, 2011; Mackenzie, 2007; Neumann et al., 2006). FTLD-U is typically developed at a relatively young age in human, and has become the second most common dementia for people younger than 60 year old (Bateman and Bennett, 2009). Mutations in *PGRN* have been found not only in the patients with FTLD-U, but also in patients with symptoms that resemble Alzheimer's disease (AD), Lewy body dementia, and corticobasal syndrome with ages ranging from 35–89 (Bateman and Bennett, 2009; Gijselinck et al., 2008; van Swieten and Heutink, 2008). To date, more than 60 mutations have been identified in *PGRN* that contribute to FTLD-U or related disorders (Bateman and Bennett, 2009; van Swieten and Heutink, 2008). Many of the mutations in GRN are hypothesized to lead to disease through haploinsufficiency of the PGRN proteins (Bateman and Bennett, 2009; van Swieten and Heutink, 2008). In addition, PGRN may play a critical role in other degenerative disorders in the CNS, including amyotrophic lateral sclerosis (ALS) (Sleegers et al., 2008) and primary progressive multiple sclerosis (Fenoglio et al., 2010). To date, the functional mechanisms of PGRN in neurodegenerative diseases are still largely unknown and

beginning to be explored. For example, it is still elusive why the cells in the frontal and temporal lobes are so much more sensitive to loss of PGRN than others.

1.4.3 The function of PGRN in inflammation

PGRN expression is upregulated by peripheral wound injury and injuries in the central nervous system (CNS). Promoter of the PGRN gene contains regulatory elements such as the IL-6 response element (Bhandari et al., 1996). Inflammatory cytokines such as TNFα induce PGRN expression in murine embryo fibroblasts (Li et al., 2002), while the anti-inflammatory cytokine IL-4 suppresses PGRN expression in myeloid cells (Ong et al., 2006). In addition, PGRN is upregulated in activated microglia upon excitotoxic stimulation by intra-striatum injection of NMDA receptor agonist quinolinic acid (Petkau et al., 2010). Injection of excitotoxin such as quinolinic acid can cause reactive gliosis and inflammatory response around the injection site (Duan et al., 1998; Heyes, 1993). Since glutamate excitotoxicity is central to the pathophysiology of epilepsy (Meldrum, 1993; Meldrum et al., 1999), it is reasonable to hypothesize that PGRN could be secreted upon seizure attacks.

PGRN influences the inflammatory response during wound healing and bacterial infection. PGRN prolongs infiltration of neutrophils and macrophages in cutaneous wounds and improves would healing (He and Bateman, 2003; He et al., 2003). Granulins, the cleaved product of PGRN, act differently from PGRN on inflammatory response. PGRN but not granulin A or B inhibits the TNFα-induced respiratory burst in cultured neutrophils (He and Bateman, 2003; Zhu et al., 2002). Granulin B but not PGRN induces the secretion of cytokine IL-8 from epithelial cells (He and Bateman, 2003; Zhu et al., 2002). IL-8 is a known chemoattractant for neutrophils and epithelial cells (Baggiolini

and Clark-Lewis, 1992). In the periphery, PGRN plays an anti-inflammatory role while granulin is proinflammatory. Although PGRN promotes infiltration of neutrophils and macrophages in the wound, whether this effect is caused by PGRN or granulin is not clear yet. Studies using PGRN deficient mice also indicate that PGRN acts against inflammation during bacterial infection (Yin et al., 2010). In response to LPS, macrophages from PGRN knockout mice secret more proinflammatory cytokines such as MCP-1, TNF, and IL6, while producing less anti-inflammatory cytokine interleukin-10 (IL-10) (Yin et al., 2010). PGRN deficient mice fail to clean away bacterial infection in liver, spleen and brain (Yin et al., 2010). The bacterial-induced infiltration of monocytes in spleen is less pronounced in PGRN deficient mice compared with controls (Yin et al., 2010). These studies suggest that PGRN may act as chemoattractant for immune cells such as neutrophils, macrophages and monocytes in the periphery.

PGRN also affects microglial migration in brain. PGRN is expressed in neurons and microglia in the CNS (Matsuwaki et al., 2011; Petkau et al., 2010). It has recently been found that application of recombinant PGRN can induce microglial migration *in vivo* and *in vitro* (Pickford et al., 2011). PGRN also induces expression of chemokines in cultured neurons (Pickford et al., 2011). Interestingly, the 18 month old PGRN deficient mice maintain a greater number of microglial cells in hypothalamus, cortex and hippocampus (Yin et al., 2010). This result suggests that PGRN may be inhibiting microglial migration, but the activation of microglia could also be a complementing reaction as a result of long-term deficiency of PGRN. Since epilepsy causes microglial activation (Borges et al., 2003), we hypothesize that PGRN may influence microglial activation and inflammatory response induced by epilepsy.

1.4.4 Other functions of PGRN in the CNS

It has been well described that elevated PGRN stimulates proliferation, survival, and motility of epithelial cells and fibroblasts (Bateman and Bennett, 2009). Recently, several studies suggest that PGRN might act as a neurotrophic factor for neurons in the CNS. Application of recombinant PGRN protein improves neuronal survival and induced neurite growth in cultured cortical and motor neurons (Gao et al., 2010; Van Damme et al., 2008). PGRN also prolongs the survival of motor neuron cultures in serum deprivation conditions (Ryan et al., 2009). PGRN-deficient neurons have increased activation of caspase-3, and are more vulnerable to normally sublethal doses of stressors such as NMDA or H2O2 (Guo et al., 2010; Kleinberger et al., 2010). Brain slices from PGRN knockout mice are subject to higher levels of tissue damage than controls when treated with LPS or oxygen glucose deprivation (Yin et al., 2010). Since epilepsy is a complicated disease affected by oxidative stress (Shin et al., 2011), inflammation (Choi and Koh, 2008), and glutamate excitotoxicity (Meldrum, 1993), we hypothesize that PGRN may play a role in seizure-induced neuronal death.

1.5 Glutamate excitotoxicity

In neurological disorders such as brain ischemia, epilepsy and dementia, excessive release of glutamate induces a series of cellular events leading to neuronal and glial damage (Lipton, 1999; Lynch and Guttmann, 2002; Morimoto et al., 2004). Failure of astrocytic glutamate transporters accelerates the accumulation of glutamate. Glutamate stimulates massive Ca^{2+} entry into postsynaptic neurons, activating a biochemical cascade that results in cell death (Pivovarova and Andrews, 2010; Sattler and Tymianski, 2001; Szydlowska and Tymianski, 2010). Studying the mechanisms by which neurons and

astrocytes respond to glutamate excitotoxicity may provide potential drug targets to cure these neurological disorders.

1.5.1 Glutamate excitotoxicity-induced neuronal cell death

During glutamate excitotoxicity, excessive synaptic release of glutamate activates postsynaptic glutamate receptors, leading to apoptotic and/or necrotic cell death. Among the glutamate receptors involved, N-methy-D-aspartate (NMDA) subtypes have been reported to be the major mediators because of their high permeability to calcium (Sattler and Tymianski, 2001). Activations of other glutamate receptors including AMPA or kainate receptors also contribute to the intracellular calcium increase (Platenik et al., 2000; Sattler and Tymianski, 2001). In addition to massive Ca^{2+} influx from extracellular space, accumulation and subsequent release of mitochondrial Ca^{2+} and its subsequent release may also play an important role in maintaining a persistent Ca^{2+} overload. It has been reported that glutamate could trigger the cleavage of the major extrusion pathways of cytoplasmic Ca^{2+}, the plasma membrane Ca^{2+} pump (PMCA) and Na^{+}/$Ca2^{+}$ exchangers (NCX), by proteases such as calpain, which might also contribute to the Ca^{2+} overload in neurons (Bano et al., 2005). Calcium overload during excitotoxicity initiates processes leading either to necrosis, apoptosis, or both (Platenik et al., 2000; Sattler and Tymianski, 2001). Apoptotic cell death, as characterized by caspase-3 activation, DNA-fragmentation and terminal deoxynucleotidyl-transferase mediated dUTP nick-end labeling (TUNEL) positive staining, has been observed in several animal models of cerebral ischemia (Chen et al., 1998; Cheng et al., 1998; Endres et al., 1998; Namura et al., 1998). Activation of caspase-3 is also required for NMDA-induced apoptosis in neuron cultures (Budd et al., 2000; Okamoto et al., 2002). Except caspase-3, glutamate

excitotoxicity-induced activations of other cysteine proteases, such as caspase-6, caspase-9, and calpain have also been reported (Capano et al., 2002; Lankiewicz et al., 2000; Wang and Qin, 2010). Interestingly, despite extensive studies, the signaling transduction pathways and subsequent downstream mechanisms that lead to cell death are still elusive. Studies have shown that several protein kinases such as protein kinase A (PKA), calmodulin-dependent protein kinase-II (CaMK-II) and some members of the protein tyrosine kinases (PTK), such as Src, may be involved in mediating Ca^{2+} signaling to the extracellular signal-regulated kinases (ERK1/2) cascade and excitotoxicity (Haddad, 2005; Wang and Qin, 2010). The identification of new proteins and genes that contribute to glutamate-induced cellular responses such as neuronal apoptosis will provide people with novel insights into the underlying mechanisms of excitotoxicity. In this dissertation, I am particularly interested in the functions of the cell signaling proteins that response early in the cell death pathway, especially the transcription factors and immediate early genes that are involved in the activation of caspase-3, because treatments targeting these early responding mediators are believed to protect neurons from damage.

1.5.2 The role of immediate early genes in glutamate excitotoxicity

Immediate early genes (IEGs) are a family of genes that are transcribed early after increased levels of activity/exaction in the brain. Expression of IEGs are induced after physiological excitation such as during learning and memory (Dragunow, 1996), and are also affected by pathological excitation of synaptic activity induced by glutamate excitotoxic insults (Xia et al., 1996) and epileptic seizures (Gass et al., 1993; Link et al., 1995). IEGs encode transcriptional factors that stimulate transcription of many other genes that lead to long-term change in the cellular function. Immunostaining of IEG-

encoded proteins such as c-fos and c-jun has been used to map areas of neuronal activation during memory, anxiety, or epileptiform events (Kubik et al., 2007; Morimoto et al., 2004).

1.5.2.1 Activation of glutamate receptors induces IEGs expression: examples of zif268, fos and jun family

Here I first introduce several members of IEGs families: *fos* family (c-*fos* and *fos*B), *jun* family (c-*jun* and *jun*B) and *zif/268*. Proteins from *fos* and *jun* families bind via leucine zipper and form heterodimeric or homodimeric transcription factors called activator protein 1 (AP-1) (Sng et al., 2004). AP-1 transcription factors recognize consensus DNA sequences such as the TPA (12-O-tetradecanoylphorbol-13-acetate) response elements (TRE) and the cAMP response elements (CRE) in the promoters of target genes (Sng et al., 2004). *Zif/268* was first identified as the transcription factor activated by growth factors (Christy et al., 1988). *Zif/268* contains three Cys2His2 zinc finger structures that form a conserved DNA binding domain which recognizes a GC-rich DNA sequence in the promoters of target genes (Knapska and Kaczmarek, 2004).

Excitotoxic activation of glutamate receptors induces expression of many IEGs. Treatment of glutamate for one hour upregulated the expression of many IEGs including *fos* family (c-*fos* and *fos*B), *jun* family (c-*jun* and *jun*B) and *zif/268* in cultured neurons (Condorelli et al., 1994) and astroglial cells (Condorelli et al., 1993). Local injection of the NMDA receptor agonist quinolinic acid into the striatum rapidly induces the expression of c-*fos*, c-*jun*, *jun*B and *zif/268* within one hour (Walker and Carlock, 1993).

Increased gene expressions of IEGs are also found in global and focal models of ischemia and in several animal models of epilepsy (Akins et al., 1996; Kiessling and Gass, 1993).

The functions of c-*fos*, c-*jun* and *zif/268* in neuronal survival during excitotoxic events have recently been reported (Behrens et al., 1999; Tureyen et al., 2008; Watson et al., 1998; Zhang et al., 2002; Zheng et al., 1998). Using site-specific knock out techniques to selectively knock out c-*fos* in the Ca1 pyramidal neurons, Zhang et al. (2002) found that these conditional c-*fos* knockout mice were more vulnerable to kainic acid-induced neuronal death (Zhang et al., 2002). These mice are subject to more severe seizures and more frequent epileptiform firings. Although c-*fos* plays a pro-survival role during kainic acid-induced seizure, phosphorylation of c-*jun* triggers apoptosis. Apoptotic signals is observed in cerebellar granule neurons when the phosphorylation site on c-*jun* is mutated to be constantly active (Watson et al., 1998). Transgenic mice with inactivated phosphorylation site of c-*jun* are less capable of transcribing promoters with AP-1 responding elements, and are more resistant to kainic acid-induced seizure and hippocampal neuronal death (Behrens et al., 1999). Cultured neurons from these mutant mice are protected from kainate-induced apoptosis (Behrens et al., 1999). In addition, *zif/268* is a key transcriptional factor in long-term synaptic plasticity and ischemia-induced inflammatory response and brain damage, but the role of *zif/268* in epilepsy is not as clear. *Zif/268* knockout mice develop normal short-term synaptic plasticity, but their long-term memory and late-phase LTP are impaired (Jones et al., 2001), suggesting *zif/268* could mediate new protein synthesis required for long-term consolidation of memory. *Zif/268* knockout mice are protected from focal ischemia, showing less infarct area, lower activation of microglia/macrophages and decreased expression of

inflammatory genes (Tureyen et al., 2008). However, using amygdala kindling seizure models, Zheng et al. (1998) found no change in the kindling rate or the DG mossy fiber sprouting pattern in *zif/268* knockout mice (Zheng et al., 1998).

1.5.2.2 The Immediate early gene KLF4

In previous findings from our laboratory using whole genome profiling techniques (Prasad et al., 2004), KLF4 mRNA was found to be rapidly and dramatically upregulated in the *in vivo* rat models of retina ischemia and cerebral ischemia. The whole-genome transcriptional profiling study conducted by Zhang et al. indicated that Krüppel-like factor 4 (KLF4/GKLF/EZF) was activated after either synaptic or extra-synaptic NMDA stimulation (Zhang et al., 2007a). While KLF4 has been shown to be expressed in epithelial cells of the cornea, skin and gastrointestinal tract (Chiambaretta et al., 2004; Garrett-Sinha et al., 1996; Segre et al., 1999; Shields et al., 1996), the expression and function of KLF4 in the CNS have not been extensively studied.

KLF4 belongs to a recently identified family of zinc finger-containing transcription factors, Krüppel-like factors (KLFs). Previous studies have shown that KLFs play important roles in proliferation, differentiation, development, and apoptosis (Garrett-Sinha et al., 1996; Rowland and Peeper, 2006; Shields et al., 1996). Malfunctions of these proteins are involved in the pathology of numerous human diseases, including cardiovascular disease, metabolic disorders, and cancer. To date, 17 KLF genes have been cloned (KLF1-17) (McConnell and Yang, 2010). Based on the functions of these proteins, KLFs are divided into four distinct subgroups. Group 1 KLFs (KLF3, KLF8, and KLF12) could interact with the carboxy-terminal binding protein (CtBP) and function as transcriptional repressors. Group 2 KLFs (KLF1, KLF2, KLF4, KLF5, KLF6,

and KLF7) are transcriptional activators. Group 3 KLFs (KLF 9, KLF10, KLF11, KLF13, KLF14, and KLF16) are also transcriptional repressors and interact with the common transcriptional corepressor Sin3A. The last two members of the KLF family, KLF15 and KLF17, are more distantly related based on phylogenetic analysis and contain no defined protein interaction motif.

Human *KLF4* gene is located at the chromosome 9q31 and the gene structure and protein domains are shown in Fig. 1.2 (Wei et al., 2006). Similar to other KLFs, KLF4 is a zinc finger transcription factor with three Cys2His2 motif at the C-terminal DNA binding domain, and recognizes GC-rich elements of target genes (Wei et al., 2006). LF4 is involved in diverse cell functions, including proliferation, differentiation and apoptosis (Garrett-Sinha et al., 1996; Rowland and Peeper, 2006; Shields et al., 1996). In recent studies, KLF4, in combination with three other transcription factors, was sufficient to reprogram mouse and human fibroblasts to pluripotent stem cells (Takahashi et al., 2007; Wernig et al., 2007), suggesting a major role of KLF4 in the cell cycle and differentiation. Related to its role in the cell cycle, KLF4 has been described as either a tumor suppressor or an oncogene, depending on the tissue type and the situation examined (Ghaleb et al., 2005; Rowland and Peeper, 2006). As a potential tumor-suppressing protein, KLF4 is downregulated in human gastric cancer (Wei et al., 2005). KLF4 has been reported to halt tumor cell cycle progression through transcriptional regulation of several cell cycle proteins. For example, KLF4 inhibits cyclin D1 expression by interacting with the Sp1 binding domain of the cyclin D1 promoter (Shie et al., 2000). KLF4 also enhances $p21^{Waf1/Cip1}$ gene expression by binding to its Sp1-like promoter region (Yoon et al., 2003; Zhang et al., 2000), and thus prevents tumor progression (Rowland and Peeper, 2006).

However, KLF4 has also been identified as a potential oncogene in other cancers including squamous cell carcinoma and breast cancer (Foster et al., 1999; Foster et al., 2005; Huang et al., 2005; Pandya et al., 2004). In human breast cancer cells, for instance, KLF4 depletion enhanced p53 levels and induced p53-dependant apoptosis (Rowland et al., 2005). Since $p21^{Waf1/Cip1}$ is required for p53-mediated apoptosis in breast cancer (Lacroix et al., 2006), the inhibition of p53 by KLF4 suggests that $p21^{Waf1/Cip1}$ might be negatively regulated in this and other situations as well. In addition, overexpression of cyclin D1 is evident in breast cancer (Bartkova et al., 1994) , and thus might neutralize the growth-arresting ability of $p21^{Waf1/Cip1}$, in conjunction with Cdk4 or Cdk6 (Sherr and Roberts, 1999). CyclinD1 is also required for KLF4-induced oncogenic transformation (Rowland et al., 2005). Taken together, these data suggest that the pro-proliferative role of KLF4 is achieved by the regulation of cyclin D1 and $p21^{Waf1/Cip1}$.

1.5.3 The contribution of cell cycle proteins to glutamate excitotoxicity

Previous evidence has suggested that various insults, including ischemia, can cause terminally differentiated neurons to attempt to reenter the cell cycle, and that this is an important path towards apoptotic cell death (Klein and Ackerman, 2003). The G0/G1 transition checkpoint is controlled by the accumulation of cyclin D1, which binds to and activates the cyclin-dependent kinase 4 (Cdk 4) that initiates subsequent cell cycle events (Sherr and Roberts, 1999). The Cdk inhibitor $p21^{Waf1/Cip1}$ binds to and inhibits the cyclin D1-Cdk4 complex, and thus arrests the cell cycle at the G1 checkpoint (Harper et al., 1993; Zhu et al., 1999). Accumulating data link aberrant regulation of cell cycle proteins to apoptosis, with evidence of abnormal upregulation of cyclin D1 protein levels and Cdk

4 activation occurring in the early stages of neuronal apoptosis (Liu and Greene, 2001; Osuga et al., 2000). Moreover, blockade of cyclin-Cdk activity prevents apoptotic death of primary cortical and sympathetic neurons in many conditions that normally lead to apoptosis (Osuga et al., 2000; Park et al., 1997a; Park et al., 1997b; Park et al., 1998).

1.5.4 Astrocytes supply the energy demand during glutamate excitotoxicity

Despite comprising only 2% of total body's weight, the brain requires about 20% of the body's energy supply to maintain its normal function (Kovac, 2010). Glucose and oxygen provided by brain blood vessels are metabolized to ATP to maintain ion gradients across neuronal membranes. ATP is also required for the uptake, synthesis and degradation of neurotransmitters. Constituting about 10 × as numerous as neurons in the CNS (O'Kusky and Colonnier, 1982; Sagduyu, 2002), astrocytes store glycogen and provide metabolic products of glucose to neurons in both physiological and pathological conditions(Brown and Ransom, 2007; Cataldo and Broadwell, 1986). In this section we will discuss the extreme energy demands associated with glutamate excitotoxicity and how astrocytes adapt to such conditions.

1.5.4.1 The importance of energy supply to glutamate excitotoxicity in neurological disorders

Brain glucose metabolism rate has been used to estimate the rate of brain energy consumption. Insufficient energy supply are associated with glutamate excitotoxicity in ischemia and AD (Astrup, 1982; Ferreira et al., 2010; Hynd et al., 2004; Molinuevo et al., 2005), while in epilepsy glucose metabolism is raised as glutamate is released (Morimoto

et al., 2004). Generally when action potential is propagated, Na+ flows in and K+ flows out of the neuronal membrane, leading to a depolarized membrane potential at the synaptic terminal, which causes glutamate release and activates ionotropic glutamate receptors. Insufficient energy supply in ischemic brain may prevent ATP-dependent pumps such as Na+-K+-ATPase from rebuilding the resting ion gradient, leaving neurons continuously depolarized and causing them to release more glutamate (Astrup, 1982). In Alzheimer's disease, glutamate excitotoxicity, reduced glucose utilization and mitochondria dysfunction have been observed and may contribute to impaired memory (Ferreira et al., 2010; Hynd et al., 2004; Molinuevo et al., 2005). In contrast, glutamate release is correlated by high levels of glucose metabolism during epilepsy (Pfund et al., 2000). Epileptic firing causes release of glutamate from depolarized presynaptic terminals, leading to brain damage (Henshall, 2007). Enhanced activity of NMDA receptors has been found in some patients with epilepsy (Meldrum et al., 1999). In TLE patients, release of glutamate occurs before the onset of seizures and continues during seizures (During and Spencer, 1993), while glucose utilization is elevated during ictal period and is decreased during the interictal period (Dube et al., 2001; Morimoto et al., 2004).

1.5.4.2 Glycolytic and oxidative metabolisms of glucose in astrocyte in physiological conditions

The structure and location of astrocytes facilitate their function of supplying energy to neurons. From the cell body astrocytes extend endfeet wrapping around intraparenchymal capillaries and thus form large surfaces absorbing glucose and oxygen from blood (Hertz et al., 2007). Other extensions from astrocytes surround different parts of neurons

including the synapses, allowing instant respond to neurotransmitter release from synapses. Glycolytic and oxidative metabolisms of glucose are the two major pathways that astrocytes utilize to generate ATP. The dominant glucose metabolic pathways vary at different subcellular locations of the astrocyte. Hertz et al. (2007) has hypothesized that cell bodies and large processes of astrocytes contain mitochondria and thus use the oxidative pathway, while fine processes from astrocyte that are closest to synapses and capillaries do not contain mitochondria and thus preferred the glycolytic pathway (Hertz et al., 2007).

1.5.4.3 Increased glycolytic metabolism of glucose in astrocyte during glutamate excitotoxicity

Extensive glutamate release increases energy demand, which can not be met solely by the oxidative metabolism of glucose, and thus energy is also supplied from glycolytic metabolism and from the breakdown of glycogen (Pellerin et al., 2007). Lactate is the product of glycolytic metabolism. Brain lactate levels increase following insults such as traumatic brain injury, and the increase of lactate can be attenuated by application of glutamate antagonist kynurenic acid (Kawamata et al., 1995). Like glutamate, extracellular lactate concentrations raise at the onset of seizures and persist during seizures in TLE patients (During et al., 1994) and in lithium-pilocarpine model (van Eijsden et al., 2004). Application of glutamate in cultured astrocyte increases lactate release (Pellerin and Magistretti, 1994), and neural activation on brain slices induces NADH release representing a late phase of glycolytic metabolism (Kasischke et al., 2004). In addition, astrocytes store glycogen and glycogen can be metabolized glycolytically

when glucose is not adequate during hypoglycemia (Brown and Ransom, 2007) and ischemia (Rossi et al., 2007).

1.5.4.4 Astrocyte-neuron lactate shuttle hypothesis: astrocytes supply neurons with lactate during glutamate excitotoxicity

Pellerin and Magistretti proposed the astrocyte-neuron lactate shuttle hypothesis (Pellerin and Magistretti, 1994). When glutamate is released during normal synaptic activity, resting ion balance is damaged, and excess glutamate is transported into astrocytes by the astrocytic glutamate transporters such as glutamate transporter 1 (GLT1) and glutamate aspartate transporter (GLAST). Each glutamate requires the cotransportation of three sodium ions. Restoring the chemical balance in both neurons and astrocytes increased the demand for ATP which is supplied from glucose metabolism. Neurons preferentially employ the oxidative pathway when glucose/oxygen is ample. As energy demand increases and glucose/oxygen is used up, astrocytes undergo glycolysis/glycogenolysis and provide lactate to the neurons as an alternative energy source. The glycolysis in neurons is limited by their ability to produce lactate because their lack of glycogen storage. Upon prolonged and strong stimulation of glutamate, glycolysis and glycogenolysis are even intensified and the glycogen reservoir could be inadequate, leading to uncoupling of the lactate shuttle. Noteworthy, accumulation of lactate acidifies the brain in ischemic conditions (Barber et al., 2003; Li et al., 1995). Low pH in cultured astrocytes (pH=6.1), either induced by lactic acid or HCl, has been shown to reduce glutamate uptake and thus may intensify the excitotoxic effect of glutamate (Bender et al., 1997).

1.6 Hypotheses and goals of research

This dissertation was designed to investigate the cellular and pathological mechanisms related to neurological diseases such as epilepsy. We aimed at discovering new protein profiles and functions by studying the cellular responses to glutamate excitotoxicity and inflammation, and the response of CNS to epileptic insults. Our study could improve our knowledge of neurological dysfunctions and might provide new potential treatment target for epilepsy. Thus, we derived our **hypotheses** as follows:

1) The immediate early gene KLF4 could be upregulated by glutamate excitotoxicity, and KLF4 could be involved in cell cycle protein expression and glutamate excitotoxicity-induced apoptosis in cultured neurons.

2) The neurotrophic factor PGRN may contribute to epilepsy-induced cell loss and microglial activation, and PGRN could also be involved in inflammatory factor-induced chemokine release and microglial migration in culture.

3) The neurotrophic factor PGRN could be involved in glutamate-induced increase of glycolysis in cultured astrocytes.

We applied a variety of methods such as molecular techniques, biochemical assays, immunostaining and pharmacological tools to address our hypotheses. The goals of this dissertation are:

1) To determine the expression pattern of KLF4 under conditions of glutamatergic stimulations in cultured neurons; to construct KLF4-overexpressing lentiviral vectors; to analyze the effect of KLF4 overexpression on the levels of cyclin D1 and $p21^{Waf1/Cip1}$; to examine whether KLF4 plays a role in NMDA-induced apoptosis by testing expression of the apoptotic protein caspase-3.

2) To examine the expression and localization of PGRN in response to pilocarpine-induced SE and to LPS stimulation; to analyze the contribution of PGRN to SE-induced cell loss and microglial activation; to investigate the role of PGRN in LPS-induced microglial activation and chemokine release.

3) To test the function of PGRN in glutamate-induced lactate release and

glucose uptake in cultured astrocytes; to examine the effect of PGRN on MCT1 expression in glutamate-treated astrocytes.

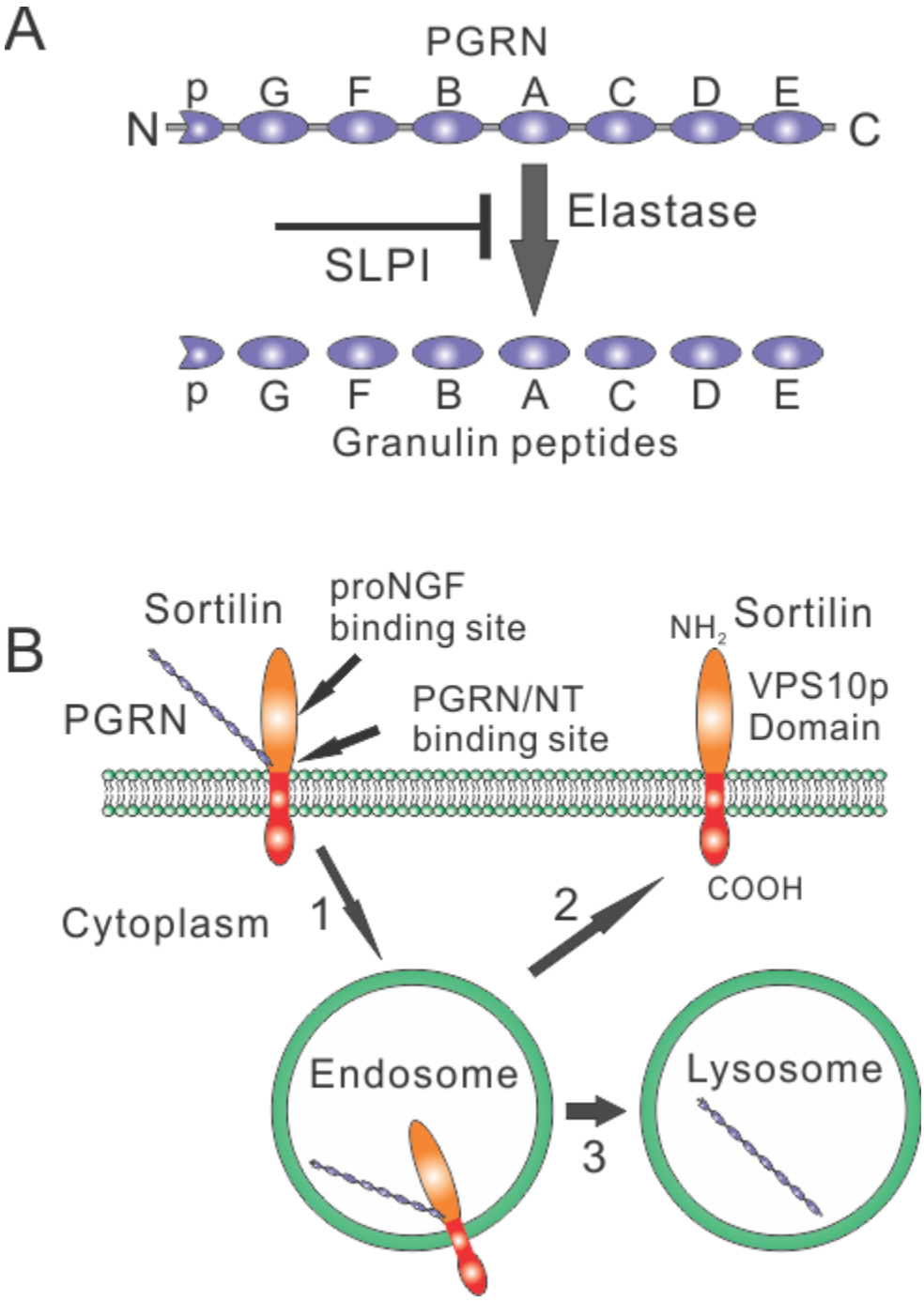
A
PGRN
p G F B A C D E
N
C
Elastase
SLPI
p G F B A C D E
Granulin peptides
B
Sortilin
proNGF
binding site
NH2
Sortilin
PGRN
PGRN/NT
binding site
VPS10p
Domain
COOH
Cytoplasm
1
2
Endosome
Lysosome
3

Fig. 1.1 The schematic structure of PGRN and the interaction between PGRN and its receptor sortilin.

The figure is adapted from (Lewis and Golde, 2010). **A,** PGRN is composed of 7.5 granulins and can be cleaved into granulins by elastase. The effect of elastase is blocked by SLPI. **B**, Sortilin is a member of VPS10p family. PGRN and NT bind to similar sites on sortilin, and proNGF binds to a different site. **C**, Binding of PGRN to Sortilin leads to endocytosis (1) of the PGRN/sortilin complex. Then PGRN is transported to the lysosome (3), whereas sortilin is recycled by endosome and return to the plasma membrane (2).

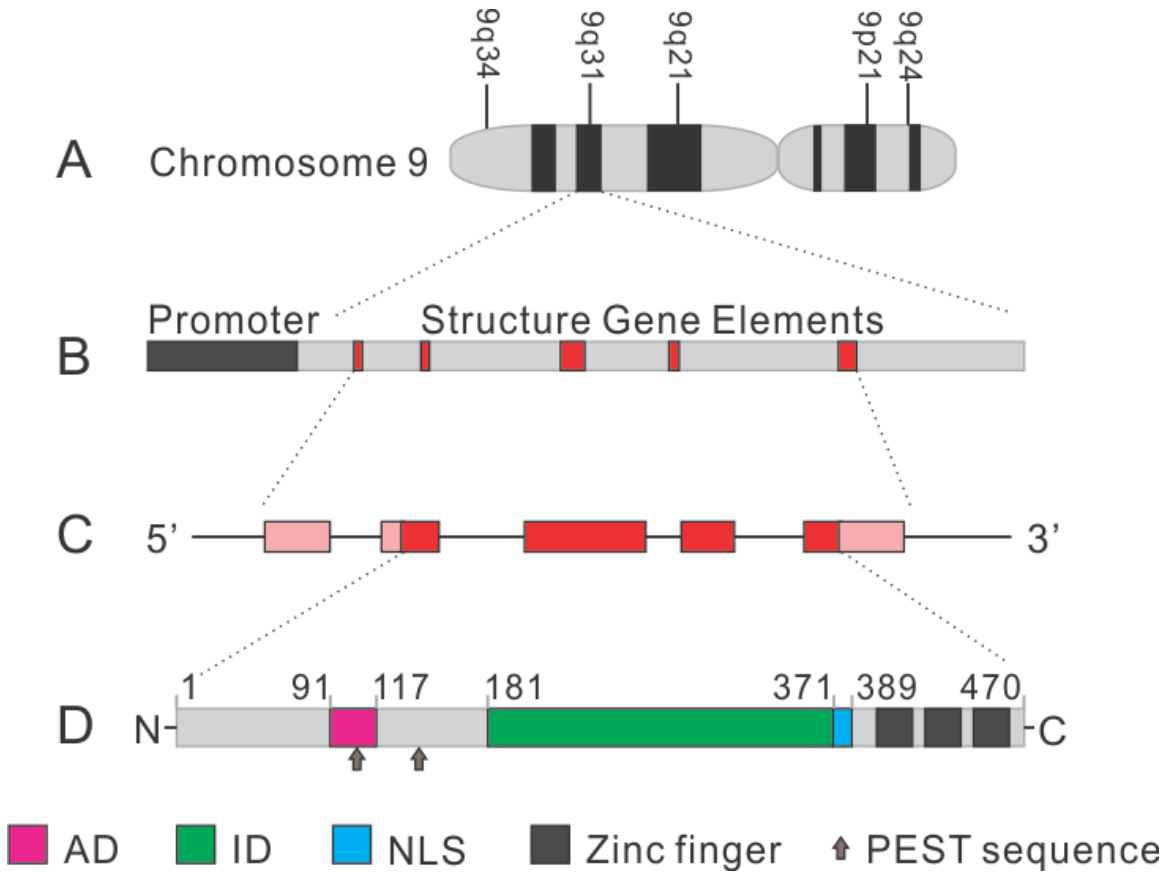

Fig. 1.2 The schematic structure of KLF4 gene and protein.

This figure is adapted from (Wei et al., 2006). **A**, *KLF4* gene is located on chromosome 9q31. B, In the KLF4 gene (6.3 kb), the red bars label the five exons of the KLF4 gene. **C**, In the KLF4 RNA transcript, the pink boxes show five exons, and the red boxes represent the KLF4 open reading frame (2639 bp). **D**, The KLF4 protein (470 amino acids) with several functional domains, including the transcriptional activation domain (AD, red), transcriptional inhibitory domain (ID, green), zinc finger DNA-binding domain, nuclear localization signal (NLS, blue), Cys2His2 zinc finger motif (black) and potential proline (P) - glutamic acid (E) - serine (S) -threonine (T) (PEST) sequence (grey).

CHAPTER TWO: THE ROLE OF KLF4 IN NMDA EXCITOTOXICITY

A version of this chapter has been published (Zhu, S., Tai, C., MacVicar, B.A., Jia, W., Cynader, M.S., 2009. Glutamatergic stimulation triggers rapid Krupple-like factor 4 expression in neurons and the overexpression of KLF4 sensitizes neurons to NMDA-induced caspase-3 activity. Brain Res. 1250**,** 49-62). The statistical analysis in this chapter is further modified and has an improved accuracy compared with that in the publication.

2.1 Summary of findings in chapter two

We report the first demonstration that KLF4 mRNA is dramatically and rapidly upregulated by NMDA application in primary cortical neuron cultures. We also report that NMDA induced significant and transient upregulation of KLF4 protein expression, in both cortical neuron cultures and native brain slices. The increase of KLF4 mRNA and protein expression in response to NMDA was time-dependent, and required NMDA receptor-mediated Ca^{2+} influx. In addition, AMPA exposure caused a time-dependent increase in KLF4 mRNA expression, which was also Ca^{2+}-dependent and involved activation of AMPA/kainate receptors and L-type voltage-sensitive calcium channels. To assess the downstream signaling pathways and functions of KLF4 activation, we used lentiviral vectors to induce ectopic overexpression of KLF4 in cultured neurons. KLF4 overexpression induced the activation of caspase-3 after a normally subtoxic dose of NMDA (10 μM). KLF4 overexpression also increased both protein and mRNA levels of the cell cycle protein cyclin D1, but reduced $p21^{Waf1/Cip1}$ protein levels. After the NMDA

treatment, cyclin D1 levels increased after a short delay (4 h), but fell back to control levels after 20 h. The effects of NMDA and KLF4 overexpression on cyclin D1 induction were additive. We conclude that glutamatergic stimulation can trigger rapid elevation of KLF4 mRNA and protein levels, and that the overexpression of KLF4 can regulate neuronal cell cycle proteins and sensitize neurons to NMDA-induced caspase-3 activity.

2.2 Experimental procedures

2.2.1 Materials

Unless stated otherwise, all chemical reagents were purchased from Sigma (Saint Louis, MO, USA). Neurobasal medium, B27 antioxidant supplement, L-glutamine, penicillin/streptomycin and trypsin were obtained from Gibco Invitrogen (Burlington, Ontario, Canada). BAPTA-AM was purchased from Calbiochem (San Diego, CA, USA). CNQX was purchased from Ascent (Bristol, UK). Glycine and sodium dodecyl sulfate (SDS) were purchased from Bio-Rad (Hercules, CA, USA). β–mercaptoethanol was purchased from Amersham (Buckinghamshire, UK). The HEK 293 T cell line was obtained from ATCC (Manassas, VA, USA).

2.2.2 DNA constructs

The lentiviral vector pFUGW was a gift from D. Baltimore (Lois et al., 2002). The backbone of pFUGW carries the human immunodeficiency virus-1 flap element between the 5’ long terminal repeat and the human ubiquitin-C internal promoter. The promoter controls an enhanced green fluorescent protein (EGFP), downstream of which a woodchuck hepatitis virus posttranscriptional regulatory element was inserted to increase the expression efficiency. The KLF4-expressing lentiviral vector was cloned as follows.

First, total RNA was extracted from mouse cortical neuron culture, and then the reverse transcription reaction was performed to generate first-strand cDNA as mentioned below. The total cDNA was used as the template to perform PCR using the primer pair: *KLF4* forward 5'-AGTAGGATCCATGAGGCAGCCACCTGGCGA-3' and *KLF4* reverse 5'-CGAGCTCGAGTTAAAAGTGCCTCTTCATGTGTAA-3'. We then replaced the EGFP in the pFUGW with the 1452 kb KLF4 fragment, to generate the viral vector called pFUKW. Sequencing results showed 100% amino acid identity to the KLF4 coding sequence (Gene bank accession number AY071827).

2.2.3 Lentiviral production and titrations

Lentiviral vectors were generated by transfecting HEK 293 T cells using a polyethyleneimine procedure (Horbinski et al., 2001; Reed et al., 2006), which yields 90% transfection efficiency. Briefly, 6 μL of 50% (wt/vol) polyethyleneimine and 3 μg DNA were separately mixed with 125 μL Dulbecco's modified Eagle's medium, combined together, and incubated at room temperature for 20 min before the mixture was added to each well. HEK 293T cells in each 10 cm dish at 90% confluency were transfected with 10 μg pFUGW or pFUKW, together with 5 μg of vesicular stomatitis virus glycoprotein and 7.5 μg of the packaging plasmid pCMV Δ 8.9 (second generation). The viral supernatants were harvested 48 h and 72 h after transfection, filtered through a 0.45-μm-pore size filter, and concentrated by ultracentrifugation (Sorvall® ultracentrifuge, Mandel, Guelph, Ontario, Canada) for 2 h at 30 000 rpm at 4 ℃. Viral pellets were then resuspended in an appropriate volume of Neurobasal medium. Aliquots of concentrated supernatants were stored at -80 ℃.

The titration of FUGW vector stock was determined by infecting HEK 293 T cells with 1 μL virus after a ten-fold serial dilution. The titer (transducing unit per μL) was calculated 3 days after infection using the formula $P*C_0*D$, where P is the percentage of green fluorescent protein (GFP) positive cells within total cells in one culture well, C_0 is the total number of cells at the time of virus infection, and D is the dilution factor. The titer of FUKW was calculated by multiplying the titer of FUGW and the fold change of viral RNA in FUKW over that in FUGW. The fold change was determined by one-step real time PCR (RT-PCR) as described below.

2.2.4 Primary mouse cortical culture, lentiviral infection and plasmid transfection

Primary neuronal cultures of mouse cortex were prepared from embryonic day 15 CD1 mice (Charles River, Quebec, Canada) as previously described (Sumrejkanchanakij et al., 2003; Willaime et al., 2001). All animal experiments were approved by the University of British Columbia Animal Care Committee. Appropriate experimental procedures were taken to minimize pain or discomfort. Briefly, the cortices were isolated and then digested with 0.25% (wt/vol) trypsin at 37 ℃ for 10-20 min. After trituration, cells were plated on poly-D-lysine coated culture plates, at a density of 1×10^6 per well in 6-well plate or 1×10^5 per well in 24-well plate. The neurons were plated in the Neurobasal medium supplemented with 2% (vol/vol) B27 antioxidant supplement, 2 mM L-glutamine, 10 μM β–mercaptoethanol, 25 μM glutamic acid and 1% (vol/vol) penicillin/streptomycin. After 2 days in culture, the glutamic acid was removed from the culture medium (so called “maintenance medium”). Culture plates were incubated at 37 ℃ in a humidified 5% CO2 chamber. Neurons were studied at or about DIV11.

2.2.4.1 Lentiviral infection

Neuron cultures were infected at 6 days *in vitro* (DIV) for 3 h at 37 ℃ with the concentrated viral stock of FUGW or FUKW using a concentration of 3 x 10^6 transducing units/well for 6-well plates and 3 x 10^5 transducing units/well for 24-well plates. Over 90% of cells infected with FUGW were GFP positive 5 days after infection.

2.2.4.2 Plasmid transfection

On DIV 9, neurons were transfected with Lipofectamine™ 2000 (Invitrogen) using a modified version of the manufacturer's protocol. In the presence of 4 μl Lipofectamine 2000, 0.1 μg of pFUKW and 0.3 μg pFUGW were added to each well in a 24-well plate, while 0.4 μg of pFUGW was applied as control. The transfection efficiency was about 1%.

2.2.5 Hippocampal slice preparation

Hippocampal slices were prepared from Sprague Dawley rats aged at postnatal days 13-16, according to standard procedures (Fraser and MacVicar, 1996). Our experiments were approved by the Canadian Council for Animal Care and the University of British Columbia Animal Care Committee. All experiments were conducted in strict accordance with the National Institutes of Health Guide for the Care and Use of Laboratory Animals. Briefly, rats were deeply anesthetized with halothane and rapidly decapitated. The brain was quickly removed and horizontal hippocampal slices (~ 400 μm) were cut with a vibratome (VT100; Leica, Willowdale, Ontario, Canada) in chilled (0-4 ℃) slicing solution containing (in mM): 75 sucrose, 87 NaCl, 25 NaHCO3, 25 D-glucose, 2.5 KCl, 1.25 NaH2PO4, 0.5 CaCl2, 7.0 MgCl2, pH 7.3. Then slices were transferred to a storage

chamber with fresh artificial cerebral spinal fluid (ACSF) containing (in mM): 126 NaCl, 2.5 KCl, 2.0 MgCl2, 2.0 CaCl2, 1.25 NaH2PO4, 26 NaHCO3, and 10 D-glucose, pH 7.3, and incubated at room temperature for more than 1 hour before recording. All solutions were saturated with 95% O2 and 5% CO2.

2.2.6 Chemical treatment

Cortical neurons were exposed to chemical treatment on DIV 11.Chemicals listed in table 2.1 were used in the control maintenance medium 30 min before NMDA application. After passing through the cytoplasmic membrane, BAPTA-AM is hydrolyzed to BAPTA by esterases and then is held in the cytosol. Neurons were treated for 1.5 h with either (1) control culture medium; (2) control culture medium with one or several of the reagents in table 2.1; (3) culture medium containing 20 μM NMDA and 20 μM glycine; (4) culture medium supplemented with NMDA, glycine, and one or several of the reagents in table 2.1. Similar experiments were performed using AMPA treatment instead of NMDA and glycine. In some cases, the dose and time of NMDA treatment were varied as described below. After treatment, gene expression was assessed using quantitative 2-step RT-PCR. In experiments requiring recovery after NMDA treatment, neurons were allowed to recover in the maintenance culture medium for 4 h or 20 h. After recovery, neurons were rinsed with cold phosphate buffered saline and protein levels were analyzed by Western blots.

2.2.7 Quantitative real time PCR

2.2.7.1 Two-step real time PCR

Total RNA from neuron cultures was isolated according to the manufacturer's instructions using Trizol® Reagent (Invitrogen). One μg of RNA was purified with DNase I (Invitrogen) and then reverse-transcribed using SuperScript™ II Reverse Transcriptase (Invitrogen), as per manufacturer's instructions. Duplicates of the 4-fold serial dilution of cDNA samples were used in a 25 μL total volume containing 12.5 μL SYBR® Green PCR master mix (Applied Biosystems**,** Foster City, CA, USA**)** and 300 nM primers for each RT-PCR reaction. Amplification was performed in the 7300 Real Time PCR System (Applied Biosystems). Cycle parameters were: 50 ℃ (2 min) and 95 ℃ (10 min), followed by 40 cycles of 95 ℃ (15 s) and 60 ℃ (1 min), followed by a dissociation stage of 95 ℃ (15 s), 60 ℃ (30 s) and 95 ℃ (15 s). Fold inductions were calculated using the formula $2^{-(\Delta\Delta^{Ct})}$, where ΔΔCt is the $\Delta Ct_{(stimulus)}$-$\Delta Ct_{(control)}$, ΔCt is $Ct(_{KLF4,\ p21,\ or\ cyclin\ D1})$-$Ct(_{actin})$ and Ct is the cycle at which the threshold is crossed. The gene specific primer pairs were as follows: *KLF4* gene forward 5'-AGGAGCCCAAGCCAAAGAG-3' and reverse 5'-ACAAGTGTGGGTGGCTGTTCT-3'; $p21^{Waf1/Cip1}$ gene forward 5'-GCAAAGTGTGCCGTTGTCTCT-3' and reverse 5'-ATGAGCGCATCGCAATCA-3'; *cyclin D1* gene forward 5'-CGAGAAGTTGTGCATCTACACTGA-3' and reverse 5'-TCACCAGAAGCAGTTCCATTTG-3'; *actin* gene forward 5'-ACGAGGCCCAGAGCAAGAG-3' and reverse 5'-TCTCCATGTCGTCCCAGTTG-3'. PCR product quality was monitored by post-PCR melt curve analysis.

2.2.7.2 One-step real time PCR

Nucleic acid samples were collected from 1 μL concentrated FUKW or FUGW viruses using phenol-chloroform (Invitrogen) extraction, as per manufacturer's instructions. After treatment with DNase I, the 2 μL sample was used in a 25 μL total volume containing SYBR® Green PCR master mix, MultiScribe™ reverse transcriptase (Applied Biosystems) and 500 nM primers for each RT-PCR reaction. Amplification was performed in the 7300 Real Time PCR System**.** The cycle parameters were similar to those used in two-step RT-PCR except that the first 2 min of 50 ℃ step was changed to 48 ℃ for 30 min. Viral RNA was measured by employing the lentiviral general antigen gene (GAG) primer as previously reported (Nishimura et al., 2002). The fold change of viral RNA in FUKW over that in FUGW was determined using the formula $2^{-(\Delta\Delta^{Ct})}$, where $\Delta\Delta Ct$ is the $\Delta Ct_{(FUKW)} - \Delta Ct_{(FUGW)}$, and ΔCt is $Ct_{(gag)} - Ct_{(actin)}$. The primers for *gag* are: forward, 5'- GGAGCTAGAACGATTCGCAGTTA-3'; reverse, 5'- GGTTGTAGCTGTCCCAGTATTTGTC-3'.

2.2.8 Western blots and immunocytochemistry

To obtain whole cell extracts, cells were homogenized with sample buffer (31 mM pH 6.8 Tris-HCl, 12.5% glycerol, 1% SDS, 0.02% Bromophenol blue). Cell lysates were boiled for 5 min and then resolved by SDS polyacrylamide gel electrophoresis. Proteins were transferred to nitrocellulose membranes (Bio-Rad, Hercules, CA). Protein bands were detected using primary antibodies including: 1:1000 rabbit polycolonal anti-KLF4 antibody (a gift from J.A. Segre's lab) (Segre et al., 1999), rabbit polycolonal anti-KLF4 (0.2 μg/mL, Millipore), anti-actin antibody (1:1000, Abcam, Cambridge, MA, USA) and anti-caspase-3 antibody (1:1000; Cell signal technology, Danvers, MA), mouse

monoclonal anti-cyclin D1 antibody (1:500; Santa Cruz Biotech, CA, USA), and anti-$p21^{Waf1/Cip1}$ antibody (1:500, BD Biosciences, Mississauga, ON Canada). Horseradish peroxidase-conjugated anti-rabbit and anti-mouse secondary antibodies (PerkinElmer, Wellesley, MA) and enhanced chemiluminescence (PerkinElmer) were used according to the manufacturer's instructions. The intensity of protein bands was measured using ImageJ software provided by NIH (http://rsb.info.nih.gov/ij/). The band that detects actin was used as a loading control.

Neurons were fixed with methanol for 10 min at -20 ℃. Nonspecific staining was blocked with 10% bovine serum albumin for 60 min at room temperature. Fixed neurons were immunostained with primary antibody in 3% bovine serum albumin overnight at 4 ℃, and then with secondary antibody for 1 h at 37 ℃. In some experiments, nuclei were counterstained by incubation with 4′,6-Diamidino-2-phenyindole (DAPI, Sigma) for 3 min. Coverslips were mounted on glass slides with anti-fade mounting medium (Vector Laboratories, Burlingame, CA, USA). The primary antibodies used were: rabbit polycolonal anti-MAP2 (1:1000, Chemicon), mouse monoclonal anti-cyclin D1 (1:100; Santa Cruz Biotech) and rabbit anti GFP (1:1000; Synaptic Systems, Goettingen, GERMANY). The secondary antibodies used were Alexa Fluor 488 conjugated anti-rabbit secondary antibodies (1:1000) and Alexa Fluor 546 conjugated anti-mouse secondary antibodies (1:1000) from Molecular Probes (Eugene, OR, USA).

2.2.9 Statistical analysis

Results were expressed as means ± SEM. One-way ANOVA was used to compare data among groups. Fisher's least significant difference post-hoc test was used to compare the differences between groups after ANOVA. When noted, two-tailed Student's *t* tests

were conducted in studies in which data from only two groups (treatment and control) are compared. Differences were considered significant at $p < 0.05$.

2.3 Results

2.3.1 Induction of KLF4 mRNA and protein levels by NMDA application in cultured neurons

In previous findings from our laboratory using whole genome profiling techniques (Prasad et al., 2004), KLF4 mRNA was found to be rapidly and dramatically upregulated in the *in vivo* rat models of retina ischemia and cerebral ischemia. These results prompted us to further investigate the regulation and function of KLF4 in a cell culture model of glutamate excitotoxicity, a critical pathological process occurring during ischemic stroke. We used an *in vitro* model of NMDA-induced excitotoxicity in mouse cortical neuron cultures (Liu et al., 2007b; Lynch and Guttmann, 2002). Our culture contained ~ 90 % microtubule-associated protein 2 (MAP2) positive neurons as measured by immunocytochemistry. We showed that the KLF4 mRNA levels were markedly elevated after NMDA application, as measured by quantitative real time PCR (RT-PCR) in Fig. 2.1. The optimal NMDA dose for inducing KLF4 expression was determined by administration of 1, 10, 20 or 50 μM NMDA for 1.5 h. The NMDA-induced KLF4 mRNA expression was most evident in the 20 μM group (57.6 ± 8.2 fold induction compared to the untreated control, $p < 0.001$). We then performed RT-PCR to evaluate time-dependent KLF4 mRNA expression following the treatment with the optimal dose of NMDA (20 μM). KLF4 mRNA induction reached maximum levels at 1.5 h and remained at elevated levels at 3 h post-treatment (Fig. 2.1B). Thus the optimal dose and

time for KLF4 induction involves 1.5 h treatment with 20 μM NMDA. There are reports indicating that NMDA treatment can induce glutamate release *in vitro* (Hamada et al., 1998), which might further activate AMPA/kainate receptors and L-type voltage-sensitive calcium channels (VSCCs) via cellular depolarization (Platenik et al., 2000). To detect whether the NMDA-induced KLF4 mRNA expression was solely dependent on NMDA receptor activation, we applied the NMDA receptor antagonist MK801, the AMPA/kainate receptor antagonist CNQX, and the L-type VSCC blocker nifedipine (Table 2.1). We found that MK801 (20 μM) completely abolished NMDA-induced KLF4 expression (Fig. 2.1C). In contrast, neither the L-type VSCC blocker nifedipine nor the AMPA/kainate receptor antagonist CNQX had any effect on NMDA-induced KLF4 expression (Fig. 2.1C). Our results indicate that KLF4 mRNA induction is mediated by NMDA receptors alone, and not by L-type VSCCs or AMPA/kainate receptors.

To investigate whether KLF4 protein levels were also upregulated by NMDA, we used immunoblotting techniques and a KLF4 antibody on neuron cultures treated with NMDA. We used the optimal NMDA treatment protocol for KLF4 mRNA induction (20 μM NMDA for 1.5 h), and further allowed neurons to recover in non-NMDA-containing medium for 0, 1, 2, 4, 6, or 8 h. We found that KLF4 protein levels were transiently upregulated during the recovery period (Fig. 2.2A and 2.2B). The induction was observed at maximal levels at 2 h (196 ± 38 % of control, $p < 0.05$) and 4 h (235 ± 49 % of control, $p < 0.01$) recovery. Thereafter KLF4 protein levels dropped at 6 h and 8 h recovery. To confirm that KLF4 protein elevation was also dependent on NMDA receptor activation, we applied MK801, CNQX and another NMDA receptor antagonist APV to neurons 30 minutes before NMDA treatment. We found that MK801 or APV significantly blocked

NMDA-induced KLF4 protein elevation (97 ± 12% of the untreated control, $p < 0.01$ compared to NMDA alone; Fig. 2.2C and 2.2D), while CNQX had no effect on the KLF4 induction by NMDA ($p = 0.42$ compared to NMDA alone; Fig. 2.2C and 2.2D).

Calcium influx through various Ca^{2+} permeable channels has been suggested to be responsible for downstream apoptotic signals following excitotoxicity (Sattler and Tymianski, 2001). To identify possible upstream regulators of KLF4, we used Ca^{2+} chelators (Table 2.1) to investigate the contribution of Ca^{2+} to NMDA-induced KLF4 mRNA and protein expression. Our results from quantitative RT-PCR showed that the cell-permeable Ca^{2+} chelator BAPTA-AM was able to partially inhibit the NMDA-induced KLF4 mRNA expression (25.6 ± 6.2 fold increase compared with 57.6 ± 8.2 fold increase with NMDA alone, $p < 0.05$; Fig. 2.1C), while the application of extracellular Ca^{2+} chelators EDTA and EGTA blocked the KLF4 induction even more strongly (2.2 ± 0.4 fold induction compared with 57.6 ± 8.2 fold induction with NMDA alone, $p < 0.001$; Fig. 2.1C). Application of BAPTA-AM, EDTA and EGTA in combination led to a complete blockade of the KLF4 mRNA elevation (1.08 ± 0.1 fold induction compared with 57.6 ± 8.2 fold induction with NMDA alone, $p < 0.001$; Fig. 2.1C). Consistent with our results from quantitative RT-PCR, Western blotting experiments also showed that application of BAPTA-AM, EDTA and EGTA completely abolished the enhancement of KLF4 protein expression by NMDA (102 ± 11 % of the untreated control, $p < 0.01$ compared with NMDA treatment alone; Fig. 2.2C and 2.2D). Thus our results suggest that Ca^{2+} influx and the associated increase in intracellular Ca^{2+} appears necessary for KLF4 induction by NMDA.

2.3.2 Induction of KLF4 protein by NMDA application in native brain slices

To determine whether the NMDA-induced enhancement of KLF4 protein level also occurred on native brain tissues, we performed Western blotting experiments on acute hippocampal slices. The slices were treated with NMDA (50 μM) for 30 minutes. NMDA was washed out following treatment and the slices were recovered for various time points: 0.5 h, 1 h, 2 h, and 3 h. Consistent with the data from cultured neurons, we observed a transient elevation of KLF4 protein level following washout. The elevation was clearly observed between 0.5 h to 2 h recovery, and the peak elevation occurred at about 1 h recovery (150 ± 12% of control, $n = 7$, $p < 0.01$; Fig. 2.3A and 2.3B). At 3 h after washout of NMDA, KLF4 protein levels decreased and returned to the baseline level (101 ± 16% of control, $n = 4$, $p > 0.95$; Fig. 2.3A and 2.3B). The time-dependency of the NMDA-induced KLF4 protein elevation is shown in Fig 3A, and the pooled data are shown in Fig. 2.3B. To confirm that the NMDA-induced effect is actually dependent on NMDA receptors, we also applied the NMDA receptor antagonist APV (50 μM) together with NMDA treatment, and found that it significantly inhibited the NMDA-induced KLF4 protein elevation (84 ± 14% of control with APV vs. 150 ± 12% of control with NMDA alone, $n = 4$, $p < 0.01$; Fig. 2.3C and 2.3D).

2.3.3 Induction of KLF4 by AMPA application

Excessive glutamate release, which occurs during brain ischemia, causes calcium influx via NMDA receptors and calcium-permeable AMPA/kainate receptors, which induces subsequent cell death signaling pathways (Platenik et al., 2000; Sattler and Tymianski, 2001).We have studied the time-dependency of NMDA-induced KLF4

expression in cultured neurons and in native tissues (Fig. 2.1-2.3). Our results suggest that *KLF4* is a gene that can be upregulated by activation of NMDA receptors and such upregulation is dependent on calcium (Fig. 2.1 and 2.2). To further explore the regulation of KLF4 in glutamate excitotoxicity, we investigated whether activation of AMPA/kainate receptors and subsequent calcium fluxes also induced KLF4 mRNA expression. We found that application of AMPA (50 μM) was able to induce KLF4 mRNA expression in a time-dependent manner. The induction time course was similar to that after NMDA stimulation: it was significant at 45 min, reached a peak at 1.5 h and lasted until 3 h (Fig. 2.4A). We also found that BAPTA-AM (Table 2.1) partially inhibited the AMPA-induced KLF4 expression (15.4 ± 1.1 fold induction with BAPTA-AM vs. 102.3 ± 8.0 fold induction with AMPA alone, $p < 0.001$; Fig. 2.4B). Application of EDTA and EGTA, or the combination of EDTA, EGTA and BAPTA-AM, completely blocked the KLF4 induction (1.9 ± 0.3 fold induction with EDTA and EGTA vs. 102.3 ± 8.0 fold induction with AMPA alone, $p < 0.001$; 1.0 ± 0.2 fold induction with EDTA, EGTA and BAPTA-AM vs. 102.3 ± 8.0 fold induction with AMPA alone, $p < 0.001$; Fig. 2.4B). Our results suggest that an increase in intracellular Ca^{2+} concentration is involved in the KLF4 induction caused by AMPA.

Since depolarization caused by AMPA may also induce activation of NMDA receptors or L-type VSCCs (Platenik et al., 2000; Sattler and Tymianski, 2001), we further asked whether AMPA/kainate receptors alone, or in combination with NMDA receptors and/or L-type VSCCs, contributed to the KLF4 mRNA upregulation caused by AMPA treatment. We found that CNQX exerted a dose-dependent blockade of the AMPA-induced KLF4 expression, with full blockade achieved using 200 μM CNQX (1.2

± 0.2 fold induction with 200 μM CNQX vs. 102.3 ± 8.0 fold induction with AMPA alone, $p < 0.001$; Fig. 2.4B). We also found that MK801 had no effect on the KLF4 induction ($p > 0.3$ compared with AMPA alone), but that nifedipine partially inhibited the KLF4 induction (22.0 ± 2.5 fold induction with nifedipine vs. 102.3 ± 8.0 fold induction with AMPA alone, $p < 0.001$; Fig. 2.4B). In conclusion, our results demonstrate that with AMPA treatment, the KLF4 induction is mediated by L-type VSCCs or AMPA/kainate receptors, but not NMDA receptors.

2.3.4 Ectopic KLF4 sensitizes NMDA-mediated caspase-3 activation in neurons

To further investigate the role of KLF4 induction in excitotoxicity, we overexpressed KLF4 in cultured cortical neurons by infecting them with a non-replicating lentiviral vector encoding either GFP (control) or mouse KLF4 under the control of the human ubiquitin promoter. We later treated the infected neurons with a subtoxic dose of NMDA (10 μM) for 1.5 h and assessed activation of caspase-3 20 h after treatment. We used caspase-3 activation, particularly the measurement of the 19 KDa cleaved fragment of caspase-3 by Western blots (Fig. 2.5A), as our criterion for identifying apoptosis (Lipton, 1999). At 20 h recovery after treatment with this normally subtoxic dose of NMDA (10 μM), endogenous KLF4 protein levels were still identifiable by Western blots in KLF4 expressing cultures but not in control cultures infected with the GFP expressing vector (Fig. 2.5A). With this subtoxic dose of NMDA, caspase-3 cleavage was not upregulated by NMDA in control cultures (lane 3 and lane 1, Fig. 2.5A). In contrast, in cultures infected with the KLF4 expressing vector, the cleaved fragment of caspase-3 was clearly upregulated at 20 h recovery after NMDA treatment (lane 4, Fig. 2.5A). Interestingly,

when neurons were not treated with NMDA, the infection with the KLF4 vector had no effect on the basal level of cleaved caspase-3 (lane 2 and lane 1, Fig. 2.5A), indicating that the activation of caspase-3 we observed in lane 4 (Fig. 2.5A) was not simply due to KLF4 overexpression itself. Our results thus suggest that in neurons treated with 10 μM NMDA, overexpression of KLF4 can sensitize cells to NMDA-induced caspase-3 activation.

2.3.5 KLF4 upregulates cyclin D1 and downregulates p21$^{Waf1/Cip1}$

Previous work in proliferative cell lines has shown that KLF4 regulates progression of the cell cycle, leading to context-dependent cell cycle arrest or oncogenesis (Rowland and Peeper, 2006). In addition, it is now well-established that apoptotic neurons can reenter the cell cycle and remain at the G_1 checkpoint, a process that is determined by the levels of cyclin D1 and cyclin D1-Cdk4/6 complex activity (Liu and Greene, 2001; Park et al., 1997b). Thus we first explored whether KLF4 had an effect on neuronal cell cycle proteins. We infected cultured cortical neurons with lentiviral vectors expressing either GFP or KLF4. Overexpression of KLF4 significantly upregulated protein levels of cyclin D1 (Fig. 2.6A and 2.6B). To further confirm and visualize this result, we transiently transfected neurons with plasmids encoding GFP, either alone (control) or together with a plasmid encoding KLF4 under the same promoter. Immunostaining for cyclin D1 was performed on the transfected cultures, and revealed a subpopulation of double positive cells (GFP^+ and cyclin $D1^+$). The percentage of double positive cells within the total population of GFP^+ cells was significantly higher in KLF4 and GFP cotransfected cultures than in controls (Fig. 2.6D). Thus our data confirm that KLF4 expression induces cyclin D1 protein expression. Further RT-PCR analysis demonstrated that mRNA levels

of cyclin D1 were 2.3-fold higher in cultures expressing KLF4 than those expressing GFP. Our data thus suggest that KLF4 overexpression transcriptionally upregulates cyclin D1 in neurons. In addition to the cyclin D1 levels, the cyclin D1-Cdk4/6 complex activity could be affected by the Cdk inhibitor $p21^{Waf1/Cip1}$, which binds to and inhibits the complex (Ekholm and Reed, 2000; Harper et al., 1993). Thus we assessed the protein and mRNA expression of $p21^{Waf1/Cip1}$ in neuron cultures infected with vectors expressing KLF4 or GFP. We found that KLF4 overexpression decreased the $p21^{Waf1/Cip1}$ protein levels (Fig. 2.6A and 2.6B), but did not change the $p21^{Waf1/Cip1}$ mRNA levels (Fig. 2.6C). These results indicate that KLF4 downregulates $p21^{Waf1/Cip1}$ at the post-transcriptional level. The combined cyclin D1 upregulation and $p21^{Waf1/Cip1}$ downregulation, both induced by KLF4, suggest that KLF4 overexpression might be involved in the regulation of cell cycle proteins.

2.3.6 The upregulation of cyclin D1 by NMDA and that by KLF4 are additive

It has been shown previously that cyclin D1 contributes to neuronal apoptosis induced by various insults including ischemia (Osuga et al., 2000; Park et al., 1997a; Park et al., 1997b; Park et al., 1998; Rashidian et al., 2005). Therefore, we tried to determine whether cyclin D1 might be involved in the KLF4-induced sensitization to caspase-3 activation in cultures treated with subtoxic NMDA stimulation. Specifically we asked whether KLF4 overexpression and NMDA application synergistically, additively, or occlusively, upregulated cyclin D1. We first used Western blots to examine whether cyclin D1 was induced after the subtoxic NMDA treatment. Five days after infection with lentiviral vectors expressing GFP (control) or KLF4, neurons were exposed to 10 μM

NMDA for 1.5 h and were allowed to recover for 4 or 20 h. In control cultures expressing GFP, cyclin D1 protein levels were enhanced after a 4 h recovery from NMDA treatment (1.5 ± 0.2 fold compared to untreated cultures), but declined to untreated levels when the recovery time was prolonged to 20 h (Fig. 2.7). The cyclin D1 expression pattern in non-infected cultures was the same as that of cultures expressing GFP (data not shown). In addition, KLF4 overexpression alone induced a 2.1 ± 0.4 fold increase in cyclin D1 protein expression compared to GFP-expressing untreated cultures (Fig. 2.7). After 4 h recovery from NMDA treatment in the cultures expressing KLF4, cyclin D1 protein was increased by 3.0 ± 0.6 fold compared to that in the GFP-expressing untreated cultures (Fig. 2.7). The induction of cyclin D1 in cultures expressing KLF4 was also transient because it decreased to basal levels at 20 h recovery (Fig. 2.7). Furthermore, the effect of combined applications of NMDA treatment and KLF4 vector infection on cyclin D1 protein levels was larger than that observed when NMDA was applied to control cultures ($p < 0.05$), suggesting an additive effect of KLF4 and NMDA on inducing cyclin D1 expression.

2.4 Conclusion

The identification of KLF4 as a gene that is rapidly and massively upregulated during retinal ischemia prompted us to study the functions of KLF4 during glutamatergic excitotoxicity. Our results demonstrate that the application of NMDA or AMPA is sufficient to induce dramatic increases in KLF4 mRNA, a process mediated by intracellular and extracellular calcium. KLF4 protein levels are also transiently increased by NMDA treatment, in both neuron cultures and brain slices. After increasing endogenous KLF4 expression using a lentiviral vector, we found that caspase-3 is

activated by a normally subtoxic dose of NMDA, suggesting that KLF4 can sensitize cells to NMDA-induced caspase-3 activity. KLF4 overexpression transcriptionally activates cyclin D1 expression, while NMDA treatment also transiently upregulates cyclin D1 protein levels. The effects of overexpressed KLF4 and those of NMDA on cyclin D1 induction are additive rather than occlusive. Our results suggest that KLF4 overexpression can modulate the activity of cell cycle proteins (Cyclin D1 and $p21^{Waf1/Cip1}$) and NMDA-induced caspase-3 activation, and can thus increase the probability of apoptotic cell death.

2.5 Discussion

2.5.1 NMDA- or AMPA- elicit calcium signals that induce KLF4

KLF4 is a critical protein in several forms of cancers (Ghaleb et al., 2005; Rowland and Peeper, 2006), but the role of KLF4 in the CNS has been little studied. Our work for the first time directly demonstrates that NMDA- or AMPA- treated cortical neurons endogenously express *KLF4* (Fig. 2.1). Both mRNA and protein levels of KLF4 are upregulated by NMDA in cultured neurons and in native brain slices (Fig. 2.2 and 2.3). This is the first demonstration of transient expression of KLF4 protein in cultured neurons and in native tissues from the CNS. These results are consistent with recent genomic profiling indicating that *KLF4* is upregulated after activation of either synaptic or extra-synaptic NMDA receptors (Zhang et al., 2007a). We further extend these observations by showing that AMPA also induces *KLF4* expression via its effects on AMPA/kainate receptors (Fig. 2.4A). In addition, our data suggest that KLF4 might be a member of the neuronal immediate early gene cohort, because of the following three

similarities between KLF4 and other IEGs. First, the induction time-course curve of KLF4 in response to NMDA or AMPA is similar to that of several other immediate early genes, for example, c-*fos* and c-*jun* (Condorelli et al., 1994). Another similarity between KLF4 and IEG is that both of them can be activated by NMDA even in the presence of Mg^{2+} (Condorelli et al., 1994), considering that we performed NMDA treatment in Neurobasal medium with Mg^{2+}. Third, we report here that KLF4 expression induced by NMDA or AMPA treatment is completely blocked by inhibition of calcium influx using EDTA/EGTA and BAPTA-AM (Table 2.1, Fig. 2.1C, 2.2C, 2.2D and 2.4B). Activation of other IEGs by glutamate also requires an increase in intracellular calcium (Platenik et al., 2000). These findings suggest the inclusion of KLF4 in the IEG cohort.

It has been shown previously that the calcium influx caused by NMDA directly involves exclusively NMDA receptors (Platenik et al., 2000). Our data confirm this conclusion first by showing that NMDA-induced KLF4 mRNA expression is dependent on calcium influx, and is completely blocked by MK801, but not by CNQX or nifedipine (Table 2.1 and Fig. 2.1C). Thus we conclude that during NMDA treatment calcium flows into the cell directly through NMDA receptors, instead of AMPA/kainate receptors and/or L-type VSCCs that might be activated, and then activates KLF4 mRNA expression. Consistent with data on KLF4 mRNA, we find that NMDA-induced enhancement of KLF4 protein expression is dependent on activation of NMDA receptors, but not AMPA/kainate receptors (Fig. 2.2C and 2.2D).

Activation of AMPA/kainate receptors causes depolarization, which then opens NMDA receptors and L-type VSCCs. Our results show that AMPA-induced KLF4 expression could be completely blocked with CNQX but not with MK801 (Table 2.1 and

Fig. 2.4B), indicating that the KLF4 reaction to AMPA is not via NMDA receptors. Considering that KLF4 activation is dependent on calcium influx, our results are consistent with previous findings indicating that AMPA-induced calcium signals are mediated by AMPA/ kainate receptors but not NMDA receptors (Poulsen et al., 2004). Interestingly, we found that L-type VSCCs also contributed to KLF4 expression induced by AMPA but not NMDA application (Fig. 2.1C and 2.4B). This is consistent with previous findings indicating that L-type VSCCs were involved in several AMPA- but not NMDA- induced cellular responses, including neurotoxicity (Weiss et al., 1990) and increase of c-*fos* mRNA (Lerea et al., 1992; Platenik et al., 2000). Taking these data together, we conclude that AMPA treatment activates AMPA/kainate receptors, which depolarizes the membrane and opens L-type VSCCs, allowing for calcium influx leading to KLF4 mRNA expression. Other channels that contribute to the calcium influx during AMPA application might involve calcium permeable AMPA receptors (Kwak and Weiss, 2006).

2.5.2 KLF4 and neuronal cell cycle

KLF4 exerts opposing effects on cell proliferation depending on the tissue type studied (Geiman et al., 2000; Rowland et al., 2005). Our findings indicate that overexpression of KLF4 in cultured neurons upregulates the cell cycle protein Cyclin D1 and downregulates $p21^{Waf1/Cip1}$, the inhibitory binding partner of the cyclin D1-Cdk4 complex (Fig. 2.6). Since induction of cyclin D1 protein is among the earliest events observed when quiescent cells reenter cell cycle (Sherr and Roberts, 1999), our results suggest that KLF4 might play a role in the regulation of neuronal cell cycle reentry. The potential role of KLF4 in regulating neuronal cell cycle is also supported by recent

studies showing that KLF4 in conjunction with three other transcription factors were able to switch mouse and human fibroblasts to pluripotent stem cells (Takahashi et al., 2007; Wernig et al., 2007), which could be further differentiated into neuronal cells both *in vitro* and *in vivo* (Wernig et al., 2008). We found that both mRNA and protein levels of cyclinD1 were elevated after induction of KLF4 (Fig. 2.6), suggesting that cyclin D1 can be transcriptionally activated by KLF4. This is consistent with a previous report showing that KLF4 interacts with the cyclin D1 promoter (Shie et al., 2000). Also supporting this conclusion is the finding that KLF4 promoted cell proliferation via regulation of cyclin D1 in Rasv12-transformed cells (Rowland et al., 2005). In addition, the cdk inhibitor $p21^{Waf1/Cip1}$ binds to and inhibits cyclin D1-CDK4, and thus causes cell arrest (Harms et al., 2007; Rowland and Peeper, 2006; Sherr and Roberts, 1999). We observed that the $p21^{Waf1/Cip1}$ protein was reduced by KLF4 (Fig. 2.6), suggesting that the inhibition of $p21^{Waf1/Cip1}$ on the neuronal cell cycle progression could be attenuated. The $p21^{Waf1/Cip1}$ mRNA was unchanged after KLF4 overexpression (Fig. 2.6). Thus the downregulation of $p21^{Waf1/Cip1}$ protein by KLF4 could be modulated either via the KLF4 suppression of the $p21^{Waf1/Cip1}$ translation machinery, or KLF4 activation of $p21^{Waf1/Cip1}$ degradation. In sum, the KLF4-induced enhancement of cyclin D1 and reduction of $p21^{Waf1/Cip1}$ protein levels suggest that ectopic KLF4 might be involved in some early events during neuronal cell cycle reentry.

Our results indicate that during the recovery from NMDA treatment, the transient induction time courses of KLF4 and of cyclin D1 protein levels are at least partially overlapped. The NMDA-induced KLF4 protein expression lasts from 2 to 4 h recovery in cultured neurons and has an even shorter duration (1 h) in native brain tissues (Fig. 2.2

and Fig. 2.3). These data are consistent with the previous reports showing that KLF4 has a PEST domain (regulatory domain of protein's half life) and a short half-life of about 2 h (Chen et al., 2005). NMDA treatment also transiently upregulates cyclin D1 protein levels with the peak induction at 4 h recovery (Fig.7), when NMDA-induced KLF4 protein levels also reach their maxima (Fig.2). This finding is supported by previous reports showing that cyclin D1 levels were increased in critical brain regions after global and focal ischemia (Osuga et al., 2000; Park et al., 2000; Timsit et al., 1999), under which circumstances, NMDA receptors were activated by released glutamate (Lipton, 1999). Based on the partially-overlapped time course of the KLF4 and cyclin D1 induction by NMDA treatment, in combination with our finding showing that overexpression of KLF4 upregulates cyclin D1, it is plausible to suggest that KLF4 might be involved in NMDA-induced cyclin D1 expression. We also found that the induction of cyclin D1 by NMDA stimulation and by KLF4 overexpression were additive (Fig. 2.7), suggesting that other pathways in addition to KLF4 might also be involved in the NMDA-induced cyclin D1 expression. For example, the PI3K-PKB/Akt pathway, which can be activated by NMDA in cultured neurons (Soriano et al., 2006), has also been shown to induce cyclin D1 expression (Treinies et al., 1999). Therefore, it is possible that the PI3K-Akt, or another pathway, and KLF4 could additively mediate the positive effect of NMDA on cyclin D1 activation.

2.5.3 KLF4 and activation of caspase-3

In our report, we show that KLF4 overexpression convert the nonlethal effect of 10 μM NMDA into higher levels of active caspase-3, while in untreated cultures KLF4 overexpression has no effect on caspase-3 activity (Fig. 2.5). Our results suggest that

KLF4 and NMDA can have a synergistic effect on the activation of caspase-3. Since caspase-3 activity is required for NMDA-induced apoptosis in neuronal cultures (Budd et al., 2000; Okamoto et al., 2002), the synergistic effect of KLF4 and NMDA on caspase-3 activation suggests a pro-apoptotic role of KLF4 during NMDA stimulation. Given the importance of the NMDA excitotoxicity during brain ischemia, the role of KLF4 in caspase-3 activation might be critical to ischemic cell death. Consistent with our results, previous reports have shown that overexpressing KLF4 in esophageal cancer cells increases the apoptotic cell death after treatment with hydrogen peroxide or after cell detachment from extracellular matrix (Yang et al., 2005). An explanation of the role of KLF4 in caspase-3 activation could be the effect of KLF4 on $p21^{Waf1/Cip1}$. Soriano et al. (Soriano et al., 2006) have showed that a subtoxic dose of NMDA (10 μM) had no effect on caspase-3 activation, and such treatment could also activate the PI3K-Akt pathway. Activated Akt has been shown to phosphorylate $p21^{Waf1/Cip1}$ and maintain $p21^{Waf1/Cip1}$ in the cytoplasm in neuronal cultures (Harms et al., 2007). Cytoplasmic $p21^{Waf1/Cip1}$ could exert an anti-apoptotic effect through the inactivation of several pro-apoptotic proteins such as JNK and pro-caspase-3 (Asada et al., 1999; Shim et al., 1996; Suzuki et al., 1998). Since overexpression of KLF4 decreases $p21^{Waf1/Cip1}$ protein levels (Fig. 2.6), it might suppress the NMDA-induced inhibitory effect of cytoplasmic $p21^{Waf1/Cip1}$ on caspase-3 activation.

In summary, we demonstrate that the application of NMDA is sufficient to induce dramatic increases in KLF4 mRNA and protein levels in cultured neurons. NMDA application also increases KLF4 protein levels in brain slice preparations. The KLF4 protein induction is also observed in native brain slices. The overexpression of KLF4 can

modulate the activity of Cyclin D1 and $p21^{Waf1/Cip1}$, and can sensitize neuron to NMDA-induced caspase-3 activation. These data suggest that KLF4 might play an important role in regulating neuronal cell cycle reentry and apoptotic neuronal death during NMDA excitotoxicity.

Table 2. 1 A list of pharmacological compounds and their purposes used in chapter two.

Compound abbreviations	Compound full names	Properties
BAPTA-AM	1,2-bis-(o-aminophenoxy)-ethane-N,N,N',N'-tetra-acetic acid tetra-acetoxy-methyl ester	Cell-permeable Ca^{2+} chelator
CNQX	1,2,3,4-tetrahydro-7-nitro-2,3-dioxoquinoxaline-6-carbonitrile disodium	AMPA/kainate receptor antagonist
EDTA	Ethylenediaminetetraacetic acid	Extracellular Ca^{2+} chelators
EGTA	Ethylene glycol-bis(2-aminoethylether)-*N*,*N*,*N′*,*N′*-tetraacetic acid	Extracellular Ca^{2+} chelators
MK801	(5R,10S)-(+)-5-Methyl-10,11-dihydro-5H-dibenzo[a,d]cyclohepten-5,10-imine hydrogen maleate	NMDA receptor antagonist
APV	DL-2-Amino-5-phosphonopentanoic acid	NMDA receptor antagonist
Nifedipine	Nifedipine	L-type VSCCs blocker

This table explains the properties of the pharmacological compounds we used in Fig. 2.1 – 2.4.

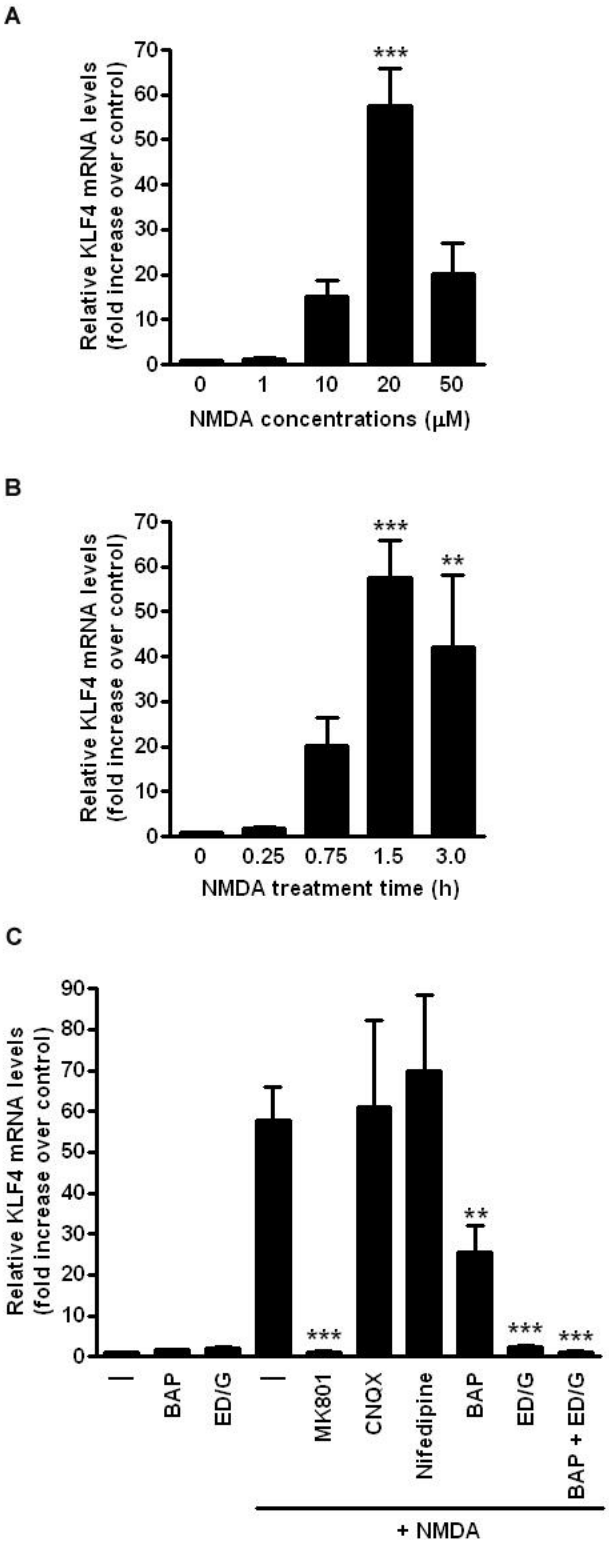
A
Relative KLF4 mRNA levels (fold increase over control)
70
60
50
40
30
20
10
0
***
0
1
10
20
50
NMDA concentrations (μM)
B
Relative KLF4 mRNA levels (fold increase over control)
70
60
50
40
30
20
10
0
***
**
0
0.25
0.75
1.5
3.0
NMDA treatment time (h)
C
Relative KLF4 mRNA levels (fold increase over control)
90
80
70
60
50
40
30
20
10
0
**
***
***
***
—
BAP
ED/G
—
MK801
CNQX
Nifedipine
BAP
ED/G
BAP + ED/G
+ NMDA

Fig. 2.1 Quantitative real-time PCR results illustrating NMDA-induced KLF4 mRNA expression.

A, Endogenous KLF4 mRNA levels were shown after neurons were incubated for 1.5 h with NMDA at doses ranging from 0 (control) to 50 μM. The mRNA levels of the control group were set to 1.0 in all panels of Fig. 2.1. B, KLF4 mRNA levels were shown after neurons were treated with 20 μM NMDA for durations ranging from 0 (control) to 3 h. C, The effects of the following reagents on NMDA-induced KLF4 mRNA expression were determined: 20 μM MK801, 50 μM CNQX, 10 μM nifedipine, 20 μM BAPTA-AM (BAP), 5 mM EDTA + 5 mM EGTA (ED/G), 20 μM BAPTA-AM + 5 mM EDTA + 5 mM EGTA (BAP + ED/G). The properties of these reagents are listed in table 2.1. In panels A and B, ** indicates $p < 0.01$ and *** indicates $p < 0.001$ compared to the untreated control groups. In panel C, ** indicates $p < 0.01$ and *** indicates $p < 0.001$ compared to NMDA-treated cells. All values are averages of results from at least three separate experiments.

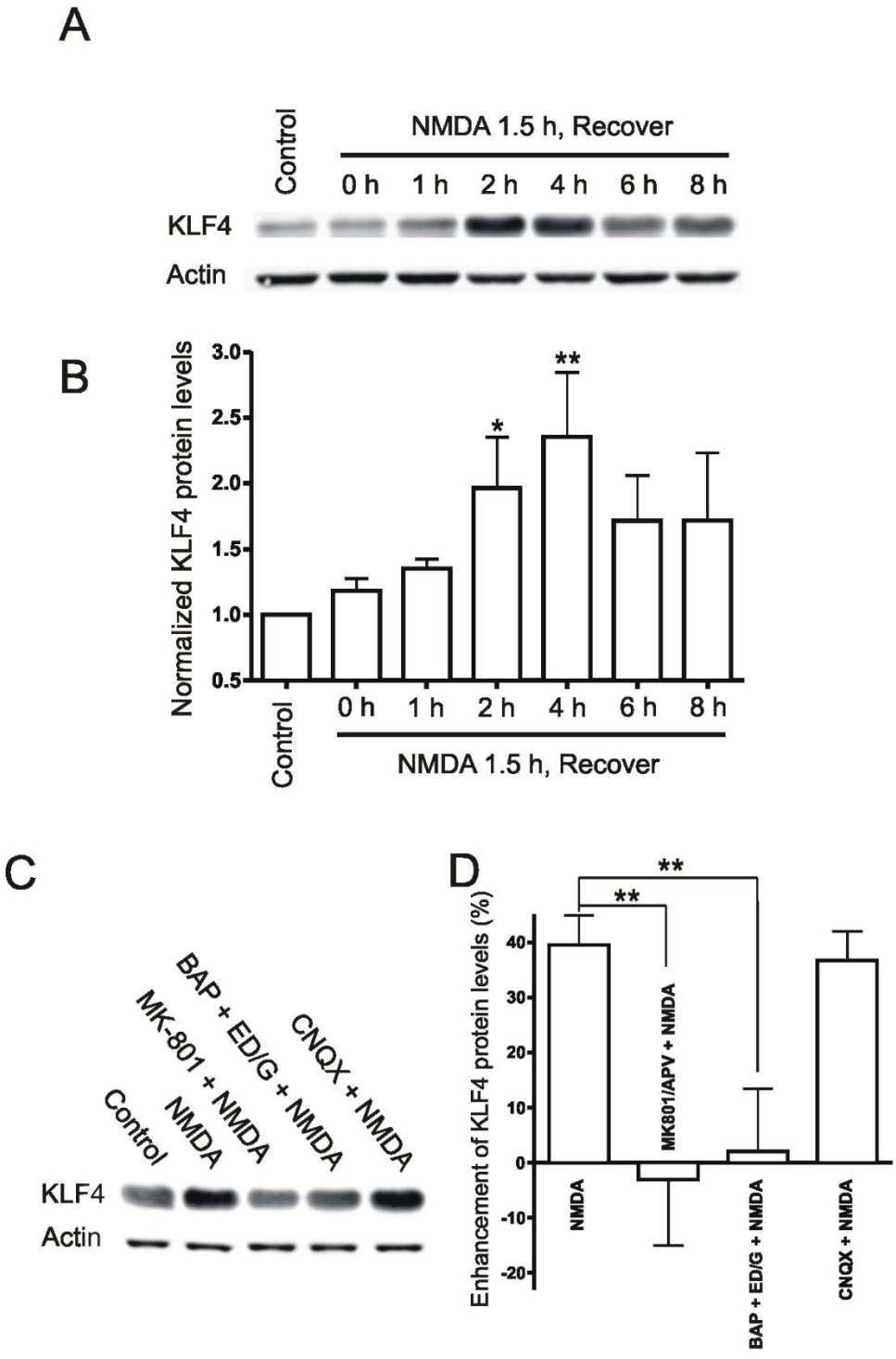
A
Control
NMDA 1.5 h, Recover
0 h
1 h
2 h
4 h
6 h
8 h
KLF4
Actin
B
Normalized KLF4 protein levels
3.0
2.5
2.0
1.5
1.0
0.5
*
**
Control
0 h
1 h
2 h
4 h
6 h
8 h
NMDA 1.5 h, Recover
C
Control
NMDA
MK-801 + NMDA
BAP + EDIG + NMDA
CNQX + NMDA
KLF4
Actin
D
Enhancement of KLF4 protein levels (%)
40
30
20
10
0
-10
-20
**
**
NMDA
MK801/APV + NMDA
BAP + ED/G + NMDA
CNQX + NMDA

Fig. 2.2 Western blot assessment of NMDA-induced KLF4 protein elevation in cultured neurons.

A and **B**, Cultured neurons were incubated with 20 μM NMDA for 1.5 h and then were allowed to recover in the culture medium for 0, 1, 2, 4, 6 and 8 h. Immunoblots of KLF4 and actin were shown in panel A. In panel B, densitometric measurements of KLF4 immunoblots were normalized to the actin expression, and the protein levels of the untreated controls were set to 1.0. * indicates $p < 0.05$ and ** indicates $p < 0.01$ compared to the control. **C**, The effects of the following reagents on NMDA-induced KLF4 protein expression were determined: 20 μM MK801 or 50 μM APV (MK801/APV), 20 μM BAPTA-AM + 5 mM EDTA + 5 mM EGTA (BAP + ED/G), and 50 μM CNQX. **D**, Densitometric measurements of the immunoblots in panel C. ** indicates $p < 0.01$ compared to NMDA-treated groups. All values are averages of results from at least three separate experiments.

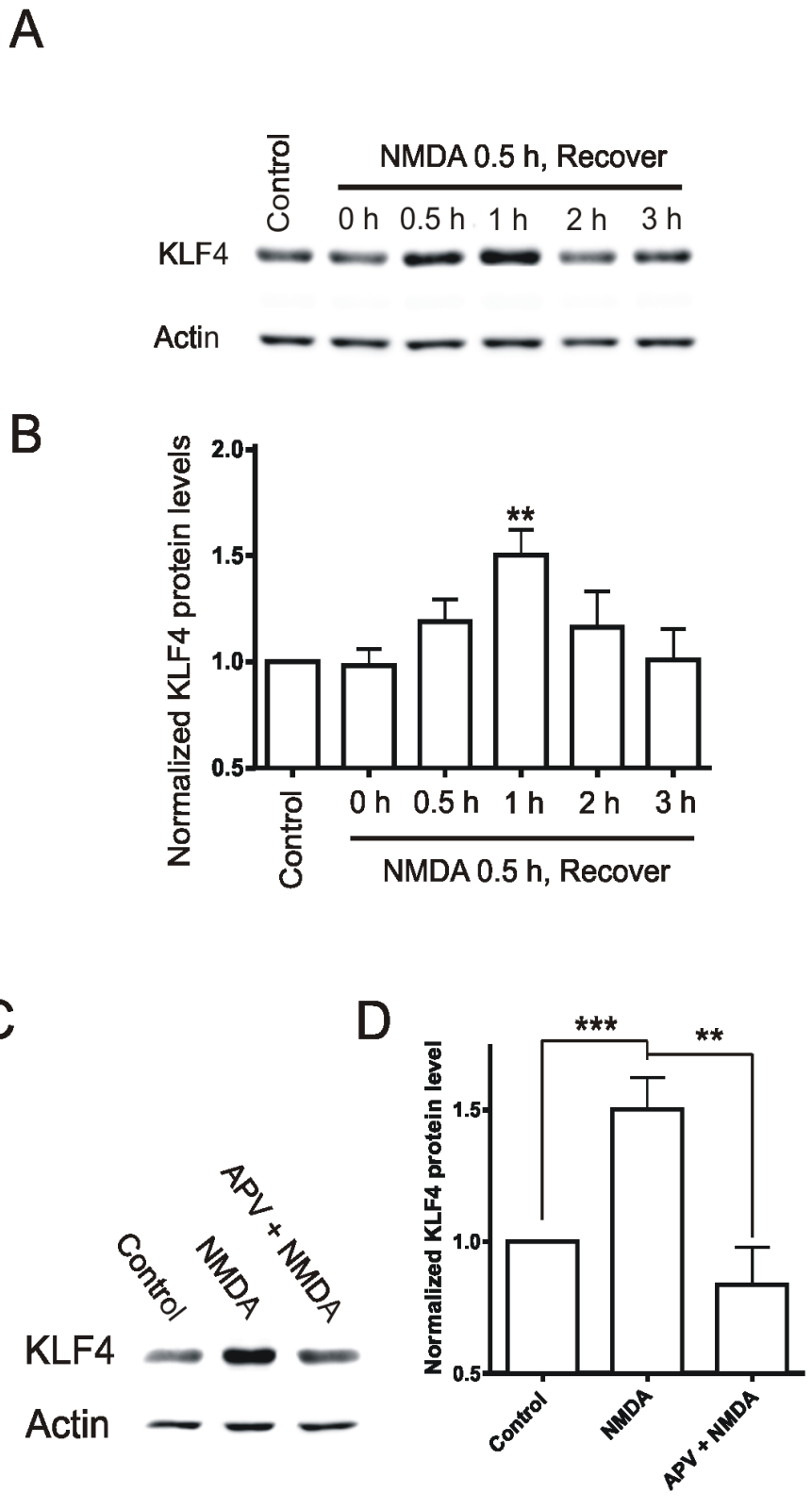
A
Control
NMDA 0.5 h, Recover
0 h
0.5 h
1 h
2 h
3 h
KLF4
Actin
B
Normalized KLF4 protein levels
2.0
1.5
1.0
0.5
**
Control
0 h
0.5 h
1 h
2 h
3 h
NMDA 0.5 h, Recover
C
Control
NMDA
APV + NMDA
KLF4
Actin
D
Normalized KLF4 protein level
1.5
1.0
0.5
***
**
Control
NMDA
APV + NMDA

Fig. 2.3 Western blot assessment of NMDA-induced KLF4 protein expression in hippocampal slices.

A and **B**, The slices were treated with NMDA (50 μM) for 30 minutes. NMDA was then washed out and the slices were incubated in fresh ACSF for different time points: 0.5 h, 1 h, 2 h, and 3 h. The enhancement of KLF4 protein levels reached maximal levels at 1 h recovery. The immunoblots of the NMDA-induced KLF4 protein elevation are shown in panel A, and the pooled data are shown in panel B. ** indicates $p < 0.01$ compared to untreated control. **C** and **D**, The effect of APV (50 μM) on NMDA-induced KLF4 protein expression were determined. Immunoblots are shown in panel A, and the pooled data are shown in panel B. ** indicates $p < 0.01$ and *** indicates $p < 0.001$. All values are averages of results from at least three separate experiments.

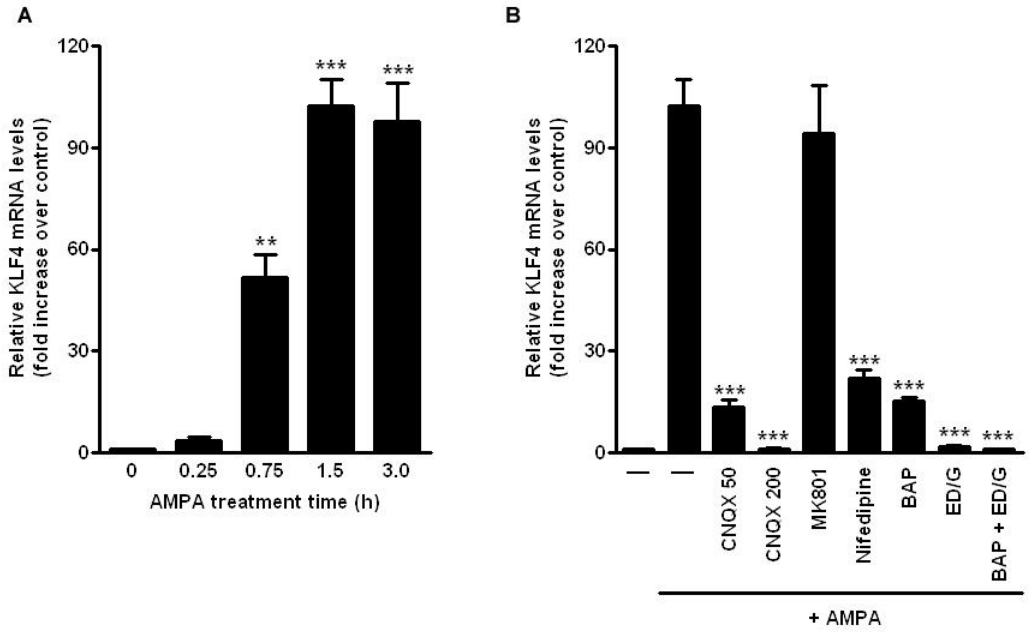

Fig. 2.4 Quantitative real-time PCR results illustrating AMPA-induced KLF4 mRNA expression.

Values were shown relative to those of the control groups that were set to 1.0. **A**, Relative endogenous KLF4 mRNA levels were shown after neurons were incubated with 50 μM AMPA for durations ranging from 0 (control) to 3 h. * indicates $p < 0.05$ and *** indicates $p < 0.001$ compared to control group. **B**, Cultures were preincubated for 30 min in medium containing the following reagents (Table 2.1): 50 μM or 200 μM CNQX (CNQX 50 or CNQX 200), 20 μM MK801, 10 μM nifedipine, 20 μM BAPTA-AM (BAP), 5 mM EDTA + 5 mM EGTA (ED/G), 20 μM BAPTA-AM + 5 mM EDTA + 5 mM EGTA (BAP + ED/G). AMPA (50 μM) was then added into the medium for 1.5 h before mRNA assessment. *** indicates $p < 0.001$ compared to (-) AMPA treated cells. All values are averages of results from at least three separate experiments.

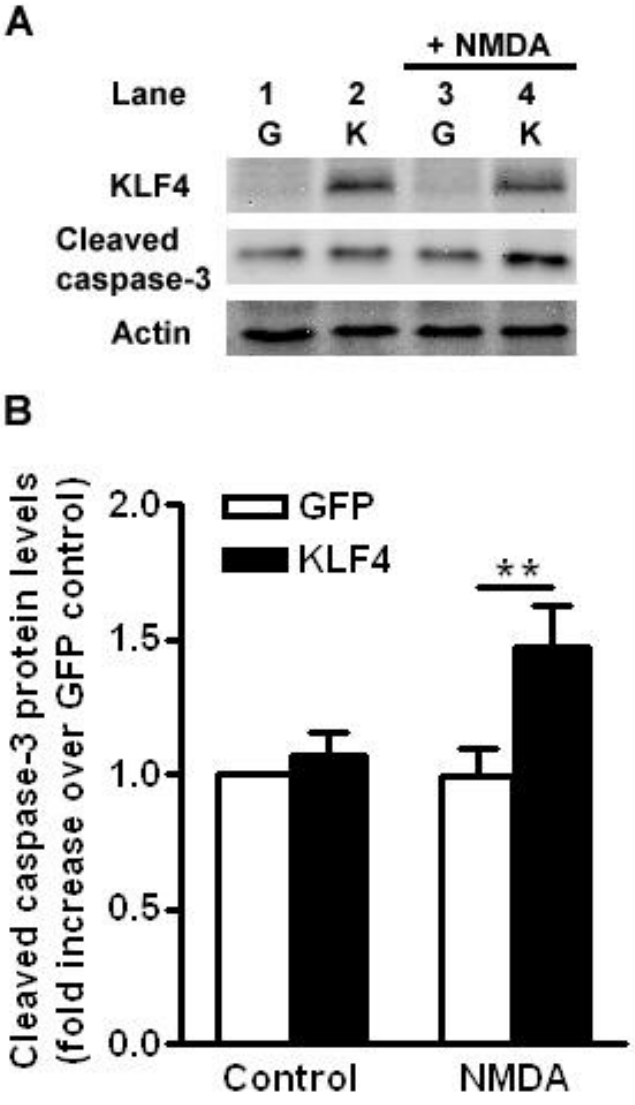
A
+ NMDA
Lane
1
2
3
4
G
K
G
K
KLF4
Cleaved caspase-3
Actin
B
Cleaved caspase-3 protein levels (fold increase over GFP control)
2.0
1.5
1.0
0.5
0.0
GFP
KLF4
**
Control
NMDA

Fig. 2.5 Western blot assessment of caspase-3 activation after KLF4 overexpression in NMDA-treated cultures.

Neurons were infected either with the lentiviral vectors expressing GFP (G, GFP) or KLF4 (K, KLF4). Five days after infection, neurons were treated with 10 μM NMDA for 1.5 h and then allowed to recover in the culture medium for 20 h. **A**, Cell lysates were immunoblotted for KLF4, cleaved caspase-3 and actin. The 19 KDa cleaved fragment of caspase-3 represented the active caspase-3. The top panel showed the marked expression of KLF4 protein following infection with lentiviral vector expressing KLF4. **B**, Densitometric measurements of the immunoblots in panel A. When normalized to actin expression, cleaved caspase-3 protein levels increased by about 50% following 10 μM NMDA treatment in KLF4 overexpressing cultures but not in GFP-expressing cultures. Control groups were analyzed when no NMDA was added. ** indicates $p < 0.01$ compared to GFP-expressing groups with NMDA treatment. All values are averages of results from at least three separate experiments.

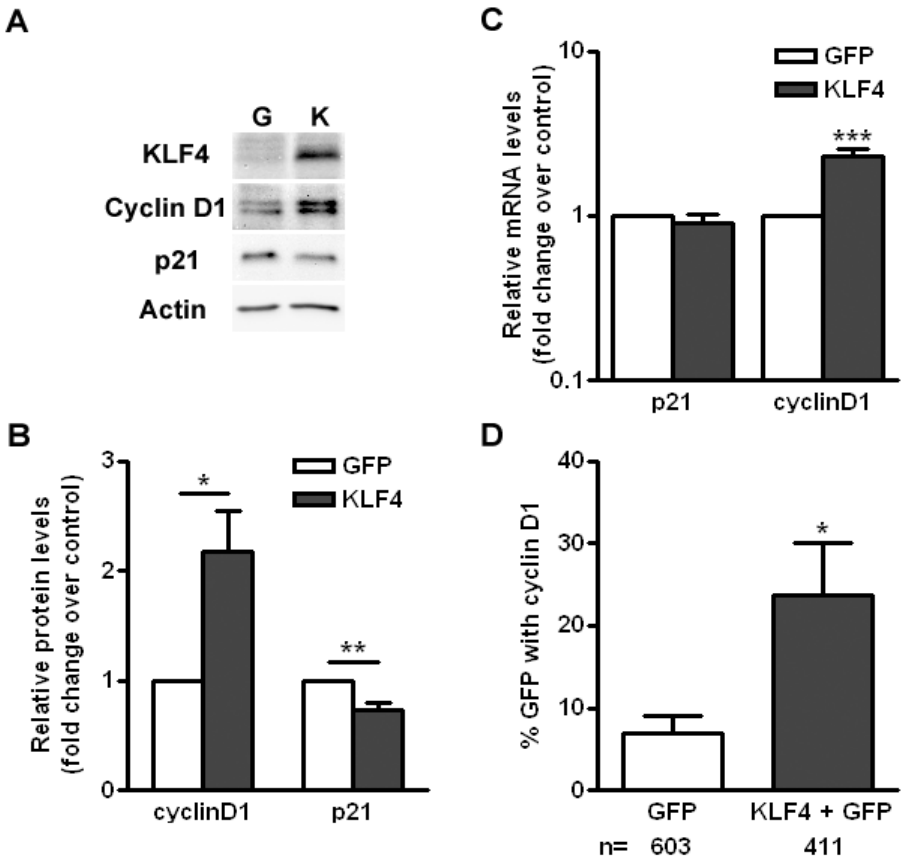
A
G
K
KLF4
Cyclin D1
p21
Actin
B
Relative protein levels
(fold change over control)
GFP
KLF4
*
**
cyclinD1
p21
C
Relative mRNA levels
(fold change over control)
GFP
KLF4
***
p21
cyclinD1
D
% GFP with cyclin D1
*
GFP
KLF4 + GFP
n= 603
411

Fig. 2.6 KLF4 upregulated cyclin D1 and downregulates p21$^{Waf1/Cip1}$.

From A to C, neuron cultures were infected with lentiviral vectors expressing either GFP (G, GFP, control) or KLF4 (K, KLF4) on DIV 6, and the protein and mRNA expression of p21$^{Waf1/Cip1}$ and cyclin D1 were analyzed on DIV 11. **A**, Western blot analysis of protein levels of KLF4, cyclin D1 and p21$^{Waf1/Cip1}$. The results showed that infection with the KLF4-expressing vector increased cyclin D1 levels and resulted in a decline in p21$^{Waf1/Cip1}$ levels. **B**, Densitometric measurement of the immunoblots in panel A. * indicates $p < 0.05$ and ** indicates $p < 0.01$ compared to control groups (GFP). **C**, Quantitative real-time PCR analysis of p21$^{Waf1/Cip1}$ and cyclin D1 mRNA levels. *** indicates $p < 0.001$ compared to control GFP group. **D**, Statistical results of cyclin D1 immunostaining in neuron cultures 48 h after transfection with plasmids expressing GFP, either alone (control, GFP), or with KLF4 (KLF4 + GFP). The percentage of cyclin D1 positive cells within the transfected GFP positive cells was shown in panel D. While only about 7% of GFP$^+$ cells were cyclin D1 immunoreactive in control, the percentage rose to about 24% for KLF4-expressing cells. * indicates $p < 0.05$ compared with control GFP groups. Two-tailed Student's *t* tests were conducted between treatment and control. All values were averages of results from at least three separate experiments.

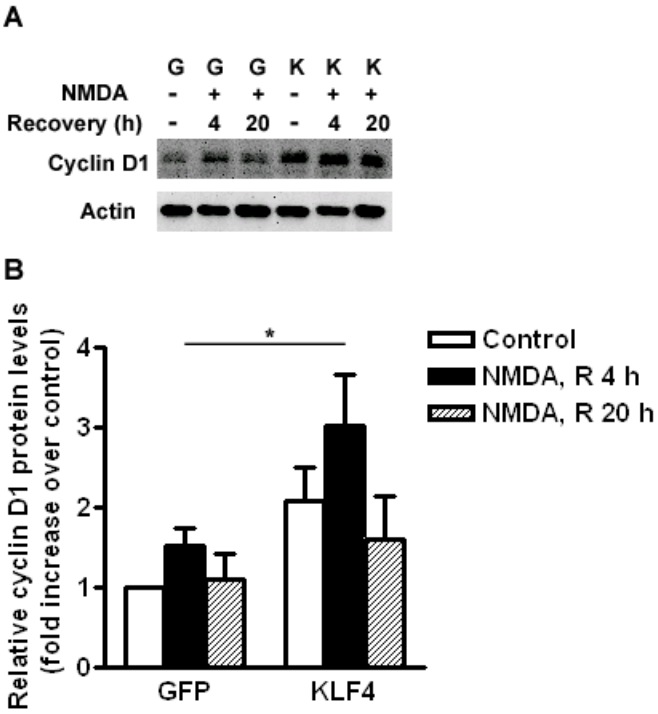
A
G G G K K K
NMDA - + + - + +
Recovery (h) - 4 20 - 4 20
Cyclin D1
Actin
B
Relative cyclin D1 protein levels (fold increase over control)
0
1
2
3
4
*
GFP
KLF4
Control
NMDA, R 4 h
NMDA, R 20 h

Fig. 2.7 The upregulation of cyclin D1 induced by NMDA and that induced by KLF4 are additive.

Neuron cultures infected with lentiviral vectors expressing GFP (G, GFP) or KLF4 (K, KLF4) were incubated with 10 μM NMDA for 1.5 h, and then allowed to recover in culture medium for 4 h (NMDA, R 4 h) or 20 h (NMDA, R 20 h). Control groups were not treated with NMDA. **A**, Cell lysates were analyzed by Western blots for detection of cyclin D1. **B**, Densitometric measurements of the immunoblots in (A). * indicates $p < 0.05$ compared between KLF4-NMDA-R4h and GFP-NMDA-R4h groups. All values are averages of results from at least three separate experiments.

CHAPTER THREE: THE ROLE OF PGRN IN MICROGLIAL MIGRATION DURING EPILEPSY AND INFLAMMATION

3.1. Summary of findings in chapter three

Haploinsufficiency of PGRN has been identified as one of the genetic causes for frontotemporal lobe dementia with ubiquitinated inclusions (FTLD-U) (Baker et al., 2006). Inflammation and microglial activation are evident in FTLD-U. Previous evidence has shown that PGRN is anti-inflammatory and chemoattractive to microglia. Depletion of PGRN increases the vulnerability of cultured slices to LPS stimulation (Yin et al., 2010). PGRN also promotes microglial migration in the brain both *in vitro* and *in vivo* (Pickford et al., 2011). However, the functions of PGRN in pathophysiological conditions remain largely unknown. Here for the first time we reported that both the protein and mRNA levels of PGRN from cortical and hippocampal extracts were significantly increased in our pilocarpine-induced seizure model. Double immunostaining showed that PGRN was upregulated in activated microglia. In our attempts to identify seizure-correlated factors that could activate PGRN, we found that LPS increased PGRN expression in a mixed neuronal-glial culture. In pure microglial culture, PGRN induced microglial migration while administration of anti-PGRN antibody abolished LPS-induced microglial migration. Using intra-hippocampal injection of recombinant PGRN protein in pilocarpine-induced status epilepticus, we found that PGRN increased seizure-induced microglial activation, but had no effect on seizure-induced neuronal injury in the dentate gyrus. However, we also found that pilocarpine-induced seizure response, microglial

activation and cell death in the dentate gyrus in PGRN knockout mice were similar to those in wildtype. Our data suggest that PGRN may act as a modulating factor for microglial migration during inflammation and seizure.

3.2. Experimental procedures

3.2.1. Reagents

Unless stated otherwise, all chemical reagents were purchased from Sigma (Saint Louis, MO, USA). Dulbecco's modified eagle medium (DMEM), fetal bovine serum (FBS), penicillin/streptomycin, and Alexa fluor-conjugated secondary antibodies were obtained from Invitrogen (Burlington, Ontario, Canada). Deoxyribonuclease I (DNase I) was purchased from Stem Cell Technologies (Vancouver, BC, Canada). Diazepam was purchased from Sandose (Boucherville, QC, Canada). Sheep Immunoglobulin G (IgG) was purchased from Cedarlane (Burlington, ON, Canada). Antibody against microtubule-associated protein 2 (MAP2) was purchased from Chemicon (Billerica, MA, USA). The rabbit anti-elastase antibody was purchased from Abcam (Cambridge, MA, USA). The rat anti-mouse rat complement receptor type 3 (CD11b) antibody and the mouse anti rat CD11b Ox42 antibody were purchased from AbD Serotec (Raleigh, NC, USA). Antibody against GFAP was purchased from Santa Cruz Biotechnology (CA, USA). Antibody against actin was purchased from Cell signal technology (Danvers, MA, USA). Antibody against PGRN was purchased from R&D Systems (Minneapolis, MN, USA). Antibody against MCP-1 was purchased from Millipore (Billerica, MA, USA). DAPI-Fluoromount-G was purchased from Southern Biotech (Birmingham, AL, USA). Fluoro-Jade B was purchased from Histo-Chem (Jefferson, AR, USA). Permount was purchased from

Fischer Scientific (Ottawa, Ontario, Canada).

3.2.2. Primary cell culture

All animal experiments were approved by the University of British Columbia Animal Care Committee. Primary neuronal cultures of mouse cortex were prepared from embryonic day 15 CD1 mice (Charles River, Quebec, Canada) as previously described in chapter 2.

Mixed neuronal-glial cultures were prepared from cerebral cortex of embryonic day 18 Sprague Dawley rats (Centre for Disease Modeling, UBC, Canada) as previously described (Kartvelishvily et al., 2006; Zhu et al., 2009). Briefly, after cortices were isolated, trypsinized, and triturated, cells were plated, at a density of 1×10^6 per well in 12-well plate. The neurons were plated in DMEM medium supplemented with 10% FBS and 1% (vol/vol) penicillin/streptomycin. Mixed cultures were studied at DIV 3 days. The mixed culture contained 52% MAP2-positive neurons and 3% Ox42-positive microglia.

Primary microglial cultures were harvested from the cerebrum of embryonic day 18 Sprague Dawley rat as previously described (Floden and Combs, 2007; Ryu et al., 2009). After isolation and trypsinization, the tissue was triturated in DMEM supplemented with 10% FBS, 1% (vol/vol) penicillin/streptomycin and 0.005 mg/ml DNase I. Cell mixtures were centrifuged and resuspended in the same DMEM without DNase I. Cells were seeded at a density of 3.5×10^7 per 10-cm culture plate pre-coated with poly-D-lysine. Culture plates were incubated at 37 ℃ in a humidified 5% CO2 chamber. The medium was replaced every 3-4 days until DIV 7. On DIV 14 plates were gently shaken by hand for 1 min and microglia were collected from the culture medium. The remaining mixed

glial cultures were kept in fresh medium and microglial cells were harvested again on DIV 21 and DIV 28. The harvested microglia contained more than 98% OX42-positive cells. Microglial cells were used immediately in the transwell migration assay.

3.2.3. *In vitro* transwell migration assay

We assessed the migration of rat microglia with a previously reported transwell assay (Horvath and DeLeo, 2009; Ryu et al., 2009). Briefly, transwell inserts (6.4 mm Diameter, 8 μm pore size, BD Biosciences) were placed inside 24-well culture plates (Corning Costar). The paradigm of the transwell apparatus is shown in Fig. 3.9A. Newly harvested microglial cells were plated at a density of 2×10^6 in the upper chamber in serum-free DMEM supplemented with 0.1% BSA. PGRN protein (100 ng/ml), control BSA (100 ng/ml) or LPS (500 ng/ml) was added to the lower chamber in DMEM/BSA medium. In some experiments, microglia in the upper chamber were pretreated with anti-PGRN antibody (1 μg/ml) or control sheep IgG (1 μg/ml) for 1 h before addition of LPS in the lower chamber. Cells were incubated at 37 ℃ in a humidified 5% CO2 chamber for 24 h. The inserts were fixed with 4% paraformaldehyde (PFA) with 2% sucrose and permeabilized with PBST (0.2% Triton X-100 in PBS). Cells on the unmigrated (top) side were gently removed using cotton Q-tips. Insert membranes were cut out, dried and mounted with the DAPI-Fluoromount-G with the migrated side facing down on microscope slides. Microglial migration was quantified by counting the number of microglia left on the membrane in 8 random fields per membrane at 20 × magnification using an inverted fluorescent microscope (Zeiss Axiovert 200). Results are illustrated as

cell migration relative to control. Data analysis was conducted with the observers blinded to the experimental conditions.

3.2.4. Expression, purification and verification of PGRN protein

To produce PGRN protein in a mammalian cell line as previously described (He and Bateman, 1999), we first subcloned HIS tag at the 5'-end of human PGRN cDNA carried in the pcDNA3.1 vector (a generous gift from Dr. Andrew Bateman, McGill University). We then transfected HEK 293T cells with this plasmid using a calcium phosphate transfection kit (ProFection Mammalian Transfection System, Promega, Madison, WI, USA) following the manufacturer's protocol. At 48 h and 72 h following transfection, culture medium were collected and used for purification. HEK 293T Cells were maintained in DMEM medium supplemented with 10% FBS and 1% (vol/vol) penicillin/streptomycin. Culture plates were kept at 37 ℃ in a humidified 5% CO2 chamber.

We first crudely purified His-tagged PGRN using the Ni-NTA purification system (Invitrogen) following the manufacturer's instructions. Briefly, 400 ml collected cultured medium was passed through a 10 ml purification column filled with Ni-NTA Agarose. Unbound protein was washed off using 200 ml native purification buffer (50 mM NaH_2PO_4, 2.5 M NaCl, pH 8.0) and 20 ml wash buffer (native purification buffer with 20 mM imidazole, pH 8.0). PGRN in the column was washed off with 10 ml elution buffer (native purification buffer with 250 mM imidazole, pH 8.0). To remove imidazole and concentrate PGRN, we then passed column eluate through an Amicon Ultra-15 Centrifugal Filter Unit (Ultracel-30 filter membrane, Millipore), and PGRN bound in the filter membrane was washed off with PBS (pH 7.4). The concentration of crudely

purified PGRN was 1 mg/ml.

We further purified PGRN using the high performance liquid chromatography (HPLC) method as previously described (He and Bateman, 1999). Crude PGRN was prepared in 0.1 % trifluoroacetic acid and then passed through the reversed-phase HPLC column (C4, 10 μm, 250 × 4.6 mm, Grace Davison Discovery Sciences company, Deerfield, IL, USA) in HPLC system (Gilson, Middleton, WI, USA).The Column was washed with a mobile mixture system providing linear gradients of 0 to 95 % acetonitrile in 0.1 % trifluoroacetic acid, at a speed of 1.5 ml/min over 80 min. The column eluate was monitored for ultraviolet absorbance at 215 nm and PGRN fractions were collected. PGRN in eluted solution was concentrated in PBS (pH 7.4) using the Amicon Ultra-15 centrifugal filter as described above. The identity of PGRN was confirmed by mass spectrometry and using Western blots with anti-PGRN antibody (Fig. 3.17).

3.2.5. Western blots

Cerebral cortex and hippocampus were isolated in ice-cold sucrose-buffer containing (in mM): 75 sucrose, 87 NaCl, 25 $NaHCO_3$, 25 D-glucose, 2.5 KCl, 1.25 NaH_2PO_4, 0.5 $CaCl_2$, 7.0 $MgCl_2$, pH 7.3. Tissues were homogenized on ice with a glass homogenizer in extraction buffer (50 mM pH 7.2 Tris base, 150 mM NaCl, 1mM EDTA, 1mM EGTA, 10% NP-40, 0.1% sodium dodecyl sulfate, 0.5% sodium deoxycholate) supplemented with complete protease inhibitor tablets (Roche) according to the manufacturer's instructions. The homogenates were centrifuged at 14,000 rpm and the supernatants were collected. Protein concentrations were tested with a RC DC™ protein assay kit (Bio-Rad, Hercules, CA) and mixed with 0.25 volume of 4 × sample buffer. For Western blots of total protein in cultured cells, cells were scraped and homogenized in 1 × sample buffer (124 mM pH

6.8 Tris-HCl, 50% glycerol, 4% SDS, 0.08% Bromophenol blue). Cell or brain lysates were boiled for 5 min and 25-50 µg protein was resolved by SDS polyacrylamide gel electrophoresis. Proteins were transferred to nitrocellulose membranes (Bio-Rad). Protein bands were detected using primary antibodies including: sheep polycolonal anti-PGRN antibody (1:1000), rabbit polycolonal anti-GFAP (1:5000), anti-elastase antibody (1:500), anti-actin antibody (1:2000), anti-beta tubulin antibody (1:2000). Horseradish peroxidase-conjugated anti-sheep and anti-rabbit secondary antibodies (PerkinElmer, Wellesley, MA) and enhanced chemiluminescence (PerkinElmer) were used according to the manufacturer's instructions. The intensity of protein bands was measured using ImageJ software provided by NIH (http://rsb.info.nih.gov/ij/). The band that detects actin was used as a loading control.

3.2.6. Quantitative real time PCR

RNA extraction and two-step RT-PCR were performed as previously described (Zhu et al., 2009). Total RNA was extracted from isolated brain tissue or cultured cells using Trizol® Reagent (Invitrogen). One µg of RNA was purified with DNase I (Invitrogen) and then reverse-transcribed to cDNA using SuperScript™ II Reverse Transcriptase (Invitrogen). Duplicates of the 4-fold serial dilution of cDNA samples were used in a 25 µL total volume containing 12.5 µL SYBR® Green PCR master mix (Applied Biosystems, Foster City, CA, USA**)** and 300 nM primers for each RT-PCR reaction. Fold inductions were calculated using the formula $2^{-(\Delta\Delta^{Ct})}$, where $\Delta\Delta Ct$ is the $\Delta Ct_{(treatment)}$-$\Delta Ct_{(control)}$, Δ Ct is $Ct_{(PGRN)}$-$Ct_{(actin)}$ and Ct is the cycle at which the threshold is crossed. The gene specific primer pairs were as follows: *rat PGRN* gene forward 5'-CACACGCGATGCATTTCAC-3' and reverse 5'-CTGCCCTGTTGGTCCTTTGT-3';

mouse PGRN gene forward 5'-GTTGTGAGGATCACATTCATTGC-3' and reverse 5'-GGGTACTTGGAGGATACCCATTTC -3'; *actin* gene forward 5'-ACGAGGCCCAGAGCAAGAG-3' and reverse 5'-TCTCCATGTCGTCCCAGTTG-3'. PCR product quality was monitored by post-PCR melt curve analysis.

3.2.7. Cannula implantation

Cannulae were implanted into 200 - 250 g Sprague Dawley rats according to previous procedures (Chen et al., 2007). All animal experiments were approved by the University of British Columbia Animal Care Committee. Appropriate experimental procedures were taken to minimize pain or discomfort. While anesthetized with inhalation of 2% isoflurane in 98% oxygen, rats were implanted with a 26-gauge stainless steel cannula (PlasticsOne, Roanoke, VA, USA) bilaterally into the each side of hippocampus (3.4 mm posterior to bregma, 1.5 mm lateral to the midline, and 2.8 mm below the skull surface). We secured each cannula to the skull with three stainless steel screws (Stoelting, Wood Dale, IL, USA). Rats were allowed at least 7 d to recover before seizure induction.

3.2.8. Pilocarpine-induced status epilepticus

We used 230 - 270 g Sprague Dawley rats and 25 - 30 g C57BL/6 mice for SE induction. Wildtype and PGRN knockout C57BL/6 mice were obtained from Dr. Blair Leavitt's lab at UBC. As previously described (Goffin et al., 2007), we induced seizures by intraperitoneal (i.p.) administration of 320 mg/kg pilocarpine hydrochloride dissolved in 0.9 % saline. Atropine methylbromide (5 mg/kg, i.p.) was used 30 min before injection of pilocarpine to minimize its peripheral convulsive effect. The animals were monitored for 8 h following pilocarpine injection. Seizures were scored according to Racine's

behavioral standards (Luttjohann et al., 2009; Racine, 1972a): 0. no response; 1.eye blinking and mouth clonus; 2. head nodding with facial jerking; 3. brief and involuntary jerks of neck and forelimbs; 4. bilateral clonic convulsions with sitting and rearing; 5. clonic convulsions with rearing, falling and loss of body control. Behaviors scored 1-3 were classified as partial seizures and those scored 4 and 5 were classified as secondarily generalized seizures. Unless specified, we determined the onset of SE by the time point at which generalized seizures (class 4 and 5) were continuously observed in animals. If seizures were not induced in animals within 45 min, they received two additional doses of pilocarpine until SE was developed (110 mg/kg for first injection, 80 mg/kg for second injection with 30 min delay from previous injection). Rats showing no behavioral response to pilocarpine were used as control animals (non-SE control) except noted. In the seizure study involving transgenic mice, all mice received one dose of pilocarpine (320 mg/kg). To terminate the SE, we injected diazepam (4 mg/kg i.p.) three hours after the onset of continual seizures. In the study to investigate the chemotactic effect of intra-hippocampus administration of PGRN protein (Fig. 3.10, 3.11 and 3.12), rats received intra-hippocampal injection of 1 μl sterilized PGRN (100 ng/μl) or BSA (100 ng/μl) in PBS at 30 min before atropine injection. PGRN was injected into one side of the brain and BSA was administered into the other side of the brain of the same animal. Drugs were injected through cannulae into the brains of free moving rats at a constant speed of 0.5 μl/min. For the 24 h post-seizure group, the same dose of PGRN or BSA was administered at 12 h after the onset of SE to supplement degraded protein, because unpublished data from our lab estimated that the half-life of PGRN recombinant protein was approximately 12 hours at 37℃. Rats receiving saline but not pilocarpine injection

were used as controls in *in vivo* chemotactic study (Fig. 3.10, 3.11 and 3.12), since all rats implanted with cannulae developed SE after one dose of pilocarpine (320 mg/kg).

3.2.9. Immunohistochemical staining

After anesthetization with urethane, animals were perfused with saline followed by 4% PFA in PBS (pH 7.4) as previously described (Ryu et al., 2009). Brains were then removed and postfixed in 4% PFA-PBS overnight at 4 ℃. After cryopreservation in 15% and then 30% sucrose-PBS at 4 °C, brains were cut into 20 μm coronal sections using a cryostat (Leica CM3050S). The immunostaining of free-floating sections was performed as previously described (Ryu et al., 2009). Briefly, nonspecific binding was blocked with 10% normal goat or donkey serum in PBST for 1 h at room temperature. Sections were then incubated overnight at 4℃ with primary antibodies prepared with 3% normal goat or donkey serum in PBST. The primary antibodies we used were mouse anti-rat OX42 (1:150), rat anti-mouse CD11b (1:50), rabbit anti-GFAP (1:500), and sheep anti-PGRN (1:50). Donkey serum was used for preparing anti-PGRN primary antibody and goat serum was used for all other antibodies. Sections were then rinsed with PBS and incubated with their respective secondary antibodies conjugated with Alexa Fluor 488 or 546 (1:1000) at room temperature for 1 h. Samples were mounted, dried, and covered in DAPI-Fluoromount-G before sealed with glass coverslip.

Quantifications of single- or double- immunostained brain sections was performed using ImageJ software on digitized images obtained with an Olympus Fluoview FV1000 confocal microscope at 20× magnification. For quantification of microglia following intra-hippocampal injection, Ox42+ cells were counted at three sections evenly spaced

through the injection site (3.4 mm posterior to bregma). To determine the number of SE-activated microglia in transgenic mice, three consecutive sections in the dentate gyrus of hippocampus (at approximately -3.0 to -4.0 from bregma) were analyzed for each animal. The quantification was conducted blinded to genotype or treatment.

3.2.10. Immunocytochemistry

Immunocytochemical staining was performed as previously described (Zhu et al., 2009). Mixed neuronal-glial cultures were seeded on glass. At DIV 5, cultures were fixed with 4% PFA with 2% sucrose in PBS (pH 7.4) at 37 ℃ for 20 min. Cultures were then permeabilized with PBST and nonspecific staining was blocked with 4% BSA-PBS. To detect the population of cell types in mixed cultures, cultures were stained with mouse anti-Ox42 (1:150) or mouse anti-MAP2 (1:1000), followed by respective secondary antibody conjugated with Alexa Fluor A488 (1:1000). Antibodies were prepared with 1% BSA-PBS. Cells were mounted in DAPI-Fluoromount-G. Images were taken using Olympus Fluoview FV1000 confocal microscope at a magnification of 40×. The cell composition was determined by the number of Ox42+ or MAP2+ cells divided by the number of DAPI+ cells in the field, as counted in the Image J. At least 1000 DAPI positive cells were counted.

3.2.11. Double immunostaining

To detect the cell types expressing PGRN, we first stained free-floating sections or mixed cultures with sheep anti-PGRN (1:50) followed by donkey anti-sheep secondary antibody conjugated with Alexa Fluor 546 (1:1000). After washing we incubated sections

or mixed cultures with specific cell-type labeling antibodies. The antibodies used were mouse anti-Ox42 (1:150), rabbit anti-GFAP (1:500), and rabbit anti-MAP2 (1:1000). We then applied the respective secondary antibodies which were raised in goat and conjugated with Alexa Fluor 488 (1:1000). Samples were mounted, dried, and covered in DAPI-Fluoromount-G before sealing with a glass coverslip. Images were taken using an Olympus Fluoview FV1000 confocal microscope. The number of Ox42+ and OX42+/PGRN+ cells in cortex, thalamus or the dentate gyrus of hippocampus were determined for 2 sections per animal at approximately -3.0 to -4.0 from bregma. The quantification was conducted in a blinded manner.

3.2.12. Fluoro-jade B staining

Neuronal death following SE was detected by Fluoro-Jade B staining at room temperature as previously described (Chen et al., 2007). Briefly, brain sections mounted on slides were subsequently immersed in 100% ethanol for 1 min, in 70% ethanol for 1 min and then washed in distilled water for 1 min. Slides were then transferred to 0.06% potassium permanganate for 15 min. After washing, slides were incubated in 0.0004% Fluoro-Jade B prepared in 0.1% acetic acid for 30 min. After three washes, slides were dried and immersed for 2 min in xylene three times, and mounted with Permount (Fischer Scientific, Ottawa, Ontario, Canada). Slides were imaged with an Olympus Fluoview FV1000 confocal microscope. Positively-stained degenerating cells in dentate gyrus of three evenly spaced sections of hippocampus (at approximately -3.0 to -4.0 from bregma) were counted using ImageJ software. The data were analyzed in a blinded manner.

3.2.13. Statistical analysis

Results were expressed as means ± SEM. One-way ANOVA was used to compare data among groups. Fisher's least significant difference post-hoc test was used to compare the differences between groups after ANOVA. Two-tailed Student's *t* tests were conducted in studies in which data from only two groups (treatment and control) are compared. Differences were considered significant at $p < 0.05$.

3.3. Results

3.3.1 Induction of PGRN protein and mRNA after pilocarpine-induced SE

Experimental status epilepticus has been shown to increase the expression of a variety of growth factors including NGF (Holtzman and Lowenstein, 1995), BDNF (Rudge et al., 1998), VEGF (Nicoletti et al., 2008), and bFGF (Riva et al., 1994; Van Der Wal et al., 1994). These growth factors may be involved in neuronal protection and glial reaction following epileptic insults (see 1.2.2 in the chapter one of this dissertation). As a growth factor recently identified as a key player in neuronal protection and microglial activation, it is opportune to study the role of PGRN in brain seizures. We first analyzed the time-dependent expression of PGRN from hippocampal and cortical lysates after the onset of SE. We found that the mRNA and protein levels of PGRN were markedly increased at 24, 48, and 96 h post-SE, but not at 3 or 12 h post-SE (Fig. 3.1). In cortex, PGRN protein levels were significantly increased after SE (2.0 ± 0.1 fold at 24 h, 4.6 ± 0.7 fold at 48 h, and 3.2 ± 0.2 fold at 96 h post-SE compared with controls). To test if upregulation of PGRN protein was due to increased mRNA expression, we used real time PCR to

measure the mRNA levels. We found that cortical PGRN mRNA levels showed a maximal elevation at 48 h, and that the elevation was persisted until 96 h following the onset of SE (1.3 ± 0.1 fold at 24 h, 2.4 ± 0.2 fold at 48 h and 2.3 ± 0.2 fold at 96 h post-SE compared with controls). In hippocampus, the PGRN induction was evident at 24 h (1.9 ± 0.2 fold for protein and 1.5 ± 0.1 fold for mRNA, compared with controls), further elevated at 48 h (3.1 ± 0.2 fold for protein and 2.3 ± 0.1 fold for mRNA, compared with controls) and 96 h (4.5 ± 0.3 fold for protein and 4.6 ± 0.2 fold for mRNA, compared with controls) after the onset of SE. The maximal levels of PGRN mRNA and protein levels were reached at 96 h in hippocampus in the time window we tested.

3.3.2 Localization of PGRN in microglia after SE

Based on our results of the time-dependent expression of PGRN following SE, we selected a single time point of 48 h to identify the types of cells expressing PGRN in post-SE brain. In control groups PGRN was expressed at a relatively low level (Fig. 3.2). However, we found a group of cells expressing distinctively high levels of PGRN immunoreactivity, much greater than other cells, at 48 h post-SE but not in control groups. These cells colocalized with microglial marker OX42 but not with the astroglial marker GFAP (Fig. 3.2D). About 90% of Ox42-immunoreactive cells expressed PGRN in both control and 48 h SE groups (Fig. 3.3). The number of PGRN/Ox42 immunoreactive cells was significantly increased at 48 h post-SE by 4.9 fold in hippocampus, 30.5 fold in thalamus and 31.5 fold in cortex, compared with control groups (Fig. 3.3A). The total number of Ox42-immunoreactive microglia was significantly increased at 48 h after SE in hippocampus, cortex and thalamus (Fig. 3.3B).

3.3.3 SE induced reactive gliosis

We also confirmed that glial cells were activated in our pilocarpine model, consistent with a finding noted previously (Cavalheiro, 1995; Yang et al., 2010). Western blotting results showed that in cortex GFAP protein levels were increased at 48 h post-SE (1.39 ± 0.03 fold compared with controls, $p < 0.001$, Fig. 3.4A and 3.4B) and at 96 h post-SE(1.52 ± 0.06 fold compared with controls, $p < 0.001$, Fig. 3.4A and 3.4B), but were not affected at other time points ($p = 0.94$ at 3 h, $p = 0.28$ at 12 h, and $p = 0.16$ at 24 h post-SE compared with controls, Fig. 3.4A and 3.4B). In hippocampus, GFAP protein levels were also increased at 24 h SE (1.28 ± 0.07 fold compared with controls, $p < 0.05$, Fig. 3.4C and 3.4D), 48 h SE (1.65 ± 0.08 fold compared with controls, $p < 0.001$, Fig. 3.4C and 3.4D) and at 96 h SE (1.63 ± 0.04 fold compared with non-SE controls, $p < 0.001$, Fig. 3.4C and 3.4D), but were not significantly affected at other time points ($p = 0.37$ at 3 h and $p = 0.34$ at 12 h post SE compared with non-SE controls, Fig. 3.4C and 3.4D) .

3.3.4 Investigation of factors that could induce PGRN expression

Based on our finding that PGRN was induced by SE in microglia, there are two major questions to ask: 1) Which factors induced by SE mediate PGRN elevation; 2) what the function of induced PGRN in microglia is. We first tried to answer the first question as follows:

3.3.4.1 The total protein expression of elastase was not affected by SE

It was reported that PGRN can be cleaved into granulin by elastase in peripheral skin cells (Zhu et al., 2002). Therefore, we asked whether elevations in PGRN protein levels could be associated with fluctuations of elastase levels. We tested elastase expression

following SE by Western blots. Our results showed that elastase protein levels were not changed in either hippocampus or cortex after pilocarpine-induced SE (p = 0.62 for cortical samples and p = 0.51 for hippocampal samples when tested with one-way ANOVA, Fig. 3.4E).

3.3.4.2 Changing synaptic activity in cultured neurons does not affect PGRN levels

During generalized seizures, intense synaptic firing has been suggested as one of the key events leading to further brain damage (Loscher and Ebert, 1996; Morimoto et al., 2004). We thus asked whether PGRN expression was affected by manipulation of synaptic activity in cultured neurons. Injection of GABAA receptor antagonist bicuculline has been used as experimental model to induce generalized seizures in animals (Ben-Ari et al., 1981; de Feo et al., 1985; Dhir et al., 2006; Meldrum and Horton, 1971). We used bicuculline to increase synaptic activity and the sodium channel blocker TTX to decrease synaptic activity in primary cortical neuron cultures. We incubated cultured neurons with TTX (2 μM) or bicuculline (50 μM) for 0.3, 1, 4, 24, 48 h. Neither TTX nor bicuculline had a significant effect on PGRN protein levels (p = 0.99 between TTX groups and p = 0.54 between bicuculline groups using one-way ANOVA, Fig 5A-5D). We also used real time PCR to test PGRN mRNA levels following bicuculline treatment, and found no change at all time points tested (p = 0.45 between groups using one-way ANOVA, Fig. 3.5E). These results suggested that increased synaptic activity during seizures may not be a direct cause for increase in PGRN levels following SE.

3.3.4.3 LPS, but not ATP, glutamate or bicuculline induced PGRN induction in mixed culture

In addition to intensified synaptic firing, other events such as elevated ATP and glutamate concentrations occur during seizures (Chapman, 1998; Meldrum, 1993; Meldrum et al., 1999; Wieraszko and Seyfried, 1989). A variety of cytokines and chemokines, which can be activated by LPS in vitro, have also been found to be induced following SE (Vezzani, 2005). Therefore, in addition to bicuculline we selected ATP, glutamate and LPS as potential seizure-correlated stimulants. Considering the complexity of cell types in brain and our observation that PGRN was upregulated in microglia, we used a mixed neuronal-glial culture as our *in vitro* model to further investigate which stimulants could upregulate PGRN. We treated mixed neuronal-glial cultures with ATP (50 μM), glutamate (1mM), bicuculline (50 μM) for 1 or 2 days, and found no difference in PGRN protein expression ($p > 0.05$ in one-way ANOVA test, Fig. 3.6C and 3.6D). However, when mixed cultures were treated with 100 ng/ml or 500 ng/ml LPS for 2 days, PGRN expression was significantly elevated (1.4 fold at 100 ng/ml LPS and 1.6 fold at 500 ng/ml LPS compared with 2-day control, Fig. 3.6A and 3.6B). One day of treatment with 500 ng/ml LPS also significantly upregulated PGRN expression (1.4 fold compared with 1-day control, Fig. 3.6A and 3.6B). Immunocytochemical staining of mixed cultures also showed a distinctively strong expression of PGRN in microglial cells (Fig. 3.7). The expression of PGRN in microglial cells in mixed culture still persisted after LPS stimulation (Fig. 3.7). Our results indicate that among all the seizure-correlated stimulants we tested in mixed neuronal-glial cultures, only LPS upregulated PGRN protein.

3.3.5 The role of PGRN in LPS-induced chemotactic responses *in vitro*

LPS has been regarded as a common way to activated microglia (Kloss et al., 2001). We next investigated whether the PGRN protein was required in LPS-induced microglial migration and release of chemoattractants.

3.3.5.1 Anti-PGRN antibody abolished LPS-induced microglial migration

We examined the contribution of PGRN to LPS-induced microglial migration with the transwell assay. Cultured microglia seeded in the upper chamber were pre-incubated with anti-PGRN antibody (1 μg/ml) or control antibody (1 μg/ml) for 1 h. LPS (500 ng/ml) was then applied to the lower chamber for 24 h. When anti-PGRN antibody was applied alone, the number of migrating microglia was similar as found with control antibody alone (0.96 ± 0.04 fold). LPS increased microglial chemotaxis by 1.47 ± 0.05 fold in control antibody. When incubated with anti-PGRN antibody, LPS induced little microglial mobility (1.07 ± 0.05 fold compared with control antibody alone). Our result thus shows that PGRN is required for LPS-induced microglial migration.

3.3.5.2 Recombinant PGRN induced microglial migration

We further tested whether PGRN is a chemoattractant for microglia. Microglia were seeded in the upper chamber, while PGRN (100 ng/mL) or control BSA (100 ng/mL) was applied to the lower chamber for 24 h. PGRN increased the number of migrating microglia by 1.4 ± 0.1 fold compared with BSA control. Our results thus indicate that PGRN act as a chemoattractive to cultured microglia.

3.3.5.3 Anti-PGRN antibody did not block LPS-induced release of MCP-1

It has been previously shown that LPS stimulation increased release of chemoattractants such as MCP-1 which was involved in microglial activation (Ambrosini and Aloisi, 2004; Kielian et al., 2001; Thompson et al., 2008). MCP-1-deficient mice showed less activation of microglia in response to LPS (Thompson et al., 2008). Therefore, we tested whether PGRN was required for LPS-induced MCP-1 expression. Pre-incubation with control antibody or anti-PGRN antibody had no effect on MCP-1 expression (1.0 ± 0.5 fold or 0.9 ± 0.2 fold compared with saline control, respectively, Fig. 3.8). LPS upregulated MCP-1 protein levels by 2.8 ± 0.5 fold in saline control, 3.3 ± 0.5 fold in control antibody, and 3.4 ± 0.3 fold in anti-PGRN antibody (Fig. 3.8). There was no significant difference in the fold change of LPS-induced MCP-1 expression when cultures were preincubated with anti-PGRN antibody, control antibody or saline (p = 0.91 between anti-PGRN-LPS and control-antibody-LPS, p = 0.21 between anti-PGRN-LPS and saline-LPS, Fig. 3.8B). Thus PGRN antibody-induced depletion exerts its effects distal to the release of MCP-1.

3.3.6 Injection of PGRN protein induced microglial activation after seizure

Based on our finding that PGRN mediated LPS-induced microglial migration *in vitro*, we asked whether PGRN might also be chemoattractive following SE *in vivo*. We first investigated the effect of recombinant PGRN on seizure-induced microglial activation. PGRN (100 ng) or BSA (100 ng) was administered symmetrically into each side of dentate gyrus of hippocampus at 30 min before atropine injection. Endogenous PGRN was induced in hippocampus at 24 h and escalated at 48 h and 96 h, but not at 12 h, after

SE initiation (Fig. 3.1). Therefore we narrowed our inspection window to no later than 24 h following SE to avoid the effect of endogenous PGRN. Rats receiving vehicle instead of pilocarpine injection was considered as "control". In control groups, PGRN had no effect on the number of Ox42-positive microglia compared with BSA. At 6 h or 12 h following SE induction, the number of microglia was not significantly changed by SE induction at the BSA-injected side (p = 0.99 between BSA-6 h SE and BSA-control, p = 0.38 between BSA-12 h SE and BSA-control, Fig. 3.10 and 3.11). However, when injected with PGRN, microglial invasion significantly increased at 6h (3.2 fold of BSA-control, 2.7 fold of PGRN-control, and 2.7 fold of BSA-SE, Fig. 3.10) and at 12 h after SE (3.4 fold of BSA-control, 2.9 fold of PGRN-control, and 2.0 fold of BSA-SE, Fig. 3.11). At 24 h post-SE, the number of microglial cells significantly upregulated at the BSA side (2.8 fold of BSA-control and 2.4 fold of PGRN-control, Fig. 3.12). PGRN injection further enhanced microglia number at 24 h post-SE (1.6 fold of BSA-SE, Fig.12). Our results thus show that PGRN protein upregulates SE-induced microglial activation *in vivo*.

3.3.7 PGRN protein had no effect on SE-induced cell death

PGRN acts as a neurotrophic factor (Van Damme et al., 2008) and depletion of PGRN rendered cultured neurons more vulnerable to NMDA or H_2O_2 (Guo et al., 2010). Thus we asked whether PGRN is protective against SE-induced neuronal degeneration. Fluoro-Jade B staining showed clear evidence of dead cells in the dentate gyrus of hippocampus at 6 h, 12 h and 24 h after SE (Fig. 3.13). However, the number of degenerating cells in PGRN-injected side were not significantly different from those in the BSA-injected side in any of the control, 6 h, 12 h and 24 h SE group (p = 0.86 between PGRN-24h and

BSA-24h, p = 0.99 between PGRN-12h and BSA-12h, p = 0.92 between PGRN-6h and BSA-6h in *post-hoc* test, Fig. 3.13B).

3.3.8 PGRN knockout mice had no difference in acute seizure development

To further investigate whether PGRN is required for convulsant effect of pilocarpine and the pilocarpine-induced microglial activation and cell death, we induced seizures in PGRN knockout mice (a generous gift from Dr. Blair Leavitt's lab) with 320 mg/kg pilocarpine. At 48 h after SE, immunostaining with PGRN protein that was evident in wildtype mice completely disappeared in PGRN knockout mice (Fig. 3.14A). However, PGRN knockout mice had similar latency to the onset of SE when compared with their wildtype littermates or normal C57BL/6 controls (p = 0.27 in one-way ANOVA test, Fig. 3.14B). There was no difference when we compared the latency at which when mice first reached behavioral seizures at class 4 and above (Racine's scale) in PGRN knockout, wildtype and control mice (p = 0.22 in one-way ANOVA test, Fig. 3.14C). All groups of mice injected with pilocarpine developed generalized seizures (class 4 and 5 in the Racine's scale). The mortality rates were 73% and 75% in WT and PGRN KO mice. Of all the 11 wildtype mice injected with pilocarpine, 4 died of seizures before developing continual seizures, 4 died 18 ± 1 min after onset of continuous generalized seizures, and 3 survived until 48 h after SE. Among all the 12 PGRN KO mice, 7 died at 22 ± 3 min after the onset of continual seizures, 2 died the second day following SE induction, and 3 survived until 48 h after SE. These preliminary data suggest that PGRN may not be required for seizure development.

3.3.9 Activation of microglia and cell death induced by SE were similar in PGRN knockout mice as in wildtype

To determine whether PGRN was necessary to SE-induce microglial activation and cell death, we used anti-Ox42 to stain microglia and Fluoro-Jade B to label degenerating cells at 48 h post SE. Deletion of PGRN had no effect on the number of microglia activated by SE (Fig. 3.15), nor did it affect SE-induced cell death (Fig. 3.16).

3.4 Conclusion

At the beginning of these studies, the role of PGRN in epilepsy was completely unknown. Here, we found that PGRN was upregulated in microglia after pilocarpine-induced seizures. We then tried to elucidate the functions of PGRN and the mechanism by which PGRN was induced. We first found that application of PGRN protein induced microglial migration at 6 h, 12 h and 24 h following seizures, but did not affect neuronal damage in the dentate gyrus. In PGRN deficient mice, seizure behavioral score, microglia numbers and neuronal damage in DG were not different from wildtype control. The role of PGRN in promoting microglial migration was also confirmed in cultured microglia, since PGRN protein increased microglial migration and PGRN-antibody abolished LPS-induced migration. The effect of PGRN on microglial migration may not be mediated by MCP-1, based on our findings that PGRN antibody did not change LPS-induced MCP-1 expression. In addition, we found that the induction of PGRN could be a result of inflammation, because LPS, but not glutamate, bicuculline or ATP, induced PGRN expression in mixed neuronal-glial culture.

3.5 Discussion

Microglial activation is a critical part of the inflammatory response and may be involved in cellular recover in many neural disorders such as FTLD-U, ischemia and epilepsy. PGRN has been shown to play an anti-inflammatory role in wounded skin (He and Bateman, 2003; Zhu et al., 2002), in arthritis (Tang et al., 2011) and in brain after bacterial infection (Yin et al., 2010). Mutations of PGRN have been identified as a major cause of FTLD-U (van Swieten and Heutink, 2008), suggesting its critical role in the CNS. However, the role of PGRN in epilepsy has not been studied. Here for the first time we show that PGRN was induced in microglia by epileptic seizures in the pilocarpine model. Expression of PGRN in microglia was previously observed in normal tissue (Baker et al., 2006) and was shown to be upregulated in mouse striatum stimulated with quinolinic acid (Petkau et al., 2010). In addition, PGRN protein is upregulated in spinal cord from ALS mice (Philips et al., 2010) and in mice subjected to spinal cord injury (Eriksen, 2010).

3.5.1 PGRN and microglial migration

We found that PGRN protein promoted microglial migration *in vitro* in purified microglial cells and *in vivo* in the pilocarpine epileptic model. Consistent with our *in vivo* result, another group has recently published that PGRN protein induced migration of microglia *in vitro* (Pickford et al., 2011). Our results expand on this finding by showing that PGRN antibody abolished LPS-stimulated migration (Fig. 3.9). We have also found that injection of PGRN protein did not induce microglial migration in control animal, but further increased microglial number at 6 – 24 h following seizure. Since seizure activated microglia (Fig. 3.2 and 3.3), a result consistent with previous work (Avignone et al.,

2008), our results suggest that PGRN is not a strong inducer of quiet microglia but rather an enhancer of microglial migration. The enhancement of PGRN on migration of purified microglial cells in culture (Fig. 3.9) is consistent with this hypothesis since cultured microglial cells are generally considered to be in a more activated state than quiet microglia in brain. Interestingly, Pickford et al. also reported that at 7d and 14 after injection of PGRN-lentivirus, *in vivo* microglial number was further increased compared with GFP-lentivirus (Pickford et al., 2011). Even GFP-lentivirus injection induced a certain degree of microglial activation, which may be due to the proinflammatory effect of lentivirus proteins such as Tat or gp41 (Lokensgard et al., 2001; Speth et al., 2000) and the inevitable trauma of the injection procedure. This work also supports our hypothesis that PGRN is an enhancer for microglial migration. Examination of the microglial responses to injury and inflammation in PGRN-overexpressing transgenic mice could be used to further examine this hypothesis.

PGRN is clearly required for the migration of cultured microglia, since we found that PGRN antibody abolished LPS-stimulated migration (Fig 3.9). There are abundant evidences showing that MCP-1 is involved in LPS-induced microglial migration (Ambrosini and Aloisi, 2004; Kielian et al., 2001; Thompson et al., 2008). We found that LPS-induced MCP-1 expression was not changed by application of PGRN antibody (Fig. 3.8). Hence PGRN may operate distal to MCP-1 in regulating microglial migration. Alternatively, PGRN may regulate LPS-induced migration through other chemokines such as CX3CL1, which has been shown to be induced by PGRN treatment (Pickford et al., 2011).

In addition to PGRN, many other growth factors also act as chemoattractants to microglia. For example, NGF has been shown to promote microglial activation, while low concentration of transforming growth factor-beta enhances (≤ 0.2 ng/ml) and high concentration of TGF-beta (≥ 2 ng/ml) reduces the NGF-induced chemotaxis (De Simone et al., 2007). VEGF and its receptor Flt-1 have been shown to participate in Abeta-induced microglial migration *in vivo* and *in vitro* (Ryu et al., 2009). Epidermal growth factor (Nolte et al., 1997) and hepatocyte growth factor-like protein (Suzuki et al., 2008) have been shown to stimulate chemotaxis of microglia and their receptors were expressed in microglia.

3.5.2 *PGRN and inflammation*

Microglial migration is accompanied by secretion of proinflammatory and anti-inflammatory signals, for example, in the case of LPS stimulation. In our efforts to search for PGRN-inducing stimulants that were associated with epilepsy-correlated sequelae, we found that LPS, but not bicuculline, glutamate, or ATP, was most effective (Fig. 3.5 and 3.6). This result suggested that inflammatory signals, but not excitatory firing or increased energy demand, might be the major cause of epilepsy-induced PGRN expression. To further confirm this hypothesis, it would be valuable to ask whether anti-inflammatory drugs can block epilepsy-induced PGRN expression in the future. Nonetheless, our result is the first report showing that the induction of anti-inflammatory PGRN could be a result of inflammatory stimulations such as LPS. LPS not only induces the release of proinflammatory agents, but also stimulates the secretion of other anti-inflammatory products such as IL-10 (Qin et al., 2006; Yin et al., 2010). Interestingly, PGRN induced expression of IL-10 in macrophages and LPS-induced secretion of IL-10

has been found to be attenuated in PGRN-deficient macrophages (Yin et al., 2010). Therefore, our results support the idea that the upregulation of PGRN by LPS might lead to increased IL-10 expression and thus exert anti-inflammatory roles, in addition to promoting migration.

Anti-inflammatory factors bind to chemoattractant receptors in peripheral inflammation, such as short-chain fatty acids binding to the GPCR 43 (Maslowski et al., 2009), and resolving E1 binding to GPCR chemokine-like receptor 1 (ChemR23) (Arita et al., 2005; Serhan et al., 2008). During neuroinflammation, LPS treatment to microglia induces the synthesis of prostaglandin E2 (PGE2) (Jang et al., 2006), which can activate proinflammatory pathways via the E-prostanoid (EP) 2 receptor and anti-inflammatory signaling via EP 4 receptor (Shi et al., 2010). Synthesis of PGE2 is required for LPS-induced macrophage migration (Tajima et al., 2008). In addition, agonist of EP4 receptor, but not that of EP2 receptor, induced migration of macrophages (Tajima et al., 2008). Based on these studies, we suggest that PGRN may have a binding receptor in microglia which can mediate the microglial migration. The identity of this receptor remains unknown. It was recently reported that PGRN bound to TNF receptors in chondrocytes and disrupted the pro-inflammatory function of TNF alpha (Tang et al., 2011). It has long been shown that microglia secreted TNF alpha and expressed TNF receptors (Kettenmann et al., 2011), and thus the interaction between PGRN and TNF receptors might be part of the mechanism by which PGRN prevents inflammation and promotes migration of microglia in the CNS.

3.5.3 PGRN in epilepsy-induced cell death

PGRN has been identified as a neurotrophic factor essential to cell survival in aging or stressed conditions (Kumar-Singh, 2011; Van Damme et al., 2008). PGRN deficiency also enhanced vulnerability of cultured neuron to normally sublethal doses of H_2O_2 and NMDA (Guo et al., 2010), and rendered cultured brain slice more vulnerable to deprivation of oxygen and glucose (Yin et al., 2010). Interestingly, exogenous PGRN also promoted survival of DIV2 motor neuron cultures, indicating the role of PGRN in neuronal development (Van Damme et al., 2008). In addition, PGRN deficiency caused caspase-dependent cleavage of TDP-43 in cultures (Zhang et al., 2007b). Deletions of PGRN led to cytoplasmic localization of TDP-43 in aged neuron cultures (Guo et al., 2010)and in aged transgenic mice (Yin et al., 2010). FTLD-U patients showed PGRN haploinsufficiency and TDP-43 pathology, recognized as toxic 35 KDa and 25 KDa TDP-43 fragments and cytoplasmic ubiquitinated aggregates (Baker et al., 2006; Neumann et al., 2006). Therefore, PGRN regulated neuron survival via regulation of cleavage and localization of TDP-43. PGRN insufficiency could cause misregulation of TDP-43 which could be toxic in neurodegenerative diseases.

However, we found that injections of PGRN did not promote cell survival after epilepsy (Fig. 3.13) and that PGRN-deficient mice had similar SE-induced damage in dentate gyrus cells as did wildtype animals (Fig. 3.16). Our results suggest that PGRN may not be involved in SE-related cell death even though it stimulated microglial activation following pilocarpine-induced SE. In fact, whether microglial activation is beneficial or detrimental to brain during epilepsy or other neurological disorders is questionable. Mice with transgenically dysfunctional microglia develop normal seizure

behaviors as control in response to pilocarpine (Mirrione et al., 2010), and ablation of microglia using minocycline does not affect neuron degeneration in DG after SE (Yang et al., 2010). In addition, microglial ablation does not alter levels of motor neuron damage in SOD1 ALS mice (Gowing et al., 2008). Studies of effects of chemokines and their receptors, which promote microglial migration, on neuronal damage demonstrate differential results. The data has shown that Chemokine CX3CL1 and its receptors CX3CR1 contributed to SE-induced neuronal damage in pilocarpine model (Yeo et al., 2011). Deficiencies in chemokine CXCL10 and its receptor CXCR3 protected CA1 and CA3 neuron from NMDA-stimulated damage in hippocampal slice cultures, but exacerbated the NMDA-induced DG neuronal death (van Weering et al., 2011).

In summary, our work suggested the role of PGRN in microglial activation induced in epilepsy and in inflammation.

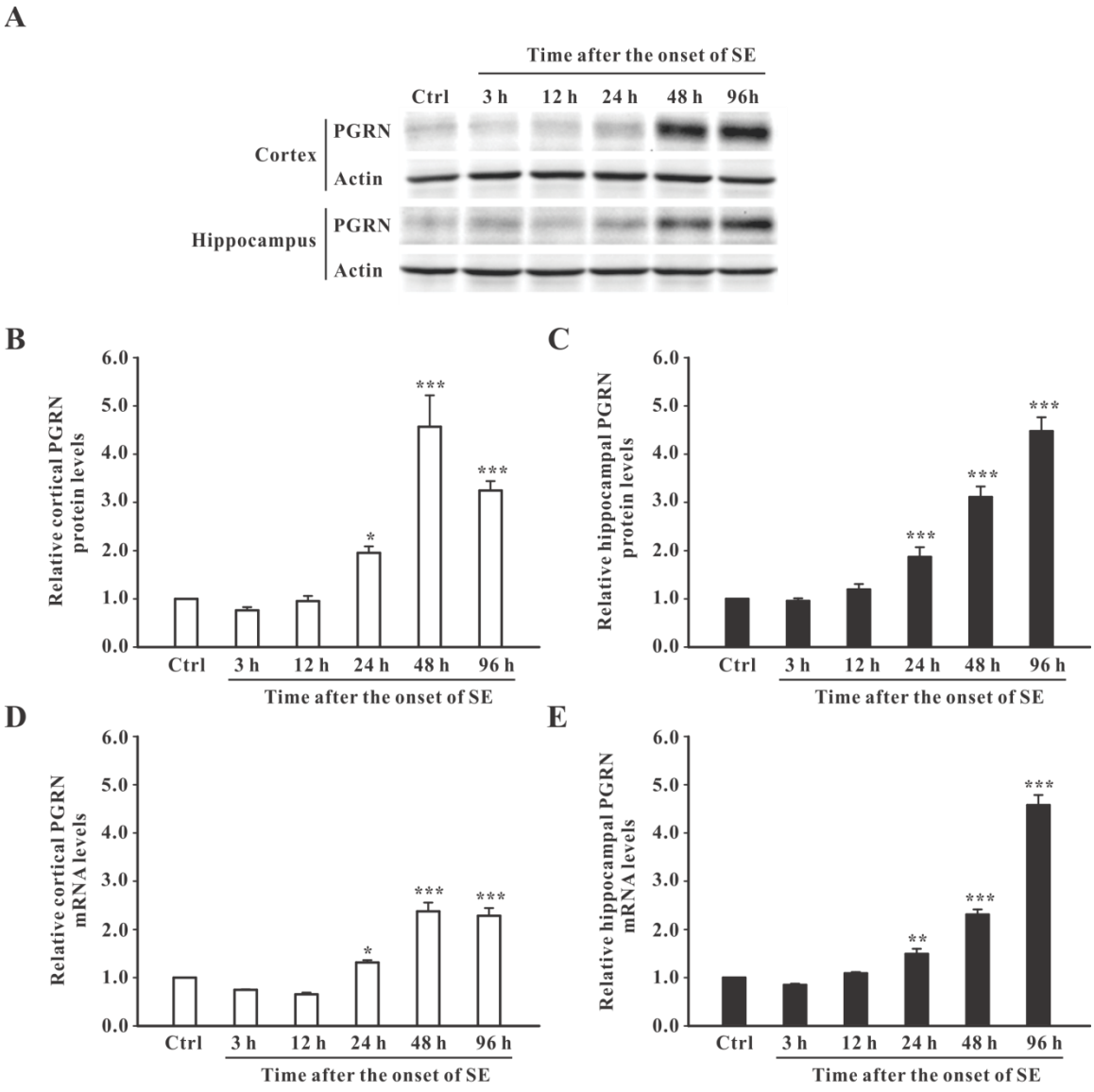
A
Time after the onset of SE
Ctrl
3 h
12 h
24 h
48 h
96h
Cortex
PGRN
Actin
Hippocampus
PGRN
Actin
B
Relative cortical PGRN protein levels
6.0
5.0
4.0
3.0
2.0
1.0
0.0
*
***
***
Ctrl
3 h
12 h
24 h
48 h
96 h
Time after the onset of SE
C
Relative hippocampal PGRN protein levels
6.0
5.0
4.0
3.0
2.0
1.0
0.0
***
***
***
Ctrl
3 h
12 h
24 h
48 h
96 h
Time after the onset of SE
D
Relative cortical PGRN mRNA levels
6.0
5.0
4.0
3.0
2.0
1.0
0.0
*
***
***
Ctrl
3 h
12 h
24 h
48 h
96 h
Time after the onset of SE
E
Relative hippocampal PGRN mRNA levels
6.0
5.0
4.0
3.0
2.0
1.0
0.0
**
***
***
Ctrl
3 h
12 h
24 h
48 h
96 h
Time after the onset of SE

Fig. 3.1 Induction of PGRN following SE.

SE was induced in rats intraperitoneally injected with pilocarpine. Total protein and mRNA were extracted from cortex and hippocampus from rats at 3, 12, 24, 48, 96 h following the onset of SE. **A**, Representative Western blots of PGRN and actin are shown. **B** and **C**, Densitometric measurements of PGRN immunoblots in panel A after normalized to the expression of actin. PGRN levels in non-SE control groups (con) were set to 1.0, and values of SE groups were expressed as relative fold change compared to control. PGRN protein levels from cortex (B) and hippocampus (C) were upregulated after the onset of SE at 24 h (n = 6), 48 h (n = 6), and 96 h (n = 5), but not at 3 h (n = 8) or 12 h (n = 5), compared with controls (n = 6). **D** and **E**, Quantitative real-time PCR assessment of PGRN mRNA levels in cortex (D) and hippocampus (E). The mRNA levels of control groups were set to 1.0, and mRNA levels of other groups were calculated as fold change compared to control group. PGRN mRNA levels were upregulated after the onset of SE at 24 h (n = 4), 48 h (n = 4), and 96 h (n = 4), but not at 3 h (n = 6) or 12 h (n = 4), compared with non-SE (n = 4). $^{*}p < 0.05$, $^{**}p < 0.01$, and $^{***}p < 0.001$ using one-way ANOVA.

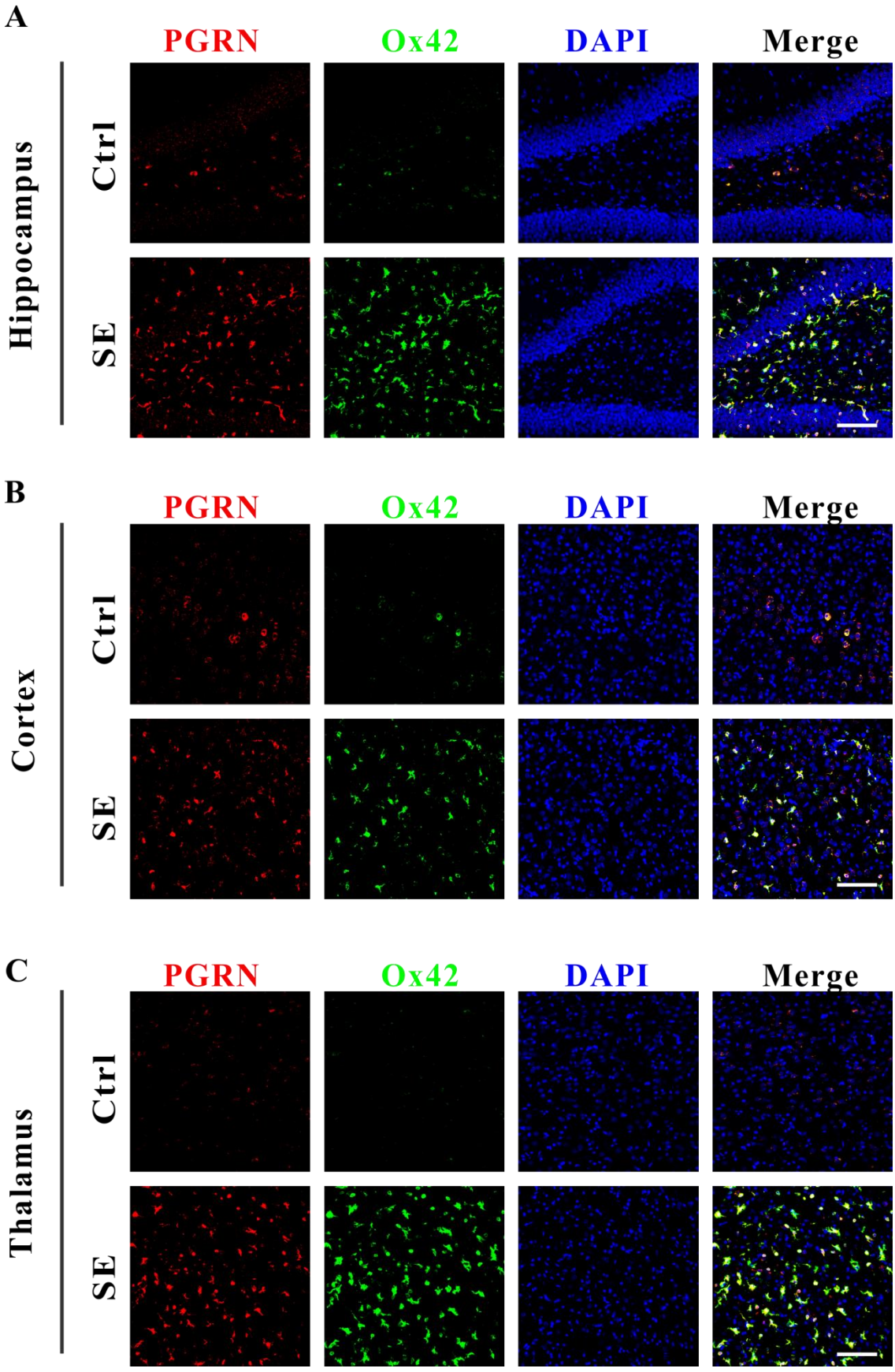
A
PGRN
Ox42
DAPI
Merge
Hippocampus
Ctrl
SE
B
PGRN
Ox42
DAPI
Merge
Cortex
Ctrl
SE
C
PGRN
Ox42
DAPI
Merge
Thalamus
Ctrl
SE

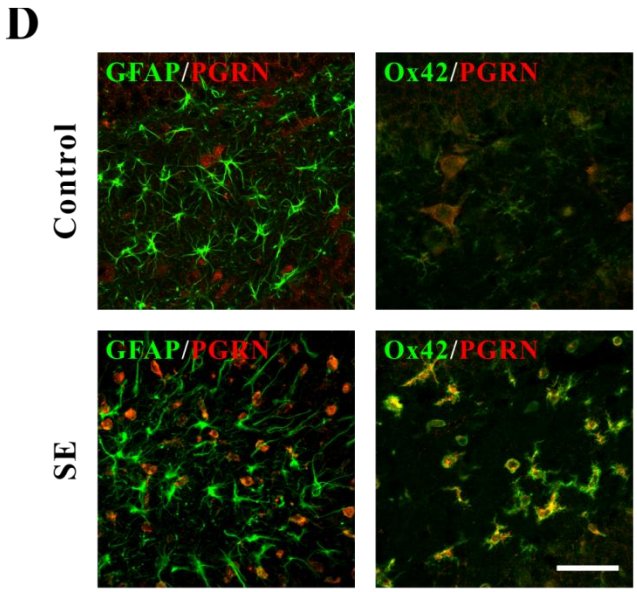

Fig. 3.2 The upregulation of PGRN-positive microglia after SE.

A-C, Representative sections from cortex (A), hippocampus (B) and thalamus (C) of non-SE control (ctrl) and of rats at 48 h after the onset of SE (SE) were double stained with anti-PGRN (red) and anti-Ox42 (green). DAPI (blue) was used to label the nucleus. Scale bar: 100 μm. **D**, High magnification of dentate gyrus immunostained with PGRN (red) and microglial marker Ox42 (green, left panels), or with PGRN (red) and astroglial marker GFAP (green, right panels). At 48 after the onset of SE (lower panels), upregulated PGRN was localized in microglia but not in astrocyte. Scale bar: 50 μm.

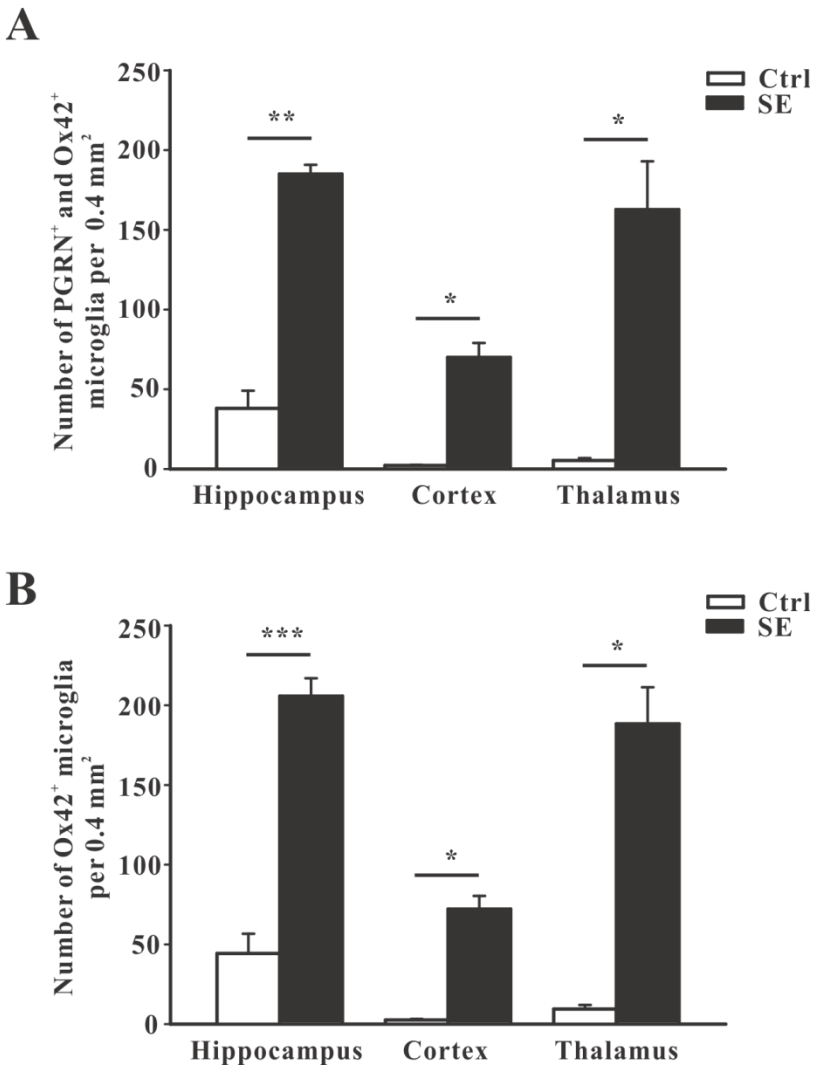

Fig. 3.3 Expression of PGRN in activated microglia.

The number of total microglia (B) and PGRN-positive microglia (A) per 0.4 square millimeter were quantified in specified regions of cerebrum (2 sections per rat and, $n = 3$ rats per group). $^{*}p < 0.05$, $^{**}p < 0.01$ and $^{*}p < 0.001$ compared with non-SE control using Student's *t* test.

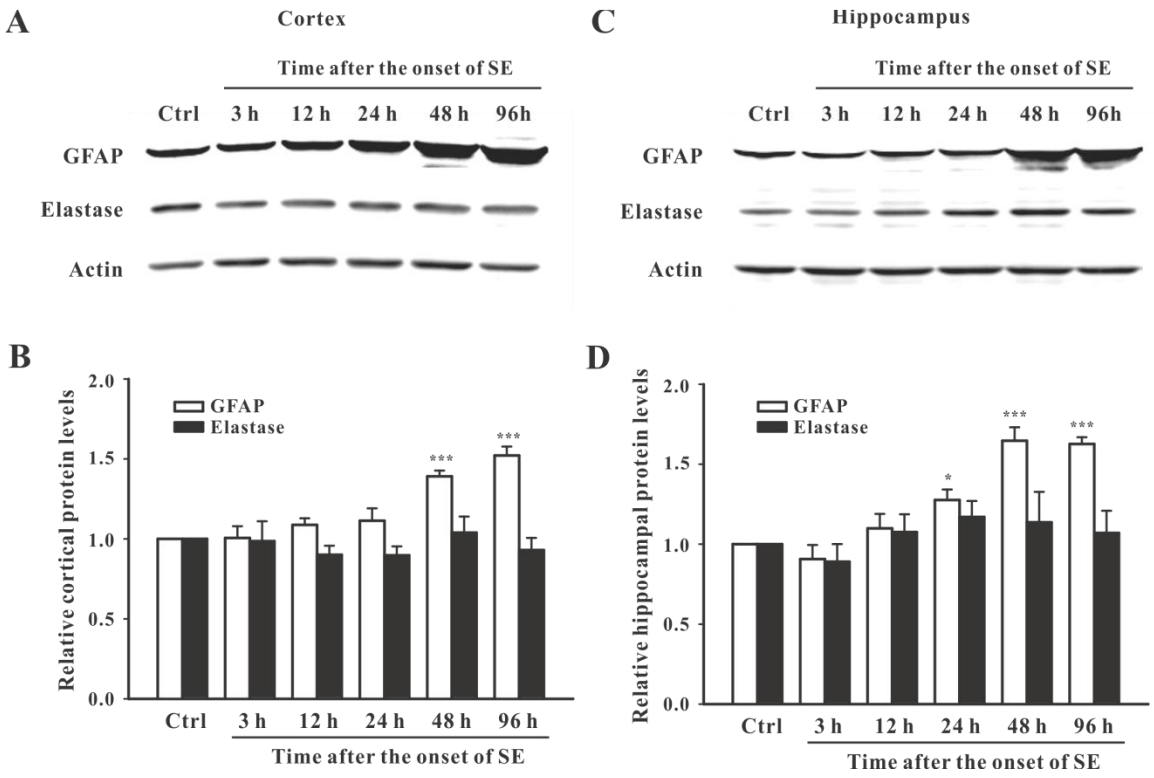

Fig. 3.4 Induction of GFAP and unaffected elastase levels following SE.

Total protein samples were extracted from cortex (A and B) and hippocampus (C and D) from rats at 3, 12, 24, 48, 96 h following pilocarpine-induced SE. Representative immunoblots of GFAP and elastase protein levels are shown in panel A (cortex) and panel C (hippocampus). The pooled data are shown in panel B (cortex) and panel D (hippocampus). Protein levels in non-SE control group were set to 1.0, and values of SE groups were expressed as relative fold change compared to control. $^{*}p < 0.05$ and $^{***}p < 0.001$ compared with non-SE control (ctrl) using one-way ANOVA. All values are averages of results from at least three animals.

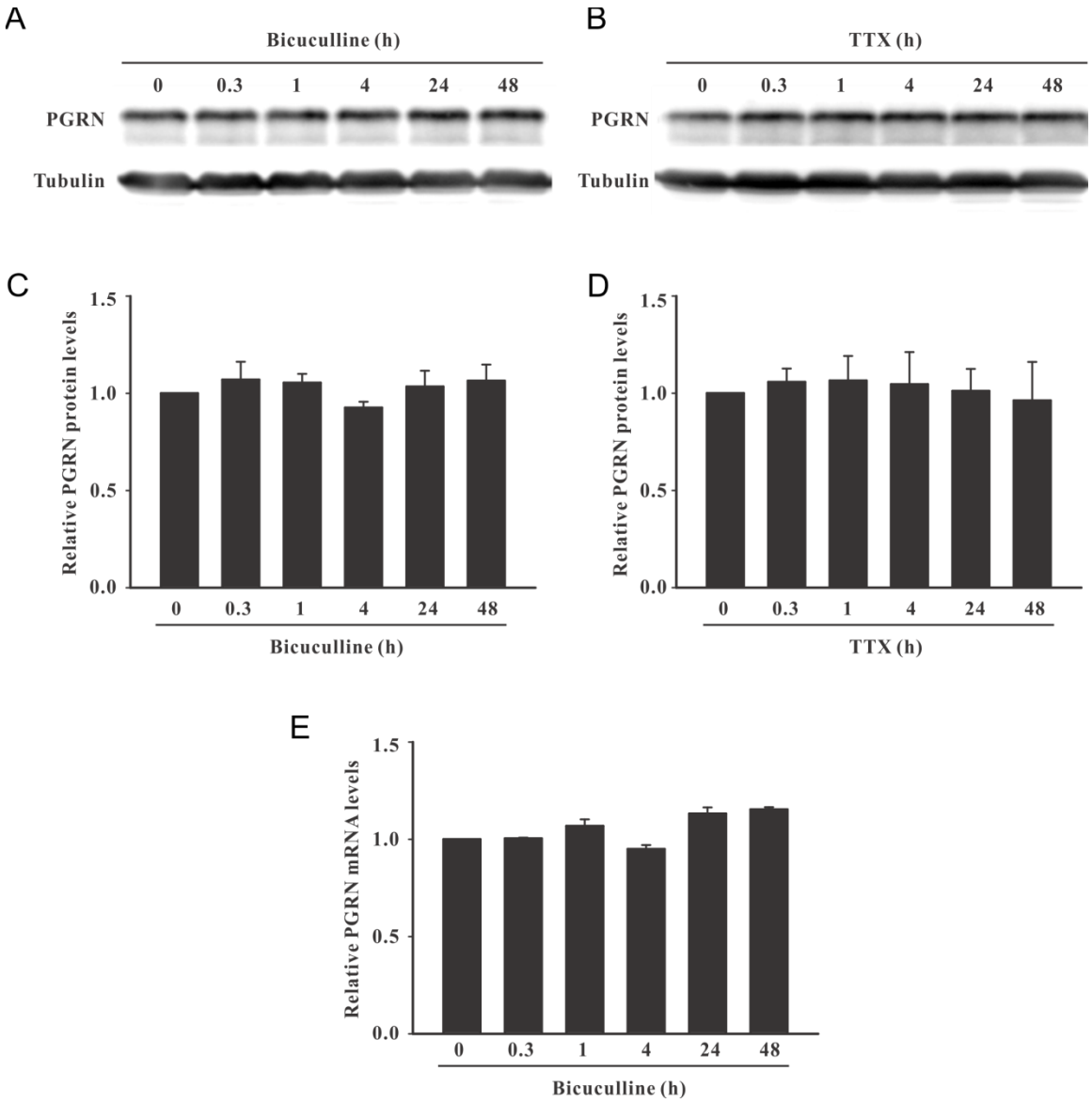
A
Bicuculline (h)
0
0.3
1
4
24
48
PGRN
Tubulin
B
TTX (h)
0
0.3
1
4
24
48
PGRN
Tubulin
C
Relative PGRN protein levels
1.5
1.0
0.5
0.0
0
0.3
1
4
24
48
Bicuculline (h)
D
Relative PGRN protein levels
1.5
1.0
0.5
0.0
0
0.3
1
4
24
48
TTX (h)
E
Relative PGRN mRNA levels
1.5
1.0
0.5
0.0
0
0.3
1
4
24
48
Bicuculline (h)

Fig. 3.5 Bicuculline or TTX had no effect on PGRN levels.

Bicuculline (50 μM) or TTX (2 μM) were added to cortical neuron cultures on DIV 10 for 48 h, on DIV11 for 24 h, and on DIV 12 for 4 h, 1 h and 0.3 h. Cultures with no treatment was considered as 0 h control. All groups were lysed on DIV 12 and analyzed with Western blots. **A**, Immunoblots of PGRN and beta-tubulin after bicuculline treatment are shown. **B**, Densitometric measurements of PGRN levels after normalized to beta-tubulin. PGRN levels in control group were set to 1.0, and values of bicuculline treatment groups were expressed as relative fold change compared to control. **C** and **D,** Following TTX treatment, immunoblots of PGRN and beta-tubulin are shown in panel C and the pooled data are shown in panel D. **E**, Quantitative real-time PCR assessment of PGRN mRNA levels after neurons were incubated for different time points with bicuculline. The mRNA levels of control groups were set to 1.0, and mRNA levels of other time points were calculated as fold change compared to control group. All values are averages of results from at least three separate experiments.

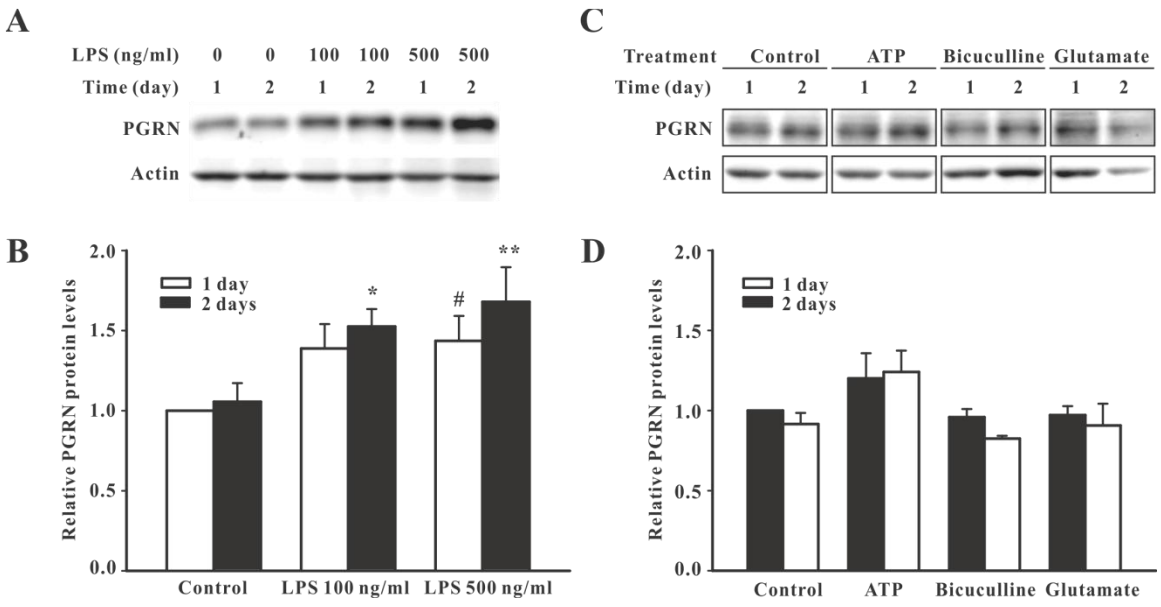

Fig. 3.6 Differential roles of LPS, ATP, bicuculline and glutamate on PGRN expression.

On DIV 3, drugs were added to mixed neuronal-glial cultures for one or two days. Untreated cultures were collected on the same day as 1-day control or 2-day control. Values are shown relative to those of 1-day control that were set to 1.0. **A** and **B**, PGRN and actin levels in cultures treated with 100 ng/mL or 500 ng/mL LPS were measured by Western blots. Representative immunoblots are shown in panel A and the pooled data are shown in panel B. $^{*}p < 0.05$ and $^{**}p < 0.001$ compared with 2-day control using one-way ANOVA, and $^{\#}p < 0.05$ compared with 1-day control using one-way ANOVA. **C** and **D**, representative immunoblots (C) and quantified results (D) of PGRN protein levels in cultures treated with ATP (50 μM), bicuculline (50 μM), and glutamate (1 mM). These treatments induced no statistically significant difference of PGRN when compared with 1-day control or 2-day control. All values are averages of results from at least three separate experiments.

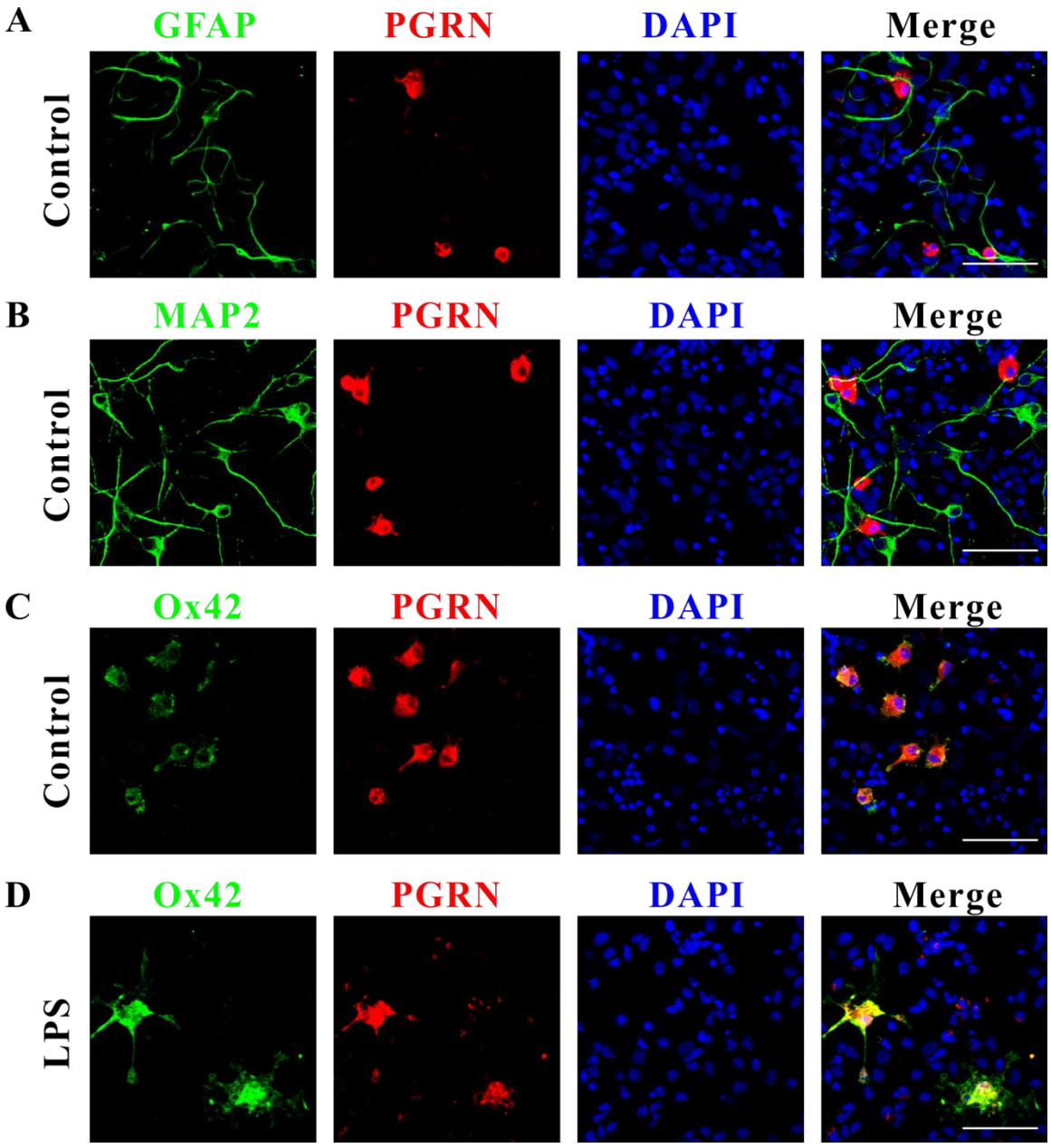
A
GFAP
PGRN
DAPI
Merge
Control
B
MAP2
PGRN
DAPI
Merge
Control
C
Ox42
PGRN
DAPI
Merge
Control
D
Ox42
PGRN
DAPI
Merge
LPS

Fig. 3.7 The localization of PGRN in microglia in mixed culture.

Panels A, B and C shows PGRN (red) double staining with astrocyte marker (GFAP, green, **A**), neuron marker (MAP2, green, B), and microglial marker (Ox42, green, C) in control cultures. **D**, Double staining of PGRN (red) and Ox42 (green) in cultures subjected to LPS (500 ng/ml) for 2 days. Note that PGRN immunoreactivity in neuron is not visible due to the low exposure required for PGRN-ir microglia. DAPI (blue) was used to label the nucleus. Scale bar is for 50 μm in all images.

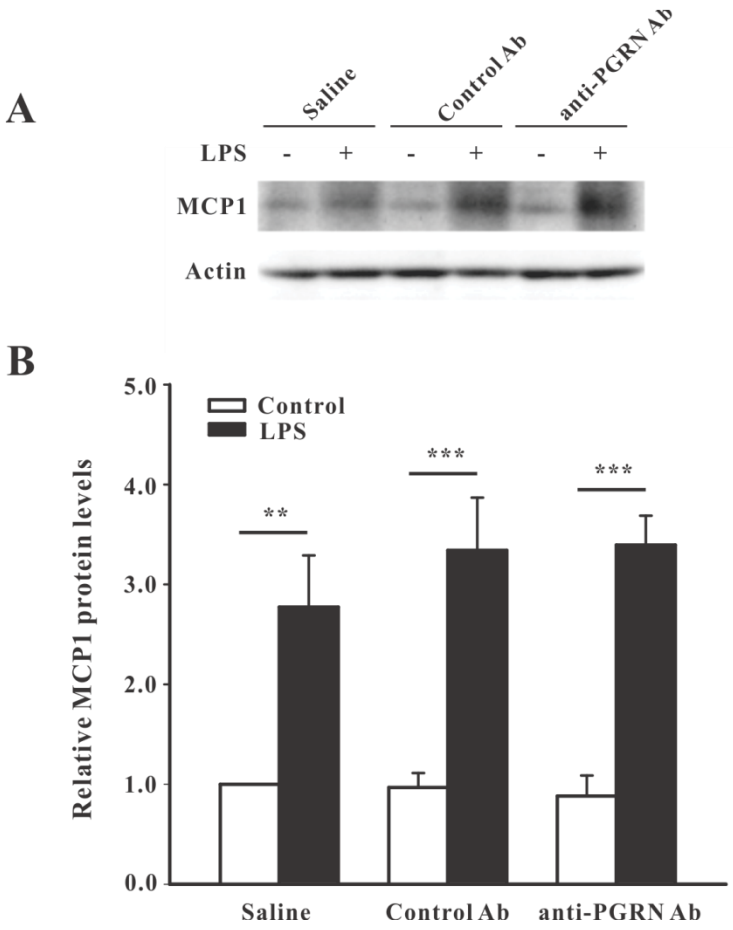

Fig. 3.8 Anti-PGRN antibody did not change LPS-induced MCP-1 expression.

On DIV 3, mixed neuronal-glial cultures were pre-incubated for one hour with sheep anti-PGRN Ab (1 μg/mL), control Ab (sheep IgG, 1 μg/mL), or saline control. Cultures were then stimulated with LPS (500 ng/mL) or vehicle control (control) for 2 days. Western blot assessment of MCP-1 and actin are shown in panel A, and the pooled data are shown in panel B. Values were shown relative to those of untreated saline control that were set to 1.0. $^{**}p < 0.01$ and $^{***}p < 0.001$ using one-way ANOVA. All values are averages of results from at least three separate experiments.

A

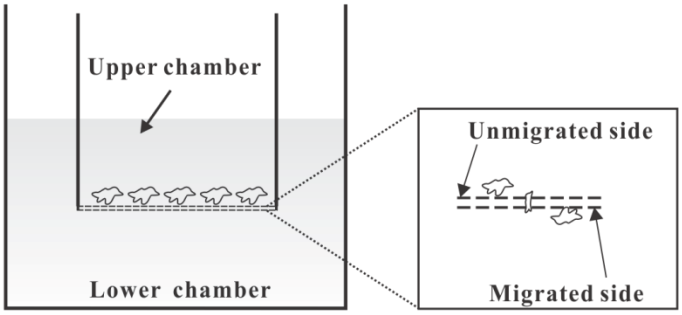
Upper chamber
Lower chamber
Unmigrated side
Migrated side

B

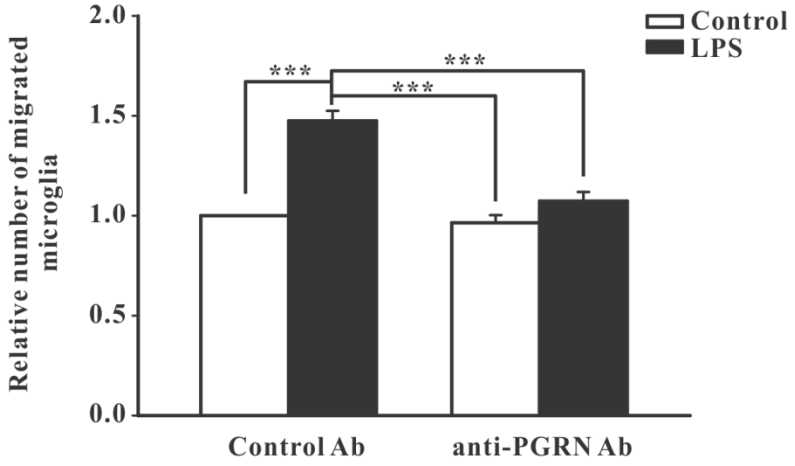
Relative number of migrated microglia
2.0
1.5
1.0
0.5
0.0
Control
LPS
***
***
***
Control Ab
anti-PGRN Ab

C

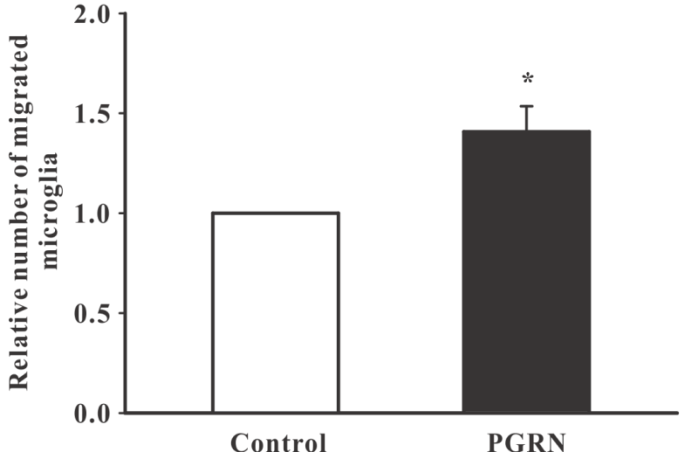
Relative number of migrated microglia
2.0
1.5
1.0
0.5
0.0
*
Control
PGRN

Fig. 3.9 *In vitro* transwell measurement of microglial migration in response to anti-PGRN Ab or PGRN protein.

A, Schematic diagram of transwell assay testing the migration of microglia is adapted from (Ryu et al., 2009). **B**, Control Ab (sheep IgG, 1 μg/mL) or sheep anti-PGRN Ab (1 μg/mL) was added to the upper chamber for 1 h, then LPS or vehicle control was added to the lower chamber for 24 h. The number of migrated microglia on the migrated side was counted and expressed as fold change to control groups (upper chamber: control Ab; lower chamber: vehicle control). $^{***}p < 0.001$ using one-way ANOVA. **C**, 100 ng/mL PGRN protein or BSA (control) was added to the lower chamber for 24 h, and the number of migrated microglia on the migrated side was counted and expressed as fold change to BSA control group. $^{*}p < 0.05$ using paired Student's *t* test. All values are averages of results from at least three separate experiments.

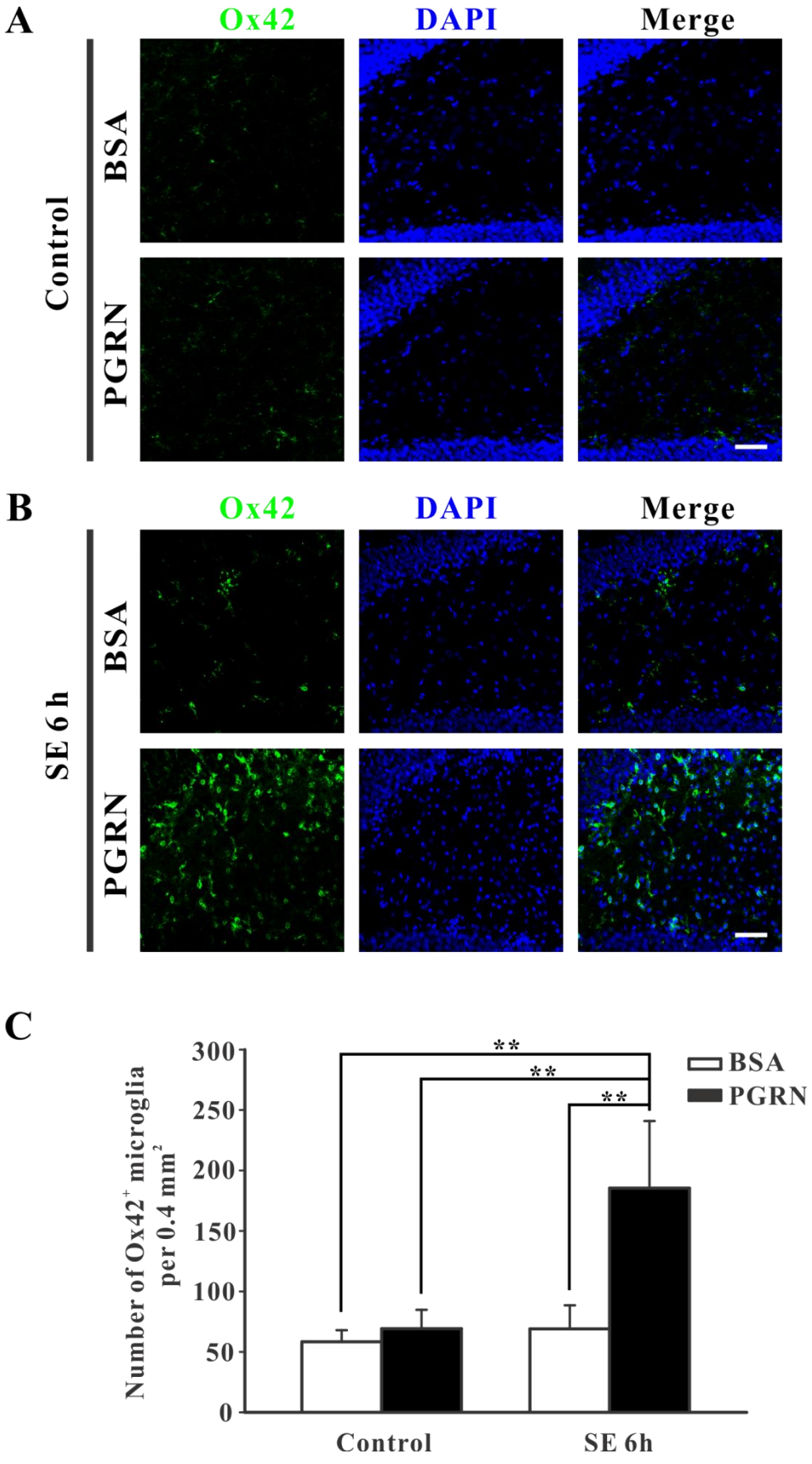
A
Ox42
DAPI
Merge
Control
BSA
PGRN
B
Ox42
DAPI
Merge
SE 6 h
BSA
PGRN
C
Number of Ox42+ microglia per 0.4 mm2
300
250
200
150
100
50
0
**
**
**
BSA
PGRN
Control
SE 6h

Fig. 3.10 Administration of PGRN increased the number of microglia at 6 h following seizure.

A and **B**, Sterilized PGRN (100 ng, bottom row in A and B) or BSA (100 ng, top row in A and B) were injected into each side of the hippocampus before seizure induction. Representative Ox42-immunoreactive (green) sections from animals at 6 h following the onset of SE (B) or control (A) are shown. Control animals received injection of vehicle instead of pilocarpine. DAPI (blue) was used to label the nucleus. Scale bar is for 50 μm in all images. **C**, The number of total microglia per 0.4 square millimeter were quantified in hippocampus (n = 5 animals for control, n = 3 animals for 6 h SE group). $^{**}p < 0.01$ using one-way ANOVA.

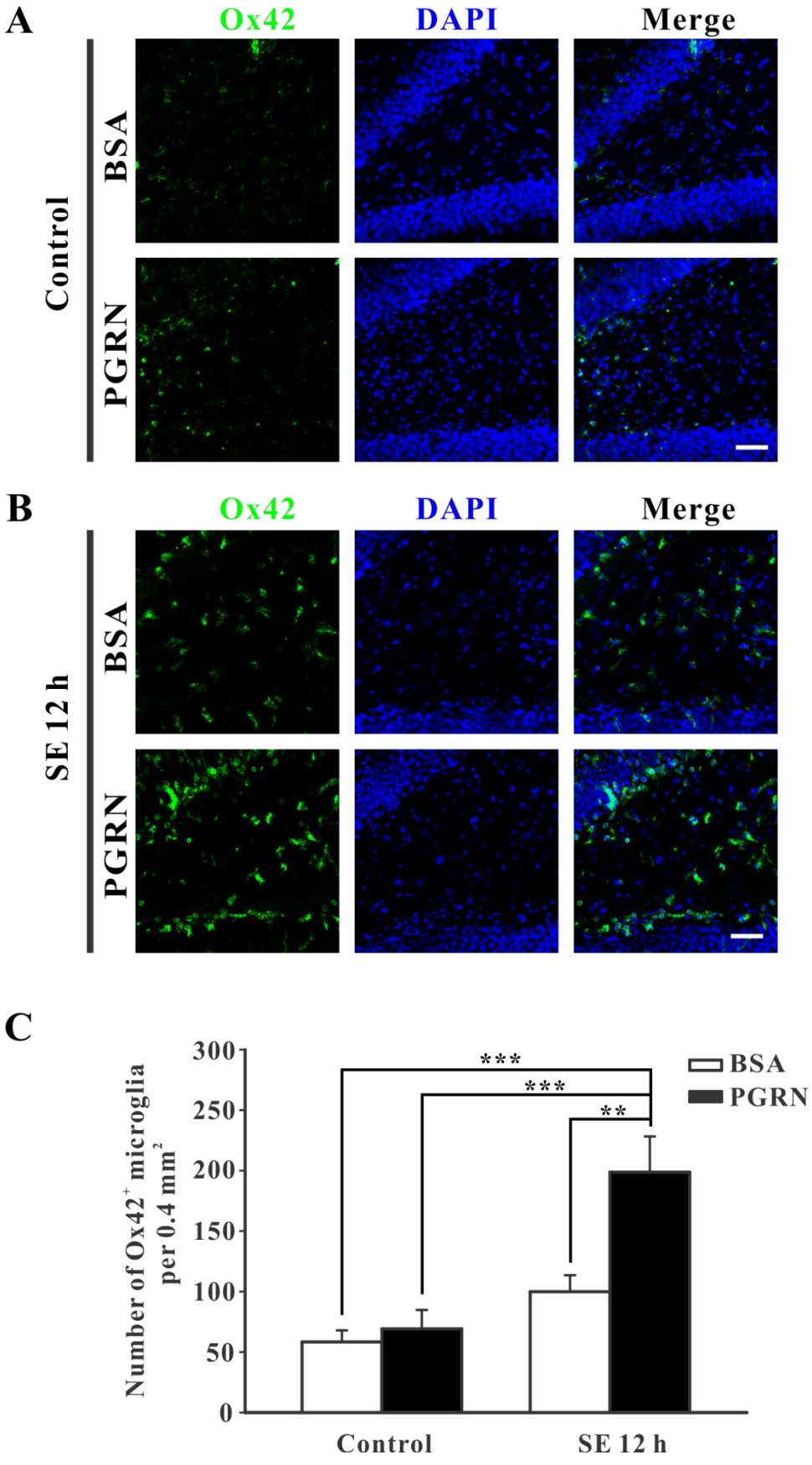
A
Ox42
DAPI
Merge
Control
BSA
PGRN
B
Ox42
DAPI
Merge
SE 12 h
BSA
PGRN
C
Number of Ox42+ microglia per 0.4 mm2
300
250
200
150
100
50
0
***
***
**
BSA
PGRN
Control
SE 12 h

Fig. 3.11 Administration of PGRN increased the number of microglia at 12 h following seizure.

A and **B**, PGRN (100 ng, bottom row in A and B) or BSA (100 ng, top row in A and B) were injected into each side of the hippocampus before seizure induction. Representative Ox42-immunoreactive (green) sections from animals at 12 h following the onset of SE (B) or control (A) are shown. Control animals were administered with same volume of saline instead of pilocarpine. DAPI (blue) was used to label the nucleus. Scale bar is for 50 μm in all images. **C**, The number of total microglia per 0.4 square millimeter were quantified in hippocampus (n = 5 animals for control, n = 4 animals for 12 h SE group). $^{**}p < 0.01$ and $^{***}p < 0.001$ using one-way ANOVA.

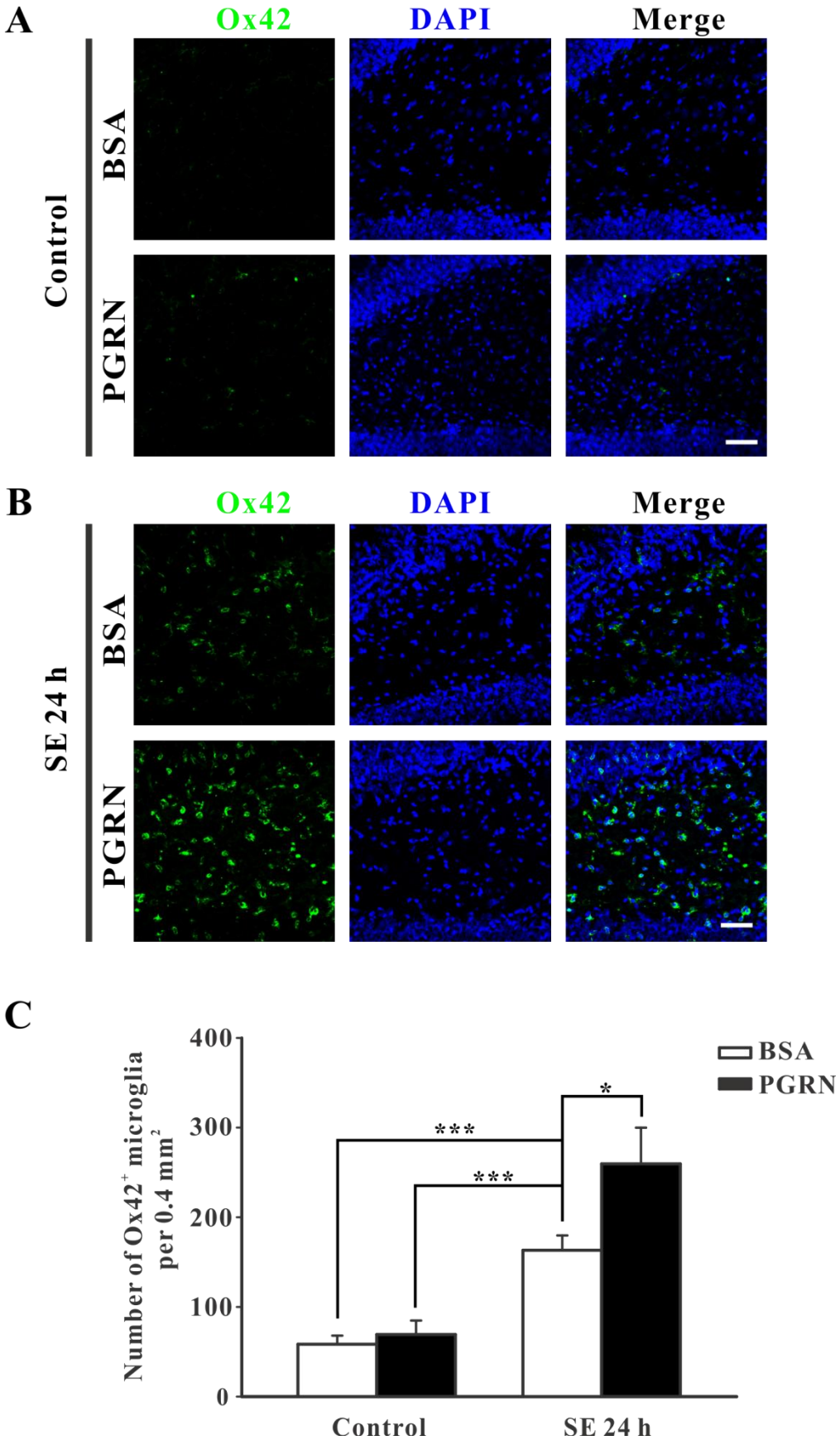
A
Ox42
DAPI
Merge
Control
BSA
PGRN
B
Ox42
DAPI
Merge
SE 24 h
BSA
PGRN
C
Number of Ox42+ microglia per 0.4 mm2
400
300
200
100
0
BSA
PGRN
***
***
*
Control
SE 24 h

Fig. 3.12 Administration of PGRN increased the number of microglia at 24 h following seizure.

A and **B**, Sterilized PGRN (100 ng, bottom row in A and B) or BSA (100 ng, top row in A and B) were injected into each side of the hippocampus before seizure induction. Representative Ox42-immunoreactive (green) sections from animals at 24 h following the onset of SE (B) or control (A) are shown. Control animals received injection of vehicle instead of pilocarpine. DAPI (blue) was used to label the nucleus. Scale bar is for 50 μm in all images. **C**, The number of total microglia per 0.4 square millimeter were quantified in hippocampus (n = 5 animals for control, n = 3 animals for 24 h SE group). $^{*}p < 0.05$ and $^{***}p < 0.001$ using one-way ANOVA.

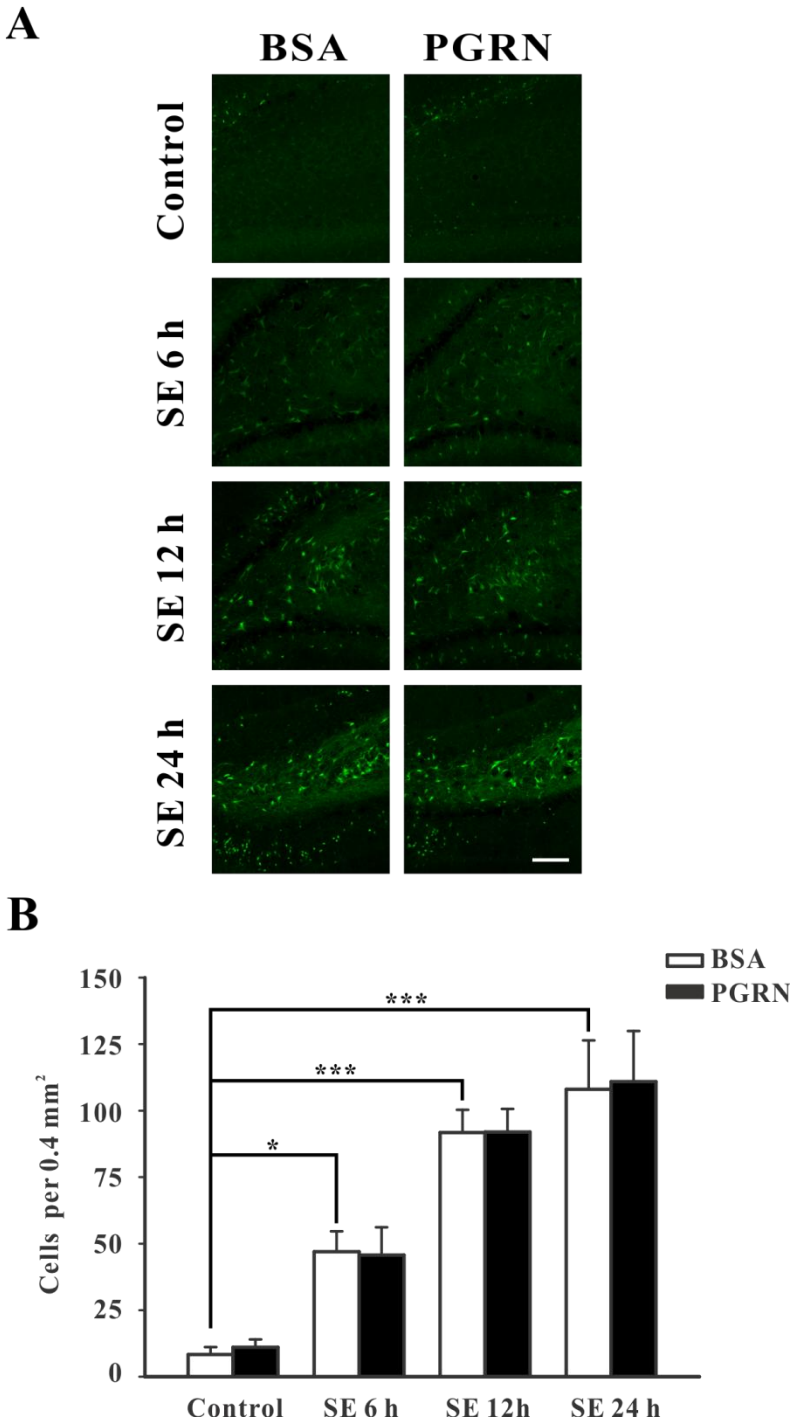
A
BSA
PGRN
Control
SE 6 h
SE 12 h
SE 24 h
B
BSA
PGRN
150
125
100
75
50
25
0
Cells per 0.4 mm²
***
***
*
Control
SE 6 h
SE 12h
SE 24 h

Fig. 3.13 Injection of PGRN had no effect on the number of degenerating cells.

Sterilized PGRN (100 ng) or BSA (100 ng) were injected bilaterally into hippocampus before seizure induction. At 6 h (n = 5), 12 h (n = 5) and 24 h (n = 3) after SE initiation, brain sections were stained with Fluoro-Jade B and the number of positively stained cells in the hilus of dentate gyrus were counted. Control animals (n = 6) received injection of vehicle instead of pilocarpine. Representative brain sections are shown in panel A (scale bar: 100 μm). The pooled data are shown in panel B. $^{*}p < 0.05$ and $^{***}p < 0.001$ using one-way ANOVA.

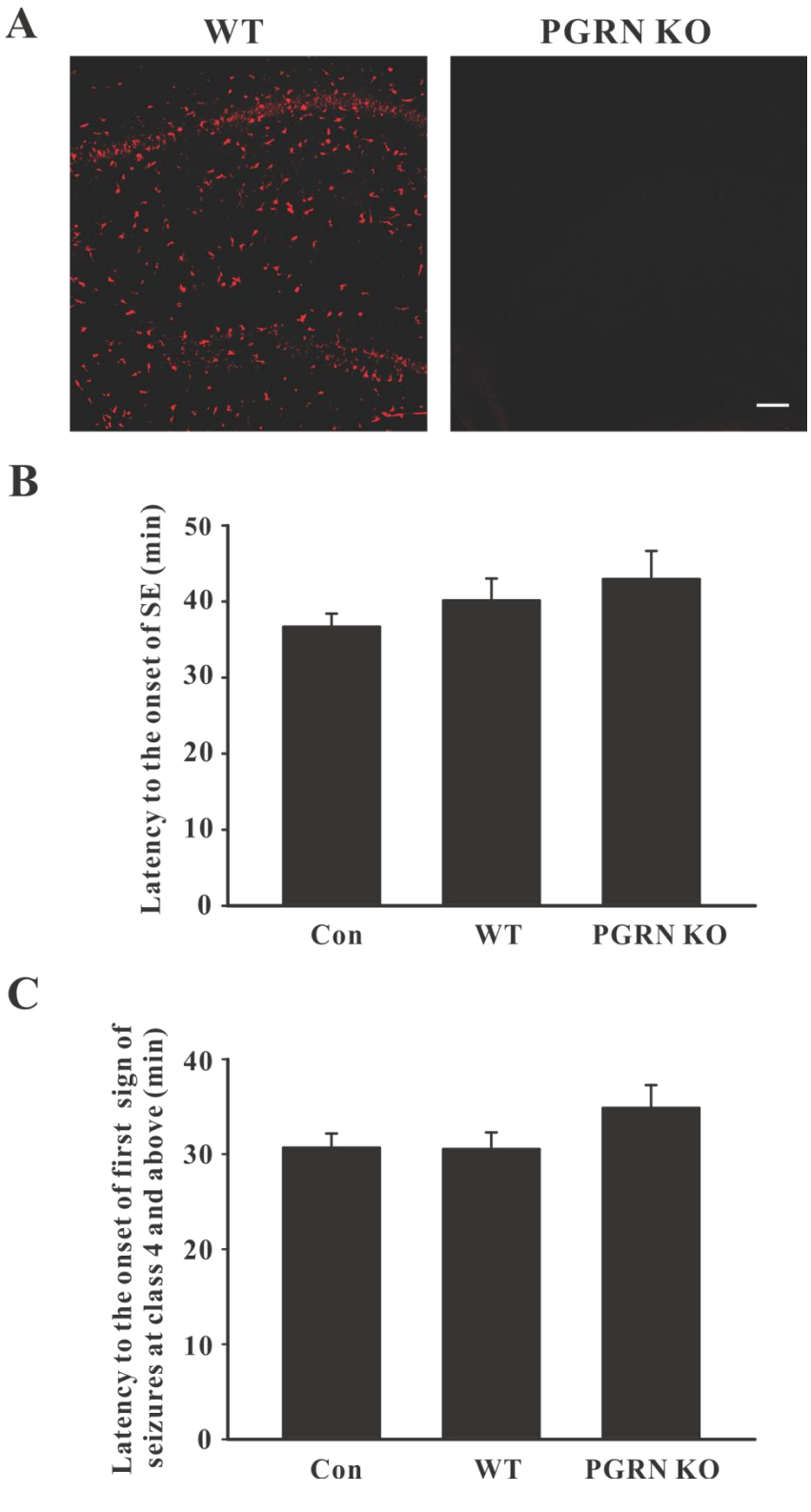
A
WT
PGRN KO
B
Latency to the onset of SE (min)
50
40
30
20
10
0
Con
WT
PGRN KO
C
Latency to the onset of first sign of seizures at class 4 and above (min)
40
30
20
10
0
Con
WT
PGRN KO

Fig. 3.14 The development of seizures was not changed in PGRN knockout mice.

A, Immunohistochemical staining of PGRN in brain sections from wildtype mice (WT) and PGRN knockout mice (PGRN KO) at 48 h after SE induction. **B**, The time from pilocarpine injection to the onset of SE in normal C57BL/6 mice (Con, *n* = 14), wildtype littermate (WT, *n* = 10) and PGRN knockout mice (PGRN KO, *n* = 11). **C**, The time between pilocarpine injection and the first sign of seizure behaviors at class 4 and above (Racine's scale) was shown for normal C57BL/6 mice (Con, *n* = 14), wildtype littermate (WT, *n* = 10) and PGRN knockout mice (PGRN KO, *n* = 12). Scale bar is for 100 μm in B and C. There is no significant difference among all three groups (B or C) using one-way ANOVA.

A

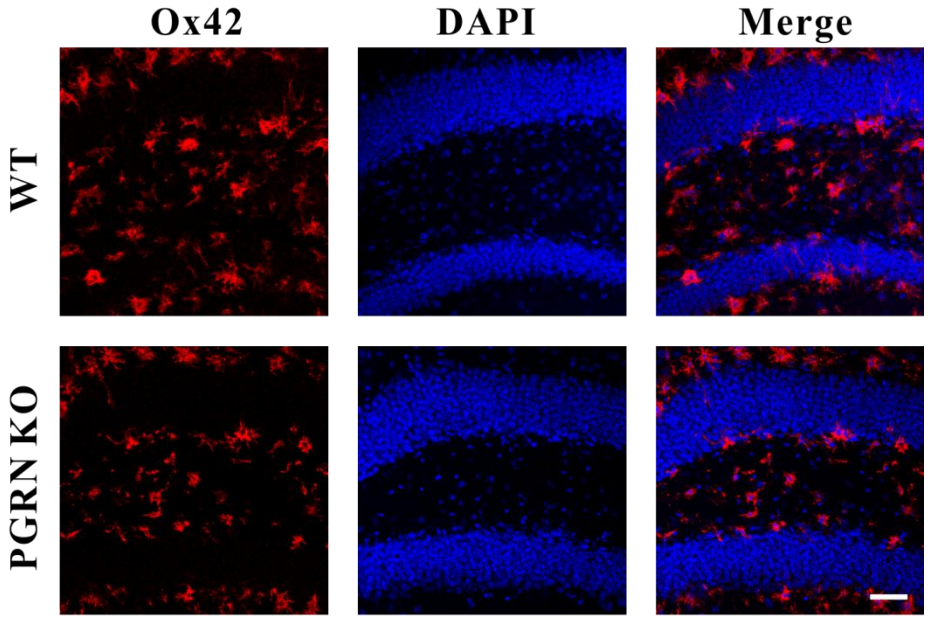
Ox42
DAPI
Merge
WT
PGRN KO

B

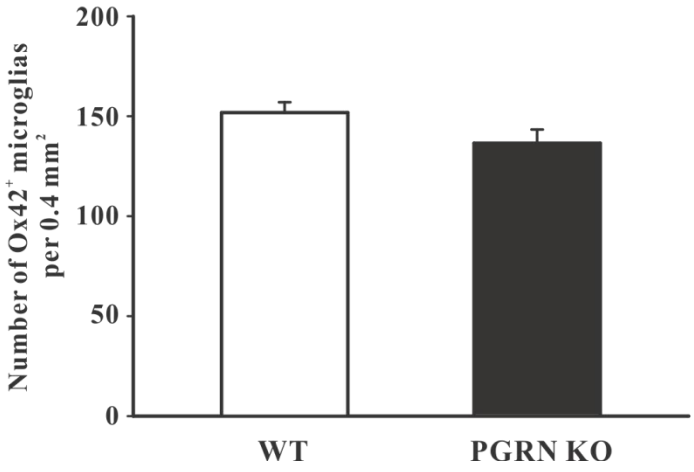
Number of Ox42+ microglias per 0.4 mm2
200
150
100
50
0
WT
PGRN KO

Fig. 3.15 SE-induced microglial activation in PGRN knockout mice was not significantly different from WT mice.

A, At 48 h following the onset of SE, dentate gyrus of PGRN knockout mice (PGRN KO, $n = 3$) and wildtype mice (WT, $n = 3$) were immunostained with anti-Ox42 antibody. DAPI was used to label nucleus. Scale bar is for 50 μm. **B**, The number of microglial cells at 48 h SE in dentate gyrus was counted. $p = 0.15$ between PGRN KO and WT groups using Student's *t* test.

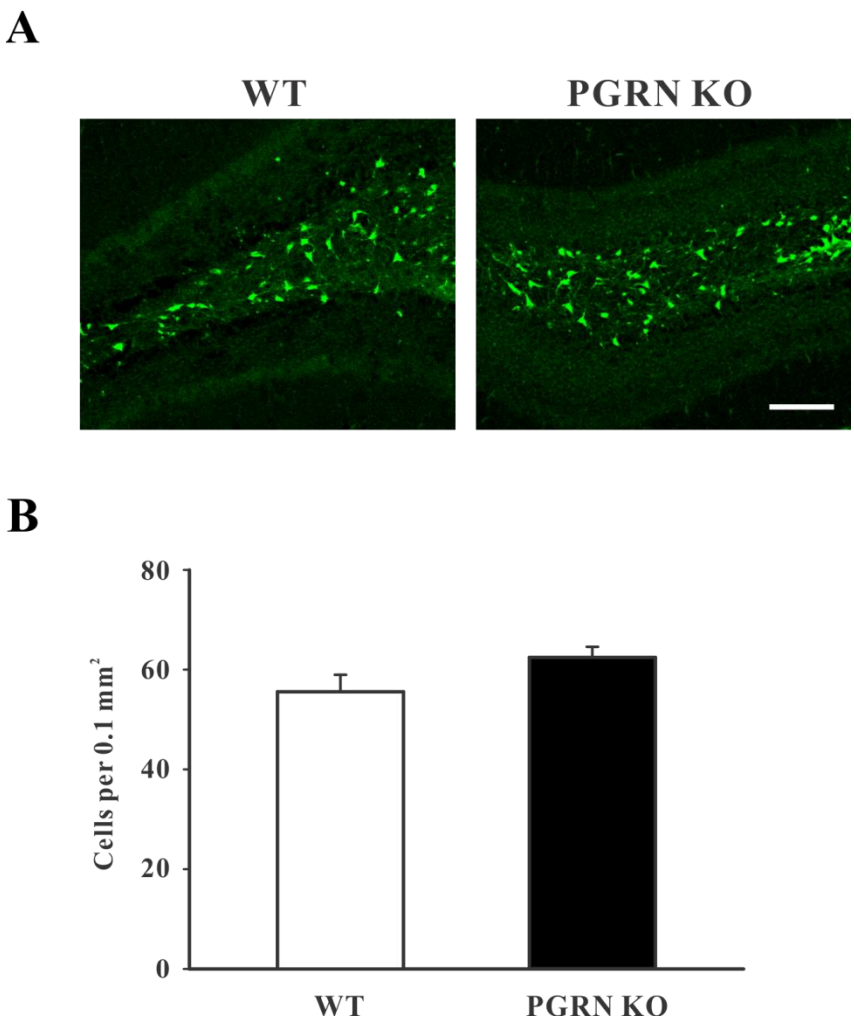

Fig. 3.16 Cell death induced by SE was not affected in PGRN knockout mice.

A, Representative Fluoro-jade B staining of dentate gyrus sections from PGRN knockout mice (PGRN KO, n = 3) and wildtype mice (WT, n = 3) at 48 h following the onset of SE (Scale bar: 100 μm). **B**, The number of Fluoro-jade B positive degenerating cells in hilus region at 48 h SE was counted. p = 0.16 between PGRN KO and WT groups using Student's t test.

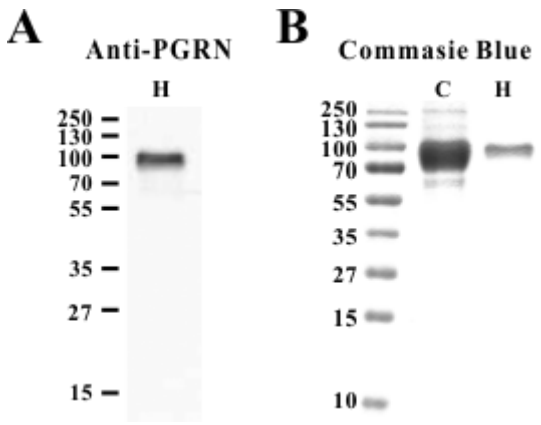

Fig. 3.17 Verification of recombinant PGRN protein.

A, Western blots with anti-PGRN antibody on HPLC-purified PGRN. **B**, Commasie-blue staining of SDS-Polyacrylamide gel. C: 2.5 μg crude PGRN in PBS from Ni-NTA purification system; H: 150 ng HPLC-purified PGRN. At least three repeats were conducted.

CHAPTER FOUR: PRELIMINARY STUDIES ON THE ROLE OF PGRN IN GLUTAMATE-INDUCED RELEASE FROM CULTURED ASTROCYTES.

4.1 Summary of findings in chapter four

In Chapter 3, we observed that GFAP and PGRN levels are both upregulated in the same time frame (48 and 96 h) after seizures. We also found that PGRN was induced in microglia but not in GFAP-positive astrocytes. However, activation of astrocytes was found in aged PGRN deficient mice (Yin et al., 2010), suggesting a possibility that PGRN might play a role in astrocytes. Since PGRN is a secretable glycoprotein and exogenous PGRN can be endocytosed (Hu et al., 2010), we postulate that PGRN produced in microglia and neurons might be secreted and affect neighboring astrocytes. Here we found that PGRN protein was expressed in cultured astrocytes. Using lentiviral vectors expressing siRNA to knock down PGRN, we found that glutamate-induced lactate release was abolished. In addition, glutamate-induced uptake of radioactive glucose was reduced by PGRN siRNA, and the protein levels of MCT1 were slightly decreased in glutamate-treated astrocytes with PGRN knocked down. Our results suggest the role of PGRN in glycolytic metabolism in cultured astrocytes.

4.2 Introduction

Nonoxidative utilization of glucose is greatly increased upon neuronal activation occurring in seizures or in physiological stimulations. Cerebral glucose utilization has been shown to be increased during ictal seizures and decreased following ictal seizures

(Engel et al., 1982). Nonoxidative metabolic fluxes, which could be neglected in normal conditions, rapidly increase and account for about one third of the total glucose utilization during bicuculline-induced seizures (Patel et al., 2004). Ictal increase of lactate concentration was also reported in human brain regions following seizure activities (Bolwig and Quistorff, 1973; During et al., 1994). These data suggest that energy provided by nonoxidative metabolism of glucose is a critical portion for balancing the energy demand during seizures. Physiological visual or somatosensory stimulations can also raise lactate concentration and nonoxidative glucose consumption (Fox and Raichle, 1986; Fox et al., 1988; Ogawa et al., 1990; Prichard et al., 1991; Sappey-Marinier et al., 1992).

The nonoxidative utilization of glucose during physiological or pathological activation of neurons had been explained by the astrocyte-neuronal lactate shuttle hypothesis (ANLSH) first proposed by Dr Magistretti and Pellerin (Pellerin and Magistretti, 1994). They first found that glutamate activated glucose uptake into astrocytes, and the subsequent metabolism of glucose mainly produced lactate (Pellerin and Magistretti, 1994). Combined with many other supporting evidences, they proposed that glycolysis in astrocytes is coupled with neuronal glucose metabolism by providing lactate to neurons when neurons were activated (Pellerin et al., 2007). In addition, astrocytes are the only cell type in brain that store glycogen, which can be broken down into glucose for glycolysis when there is acute energy demand in conditions such as seizure or ischemia (Cloix and Hevor, 2009; Pellerin et al., 2007; Rossi et al., 2007).

It was recently found that serum concentrations of PGRN were elevated in obese individuals and patients with increased plasma glucose (Yoon et al., 2009), suggesting a

potential role of PGRN in glucose metabolism. Therefore, our initial attempt to verify PGRN's function in astrocytes was to test the role of PGRN in nonoxidative glucose metabolism in primary astrocyte cultures.

4.2 Methods

4.2.1 Preparation of astrocyte cultures

Astrocyte culture was prepared from Cortices from 1-day-old Sprague Dawley rat brain as previously described (Allaman et al., 2004; McCarthy and de Vellis, 1980). Briefly, after removal of meninges, the cerebrums were minced, homogenized in a tissue grinder (Fischer), and passed through a filter mash (90 μm). Cells were seeded on poly-D-lysine-coated 75 cm^2 flasks at a density of 2-3 $\times 10^6$ per flask. After 7-10 days, astrocytes grew to 100 % confluent monolayer in DMEM (Gibco) supplemented with 10% fetal bovine serum and 1% (vol/vol) penicillin/streptomycin. Confluent astrocytes were trypsinized and frozen in liquid nitrogen. On experiment day (DIV 1), astrocytes were thawed and seeded on 6 well plates in DMEM (Gibco) supplemented with 10% fetal bovine serum and 1% (vol/vol) penicillin/streptomycin at a density of 4-5 $\times 10^5$ per well in 6-well culture plate. Medium was changed twice a week and maintained in a humidified chamber with 5% CO2/95% air. More than 90% of the cells yielded by this protocol are GFAP-positive astrocytes.

4.2.2 Infection of lentiviral vectors expressing PGRN siRNA and scrambled siRNA

On DIV 7, astrocyte was more than 80% confluent and was infected with lentiviral vectors expressing PGRN siRNA (siRNA) or scrambled siRNA (sc). The lentiviral

vectors were designed and prepared by Aobo Guo as stated in Guo's publication (Guo et al., 2010).The sequence of PGRN siRNA was 5'-GACAGAGTGCATTGCTGTC-3' and that of scrambled siRNA was 5'-GCCTATGGTCACAGGTAGT-3'. Preparation, trituration and infection of lentivirus were the same as those written in Chapter two. The titer we used were 5 MOI (Multiplicity of Infection = ratio of infectious virus particles to cells).

4.2.3 Treatment of cultured astrocytes

On DIV 21, PGRN protein (120 ng/ml) was added to "PGRN protein" groups for 1 day and was maintained throughout all incubations the next day. On DIV 22, cultured astrocytes were treated as previously described (Pellerin and Magistretti, 1994). Culture medium was replaced with D5 medium: DMEM (Sigma_D5030) supplemented with 5 mM glucose, 44 mM NaHCO3 and 1 % (vol/vol) penicillin/streptomycin. After 2 h incubation, culture medium was replaced with 2 ml D5 medium with or without 0.3 mM glutamic acid and incubated for another 30 min.

4.2.4 Measurement of lactate release

After treatment, supernatant was collected and lactate concentration was measured using a enzymatic assay following the manufacturer's instructions (Biomedical Research Service, Buffalo, NY, USA) as previously described (Allaman et al., 2004). Briefly, to each aliquot of 20 µl culture medium, 50 µl lactate assay solution in the kit was added. The plate was then incubated in a humidified 37 ℃ incubator for 30-60 min. The reaction was stopped by adding 50 µl 3 % acetic acid. The absorbance was read at 485 nm and

absolute values was calculated from a standard curve. The lactate concentration was normalized to the total protein amount in the cultured cells.

4.2.5 Western blots

After treatment, cultured astrocytes were rinsed in ice-cold PBS and homogenized with 1x sample buffer (124 mM pH 6.8 Tris-HCl, 50% glycerol, 4% SDS, 0.08% Bromophenol blue). Protein concentrations were tested with RC DC™ protein assay kit (Bio-Rad, Hercules, CA). Cell lysates was analyzed by Western blots as described in Chapters two and three. Primary antibody we used are: rabbit polycolonal anti-MCT1 antibody (1:1000, Millipore, Billerica, MA, USA), sheep polycolonal anti-PGRN antibody (1:1000, R&D Systems, Minneapolis, MN, USA), rabbit polycolonal anti-GFAP (1:5000, Santa Cruz Biotechnology CA, USA), anti-actin antibody (1:2000, Cell signal technology, Danvers, MA, USA).

4.2.5 [^{3}H]2DG uptake

Glucose uptake was measured as previously described (Allaman et al., 2004). After 2 h pre-incubation of D5 medium on DIV 22, culture medium in each group was replaced with 2 mL D5 medium containing 4 μCi/mL deoxy-d-glucose 2-[1,2–3H(N)] ([3H]2DG) (PerkinElmer) with or without glucose transporter inhibitor cytochalasin B (25 μM). After 30 min incubation, the supernatant culture medium was saved on ice for detection of lactate release as described above. Cells were rinsed three times with ice-cold PBS and lysed with 1 mL 10 mM NaOH/0.1% Triton X-100. The radioactivity in aliquots of 400 μl lysates was analyzed by liquid scintillation counting. Protein concentration of the lysates was determined as described above. The total radioactive counts were subtracted

by the counts in wells treated with cytochalasin B, and thus represented the amount of glucose uptake mediated by glucose transporters. The results in each group were divided by protein content and were then normalized to the value of sc-control group which was set to 1.0.

4.3 Results

Interestingly, we found that PGRN was expressed in cultured astrocytes. Our lab has previously constructed a lentiviral vector expressing PGRN siRNA (siRNA) which efficiently knocked down PGRN and has used a lentiviral vector expressing scrambled siRNA (sc) as a control (Fig. 4.1C) (Guo et al., 2010). PGRN knock down did not affect basal levels of lactate (siRNA at 0.86 ± 0.08 fold compared to sc, $p = 0.37$, Fig. 4.1A). We then examined whether PGRN contributed to glutamate-induced lactate release. Consistent with previous work (Pellerin and Magistretti, 1994), we found that lactate release was greatly increased by glutamate treatment in cultured astrocytes ($p < 0.01$, sc-glutamate at 1.54 ± 0.08 fold compared to sc, Fig. 4.1A). Interestingly, knocking down PGRN abolished the effect of glutamate on lactate release (p = 0.32, siRNA-glutamate at 1.15 ± 0.10 fold of sc versus siRNA at 0.86 ± 0.08 fold of sc, Fig.4.1A). Application of recombinant PGRN protein to astrocytes infected with PGRN siRNA restored the effect of glutamate on lactate release ($p < 0.05$, siRNA-PGRN-glutamate at 1.69 ± 0.15 fold of sc versus siRNA-PGRN at 1.05 ± 0.17 fold of sc; Fig 4.1A), illustrating the specificity of the effect. Our results thus suggest that PGRN is required for the glutamate-induced glycolysis. An alternative explanation is that with knockdown of PGRN, the ability of astrocyte to supply lactate upon excitatory stimulation was impaired.

We then examined possible causes for lowered lactate release. Glucose utilization contributes positively to glycolysis and hence the production of lactate (Pellerin et al., 2007), and lactate has been shown to be released by MCT1 such as MCT1 (Broer et al., 1997; Pellerin et al., 2005). Fluctuations in MCT1 expression levels sometimes correlates positively with the release and uptake of lactate (Becker et al., 2004; Dubouchaud et al., 2000).Therefore we tested glucose uptake and MCT1 expression in PGRN-siRNA-treated astrocytes in response to glutamate. We found that glutamate-induced [3H]2DG uptake($p < 0.05$, sc-glutamate at 1.52 ± 0.08 fold compared to sc, Fig. 4.1B) no longer existed when PGRN was knocked down ($p = 0.23$, siRNA-glutamate at 1.16 ± 0.22 fold of sc versus siRNA at 0.89 ± 0.11 fold of sc, Fig.4.1B), but was reestablished by application of recombinant PGRN protein ($p < 0.05$, siRNA-PGRN-glutamate at 1.58 ± 0.05 fold of sc versus siRNA-PGRN at 0.93 ± 0.01 fold of sc; Fig 4.1B).We also found that MCT1 was expressed in our cultured astrocytes. PGRN siRNA or glutamate stimulation did not change basal expression of MCT1 (siRNA at 0.90 ± 0.04 fold versus sc, $p = 0.10$; glutamate at 0.98 ± 0.04 fold versus sc, $p = 0.66$; Fig. 4.1C and 4.1D). Our results suggested that astrocytes may not require extra levels of MCT1 protein for glutamate-induced lactate release. It is possible that basal MCT1 protein is already at such an abundant level that it could supply both basal and elevated lactate transportation. We also found less MCT1 protein when astrocytes with reduced levels of PGRN were stressed with glutamate, compared with control astrocytes that were treated with glutamate (siRNA-glutamate at 0.82 ± 0.12 fold of sc versus sc-glutamate at 0.98 ± 0.04 fold of sc, $p < 0.05$, Fig. 4.1C and 4.1D). This result may explain the reduction of lactate release in the siRNA-glutamate groups (lactate concentrations of siRNA-glutamate at 1.15 ± 0.10

fold of sc versus that of sc-glutamate at 1.54 ± 0.08 fold of sc, $p < 0.05$, Fig.4.1A). Interestingly, our cultured astrocytes were not activated by either glutamate or PGRN knockdown since the GFAP expression levels was not changed (Fig. 4.1C and 4.1E). Therefore, the change in MCT1 expression is not necessarily the result of astrocyte activation.

4.4 Conclusion

At the start of this study, the role of PGRN in astrocyte remains largely unknown. Here, we found that PGRN was required for glutamate-induced lactate release in cultured astrocytes. Glucose uptake creates the resource for lactate production (Allaman et al., 2004; Pellerin and Magistretti, 1994; Pellerin et al., 2007), and lactate is secreted from astrocytes via MCTs such as MCT1 (Broer et al., 1997; Pellerin et al., 2005). We found that PGRN was also required for glucose uptake and the maintenance of MCT1 protein levels upon glutamate stimulation (Fig. 4.1). Our preliminary data suggest that PGRN may play a critical role in ANLSH by regulating the supply of lactate from astrocytes to neurons under conditions of excitatory stimulation.

4.5 Discussion

4.5.1 Expression of PGRN in cultured astrocytes

Previous reports showed that PGRN was not expressed in astrocyte in adult animals (chapter 3) and also in human subjects (Baker et al., 2006). To our surprise, the astrocyte cultures express PGRN, making us wonder what causes this different observation. Astrocytes in culture and those in adult brain are different in several ways: 1. The morphology appears different; 2. The cultured astrocytes exist as a purified colony but *in*

vivo they form complex networks with neurons, microglia, and blood vessels. 3. Cultured astrocyte can proliferate and be further differentiated and activated by compounds such as dibutyryl cyclic AMP (Fahrig and Sommermeyer, 1993), and most astrocyte in adult brain are already differentiated. Previous work has shown that PGRN was detected by enzyme-linked immunosorbent assay (ELISA) in neural progenitor cell cultures which contained 50% astrocyte progenitors and15% neural stem cells (Nedachi et al., 2011). However, this study lacks the immunocytochemical experiments to identify exactly which cell type expressed PGRN. In contrast, another group has found that PGRN did not colocalize with embryonic neural stem cells labeled with nestin (Petkau et al., 2010). Thus PGRN might be expressed in astrocyte progenitors, which may explain why our cultured astrocytes expressed PGRN. However, we can not exclude other possible reasons causing difference between our result and previous work. In the future, we can investigate whether PGRN localize in astrocyte progenitor cells in embryonic CNS to consolidate these findings.

4.5.2 PGRN and glucose metabolism

Our results suggest that PGRN could be required for glycolytic metabolism in astrocytes. Consistent with our findings, a correlation of PGRN levels and glucose metabolism was also found in patients with diabetes. Serum PGRN concentrations were elevated in patients with high plasma glucose and type-2 diabetes patients (Tonjes et al., 2010; Youn et al., 2009). Diabetic or obese mice had a higher level of MCT1 protein in brain (Pierre et al., 2007), supporting the high demand of glucose metabolism. In combination with these findings, our results imply that increased PGRN might contribute to elevated glucose metabolism in these patients.

In summary, here for the first time we showed that PGRN was expressed by cultured astrocytes. We also found the novel functions of PGRN in regulating lactate release, glucose uptake and MCT1 expression in astrocytes.

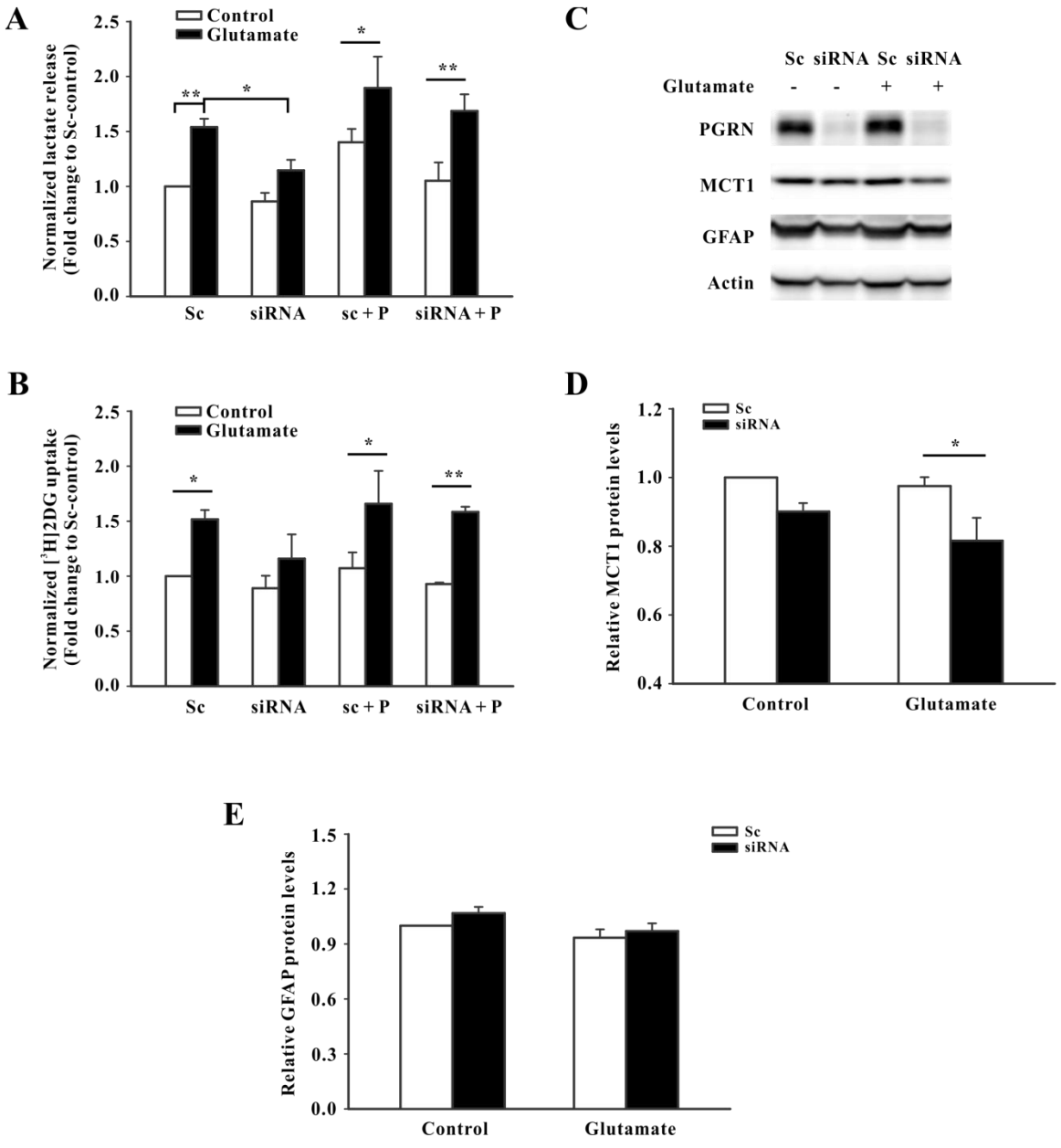
A
Control
Glutamate
Normalized lactate release
(Fold change to Sc-control)
2.5
2.0
1.5
1.0
0.5
0.0
Sc
siRNA
sc + P
siRNA + P
C
Sc siRNA Sc siRNA
Glutamate - - + +
PGRN
MCT1
GFAP
Actin
B
Control
Glutamate
Normalized [3H]2DG uptake
(Fold change to Sc-control)
D
Sc
siRNA
Relative MCT1 protein levels
1.2
1.0
0.8
0.6
0.4
Control
Glutamate
E
Sc
siRNA
Relative GFAP protein levels
1.5
1.2
0.9
0.6
0.3
0.0
Control
Glutamate

Fig. 4.1 PGRN contributed to lactate release in cultured astrocyte.

A, Astrocyte infected with lentiviral vectors expressing scrambled siRNA (sc) or PGRN siRNA (siRNA) were pretreated with recombinant PGRN protein (P). After 30 min treatment with or without glutamate, lactate concentration in cultured medium was determined and divided by total amount of protein in astrocytes. This value in each group was normalized to the value of sc-control group which was set to 1.0. $^{*}p < 0.05$ and $^{**}p < 0.01$ between compared groups in Student-Newman-Keuls post-hoc test after one-way ANOVA is significant. **B**, The glucose uptake of each group in panel A was determined by the radioactivity of astrocyte after 30 min incubation with [3H]2DG. $^{*}p < 0.05$ and $^{**}p < 0.01$ between compared groups in Fisher's least significant difference post-hoc test after one-way ANOVA is significant. **C**, sc- or siRNA- infected astrocyte were treated with or without glutamate for 30 min, and PGRN, MCT1, GFAP and actin proteins levels were analyzed by Western blots. **D** and **E**, Densitometric measurements of MCT1 (C) and GFAP (D) immunoblots in panel B after normalization to the expression of actin. Protein levels of groups were expressed as fold changes compared to the levels of untreated sc groups which were set to 1.0. In panel C, $^{*}p < 0.05$ between compared groups using Fisher's least significant difference post-hoc test after one-way ANOVA is significant. In panel D, GFAP levels is not significantly different among groups ($p = 0.067$) in one-way ANOVA. All values are averages of results from at least three separate experiments.

CHAPTER FIVE: CONCLUSIONS AND GENEARAL DISCUSSION

5.1 Conclusions

In this dissertation, I designed several experiments to investigate the cellular and pathological mechanisms related to neurological diseases such as epilepsy. I discovered the novel expression and function of KLF4 and PGRN in the CNS under conditions of harmful insults *in vivo* and *in vitro*. I observed the role of KLF4 in promoting apoptotic signals in response to glutamate excitotoxicity. I also found the role of PGRN in microglial migration in response to inflammatory or epileptic insults, and the contribution of PGRN to astrocytic glycolysis in response to glutamate excitotoxicity. My studies suggest that KLF4 and PGRN could be involved in neurological dysfunction. My work also suggest that the involvement of PGRN in the pathophysiology of epilepsy. I achieve my research goals, and my work supports and verifies the hypotheses proposed in this dissertation (section 1.6), as indicated in details as follows:

1) I found that KLF4 mRNA and protein levels were induced by excitotoxic application of NMDA or AMPA in cultured neurons, and that KLF4 protein levels rapidly increased in response to activation of NMDA receptors in both neuron cultures and brain slices. Using the KLF4-overexpressing lentiviral vector, I found that overexpressing KLF4 increased both protein and mRNA levels of the cell cycle protein cyclin D1, but reduced p21Waf1/Cip1 protein levels. Using this vector I also found that KLF4 overexpression induced the activation of caspase-3 after a normally subtoxic dose of NMDA (10 μM). Our findings support our hypothesis that KLF4 could be an

immediate early gene induced by glutamate excitotoxicity, and that KLF4 could be involved in cell cycle protein expression and glutamate excitotoxicity-induced apoptosis in cultured neurons.

2) I found that PGRN was induced in microglia in response to pilocarpine-induced SE, and that PGRN was also induced by LPS stimulation in mixed neuronal-glial cultures. Using recombinant PGRN protein, I observed that the administration of PGRN promoted microglial migration in the pilocarpine-induced SE. Applying recombinant PGRN protein and anti-PGRN antibody, I found and that PGRN also mediated the LPS-induced microglial activation in purified microglial cultures. However, application of anti-PGRN antibody did not affect LPS-induced MCP-1 expression. Administration of PGRN did not affect DG cell loss following pilocarpine-induced SE. In a preliminary study, my results indicated that the latency to acute seizures induced by pilocarpine, and SE-induced microglial activation and DG cell loss were not affected in PGRN deficient mice. My results suggest that PGRN could enhance, but may not be required for, epilepsy-induced microglial activation, and that PGRN could contribute to LPS-induced microglial migration in cultured microglia. My research also suggests that PGRN may not contribute to SE-induced DG cell loss or development of acute seizure induced by pilocarpine, and that PGRN may not be required for LPS-induced MCP-1 expression. My findings modify the hypothesis proposed earlier.

3) I found that cultured astrocytes expressed PGRN protein. Using lentiviral vector expressing PGRN siRNA to deplete PGRN, we found that PGRN was required for glutamate-induced lactated release. PGRN siRNA also caused a reduction in glutamate-induced uptake of glucose, and slightly decreased the protein levels of MCT1 glutamate-treated astrocytes. Our results support our hypothesis that PGRN could be involved in glutamate-induced increase of

glycolysis in cultured astrocyte.

5.2 Significance of findings

5.2.1 The role of KLF4 and PGRN in glutamate excitotoxicity

Excessive release of glutamate during neurological disorders such as epilepsy and ischemia causes huge impact on CNS cells including neurons and astrocytes. It has been shown that immediate early genes were rapidly increased upon glutamate stimulations, including *fos* family (c-*fos* and *fos*B), *jun* family (c-*jun* and *jun*B) and *zif/268* in cultured neurons (Condorelli et al., 1994). Studies manipulating levels of these genes using transgenic mice suggested a pro-apoptotic role of c-*jun* (Behrens et al., 1999) and c-*fos* (Watson et al., 1998) in kainic acid-induced SE, and a pro-apoptotic role of *zif/268* in focal ischemia (Tureyen et al., 2008). At the beginning of this study, the role of the immediate early gene KLF4 in glutamate excitotoxicity was completely unknown. We found that KLF4 was rapidly induced by NMDA or AMPA (Fig. 2.1-2.4), and could activate caspase-3 in a normally sublethal dose of NMDA (Fig. 2.5), suggesting a potential pro-apoptotic role of KLF4. Our work suggests the regulation and function of KLF4 during glutamate excitotoxicity, and expands the pool of immediate early genes that respond to glutamate.

In addition, augmentation of extracellular glutamate concentrations epilepsy has been shown to be correlated with enhanced glucose metabolism and lactate release (During et al., 1994; Henshall, 2007; Meldrum et al., 1999). The astrocyte-neuronal lactate shuttle hypothesis (ANLSH) suggests that glutamate induced lactate release from astrocytes, which could supply the increased energy demand of neighboring neurons activated in

physiological or pathological conditions (Pellerin et al., 2007). The role of neurotrophic factors in ANLSH has been largely unknown, and whether PGRN was involved in ANLSH was completely not clear before our study. Our preliminary study in chapter four showed that PGRN was required for glutamate-induced lactate release in cultured astrocytes. Our study suggests a novel function of PGRN in modulating glycolysis in astrocytes.

5.2.2 The role of PGRN in microglial activation stimulated by epilepsy and inflammation

Microglial activation represents one of major immune responses of CNS in neurological disorders such as epilepsy and in inflammatory insults. Chemokines and cytokines can induce activation of microglia. Primary microglial cultures have been shown to express a few growth factors such as BDNF and PGRN, but an NGF or neurotrophin-3 (Nakajima et al., 2001; Pickford et al., 2011). LPS induces secretion of BDNF (Nakajima et al., 2001). Cultured microglial cells also express several Trks and a NGF receptor, and application of BDNF, NGF or neurotrophin-3, suppressed LPS-induced production of nitric oxide (Nakajima et al., 1998). But very few groups have reported the role of growth factors in regulating microglial migration during epilepsy and/or inflammation. Recently, PGRN has been shown to induce microglial migration *in vitro* and *in vivo* (Pickford et al., 2011). Our work confirmed their results *in vitro* but our results showed that PGRN activated microglia only in animals subjected to SE but not in non-SE controls. A discussion of the difference between our result and Pickford's work is shown in section 3.5.1 of chapter three. We also found that LPS stimulated PGRN expression, and PGRN was required for LPS-induced microglial migration *in vitro*. Our

results expand Pickford's findings and suggest that PGRN could be involved in microglial migration during epilepsy and inflammation.

5.2.3 Potential applications of our findings in diagnosis of diseases with microglial activation

Our findings indicate that PGRN was significantly increased by LPS and was induced in microglia by epilepsy. Microglial cells are transiently activated in acute neurological disorders such as ischemia and epilepsy and in brain inflammation (Avignone et al., 2008; Bruce et al., 1996; Kielian, 2004). Activation of microglia can last as long as years in neurodegenerative diseases (Gerhard et al., 2006; Giulian, 1999; Yin et al., 2010). Diagnosing these diseases can be difficult. For example, some epileptic patients have no convulsive syndromes and show other complicated syndromes such as vomiting, nausea and language disorder (Pro et al., 2011; Tiamkao et al., 2011). PGRN is a secreted protein which can be detected in plasma, and PGRN has been studied as a biomarker for other neurological disorders and cancers (Ghidoni et al., 2008; Han et al., 2011; Hu et al., 2010; Youn et al., 2009). Therefore, our work suggests a correlation between PGRN and microglial activation and inflammation, making PGRN a potential biomarker for diagnosing epilepsy and brain inflammation caused by bacterial infections. More clinical studies must be conducted to verify this possibility.

5.4 Future directions

Several interesting questions emerge from this dissertation. Investigations on these future directions can improve our understandings of the function of KLF4 and PGRN in

the CNS, and can provide insights to the pathophysiology of glutamate excitotoxicity, inflammation and epilepsy.

5.4.1 The involvement of KLF4 in NMDA excitotoxicity

A few questions can be asked based on our findings in chapter two.

First, we are curious about how calcium flow via NMDA receptors induced KLF4 expression. Calcium influx through NMDA receptors activates several signaling pathways that regulate early gene expression. Among others, NMDA activates mitogen activated protein kinases kinase 4 and/or 7, which in turn phosphorylate the c-jun N-terminal kinase (JNK). C-jun belongs to the AP-1 transcription factor complex, and the phosphorylation of c-jun by JNK potentiates its transcriptional activity. We analyzed the KLF4 promoter sequence with MatInspector (http://www.genomatix.de/) and found an AP-1 binding site about 1.2 kb upstream of the ATG start codon, suggesting possible activation of AP-1 in the KLF4 promoter. Further experiment defining the aforementioned calcium/c-jun/KLF4 signaling pathway would help to explain the mechanism of calcium-regulated KLF4 expression.

Secondly, it would be interesting to investigate whether KLF4 was required for NMDA-induced caspase-3 activation. We have tried to use the small interfering RNA (siRNA) to knock down KLF4 (Fig. 5.1). Working with COS cells, we have designed and tested the activity of several siRNAs, and determined a very efficient one (siRNA 3, lane 5 in panel A of the attached Fig. 5.1). This siRNA could completely knock down the overexpressed KLF4 protein in COS cells. Unfortunately, when we tried this siRNA on the primary cultured neurons, it could only knockdown about 40% of the endogenous

KLF4 mRNA (panel B of Fig. 5.1). We did not achieve any KLF4 siRNAs with better efficiency. With this siRNA 3, we tested its effect in subtoxic NMDA (10 μM) - induced Caspase-3 protein level, and did not find any significant change (panel C of Fig. 5.1). We also tested the effect of this siRNA on cell death induced by NMDA (20 μM), and did not find any significant difference compared with control siRNA (panel D of Fig. 5.1). Most likely, the lack of efficacy of the siRNA in the knockdown experiments is due to its low efficiency. We will continue to devise new approaches to knock down KLF4 expression and these will be presented in future papers.

5.4.2 Implications of our findings in epilepsy study

5.4.2.1 Upregulation of PGRN by epileptic seizures

In our investigations to discover potential inducing factors for PGRN expression, we found that inflammation could be an inducing factor for PGRN expression in chapter three (Fig. 3.6). But the questions of whether inflammation is required for SE-induced PGRN expression are not explained. To address this question, we can test whether anti-inflammatory drugs can block epilepsy-induced PGRN expression in the future. Furthermore, although we found that PGRN promoted microglial migration following SE, it is possible that PGRN act in an autocrine manner. We can examine whether microglial activation is required for epilepsy-induced PGRN expression, using the minocycline to intervene microglial activation.

5.4.2.2 PGRN in neural circuit reorganization following epileptic attacks

Reorganization of neural networks was caused by epileptic seizures. Mossy fiber sprouting (the axon projections of DG granule cells), aberrant neurogenesis of DG

granule cells, and abnormal migration of newborn granule cells into the hilus were detected in TLE patients and in experimental models of epilepsy (Curia et al., 2008; Parent and Lowenstein, 1997; Parent and Murphy, 2008; Sharma et al., 2008; Yang et al., 2010). Many growth factors are involved in regulation of these events. We expect a role of PGRN in neural circuit reorganization after seizures for the following reasons. First, previous work has suggested a role of PGRN in neurite generation (Gao et al., 2010; Tapia et al., 2011; Van Damme et al., 2008). Application of PGRN has been shown to stimulate outgrowth of axon in cultured motor neurons (Van Damme et al., 2008) and in cortical neuron cultures (Gao et al., 2010). Knocking down PGRN resulted a reduction in dendritic arborization (Tapia et al., 2011). Secondly, our results indicated that PGRN existed in activated microglia (Fig. 3.2), and it has been shown that activated microglia played a role in neurogenesis during development and in a lithium pilocarpine model (Ekdahl et al., 2009; Yang et al., 2010). Yang et al. (2009) found that ablation of microglia by minocycline, but not dysfunction of astrocyte by fluorocitrate, blocked the migration of new born neurons in pilocarpine epilepsy model. In addition, mossy fiber sprouting can last at least for a month after SE induction, as long as microglia was still activated (Curia et al., 2008; Sharma et al., 2008; Yang et al., 2010). Therefore, PGRN may be involved in SE-induced neurite reorganization. Since PGRN was mainly expressed by activated microglia, we can examine the expression of PGRN at later time points when these events of neural circuit rewiring occurred. For example, previous studies have shown increased levels of DG granule cell neurogenesis at day 7 (Kuramoto et al., 2011), aberrant migration of newborn granule cells at day 14 (Yang et al., 2010), and abnormal sprouting of mossy fibers at the 8 weeks (Chen et al., 2007) following SE

induction. Using PGRN deficient mouse, we could investigate whether PGRN is involved in epilepsy-induced generation and migration of granule neurons, and mossy fiber sprouting in the future.

5.4.2.3 The role of PGRN in epileptogenesis

Although many anti-epileptic drugs are available on the market, 30% of patients suffering from epilepsy are resistant to these drugs. As described in section 1.2.2 of Chapter one, many growth factors have been shown to play a complicated role in spontaneous recurrent seizures (SRSs), including NGF, BDNF and bFGF. The receptors of these growth factors also mediate their role in epileptogenesis. In the case of BDNF, different doses and timing of BDNF caused contradictory effects on development of SRSs following SE or kindling procedures, possibly due to different levels of activation of the receptor TrkB. Therefore, as a growth factor, PGRN might be involved in epileptogenesis but the activation levels of its receptors shall be a critical concern. To test this hypothesis, first we need to examine PGRN expression during chronic phase when SRSs occur. If PGRN is still expressed during chronic phase, we can use PGRN null mice to examine the pilocarpine-induced SRSs. We can also test the effect of a wide range of doses of PGRN on epileptogenesis.

Since our preliminary study showed that the latency to behavioral seizures was not affected in PGRN knockout mice (Fig. 3.14), we should be aware of the risk of this proposed study. We also found that PGRN was sufficient but was not required for SE-induced microglial migration in DG (Fig. 3.10, 3.11, 3.12). A recent study indicated that ablation of microglia had no effect on behavioral scores of acute seizures induced by pilocarpine (Mirrione et al., 2010), but there is no direct evidence showing that activation

of microglia was required for SRSs. In addition, it was suggested that abnormal firing provided by reorganized neural circuit was related with epileptogenesis (Santhakumar et al., 2005; Sharma et al., 2008), but contradictory evidences also existed (Dudek and Shao, 2004) since intervening mossy fiber sprouting with cycloheximide failed to affect the SE-induced SRSs (Dos Santos et al., 2005; Longo and Mello, 1997; Longo et al., 2002). Therefore, we shall be aware of the risk of the investigation on the role of PGRN in SRSs.

5.4.2.4 The involvement of PGRN in lactate release during epilepsy

The PGRN expression, glutamate release, and glycolytic metabolism were independently observed in epilepsy. Extracellular glutamate concentration increased during epileptic firing (During and Spencer, 1993), leading to augmented energy demand. Lactate concentration and glucose metabolism were also raised during ictal seizures (Bolwig and Quistorff, 1973; Dube et al., 2001; During et al., 1994; Engel et al., 1982; Morimoto et al., 2004; Patel et al., 2004; van Eijsden et al., 2004). Increased levels of MCT1 expression has been observed in astrocytes in animal models of temporal lobe epilepsy (Lauritzen et al., 2011). Our results in chapter three showed the upregulation of PGRN after seizures (Fig. 3.1A). We also found that PGRN in involved in lactate release, glucose uptake and MCT1 expression in our cultured astrocyte (Fig. 4.1). Thus we postulate that regulation of PGRN in astrocytic glycolysis and MCT1 expression may exist *in vivo* during seizures. To support the hypothesis, we can examine the microdialysate lactate concentration and the MCT1 protein expression levels in epileptic PGRN KO mice in the future. In addition, glycogen break down is another unique astrocytic resource for producing lactate and thus can also be tested in our experimental settings in the future.

5.4.3 Implications of our findings in FTLD-U with PGRN mutations

FTLD-U patients that possessed PGRN mutations throughout their lives developed dementia when they aged (Baker et al., 2006), and thus it is likely that aging related phenomena are involved in the etiology of FTLD-U. It was found that cognitive stimulation-induced lactate response disappeared in aged subjects (Urrila et al., 2004), suggesting the age-dependency of lactate response. Mice with MCT1 deletion developed amnesia which can be rescued by lactate (Suzuki et al., 2011), suggesting the requirement of lactate and MCT1 expression for long-term memory. In addition, FTLD-U Patients with PGRN mutation and decreased levels of PGRN also demonstrated a reduction in glucose metabolism (Spina et al., 2007). Therefore, based on our results in Chapter four (Fig. 4.1), we can hypothesize that PGRN mutation in FTLD-U might reduced lactate response and MCT1 expression, and may lead to lack of lactate response at older age. Considering the role of MCT1 and lactate in learning and memory, this hypothesis could explain the exacerbated conditions in aged FTLD-U patients. More experiments needed to be done to support this possibility, for example, the lactate and MCT1 levels in FTLD-U patients with haploinsufficiency of PGRN can be studied in the future.

Overall, this dissertation demonstrates novel functions of KLF4 and PGRN. During glutamate excitotoxicity, KLF4 may contribute to caspase 3 activation in cultured neurons, and PGRN could be required for lactate release from cultured astrocytes. In addition, our results suggest the role of PGRN in microglial activation upon inflammatory or epileptic stimulations. However, PGRN is not required for seizure development in the pilocarpine model, neither is PGRN required for SE-induced cell death in dentate gyrus.

Figure B

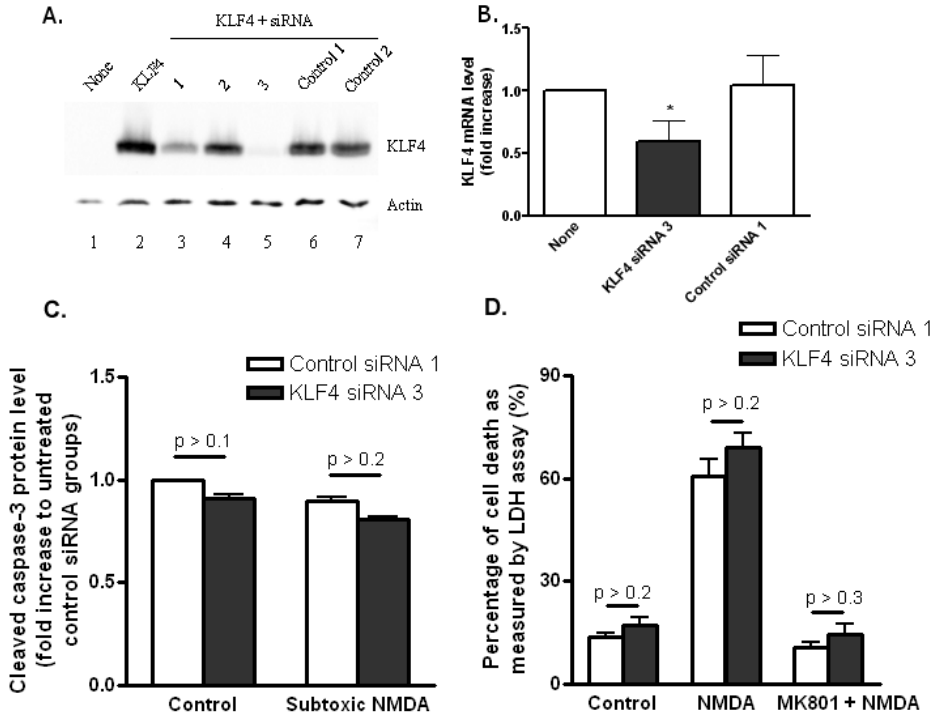
A.
KLF4 + siRNA
None
KLF4
1
2
3
Control 1
Control 2
KLF4
Actin
1 2 3 4 5 6 7
B.
KLF4 mRNA level (fold increase)
1.5
1.0
0.5
0.0
*
None
KLF4 siRNA 3
Control siRNA 1
C.
Cleaved caspase-3 protein level (fold increase to untreated control siRNA groups)
Control siRNA 1
KLF4 siRNA 3
1.5
1.0
0.5
0.0
p > 0.1
p > 0.2
Control
Subtoxic NMDA
D.
Percentage of cell death as measured by LDH assay (%)
Control siRNA 1
KLF4 siRNA 3
90
60
30
0
p > 0.2
p > 0.2
p > 0.3
Control
NMDA
MK801 + NMDA

Fig. 5.1 The preliminary study on constructing and testing of the KLF4 siRNA.

In panel **A**, Western blot analysis of KLF4 protein levels in COS cells transfected with plasmids expressing KLF4, either alone (lane 2), or together with plasmids expressing various small interference RNA designed to knock down KLF4 (KLF4 siRNA 1 to 3, lane 3-5), or together with plasmids expressing two scrambled siRNAs (Control 1 and 2, lane 6 and 7). KLF4 siRNA 3 completely knocked down the overexpressed KLF4, and the scrambled control siRNA 1 had the least effect on knocking down KLF4. From **B** to **D**, Data were analyzed in neurons with 5-day infection of lentiviral vectors expressing either KLF4 siRNA 3, or the scramble control siRNA 1. On DIV 11, quantitative real-time PCR analysis of endogenous KLF4 mRNA levels was performed as shown in panel B. The KLF4 siRNA 3 knocked down about 40% of the endogenous KLF4 mRNA compared to control siRNA 1 (*$p < 0.05$). In panel C, infected neurons were treated with 10 μM NMDA (subtoxic dose of NMDA) for 1.5 h, and then allowed to recover in non-NMDA-containing culture medium for 20 h before Western blot assessment of cleaved Caspase-3. In both untreated and NMDA-treated cultures, there were no significant differences between KLF4 siRNA 3 and control siRNA 1 groups. In panel D, infected neurons were treated with 20 μM NMDA (lethal dose of NMDA) for 1.5 h. After 20 h recovery in non-NMDA-containing culture medium, cell death was assessed with the lactate hydrogenase (LDH) assay. MK801 (20 μM) was applied together with NMDA to ensure that cell death was caused by activation of NMDA receptors (MK801 + NMDA). In control siRNA 1 groups, NMDA treatment caused 61 ± 10 % cell death, which was completely blocked by application of MK801 (11 ± 3 % cell death in MK801 + NMDA groups vs. 14 ± 3 % cell death in untreated control). However, expression of KLF4

siRNA 3 had a similar effect on cell death as did the control siRNA 1 in all three conditions: control, NMDA, and MK801 + NMDA. No significant change was observed. All values are averages of results from at least three separate experiments.

REFERENCES

Adams, B., Sazgar, M., Osehobo, P., Van der Zee, C.E., Diamond, J., Fahnestock, M., Racine, R.J., 1997. Nerve growth factor accelerates seizure development, enhances mossy fiber sprouting, and attenuates seizure-induced decreases in neuronal density in the kindling model of epilepsy. J Neurosci. 17**,** 5288-96.

Akins, P.T., Liu, P.K., Hsu, C.Y., 1996. Immediate early gene expression in response to cerebral ischemia. Friend or foe? Stroke. 27**,** 1682-7.

Allaman, I., Pellerin, L., Magistretti, P.J., 2004. Glucocorticoids modulate neurotransmitter-induced glycogen metabolism in cultured cortical astrocytes. J Neurochem. 88**,** 900-8.

Amaral, D.G., Scharfman, H.E., Lavenex, P., 2007. The dentate gyrus: fundamental neuroanatomical organization (dentate gyrus for dummies). Prog Brain Res. 163**,** 3-22.

Ambrosini, E., Aloisi, F., 2004. Chemokines and glial cells: a complex network in the central nervous system. Neurochem Res. 29**,** 1017-38.

Andersen, P., 2007. The hippocampus book, Vol., Oxford University Press, Oxford ; New York.

Arita, M., Bianchini, F., Aliberti, J., Sher, A., Chiang, N., Hong, S., Yang, R., Petasis, N.A., Serhan, C.N., 2005. Stereochemical assignment, antiinflammatory properties, and receptor for the omega-3 lipid mediator resolvin E1. J Exp Med. 201**,** 713-22.

Asada, M., Yamada, T., Ichijo, H., Delia, D., Miyazono, K., Fukumuro, K., Mizutani, S., 1999. Apoptosis inhibitory activity of cytoplasmic p21(Cip1/WAF1) in monocytic differentiation. Embo J. 18**,** 1223-34.

Astrup, J., 1982. Energy-requiring cell functions in the ischemic brain. Their critical supply and possible inhibition in protective therapy. J Neurosurg. 56**,** 482-97.

Avignone, E., Ulmann, L., Levavasseur, F., Rassendren, F., Audinat, E., 2008. Status epilepticus induces a particular microglial activation state characterized by enhanced purinergic signaling. J Neurosci. 28**,** 9133-44.

Avoli, M., Louvel, J., Kurcewicz, I., Pumain, R., Barbarosie, M., 1996. Extracellular free potassium and calcium during synchronous activity induced by 4-aminopyridine in the juvenile rat hippocampus. J Physiol. 493 (Pt 3)**,** 707-17.

Babcock, A.A., Kuziel, W.A., Rivest, S., Owens, T., 2003. Chemokine expression by glial cells directs leukocytes to sites of axonal injury in the CNS. J Neurosci. 23**,** 7922-30.

Baggiolini, M., Clark-Lewis, I., 1992. Interleukin-8, a chemotactic and inflammatory cytokine. FEBS Lett. 307**,** 97-101.

Baker, M., Mackenzie, I.R., Pickering-Brown, S.M., Gass, J., Rademakers, R., Lindholm, C., Snowden, J., Adamson, J., Sadovnick, A.D., Rollinson, S., Cannon, A., Dwosh, E., Neary, D., Melquist, S., Richardson, A., Dickson, D., Berger, Z., Eriksen, J., Robinson, T., Zehr, C., Dickey, C.A., Crook, R., McGowan, E., Mann, D., Boeve, B., Feldman, H., Hutton, M., 2006. Mutations in progranulin cause tau-negative frontotemporal dementia linked to chromosome 17. Nature. 442**,** 916-9.

Ballabriga, J., Pozas, E., Planas, A.M., Ferrer, I., 1997. bFGF and FGFR-3 immunoreactivity in the rat brain following systemic kainic acid administration at convulsant doses: localization of bFGF and FGFR-3 in reactive astrocytes, and FGFR-3 in reactive microglia. Brain Res. 752**,** 315-8.

Bandtlow, C.E., Meyer, M., Lindholm, D., Spranger, M., Heumann, R., Thoenen, H., 1990. Regional and cellular codistribution of interleukin 1 beta and nerve growth factor mRNA in the adult rat brain: possible relationship to the regulation of nerve growth factor synthesis. J Cell Biol. 111**,** 1701-11.

Bano, D., Young, K.W., Guerin, C.J., Lefeuvre, R., Rothwell, N.J., Naldini, L., Rizzuto, R., Carafoli, E., Nicotera, P., 2005. Cleavage of the plasma membrane Na+/Ca2+ exchanger in excitotoxicity. Cell. 120**,** 275-85.

Barber, P.A., Demchuk, A.M., Hirt, L., Buchan, A.M., 2003. Biochemistry of ischemic stroke. Adv Neurol. 92**,** 151-64.

Bartkova, J., Lukas, J., Muller, H., Lutzhoft, D., Strauss, M., Bartek, J., 1994. Cyclin D1 protein expression and function in human breast cancer. Int J Cancer. 57**,** 353-61.

Bateman, A., Bennett, H.P., 2009. The granulin gene family: from cancer to dementia. Bioessays. 31**,** 1245-54.

Becker, H.M., Broer, S., Deitmer, J.W., 2004. Facilitated lactate transport by MCT1 when coexpressed with the sodium bicarbonate cotransporter (NBC) in Xenopus oocytes. Biophys J. 86**,** 235-47.

Behrens, A., Sibilia, M., Wagner, E.F., 1999. Amino-terminal phosphorylation of c-Jun regulates stress-induced apoptosis and cellular proliferation. Nat Genet. 21**,** 326-9.

Ben-Ari, Y., Tremblay, E., Riche, D., Ghilini, G., Naquet, R., 1981. Electrographic, clinical and pathological alterations following systemic administration of kainic acid, bicuculline or pentetrazole: metabolic mapping using the deoxyglucose method with special reference to the pathology of epilepsy. Neuroscience. 6**,** 1361-91.

Bender, A.S., Young, L.P., Norenberg, M.D., 1997. Effect of lactic acid on L-glutamate uptake in cultured astrocytes: mechanistic considerations. Brain Res. 750**,** 59-66.

Bender, R., Heimrich, B., Meyer, M., Frotscher, M., 1998. Hippocampal mossy fiber sprouting is not impaired in brain-derived neurotrophic factor-deficient mice. Exp Brain Res. 120**,** 399-402.

Berg, A.T., 2011. Epilepsy, cognition, and behavior: The clinical picture. Epilepsia. 52 Suppl 1**,** 7-12.

Bhalla, D., Godet, B., Druet-Cabanac, M., Preux, P.M., 2011. Etiologies of epilepsy: a comprehensive review. Expert Rev Neurother. 11**,** 861-76.

Bhandari, V., Bateman, A., 1992. Structure and chromosomal location of the human granulin gene. Biochem Biophys Res Commun. 188**,** 57-63.

Bhandari, V., Daniel, R., Lim, P.S., Bateman, A., 1996. Structural and functional analysis of a promoter of the human granulin/epithelin gene. Biochem J. 319 (Pt 2)**,** 441-7.

Binder, D.K., Routbort, M.J., Ryan, T.E., Yancopoulos, G.D., McNamara, J.O., 1999. Selective inhibition of kindling development by intraventricular administration of TrkB receptor body. J Neurosci. 19**,** 1424-36.

Bolwig, T.G., Quistorff, B., 1973. In vivo concentration of lactate in the brain of consious rats beford and during seizures: a new ultra-rapid technique for the freeze-sampling of brain tissue. J Neurochem. 21**,** 1345-8.

Borges, K., Gearing, M., McDermott, D.L., Smith, A.B., Almonte, A.G., Wainer, B.H., Dingledine, R., 2003. Neuronal and glial pathological changes during epileptogenesis in the mouse pilocarpine model. Exp Neurol. 182**,** 21-34.

Brett, F.M., Mizisin, A.P., Powell, H.C., Campbell, I.L., 1995. Evolution of neuropathologic abnormalities associated with blood-brain barrier breakdown in transgenic mice expressing interleukin-6 in astrocytes. J Neuropathol Exp Neurol. 54**,** 766-75.

Broer, S., Rahman, B., Pellegri, G., Pellerin, L., Martin, J.L., Verleysdonk, S., Hamprecht, B., Magistretti, P.J., 1997. Comparison of lactate transport in astroglial cells and monocarboxylate transporter 1 (MCT 1) expressing Xenopus laevis oocytes. Expression of two different monocarboxylate transporters in astroglial cells and neurons. J Biol Chem. 272**,** 30096-102.

Brouwers, N., Nuytemans, K., van der Zee, J., Gijselinck, I., Engelborghs, S., Theuns, J., Kumar-Singh, S., Pickut, B.A., Pals, P., Dermaut, B., Bogaerts, V., De Pooter, T., Serneels, S., Van den Broeck, M., Cuijt, I., Mattheijssens, M., Peeters, K., Sciot, R., Martin, J.J., Cras, P., Santens, P., Vandenberghe, R., De Deyn, P.P., Cruts, M., Van Broeckhoven, C., Sleegers, K., 2007. Alzheimer and Parkinson diagnoses in progranulin null mutation carriers in an extended founder family. Arch Neurol. 64**,** 1436-46.

Brown, A.M., Ransom, B.R., 2007. Astrocyte glycogen and brain energy metabolism. Glia. 55**,** 1263-71.

Bruce, A.J., Boling, W., Kindy, M.S., Peschon, J., Kraemer, P.J., Carpenter, M.K., Holtsberg, F.W., Mattson, M.P., 1996. Altered neuronal and microglial responses to excitotoxic and ischemic brain injury in mice lacking TNF receptors. Nat Med. 2**,** 788-94.

Bucan, M., Gatalica, B., Baba, T., Gerton, G.L., 1996. Mapping of Grn, the gene encoding the granulin/epithelin precursor (acrogranin), to mouse chromosome 11. Mamm Genome. 7**,** 704-5.

Budd, S.L., Tenneti, L., Lishnak, T., Lipton, S.A., 2000. Mitochondrial and extramitochondrial apoptotic signaling pathways in cerebrocortical neurons. Proc Natl Acad Sci U S A. 97**,** 6161-6.

Cajal, S.R.y., 1911. Histologie du syst ème nerveux Vol. II, A. Maloine. , Paris.

Campbell, I.L., Abraham, C.R., Masliah, E., Kemper, P., Inglis, J.D., Oldstone, M.B., Mucke, L., 1993. Neurologic disease induced in transgenic mice by cerebral overexpression of interleukin 6. Proc Natl Acad Sci U S A. 90**,** 10061-5.

Capano, M., Virji, S., Crompton, M., 2002. Cyclophilin-A is involved in excitotoxin-induced caspase activation in rat neuronal B50 cells. Biochem J. 363**,** 29-36.

Cataldo, A.M., Broadwell, R.D., 1986. Cytochemical identification of cerebral glycogen and glucose-6-phosphatase activity under normal and experimental conditions. II. Choroid plexus and ependymal epithelia, endothelia and pericytes. J Neurocytol. 15**,** 511-24.

Cavalheiro, E.A., 1995. The pilocarpine model of epilepsy. Ital J Neurol Sci. 16**,** 33-7.

Cavazos, J.E., Sutula, T.P., 1990. Progressive neuronal loss induced by kindling: a possible mechanism for mossy fiber synaptic reorganization and hippocampal sclerosis. Brain Res. 527**,** 1-6.

Chao, M., Casaccia-Bonnefil, P., Carter, B., Chittka, A., Kong, H., Yoon, S.O., 1998. Neurotrophin receptors: mediators of life and death. Brain Res Brain Res Rev. 26**,** 295-301.
Chapman, A.G., 1998. Glutamate receptors in epilepsy. Prog Brain Res. 116**,** 371-83.
Chen, J., Nagayama, T., Jin, K., Stetler, R.A., Zhu, R.L., Graham, S.H., Simon, R.P., 1998. Induction of caspase-3-like protease may mediate delayed neuronal death in the hippocampus after transient cerebral ischemia. J Neurosci. 18**,** 4914-28.
Chen, Q., He, S., Hu, X.L., Yu, J., Zhou, Y., Zheng, J., Zhang, S., Zhang, C., Duan, W.H., Xiong, Z.Q., 2007. Differential roles of NR2A- and NR2B-containing NMDA receptors in activity-dependent brain-derived neurotrophic factor gene regulation and limbic epileptogenesis. J Neurosci. 27**,** 542-52.
Chen, Z.Y., Wang, X., Zhou, Y., Offner, G., Tseng, C.C., 2005. Destabilization of Kruppel-like factor 4 protein in response to serum stimulation involves the ubiquitin-proteasome pathway. Cancer Res. 65**,** 10394-400.
Cheng, Y., Deshmukh, M., D'Costa, A., Demaro, J.A., Gidday, J.M., Shah, A., Sun, Y., Jacquin, M.F., Johnson, E.M., Holtzman, D.M., 1998. Caspase inhibitor affords neuroprotection with delayed administration in a rat model of neonatal hypoxic-ischemic brain injury. J Clin Invest. 101**,** 1992-9.
Chiambaretta, F., De Graeve, F., Turet, G., Marceau, G., Gain, P., Dastugue, B., Rigal, D., Sapin, V., 2004. Cell and tissue specific expression of human Kruppel-like transcription factors in human ocular surface. Mol Vis. 10**,** 901-9.
Choi, J., Koh, S., 2008. Role of brain inflammation in epileptogenesis. Yonsei Med J. 49**,** 1-18.
Christy, B.A., Lau, L.F., Nathans, D., 1988. A gene activated in mouse 3T3 cells by serum growth factors encodes a protein with "zinc finger" sequences. Proc Natl Acad Sci U S A. 85**,** 7857-61.
Cloix, J.F., Hevor, T., 2009. Epilepsy, regulation of brain energy metabolism and neurotransmission. Curr Med Chem. 16**,** 841-53.
Cohen, I., Navarro, V., Clemenceau, S., Baulac, M., Miles, R., 2002. On the origin of interictal activity in human temporal lobe epilepsy in vitro. Science. 298**,** 1418-21.
Condorelli, D.F., Dell'Albani, P., Amico, C., Kaczmarek, L., Nicoletti, F., Lukasiuk, K., Stella, A.M., 1993. Induction of primary response genes by excitatory amino acid receptor agonists in primary astroglial cultures. J Neurochem. 60**,** 877-85.
Condorelli, D.F., Dell'Albani, P., Amico, C., Lukasiuk, K., Kaczmarek, L., Giuffrida-Stella, A.M., 1994. Glutamate receptor-driven activation of transcription factors in primary neuronal cultures. Neurochem Res. 19**,** 489-99.
Corkin, S., 1968. Acquisition of Motor Skill after Bilateral Medial Temporal-Lobe Excision. Neuropsychologia. 6**,** 255-&.
Cortini, F., Fenoglio, C., Guidi, I., Venturelli, E., Pomati, S., Marcone, A., Scalabrini, D., Villa, C., Clerici, F., Dalla Valle, E., Mariani, C., Cappa, S., Bresolin, N., Scarpini, E., Galimberti, D., 2008. Novel exon 1 progranulin gene variant in Alzheimer's disease. Eur J Neurol. 15**,** 1111-7.
Croll, S.D., Suri, C., Compton, D.L., Simmons, M.V., Yancopoulos, G.D., Lindsay, R.M., Wiegand, S.J., Rudge, J.S., Scharfman, H.E., 1999. Brain-derived neurotrophic factor transgenic mice exhibit passive avoidance deficits, increased seizure

severity and in vitro hyperexcitability in the hippocampus and entorhinal cortex. Neuroscience. 93**,** 1491-506.
Croll, S.D., Goodman, J.H., Scharfman, H.E., 2004a. Vascular endothelial growth factor (VEGF) in seizures: a double-edged sword. Adv Exp Med Biol. 548**,** 57-68.
Croll, S.D., Ransohoff, R.M., Cai, N., Zhang, Q., Martin, F.J., Wei, T., Kasselman, L.J., Kintner, J., Murphy, A.J., Yancopoulos, G.D., Wiegand, S.J., 2004b. VEGF-mediated inflammation precedes angiogenesis in adult brain. Exp Neurol. 187**,** 388-402.
Cruts, M., Gijselinck, I., van der Zee, J., Engelborghs, S., Wils, H., Pirici, D., Rademakers, R., Vandenberghe, R., Dermaut, B., Martin, J.J., van Duijn, C., Peeters, K., Sciot, R., Santens, P., De Pooter, T., Mattheijssens, M., Van den Broeck, M., Cuijt, I., Vennekens, K., De Deyn, P.P., Kumar-Singh, S., Van Broeckhoven, C., 2006. Null mutations in progranulin cause ubiquitin-positive frontotemporal dementia linked to chromosome 17q21. Nature. 442**,** 920-4.
Curia, G., Longo, D., Biagini, G., Jones, R.S., Avoli, M., 2008. The pilocarpine model of temporal lobe epilepsy. J Neurosci Methods. 172**,** 143-57.
Daniel, R., He, Z., Carmichael, K.P., Halper, J., Bateman, A., 2000. Cellular localization of gene expression for progranulin. J Histochem Cytochem. 48**,** 999-1009.
Daniel, R., Daniels, E., He, Z., Bateman, A., 2003. Progranulin (acrogranin/PC cell-derived growth factor/granulin-epithelin precursor) is expressed in the placenta, epidermis, microvasculature, and brain during murine development. Dev Dyn. 227**,** 593-9.
Dasheiff, R.M., McNamara, J.O., 1982. Intradentate colchicine retards the development of amygdala kindling. Ann Neurol. 11**,** 347-52.
de Bock, F., Dornand, J., Rondouin, G., 1996. Release of TNF alpha in the rat hippocampus following epileptic seizures and excitotoxic neuronal damage. Neuroreport. 7**,** 1125-9.
de Feo, M.R., Mecarelli, O., Ricci, G.F., 1985. Bicuculline- and allylglycine-induced epilepsy in developing rats. Exp Neurol. 90**,** 411-21.
de Guzman, P., Inaba, Y., Biagini, G., Baldelli, E., Mollinari, C., Merlo, D., Avoli, M., 2006. Subiculum network excitability is increased in a rodent model of temporal lobe epilepsy. Hippocampus. 16**,** 843-60.
de Lanerolle, N.C., Kim, J.H., Robbins, R.J., Spencer, D.D., 1989. Hippocampal interneuron loss and plasticity in human temporal lobe epilepsy. Brain Res. 495**,** 387-95.
De Simone, R., Ambrosini, E., Carnevale, D., Ajmone-Cat, M.A., Minghetti, L., 2007. NGF promotes microglial migration through the activation of its high affinity receptor: modulation by TGF-beta. J Neuroimmunol. 190**,** 53-60.
Dhir, A., Naidu, P.S., Kulkarni, S.K., 2006. Effect of cyclooxygenase-2 (COX-2) inhibitors in various animal models (bicuculline, picrotoxin, maximal electroshock-induced convulsions) of epilepsy with possible mechanism of action. Indian J Exp Biol. 44**,** 286-91.
Dimitrijevic, O.B., Stamatovic, S.M., Keep, R.F., Andjelkovic, A.V., 2007. Absence of the chemokine receptor CCR2 protects against cerebral ischemia/reperfusion injury in mice. Stroke. 38**,** 1345-53.

Dos Santos, J.G., Jr., Longo, B.M., Blanco, M.M., Menezes de Oliveira, M.G., Mello, L.E., 2005. Behavioral changes resulting from the administration of cycloheximide in the pilocarpine model of epilepsy. Brain Res. 1066**,** 37-48.
Dragunow, M., 1996. A role for immediate-early transcription factors in learning and memory. Behav Genet. 26**,** 293-9.
Duan, W.M., Widner, H., Cameron, R.M., Brundin, P., 1998. Quinolinic acid-induced inflammation in the striatum does not impair the survival of neural allografts in the rat. Eur J Neurosci. 10**,** 2595-606.
Dube, C., Boyet, S., Marescaux, C., Nehlig, A., 2001. Relationship between neuronal loss and interictal glucose metabolism during the chronic phase of the lithium-pilocarpine model of epilepsy in the immature and adult rat. Exp Neurol. 167**,** 227-41.
Dubouchaud, H., Butterfield, G.E., Wolfel, E.E., Bergman, B.C., Brooks, G.A., 2000. Endurance training, expression, and physiology of LDH, MCT1, and MCT4 in human skeletal muscle. Am J Physiol Endocrinol Metab. 278**,** E571-9.
Dudek, F.E., Shao, L.R., 2004. Mossy fiber sprouting and recurrent excitation: direct electrophysiologic evidence and potential implications. Epilepsy Curr. 4**,** 184-7.
During, M.J., Spencer, D.D., 1993. Extracellular hippocampal glutamate and spontaneous seizure in the conscious human brain. Lancet. 341**,** 1607-10.
During, M.J., Fried, I., Leone, P., Katz, A., Spencer, D.D., 1994. Direct measurement of extracellular lactate in the human hippocampus during spontaneous seizures. J Neurochem. 62**,** 2356-61.
Eikelenboom, P., Veerhuis, R., Scheper, W., Rozemuller, A.J., van Gool, W.A., Hoozemans, J.J., 2006. The significance of neuroinflammation in understanding Alzheimer's disease. J Neural Transm. 113**,** 1685-95.
Ekdahl, C.T., Claasen, J.H., Bonde, S., Kokaia, Z., Lindvall, O., 2003. Inflammation is detrimental for neurogenesis in adult brain. Proc Natl Acad Sci U S A. 100**,** 13632-7.
Ekdahl, C.T., Kokaia, Z., Lindvall, O., 2009. Brain inflammation and adult neurogenesis: the dual role of microglia. Neuroscience. 158**,** 1021-9.
Ekholm, S.V., Reed, S.I., 2000. Regulation of G(1) cyclin-dependent kinases in the mammalian cell cycle. Curr Opin Cell Biol. 12**,** 676-84.
Endres, M., Namura, S., Shimizu-Sasamata, M., Waeber, C., Zhang, L., Gomez-Isla, T., Hyman, B.T., Moskowitz, M.A., 1998. Attenuation of delayed neuronal death after mild focal ischemia in mice by inhibition of the caspase family. J Cereb Blood Flow Metab. 18**,** 238-47.
Engel, J., Pedley, T.A., 2008. Epilepsy: A comprehensive textbook. Vol., ed.^eds. Lippincott Williams & Wilkins, Philadelphia.
Engel, J., Jr., Kuhl, D.E., Phelps, M.E., 1982. Patterns of human local cerebral glucose metabolism during epileptic seizures. Science. 218**,** 64-6.
Eriksen, J.L., Mackenzie, I.R., 2008. Progranulin: normal function and role in neurodegeneration. J Neurochem. 104**,** 287-97.
Eriksen, J.L., 2010. The enigmatic roles of microglial versus neuronal progranulin in neurological disease. Acta Neuropathol. 119**,** 107-9.

Eriksson, C., Winblad, B., Schultzberg, M., 1998. Kainic acid induced expression of interleukin-1 receptor antagonist mRNA in the rat brain. Brain Res Mol Brain Res. 58**,** 195-208.

Fabene, P.F., Bramanti, P., Constantin, G., 2010. The emerging role for chemokines in epilepsy. J Neuroimmunol. 224**,** 22-7.

Fahrig, T., Sommermeyer, H., 1993. Dibutyryl cyclic AMP-induced morphological differentiation of rat brain astrocytes increases alpha 1-adrenoceptor induced phosphoinositide breakdown by a mechanism involving protein synthesis. Brain Res. 602**,** 318-24.

Fenoglio, C., Scalabrini, D., Esposito, F., Comi, C., Cavalla, P., De Riz, M., Martinelli, V., Piccio, L.M., Venturelli, E., Fumagalli, G., Capra, R., Collimedaglia, L., Ghezzi, A., Rodegher, M.E., Vercellino, M., Leone, M., Giordana, M.T., Bresolin, N., Monaco, F., Comi, G., Scarpini, E., Martinelli-Boneschi, F., Galimberti, D., 2010. Progranulin gene variability increases the risk for primary progressive multiple sclerosis in males. Genes Immun. 11**,** 497-503.

Ferreira, I.L., Resende, R., Ferreiro, E., Rego, A.C., Pereira, C.F., 2010. Multiple defects in energy metabolism in Alzheimer's disease. Curr Drug Targets. 11**,** 1193-206.

Floden, A.M., Combs, C.K., 2007. Microglia repetitively isolated from in vitro mixed glial cultures retain their initial phenotype. J Neurosci Methods. 164**,** 218-24.

Foresti, M.L., Arisi, G.M., Katki, K., Montanez, A., Sanchez, R.M., Shapiro, L.A., 2009. Chemokine CCL2 and its receptor CCR2 are increased in the hippocampus following pilocarpine-induced status epilepticus. J Neuroinflammation. 6**,** 40.

Foster, K.W., Ren, S., Louro, I.D., Lobo-Ruppert, S.M., McKie-Bell, P., Grizzle, W., Hayes, M.R., Broker, T.R., Chow, L.T., Ruppert, J.M., 1999. Oncogene expression cloning by retroviral transduction of adenovirus E1A-immortalized rat kidney RK3E cells: transformation of a host with epithelial features by c-MYC and the zinc finger protein GKLF. Cell Growth Differ. 10**,** 423-34.

Foster, K.W., Liu, Z., Nail, C.D., Li, X., Fitzgerald, T.J., Bailey, S.K., Frost, A.R., Louro, I.D., Townes, T.M., Paterson, A.J., Kudlow, J.E., Lobo-Ruppert, S.M., Ruppert, J.M., 2005. Induction of KLF4 in basal keratinocytes blocks the proliferation-differentiation switch and initiates squamous epithelial dysplasia. Oncogene. 24**,** 1491-500.

Fox, P.T., Raichle, M.E., 1986. Focal physiological uncoupling of cerebral blood flow and oxidative metabolism during somatosensory stimulation in human subjects. Proc Natl Acad Sci U S A. 83**,** 1140-4.

Fox, P.T., Raichle, M.E., Mintun, M.A., Dence, C., 1988. Nonoxidative glucose consumption during focal physiologic neural activity. Science. 241**,** 462-4.

Frade, J.M., Barde, Y.A., 1998. Nerve growth factor: two receptors, multiple functions. Bioessays. 20**,** 137-45.

Frank, L., Ventimiglia, R., Anderson, K., Lindsay, R.M., Rudge, J.S., 1996. BDNF down-regulates neurotrophin responsiveness, TrkB protein and TrkB mRNA levels in cultured rat hippocampal neurons. Eur J Neurosci. 8**,** 1220-30.

Fraser, D.D., MacVicar, B.A., 1996. Cholinergic-dependent plateau potential in hippocampal CA1 pyramidal neurons. J Neurosci. 16**,** 4113-28.

Friedman, W.J., Larkfors, L., Ayer-LeLievre, C., Ebendal, T., Olson, L., Persson, H., 1990. Regulation of beta-nerve growth factor expression by inflammatory mediators in hippocampal cultures. J Neurosci Res. 27**,** 374-82.

Gadient, R.A., Cron, K.C., Otten, U., 1990. Interleukin-1 beta and tumor necrosis factor-alpha synergistically stimulate nerve growth factor (NGF) release from cultured rat astrocytes. Neurosci Lett. 117**,** 335-40.

Galic, M.A., Riazi, K., Heida, J.G., Mouihate, A., Fournier, N.M., Spencer, S.J., Kalynchuk, L.E., Teskey, G.C., Pittman, Q.J., 2008. Postnatal inflammation increases seizure susceptibility in adult rats. J Neurosci. 28**,** 6904-13.

Gall, C.M., Berschauer, R., Isackson, P.J., 1994. Seizures increase basic fibroblast growth factor mRNA in adult rat forebrain neurons and glia. Brain Res Mol Brain Res. 21**,** 190-205.

Gao, X., Joselin, A.P., Wang, L., Kar, A., Ray, P., Bateman, A., Goate, A.M., Wu, J.Y., 2010. Progranulin promotes neurite outgrowth and neuronal differentiation by regulating GSK-3beta. Protein Cell. 1**,** 552-62.

Garrett-Sinha, L.A., Eberspaecher, H., Seldin, M.F., de Crombrugghe, B., 1996. A gene for a novel zinc-finger protein expressed in differentiated epithelial cells and transiently in certain mesenchymal cells. J Biol Chem. 271**,** 31384-90.

Gass, P., Herdegen, T., Bravo, R., Kiessling, M., 1993. Spatiotemporal induction of immediate early genes in the rat brain after limbic seizures: effects of NMDA receptor antagonist MK-801. Eur J Neurosci. 5**,** 933-43.

Geiman, D.E., Ton-That, H., Johnson, J.M., Yang, V.W., 2000. Transactivation and growth suppression by the gut-enriched Kruppel-like factor (Kruppel-like factor 4) are dependent on acidic amino acid residues and protein-protein interaction. Nucleic Acids Res. 28**,** 1106-13.

Gerhard, A., Pavese, N., Hotton, G., Turkheimer, F., Es, M., Hammers, A., Eggert, K., Oertel, W., Banati, R.B., Brooks, D.J., 2006. In vivo imaging of microglial activation with [11C](R)-PK11195 PET in idiopathic Parkinson's disease. Neurobiol Dis. 21**,** 404-12.

Ghaleb, A.M., Nandan, M.O., Chanchevalap, S., Dalton, W.B., Hisamuddin, I.M., Yang, V.W., 2005. Kruppel-like factors 4 and 5: the yin and yang regulators of cellular proliferation. Cell Res. 15**,** 92-6.

Ghidoni, R., Benussi, L., Glionna, M., Franzoni, M., Binetti, G., 2008. Low plasma progranulin levels predict progranulin mutations in frontotemporal lobar degeneration. Neurology. 71**,** 1235-9.

Gijselinck, I., Van Broeckhoven, C., Cruts, M., 2008. Granulin mutations associated with frontotemporal lobar degeneration and related disorders: an update. Hum Mutat. 29**,** 1373-86.

Giulian, D., Li, J., Li, X., George, J., Rutecki, P.A., 1994. The impact of microglia-derived cytokines upon gliosis in the CNS. Dev Neurosci. 16**,** 128-36.

Giulian, D., 1999. Microglia and the immune pathology of Alzheimer disease. Am J Hum Genet. 65**,** 13-8.

Goddard, G.V., 1967. Development of epileptic seizures through brain stimulation at low intensity. Nature. 214**,** 1020-1.

Goffin, K., Nissinen, J., Van Laere, K., Pitkanen, A., 2007. Cyclicity of spontaneous recurrent seizures in pilocarpine model of temporal lobe epilepsy in rat. Exp Neurol. 205**,** 501-5.

Gowing, G., Philips, T., Van Wijmeersch, B., Audet, J.N., Dewil, M., Van Den Bosch, L., Billiau, A.D., Robberecht, W., Julien, J.P., 2008. Ablation of proliferating microglia does not affect motor neuron degeneration in amyotrophic lateral sclerosis caused by mutant superoxide dismutase. J Neurosci. 28**,** 10234-44.

Guo, A., Tapia, L., Bamji, S.X., Cynader, M.S., Jia, W., 2010. Progranulin deficiency leads to enhanced cell vulnerability and TDP-43 translocation in primary neuronal cultures. Brain Res. 1366**,** 1-8.

Gutierrez, R., 2003. The GABAergic phenotype of the "glutamatergic" granule cells of the dentate gyrus. Prog Neurobiol. 71**,** 337-58.

Gutierrez, R., Romo-Parra, H., Maqueda, J., Vivar, C., Ramirez, M., Morales, M.A., Lamas, M., 2003. Plasticity of the GABAergic phenotype of the "glutamatergic" granule cells of the rat dentate gyrus. J Neurosci. 23**,** 5594-8.

Guzik-Kornacka, A., Sliwa, A., Plucinska, G., Lukasiuk, K., 2011. Status epilepticus evokes prolonged increase in the expression of CCL3 and CCL4 mRNA and protein in the rat brain. Acta Neurobiol Exp (Wars). 71**,** 193-207.

Haddad, J.J., 2005. N-methyl-D-aspartate (NMDA) and the regulation of mitogen-activated protein kinase (MAPK) signaling pathways: a revolving neurochemical axis for therapeutic intervention? Prog Neurobiol. 77**,** 252-82.

Hamada, T., Sonoda, R., Watanabe, A., Ono, M., Shibata, S., Watanabe, S., 1998. NMDA induced glutamate release from the suprachiasmatic nucleus: an in vitro study in the rat. Neurosci Lett. 256**,** 93-6.

Han, J.J., Yu, M., Houston, N., Steinberg, S.M., Kohn, E.C., 2011. Progranulin is a potential prognostic biomarker in advanced epithelial ovarian cancers. Gynecol Oncol. 120**,** 5-10.

Harms, C., Albrecht, K., Harms, U., Seidel, K., Hauck, L., Baldinger, T., Hubner, D., Kronenberg, G., An, J., Ruscher, K., Meisel, A., Dirnagl, U., von Harsdorf, R., Endres, M., Hortnagl, H., 2007. Phosphatidylinositol 3-Akt-kinase-dependent phosphorylation of p21(Waf1/Cip1) as a novel mechanism of neuroprotection by glucocorticoids. J Neurosci. 27**,** 4562-71.

Harper, J.W., Adami, G.R., Wei, N., Keyomarsi, K., Elledge, S.J., 1993. The p21 Cdk-interacting protein Cip1 is a potent inhibitor of G1 cyclin-dependent kinases. Cell. 75**,** 805-16.

He, X.P., Kotloski, R., Nef, S., Luikart, B.W., Parada, L.F., McNamara, J.O., 2004. Conditional deletion of TrkB but not BDNF prevents epileptogenesis in the kindling model. Neuron. 43**,** 31-42.

He, Z., Bateman, A., 1999. Progranulin gene expression regulates epithelial cell growth and promotes tumor growth in vivo. Cancer Res. 59**,** 3222-9.

He, Z., Ismail, A., Kriazhev, L., Sadvakassova, G., Bateman, A., 2002. Progranulin (PC-cell-derived growth factor/acrogranin) regulates invasion and cell survival. Cancer Res. 62**,** 5590-6.

He, Z., Bateman, A., 2003. Progranulin (granulin-epithelin precursor, PC-cell-derived growth factor, acrogranin) mediates tissue repair and tumorigenesis. J Mol Med (Berl). 81**,** 600-12.

He, Z., Ong, C.H., Halper, J., Bateman, A., 2003. Progranulin is a mediator of the wound response. Nat Med. 9**,** 225-9.
Heese, K., Hock, C., Otten, U., 1998. Inflammatory signals induce neurotrophin expression in human microglial cells. J Neurochem. 70**,** 699-707.
Heinemann, U., Beck, H., Dreier, J.P., Ficker, E., Stabel, J., Zhang, C.L., 1992. The Dentate Gyrus as a Regulated Gate for the Propagation of Epileptiform Activity. Epilepsy Research. 273-280.
Henshall, D.C., 2007. Apoptosis signalling pathways in seizure-induced neuronal death and epilepsy. Biochem Soc Trans. 35**,** 421-3.
Hertz, L., Peng, L., Dienel, G.A., 2007. Energy metabolism in astrocytes: high rate of oxidative metabolism and spatiotemporal dependence on glycolysis/glycogenolysis. J Cereb Blood Flow Metab. 27**,** 219-49.
Heyes, M.P., 1993. Quinolinic acid and inflammation. Ann N Y Acad Sci. 679**,** 211-6.
Holtzman, D.M., Lowenstein, D.H., 1995. Selective inhibition of axon outgrowth by antibodies to NGF in a model of temporal lobe epilepsy. J Neurosci. 15**,** 7062-70.
Horbinski, C., Stachowiak, M.K., Higgins, D., Finnegan, S.G., 2001. Polyethyleneimine-mediated transfection of cultured postmitotic neurons from rat sympathetic ganglia and adult human retina. BMC Neurosci. 2**,** 2.
Horvath, R.J., DeLeo, J.A., 2009. Morphine enhances microglial migration through modulation of P2X4 receptor signaling. J Neurosci. 29**,** 998-1005.
Hou, X., Wang, X., Zhang, L., 2010. Conditional downregulation of brain- derived neurotrophic factor and tyrosine kinase receptor B blocks epileptogenesis in the human temporal lobe epilepsy hippocampus. Neurol India. 58**,** 29-34.
Houser, C.R., 1990. Granule cell dispersion in the dentate gyrus of humans with temporal lobe epilepsy. Brain Res. 535**,** 195-204.
Hu, F., Padukkavidana, T., Vaegter, C.B., Brady, O.A., Zheng, Y., Mackenzie, I.R., Feldman, H.H., Nykjaer, A., Strittmatter, S.M., 2010. Sortilin-mediated endocytosis determines levels of the frontotemporal dementia protein, progranulin. Neuron. 68**,** 654-67.
Huang, C.C., Liu, Z., Li, X., Bailey, S.K., Nail, C.D., Foster, K.W., Frost, A.R., Ruppert, J.M., Lobo-Ruppert, S.M., 2005. KLF4 and PCNA identify stages of tumor initiation in a conditional model of cutaneous squamous epithelial neoplasia. Cancer Biol Ther. 4**,** 1401-8.
Hughes, P.M., Allegrini, P.R., Rudin, M., Perry, V.H., Mir, A.K., Wiessner, C., 2002. Monocyte chemoattractant protein-1 deficiency is protective in a murine stroke model. J Cereb Blood Flow Metab. 22**,** 308-17.
Humpel, C., Lippoldt, A., Chadi, G., Ganten, D., Olson, L., Fuxe, K., 1993. Fast and widespread increase of basic fibroblast growth factor messenger RNA and protein in the forebrain after kainate-induced seizures. Neuroscience. 57**,** 913-22.
Hynd, M.R., Scott, H.L., Dodd, P.R., 2004. Glutamate-mediated excitotoxicity and neurodegeneration in Alzheimer's disease. Neurochem Int. 45**,** 583-95.
Ikonomidou-Turski, C., Cavalheiro, E.A., Turski, L., Bortolotto, Z.A., Kleinrok, Z., Calderazzo-Filho, L.S., Turski, W.A., 1988. Differential effects of non-steroidal anti-inflammatory drugs on seizures produced by pilocarpine in rats. Brain Res. 462**,** 275-85.

Ishizuka, K., Kimura, T., Igata-yi, R., Katsuragi, S., Takamatsu, J., Miyakawa, T., 1997. Identification of monocyte chemoattractant protein-1 in senile plaques and reactive microglia of Alzheimer's disease. Psychiatry Clin Neurosci. 51**,** 135-8.

Jang, M.H., Kim, C.J., Kim, E.H., Kim, M.G., Leem, K.H., Kim, J., 2006. Effects of Platycodon grandiflorum on lipopolysaccharide-stimulated production of prostaglandin E2, nitric oxide, and interleukin-8 in mouse microglial BV2 cells. J Med Food. 9**,** 169-74.

Jankowsky, J.L., Patterson, P.H., 2001. The role of cytokines and growth factors in seizures and their sequelae. Prog Neurobiol. 63**,** 125-49.

Jensen, M.S., Azouz, R., Yaari, Y., 1994. Variant firing patterns in rat hippocampal pyramidal cells modulated by extracellular potassium. J Neurophysiol. 71**,** 831-9.

Jones, M.W., Errington, M.L., French, P.J., Fine, A., Bliss, T.V., Garel, S., Charnay, P., Bozon, B., Laroche, S., Davis, S., 2001. A requirement for the immediate early gene Zif268 in the expression of late LTP and long-term memories. Nat Neurosci. 4**,** 289-96.

Kartvelishvily, E., Shleper, M., Balan, L., Dumin, E., Wolosker, H., 2006. Neuron-derived D-serine release provides a novel means to activate N-methyl-D-aspartate receptors. J Biol Chem. 281**,** 14151-62.

Kasischke, K.A., Vishwasrao, H.D., Fisher, P.J., Zipfel, W.R., Webb, W.W., 2004. Neural activity triggers neuronal oxidative metabolism followed by astrocytic glycolysis. Science. 305**,** 99-103.

Kato, M., Hasunuma, N., Nakayama, R., Takeda, J., Itami, S., Taira, M., Manabe, M., Osada, S., 2009. Progranulin, a secreted tumorigenesis and dementia-related factor, regulates mouse hair growth. J Dermatol Sci. 53**,** 234-6.

Kawamata, T., Katayama, Y., Hovda, D.A., Yoshino, A., Becker, D.P., 1995. Lactate accumulation following concussive brain injury: the role of ionic fluxes induced by excitatory amino acids. Brain Res. 674**,** 196-204.

Kayasuga, Y., Chiba, S., Suzuki, M., Kikusui, T., Matsuwaki, T., Yamanouchi, K., Kotaki, H., Horai, R., Iwakura, Y., Nishihara, M., 2007. Alteration of behavioural phenotype in mice by targeted disruption of the progranulin gene. Behav Brain Res. 185**,** 110-8.

Kettenmann, H., Hanisch, U.K., Noda, M., Verkhratsky, A., 2011. Physiology of microglia. Physiol Rev. 91**,** 461-553.

Kielian, T., Barry, B., Hickey, W.F., 2001. CXC chemokine receptor-2 ligands are required for neutrophil-mediated host defense in experimental brain abscesses. J Immunol. 166**,** 4634-43.

Kielian, T., 2004. Microglia and chemokines in infectious diseases of the nervous system: views and reviews. Front Biosci. 9**,** 732-50.

Kiessling, M., Gass, P., 1993. Immediate early gene expression in experimental epilepsy. Brain Pathol. 3**,** 381-93.

Klein, J.A., Ackerman, S.L., 2003. Oxidative stress, cell cycle, and neurodegeneration. J Clin Invest. 111**,** 785-93.

Kleinberger, G., Wils, H., Ponsaerts, P., Joris, G., Timmermans, J.P., Van Broeckhoven, C., Kumar-Singh, S., 2010. Increased caspase activation and decreased TDP-43 solubility in progranulin knockout cortical cultures. J Neurochem. 115**,** 735-47.

Kloss, C.U., Bohatschek, M., Kreutzberg, G.W., Raivich, G., 2001. Effect of lipopolysaccharide on the morphology and integrin immunoreactivity of ramified microglia in the mouse brain and in cell culture. Exp Neurol. 168**,** 32-46.

Knapska, E., Kaczmarek, L., 2004. A gene for neuronal plasticity in the mammalian brain: Zif268/Egr-1/NGFI-A/Krox-24/TIS8/ZENK? Prog Neurobiol. 74**,** 183-211.

Knusel, B., Gao, H., Okazaki, T., Yoshida, T., Mori, N., Hefti, F., Kaplan, D.R., 1997. Ligand-induced down-regulation of Trk messenger RNA, protein and tyrosine phosphorylation in rat cortical neurons. Neuroscience. 78**,** 851-62.

Kokaia, M., Ernfors, P., Kokaia, Z., Elmer, E., Jaenisch, R., Lindvall, O., 1995. Suppressed epileptogenesis in BDNF mutant mice. Exp Neurol. 133**,** 215-24.

Kondratyev, A., Ved, R., Gale, K., 2002. The effects of repeated minimal electroconvulsive shock exposure on levels of mRNA encoding fibroblast growth factor-2 and nerve growth factor in limbic regions. Neuroscience. 114**,** 411-6.

Kotti, T., Tapiola, T., Riekkinen, P.J., Sr., Miettinen, R., 1996. The calretinin-containing mossy cells survive excitotoxic insult in the gerbil dentate gyrus. Comparison of excitotoxicity-induced neuropathological changes in the gerbil and rat. Eur J Neurosci. 8**,** 2371-8.

Kovac, L., 2010. The 20 W sleep-walkers. EMBO Rep. 11**,** 2.

Kubik, S., Miyashita, T., Guzowski, J.F., 2007. Using immediate-early genes to map hippocampal subregional functions. Learn Mem. 14**,** 758-70.

Kumai, Y., Ooboshi, H., Takada, J., Kamouchi, M., Kitazono, T., Egashira, K., Ibayashi, S., Iida, M., 2004. Anti-monocyte chemoattractant protein-1 gene therapy protects against focal brain ischemia in hypertensive rats. J Cereb Blood Flow Metab. 24**,** 1359-68.

Kumar-Singh, S., 2011. Progranulin and TDP-43: Mechanistic Links and Future Directions. J Mol Neurosci.

Kuramoto, S., Yasuhara, T., Agari, T., Kondo, A., Jing, M., Kikuchi, Y., Shinko, A., Wakamori, T., Kameda, M., Wang, F., Kin, K., Edahiro, S., Miyoshi, Y., Date, I., 2011. BDNF-secreting capsule exerts neuroprotective effects on epilepsy model of rats. Brain Res. 1368**,** 281-9.

Kuruba, R., Hattiangady, B., Parihar, V.K., Shuai, B., Shetty, A.K., 2011. Differential susceptibility of interneurons expressing neuropeptide y or parvalbumin in the aged hippocampus to acute seizure activity. PLoS One. 6**,** e24493.

Kwak, S., Weiss, J.H., 2006. Calcium-permeable AMPA channels in neurodegenerative disease and ischemia. Curr Opin Neurobiol. 16**,** 281-7.

Lacroix, M., Toillon, R.A., Leclercq, G., 2006. p53 and breast cancer, an update. Endocr Relat Cancer. 13**,** 293-325.

LaFrance, W.C., Jr., Leaver, K., Stopa, E.G., Papandonatos, G.D., Blum, A.S., 2010. Decreased serum BDNF levels in patients with epileptic and psychogenic nonepileptic seizures. Neurology. 75**,** 1285-91.

Lahteinen, S., Pitkanen, A., Saarelainen, T., Nissinen, J., Koponen, E., Castren, E., 2002. Decreased BDNF signalling in transgenic mice reduces epileptogenesis. Eur J Neurosci. 15**,** 721-34.

Lankiewicz, S., Marc Luetjens, C., Truc Bui, N., Krohn, A.J., Poppe, M., Cole, G.M., Saido, T.C., Prehn, J.H., 2000. Activation of calpain I converts excitotoxic neuron death into a caspase-independent cell death. J Biol Chem. 275**,** 17064-71.

Larmet, Y., Reibel, S., Carnahan, J., Nawa, H., Marescaux, C., Depaulis, A., 1995. Protective effects of brain-derived neurotrophic factor on the development of hippocampal kindling in the rat. Neuroreport. 6**,** 1937-41.

Lauritzen, F., Perez, E.L., Melillo, E.R., Roh, J.M., Zaveri, H.P., Lee, T.S., Wang, Y., Bergersen, L.H., Eid, T., 2011. Altered expression of brain monocarboxylate transporter 1 in models of temporal lobe epilepsy. Neurobiol Dis.

Lee, M.J., Chen, T.F., Cheng, T.W., Chiu, M.J., 2011. rs5848 variant of progranulin gene is a risk of Alzheimer's disease in the Taiwanese population. Neurodegener Dis. 8**,** 216-20.

Lee, T.S., Mane, S., Eid, T., Zhao, H.Y., Lin, A.P., Guan, Z., Kim, J.H., Schweitzer, J., King-Stevens, D., Weber, P., Spencer, S.S., Spencer, D.D., de Lanerolle, N.C., 2007. Gene expression in temporal lobe epilepsy is consistent with increased release of glutamate by astrocytes. Molecular Medicine. 13**,** 1-13.

Lerea, L.S., Butler, L.S., McNamara, J.O., 1992. NMDA and non-NMDA receptor-mediated increase of c-fos mRNA in dentate gyrus neurons involves calcium influx via different routes. J Neurosci. 12**,** 2973-81.

Lewis, J., Golde, T.E., 2010. Sorting out frontotemporal dementia? Neuron. 68**,** 601-3.

Li, F., Zhu, S., Wu, C., Yan, C., Liu, Y., Shugan, L., 2011. Neuroinflammation and cell therapy for Parkinson's disease. Front Biosci (Schol Ed). 3**,** 1407-20.

Li, L.M., Cendes, F., Andermann, F., Watson, C., Fish, D.R., Cook, M.J., Dubeau, F., Duncan, J.S., Shorvon, S.D., Berkovic, S.F., Free, S., Olivier, A., Harkness, W., Arnold, D.L., 1999. Surgical outcome in patients with epilepsy and dual pathology. Brain. 122 (Pt 5)**,** 799-805.

Li, P.A., Shamloo, M., Katsura, K., Smith, M.L., Siesjo, B.K., 1995. Critical values for plasma glucose in aggravating ischaemic brain damage: correlation to extracellular pH. Neurobiol Dis. 2**,** 97-108.

Li, X., Massa, P.E., Hanidu, A., Peet, G.W., Aro, P., Savitt, A., Mische, S., Li, J., Marcu, K.B., 2002. IKKalpha, IKKbeta, and NEMO/IKKgamma are each required for the NF-kappa B-mediated inflammatory response program. J Biol Chem. 277**,** 45129-40.

Link, W., Konietzko, U., Kauselmann, G., Krug, M., Schwanke, B., Frey, U., Kuhl, D., 1995. Somatodendritic expression of an immediate early gene is regulated by synaptic activity. Proc Natl Acad Sci U S A. 92**,** 5734-8.

Lipton, P., 1999. Ischemic cell death in brain neurons. Physiol Rev. 79**,** 1431-568.

Liu, D.X., Greene, L.A., 2001. Neuronal apoptosis at the G1/S cell cycle checkpoint. Cell Tissue Res. 305**,** 217-28.

Liu, J.X., Cao, X., Tang, Y.C., Liu, Y., Tang, F.R., 2007a. CCR7, CCR8, CCR9 and CCR10 in the mouse hippocampal CA1 area and the dentate gyrus during and after pilocarpine-induced status epilepticus. J Neurochem. 100**,** 1072-88.

Liu, Y., Wong, T.P., Aarts, M., Rooyakkers, A., Liu, L., Lai, T.W., Wu, D.C., Lu, J., Tymianski, M., Craig, A.M., Wang, Y.T., 2007b. NMDA receptor subunits have differential roles in mediating excitotoxic neuronal death both in vitro and in vivo. J Neurosci. 27**,** 2846-57.

Liu, Z., Holmes, G.L., 1997a. Basic fibroblast growth factor is highly neuroprotective against seizure-induced long-term behavioural deficits. Neuroscience. 76**,** 1129-38.

Liu, Z., Holmes, G.L., 1997b. Basic fibroblast growth factor-induced seizures in rats. Neurosci Lett. 233**,** 85-8.
Lois, C., Hong, E.J., Pease, S., Brown, E.J., Baltimore, D., 2002. Germline transmission and tissue-specific expression of transgenes delivered by lentiviral vectors. Science. 295**,** 868-72.
Lokensgard, J.R., Hu, S., Hegg, C.C., Thayer, S.A., Gekker, G., Peterson, P.K., 2001. Diazepam inhibits HIV-1 Tat-induced migration of human microglia. J Neurovirol. 7**,** 481-6.
Longo, B.M., Mello, L.E., 1997. Blockade of pilocarpine- or kainate-induced mossy fiber sprouting by cycloheximide does not prevent subsequent epileptogenesis in rats. Neurosci Lett. 226**,** 163-6.
Longo, B.M., Sanabria, E.R., Gabriel, S., Mello, L.E., 2002. Electrophysiologic abnormalities of the hippocampus in the pilocarpine/cycloheximide model of chronic spontaneous seizures. Epilepsia. 43 Suppl 5**,** 203-8.
Loscher, W., Ebert, U., 1996. The role of the piriform cortex in kindling. Prog Neurobiol. 50**,** 427-81.
Loscher, W., 2011. Critical review of current animal models of seizures and epilepsy used in the discovery and development of new antiepileptic drugs. Seizure. 20**,** 359-68.
Losy, J., Zaremba, J., 2001. Monocyte chemoattractant protein-1 is increased in the cerebrospinal fluid of patients with ischemic stroke. Stroke. 32**,** 2695-6.
Louboutin, J.P., Chekmasova, A., Marusich, E., Agrawal, L., Strayer, D.S., 2011. Role of CCR5 and its ligands in the control of vascular inflammation and leukocyte recruitment required for acute excitotoxic seizure induction and neural damage. FASEB J. 25**,** 737-53.
Louis, E.D., Williamson, P.D., Darcey, T.M., 1987. Experimental models of chronic focal epilepsy: a critical review of four models. Yale J Biol Med. 60**,** 255-72.
Lowenstein, D.H., Arsenault, L., 1996. Dentate granule cell layer collagen explant cultures: spontaneous axonal growth and induction by brain-derived neurotrophic factor or basic fibroblast growth factor. Neuroscience. 74**,** 1197-208.
Lu, M.O., Zhang, X.M., Mix, E., Quezada, H.C., Jin, T., Zhu, J., Adem, A., 2008. TNF-alpha receptor 1 deficiency enhances kainic acid-induced hippocampal injury in mice. J Neurosci Res. 86**,** 1608-14.
Luttjohann, A., Fabene, P.F., van Luijtelaar, G., 2009. A revised Racine's scale for PTZ-induced seizures in rats. Physiol Behav. 98**,** 579-86.
Lynch, D.R., Guttmann, R.P., 2002. Excitotoxicity: perspectives based on N-methyl-D-aspartate receptor subtypes. J Pharmacol Exp Ther. 300**,** 717-23.
Mackenzie, I.R., 2007. The neuropathology and clinical phenotype of FTD with progranulin mutations. Acta Neuropathol. 114**,** 49-54.
Manley, N.C., Bertrand, A.A., Kinney, K.S., Hing, T.C., Sapolsky, R.M., 2007. Characterization of monocyte chemoattractant protein-1 expression following a kainate model of status epilepticus. Brain Res. 1182**,** 138-43.
Martin, J.A., Craft, D.K., Su, J.H., Kim, R.C., Cotman, C.W., 2001. Astrocytes degenerate in frontotemporal dementia: possible relation to hypoperfusion. Neurobiol Aging. 22**,** 195-207.

Maslowski, K.M., Vieira, A.T., Ng, A., Kranich, J., Sierro, F., Yu, D., Schilter, H.C., Rolph, M.S., Mackay, F., Artis, D., Xavier, R.J., Teixeira, M.M., Mackay, C.R., 2009. Regulation of inflammatory responses by gut microbiota and chemoattractant receptor GPR43. Nature. 461**,** 1282-6.

Matsuwaki, T., Asakura, R., Suzuki, M., Yamanouchi, K., Nishihara, M., 2011. Age-dependent changes in progranulin expression in the mouse brain. J Reprod Dev. 57**,** 113-9.

McCarthy, K.D., de Vellis, J., 1980. Preparation of separate astroglial and oligodendroglial cell cultures from rat cerebral tissue. J Cell Biol. 85**,** 890-902.

McConnell, B.B., Yang, V.W., 2010. Mammalian Kruppel-like factors in health and diseases. Physiol Rev. 90**,** 1337-81.

Meldrum, B.S., Horton, R.W., 1971. Convulsive effects of 4-deoxypyridoxine and of bicuculline in photosensitive baboons (Papio papio) and in rhesus monkeys (Macaca mulatta). Brain Res. 35**,** 419-36.

Meldrum, B.S., 1993. Excitotoxicity and selective neuronal loss in epilepsy. Brain Pathol. 3**,** 405-12.

Meldrum, B.S., Akbar, M.T., Chapman, A.G., 1999. Glutamate receptors and transporters in genetic and acquired models of epilepsy. Epilepsy Res. 36**,** 189-204.

Mirnajafi-Zadeh, J., Mortazavi, M., Fathollahi, Y., Alasvand Zarasvand, M., Reza Palizvan, M., 2002. Effect of transient hippocampal inhibition on amygdaloid kindled seizures and amygdaloid kindling rate. Brain Res. 954**,** 220-6.

Mirrione, M.M., Konomos, D.K., Gravanis, I., Dewey, S.L., Aguzzi, A., Heppner, F.L., Tsirka, S.E., 2010. Microglial ablation and lipopolysaccharide preconditioning affects pilocarpine-induced seizures in mice. Neurobiol Dis. 39**,** 85-97.

Molinuevo, J.L., Llado, A., Rami, L., 2005. Memantine: targeting glutamate excitotoxicity in Alzheimer's disease and other dementias. Am J Alzheimers Dis Other Demen. 20**,** 77-85.

Monje, M.L., Toda, H., Palmer, T.D., 2003. Inflammatory blockade restores adult hippocampal neurogenesis. Science. 302**,** 1760-5.

Moody, W.J., Futamachi, K.J., Prince, D.A., 1974. Extracellular potassium activity during epileptogenesis. Exp Neurol. 42**,** 248-63.

Morimoto, K., Fahnestock, M., Racine, R.J., 2004. Kindling and status epilepticus models of epilepsy: rewiring the brain. Prog Neurobiol. 73**,** 1-60.

Moser, B., Wolf, M., Walz, A., Loetscher, P., 2004. Chemokines: multiple levels of leukocyte migration control. Trends Immunol. 25**,** 75-84.

Mukherjee, O., Wang, J., Gitcho, M., Chakraverty, S., Taylor-Reinwald, L., Shears, S., Kauwe, J.S., Norton, J., Levitch, D., Bigio, E.H., Hatanpaa, K.J., White, C.L., Morris, J.C., Cairns, N.J., Goate, A., 2008. Molecular characterization of novel progranulin (GRN) mutations in frontotemporal dementia. Hum Mutat. 29**,** 512-21.

Nadler, J.V., 2003. The recurrent mossy fiber pathway of the epileptic brain. Neurochem Res. 28**,** 1649-58.

Nakajima, K., Kikuchi, Y., Ikoma, E., Honda, S., Ishikawa, M., Liu, Y., Kohsaka, S., 1998. Neurotrophins regulate the function of cultured microglia. Glia. 24**,** 272-89.

Nakajima, K., Honda, S., Tohyama, Y., Imai, Y., Kohsaka, S., Kurihara, T., 2001. Neurotrophin secretion from cultured microglia. J Neurosci Res. 65**,** 322-31.

Namura, S., Zhu, J., Fink, K., Endres, M., Srinivasan, A., Tomaselli, K.J., Yuan, J., Moskowitz, M.A., 1998. Activation and cleavage of caspase-3 in apoptosis induced by experimental cerebral ischemia. J Neurosci. 18**,** 3659-68.

Nedachi, T., Kawai, T., Matsuwaki, T., Yamanouchi, K., Nishihara, M., 2011. Progranulin enhances neural progenitor cell proliferation through glycogen synthase kinase 3beta phosphorylation. Neuroscience. 185**,** 106-15.

Neumann, M., Sampathu, D.M., Kwong, L.K., Truax, A.C., Micsenyi, M.C., Chou, T.T., Bruce, J., Schuck, T., Grossman, M., Clark, C.M., McCluskey, L.F., Miller, B.L., Masliah, E., Mackenzie, I.R., Feldman, H., Feiden, W., Kretzschmar, H.A., Trojanowski, J.Q., Lee, V.M., 2006. Ubiquitinated TDP-43 in frontotemporal lobar degeneration and amyotrophic lateral sclerosis. Science. 314**,** 130-3.

Nicoletti, J.N., Shah, S.K., McCloskey, D.P., Goodman, J.H., Elkady, A., Atassi, H., Hylton, D., Rudge, J.S., Scharfman, H.E., Croll, S.D., 2008. Vascular endothelial growth factor is up-regulated after status epilepticus and protects against seizure-induced neuronal loss in hippocampus. Neuroscience. 151**,** 232-41.

Nishimura, Y., Igarashi, T., Haigwood, N., Sadjadpour, R., Plishka, R.J., Buckler-White, A., Shibata, R., Martin, M.A., 2002. Determination of a statistically valid neutralization titer in plasma that confers protection against simian-human immunodeficiency virus challenge following passive transfer of high-titered neutralizing antibodies. J Virol. 76**,** 2123-30.

Nolte, C., Kirchhoff, F., Kettenmann, H., 1997. Epidermal growth factor is a motility factor for microglial cells in vitro: evidence for EGF receptor expression. Eur J Neurosci. 9**,** 1690-8.

O'Kusky, J., Colonnier, M., 1982. A laminar analysis of the number of neurons, glia, and synapses in the adult cortex (area 17) of adult macaque monkeys. J Comp Neurol. 210**,** 278-90.

Ogawa, S., Lee, T.M., Nayak, A.S., Glynn, P., 1990. Oxygenation-sensitive contrast in magnetic resonance image of rodent brain at high magnetic fields. Magn Reson Med. 14**,** 68-78.

Okamoto, S., Li, Z., Ju, C., Scholzke, M.N., Mathews, E., Cui, J., Salvesen, G.S., Bossy-Wetzel, E., Lipton, S.A., 2002. Dominant-interfering forms of MEF2 generated by caspase cleavage contribute to NMDA-induced neuronal apoptosis. Proc Natl Acad Sci U S A. 99**,** 3974-9.

Ong, C.H., He, Z., Kriazhev, L., Shan, X., Palfree, R.G., Bateman, A., 2006. Regulation of progranulin expression in myeloid cells. Am J Physiol Regul Integr Comp Physiol. 291**,** R1602-12.

Osuga, H., Osuga, S., Wang, F., Fetni, R., Hogan, M.J., Slack, R.S., Hakim, A.M., Ikeda, J.E., Park, D.S., 2000. Cyclin-dependent kinases as a therapeutic target for stroke. Proc Natl Acad Sci U S A. 97**,** 10254-9.

Pallud, J., Haussler, U., Langlois, M., Hamelin, S., Devaux, B., Deransart, C., Depaulis, A., 2010. Dentate gyrus and hilus transection blocks seizure propagation and granule cell dispersion in a mouse model for mesial temporal lobe epilepsy. Hippocampus.

Pandya, A.Y., Talley, L.I., Frost, A.R., Fitzgerald, T.J., Trivedi, V., Chakravarthy, M., Chhieng, D.C., Grizzle, W.E., Engler, J.A., Krontiras, H., Bland, K.I., LoBuglio, A.F., Lobo-Ruppert, S.M., Ruppert, J.M., 2004. Nuclear localization of KLF4 is

associated with an aggressive phenotype in early-stage breast cancer. Clin Cancer Res. 10**,** 2709-19.
Panuccio, G., D'Antuono, M., de Guzman, P., De Lannoy, L., Biagini, G., Avoli, M., 2010. In vitro ictogenesis and parahippocampal networks in a rodent model of temporal lobe epilepsy. Neurobiol Dis. 39**,** 372-80.
Parent, J.M., Lowenstein, D.H., 1997. Mossy fiber reorganization in the epileptic hippocampus. Curr Opin Neurol. 10**,** 103-9.
Parent, J.M., Murphy, G.G., 2008. Mechanisms and functional significance of aberrant seizure-induced hippocampal neurogenesis. Epilepsia. 49 Suppl 5**,** 19-25.
Park, D.S., Levine, B., Ferrari, G., Greene, L.A., 1997a. Cyclin dependent kinase inhibitors and dominant negative cyclin dependent kinase 4 and 6 promote survival of NGF-deprived sympathetic neurons. J Neurosci. 17**,** 8975-83.
Park, D.S., Morris, E.J., Greene, L.A., Geller, H.M., 1997b. G1/S cell cycle blockers and inhibitors of cyclin-dependent kinases suppress camptothecin-induced neuronal apoptosis. J Neurosci. 17**,** 1256-70.
Park, D.S., Morris, E.J., Padmanabhan, J., Shelanski, M.L., Geller, H.M., Greene, L.A., 1998. Cyclin-dependent kinases participate in death of neurons evoked by DNA-damaging agents. J Cell Biol. 143**,** 457-67.
Park, D.S., Obeidat, A., Giovanni, A., Greene, L.A., 2000. Cell cycle regulators in neuronal death evoked by excitotoxic stress: implications for neurodegeneration and its treatment. Neurobiol Aging. 21**,** 771-81.
Patel, A.B., de Graaf, R.A., Mason, G.F., Kanamatsu, T., Rothman, D.L., Shulman, R.G., Behar, K.L., 2004. Glutamatergic neurotransmission and neuronal glucose oxidation are coupled during intense neuronal activation. J Cereb Blood Flow Metab. 24**,** 972-85.
Patel, M.N., McNamara, J.O., 1995. Selective enhancement of axonal branching of cultured dentate gyrus neurons by neurotrophic factors. Neuroscience. 69**,** 763-70.
Pellerin, L., Magistretti, P.J., 1994. Glutamate uptake into astrocytes stimulates aerobic glycolysis: a mechanism coupling neuronal activity to glucose utilization. Proc Natl Acad Sci U S A. 91**,** 10625-9.
Pellerin, L., Bergersen, L.H., Halestrap, A.P., Pierre, K., 2005. Cellular and subcellular distribution of monocarboxylate transporters in cultured brain cells and in the adult brain. J Neurosci Res. 79**,** 55-64.
Pellerin, L., Bouzier-Sore, A.K., Aubert, A., Serres, S., Merle, M., Costalat, R., Magistretti, P.J., 2007. Activity-dependent regulation of energy metabolism by astrocytes: an update. Glia. 55**,** 1251-62.
Peltola, J., Hurme, M., Miettinen, A., Keranen, T., 1998. Elevated levels of interleukin-6 may occur in cerebrospinal fluid from patients with recent epileptic seizures. Epilepsy Res. 31**,** 129-33.
Penkowa, M., Molinero, A., Carrasco, J., Hidalgo, J., 2001. Interleukin-6 deficiency reduces the brain inflammatory response and increases oxidative stress and neurodegeneration after kainic acid-induced seizures. Neuroscience. 102**,** 805-18.
Petkau, T.L., Neal, S.J., Orban, P.C., MacDonald, J.L., Hill, A.M., Lu, G., Feldman, H.H., Mackenzie, I.R., Leavitt, B.R., 2010. Progranulin expression in the developing and adult murine brain. J Comp Neurol. 518**,** 3931-47.

Pfund, Z., Chugani, D.C., Juhasz, C., Muzik, O., Chugani, H.T., Wilds, I.B., Seraji-Bozorgzad, N., Moore, G.J., 2000. Evidence for coupling between glucose metabolism and glutamate cycling using FDG PET and 1H magnetic resonance spectroscopy in patients with epilepsy. J Cereb Blood Flow Metab. 20**,** 871-8.

Philips, T., De Muynck, L., Thu, H.N., Weynants, B., Vanacker, P., Dhondt, J., Sleegers, K., Schelhaas, H.J., Verbeek, M., Vandenberghe, R., Sciot, R., Van Broeckhoven, C., Lambrechts, D., Van Leuven, F., Van Den Bosch, L., Robberecht, W., Van Damme, P., 2010. Microglial upregulation of progranulin as a marker of motor neuron degeneration. J Neuropathol Exp Neurol. 69**,** 1191-200.

Pickford, F., Marcus, J., Camargo, L.M., Xiao, Q., Graham, D., Mo, J.R., Burkhardt, M., Kulkarni, V., Crispino, J., Hering, H., Hutton, M., 2011. Progranulin is a chemoattractant for microglia and stimulates their endocytic activity. Am J Pathol. 178**,** 284-95.

Pierre, K., Parent, A., Jayet, P.Y., Halestrap, A.P., Scherrer, U., Pellerin, L., 2007. Enhanced expression of three monocarboxylate transporter isoforms in the brain of obese mice. J Physiol. 583**,** 469-86.

Pitkanen, A., Lukasiuk, K., 2011. Mechanisms of epileptogenesis and potential treatment targets. Lancet Neurol. 10**,** 173-86.

Pivovarova, N.B., Andrews, S.B., 2010. Calcium-dependent mitochondrial function and dysfunction in neurons. FEBS J. 277**,** 3622-36.

Platenik, J., Kuramoto, N., Yoneda, Y., 2000. Molecular mechanisms associated with long-term consolidation of the NMDA signals. Life Sci. 67**,** 335-64.

Polascheck, N., Bankstahl, M., Loscher, W., 2010. The COX-2 inhibitor parecoxib is neuroprotective but not antiepileptogenic in the pilocarpine model of temporal lobe epilepsy. Exp Neurol. 224**,** 219-33.

Poulsen, C.F., Simeone, T.A., Maar, T.E., Smith-Swintosky, V., White, H.S., Schousboe, A., 2004. Modulation by topiramate of AMPA and kainate mediated calcium influx in cultured cerebral cortical, hippocampal and cerebellar neurons. Neurochem Res. 29**,** 275-82.

Prasad, S.S., Nie, W., Kojic, L.Z., Wen, Y.H., Jia, W., Biernaskie, J.A., McKay, K., Corbett, D., Lu, J., Cynader, M.S., 2004. Toward the development of a stroke-triggered vector: gene expression analysis during cerebral ischemia Society for Neuroscience Abstracts. 343.10.

Prichard, J., Rothman, D., Novotny, E., Petroff, O., Kuwabara, T., Avison, M., Howseman, A., Hanstock, C., Shulman, R., 1991. Lactate rise detected by 1H NMR in human visual cortex during physiologic stimulation. Proc Natl Acad Sci U S A. 88**,** 5829-31.

Pro, S., Randi, F., Pulitano, P., Vicenzini, E., Mecarelli, O., 2011. Non-convulsive status epilepticus characterised exclusively by a language disorder induced by non-ketotic hyperglycaemia. Epileptic Disord. 13**,** 193-6.

Qin, H., Wilson, C.A., Roberts, K.L., Baker, B.J., Zhao, X., Benveniste, E.N., 2006. IL-10 inhibits lipopolysaccharide-induced CD40 gene expression through induction of suppressor of cytokine signaling-3. J Immunol. 177**,** 7761-71.

Racine, R.J., 1972a. Modification of seizure activity by electrical stimulation. II. Motor seizure. Electroencephalogr Clin Neurophysiol. 32**,** 281-94.

Racine, R.J., 1972b. Modification of seizure activity by electrical stimulation. I. After-discharge threshold. Electroencephalogr Clin Neurophysiol. 32**,** 269-79.
Rafiq, A., Zhang, Y.F., DeLorenzo, R.J., Coulter, D.A., 1995. Long-duration self-sustained epileptiform activity in the hippocampal-parahippocampal slice: a model of status epilepticus. J Neurophysiol. 74**,** 2028-42.
Rashid, K., Van der Zee, C.E., Ross, G.M., Chapman, C.A., Stanisz, J., Riopelle, R.J., Racine, R.J., Fahnestock, M., 1995. A nerve growth factor peptide retards seizure development and inhibits neuronal sprouting in a rat model of epilepsy. Proc Natl Acad Sci U S A. 92**,** 9495-9.
Rashidian, J., Iyirhiaro, G., Aleyasin, H., Rios, M., Vincent, I., Callaghan, S., Bland, R.J., Slack, R.S., During, M.J., Park, D.S., 2005. Multiple cyclin-dependent kinases signals are critical mediators of ischemia/hypoxic neuronal death in vitro and in vivo. Proc Natl Acad Sci U S A. 102**,** 14080-5.
Ravizza, T., Rizzi, M., Perego, C., Richichi, C., Veliskova, J., Moshe, S.L., De Simoni, M.G., Vezzani, A., 2005. Inflammatory response and glia activation in developing rat hippocampus after status epilepticus. Epilepsia. 46 Suppl 5**,** 113-7.
Reed, S.E., Staley, E.M., Mayginnes, J.P., Pintel, D.J., Tullis, G.E., 2006. Transfection of mammalian cells using linear polyethylenimine is a simple and effective means of producing recombinant adeno-associated virus vectors. J Virol Methods. 138**,** 85-98.
Riazi, K., Galic, M.A., Kuzmiski, J.B., Ho, W., Sharkey, K.A., Pittman, Q.J., 2008. Microglial activation and TNFalpha production mediate altered CNS excitability following peripheral inflammation. Proc Natl Acad Sci U S A. 105**,** 17151-6.
Rigau, V., Morin, M., Rousset, M.C., de Bock, F., Lebrun, A., Coubes, P., Picot, M.C., Baldy-Moulinier, M., Bockaert, J., Crespel, A., Lerner-Natoli, M., 2007. Angiogenesis is associated with blood-brain barrier permeability in temporal lobe epilepsy. Brain. 130**,** 1942-56.
Riva, M.A., Donati, E., Tascedda, F., Zolli, M., Racagni, G., 1994. Short- and long-term induction of basic fibroblast growth factor gene expression in rat central nervous system following kainate injection. Neuroscience. 59**,** 55-65.
Rodriguez, J.J., Olabarria, M., Chvatal, A., Verkhratsky, A., 2009. Astroglia in dementia and Alzheimer's disease. Cell Death Differ. 16**,** 378-85.
Rossi, D.J., Brady, J.D., Mohr, C., 2007. Astrocyte metabolism and signaling during brain ischemia. Nat Neurosci. 10**,** 1377-86.
Rovelet-Lecrux, A., Deramecourt, V., Legallic, S., Maurage, C.A., Le Ber, I., Brice, A., Lambert, J.C., Frebourg, T., Hannequin, D., Pasquier, F., Campion, D., 2008. Deletion of the progranulin gene in patients with frontotemporal lobar degeneration or Parkinson disease. Neurobiol Dis. 31**,** 41-5.
Rowland, B.D., Bernards, R., Peeper, D.S., 2005. The KLF4 tumour suppressor is a transcriptional repressor of p53 that acts as a context-dependent oncogene. Nat Cell Biol. 7**,** 1074-82.
Rowland, B.D., Peeper, D.S., 2006. KLF4, p21 and context-dependent opposing forces in cancer. Nat Rev Cancer. 6**,** 11-23.
Rudge, J.S., Mather, P.E., Pasnikowski, E.M., Cai, N., Corcoran, T., Acheson, A., Anderson, K., Lindsay, R.M., Wiegand, S.J., 1998. Endogenous BDNF protein is

increased in adult rat hippocampus after a kainic acid induced excitotoxic insult but exogenous BDNF is not neuroprotective. Exp Neurol. 149**,** 398-410.
Rutecki, P.A., Yang, Y., 1998. Ictal epileptiform activity in the CA3 region of hippocampal slices produced by pilocarpine. J Neurophysiol. 79**,** 3019-29.
Ryan, C.L., Baranowski, D.C., Chitramuthu, B.P., Malik, S., Li, Z., Cao, M., Minotti, S., Durham, H.D., Kay, D.G., Shaw, C.A., Bennett, H.P., Bateman, A., 2009. Progranulin is expressed within motor neurons and promotes neuronal cell survival. BMC Neurosci. 10**,** 130.
Ryu, J.K., Cho, T., Choi, H.B., Wang, Y.T., McLarnon, J.G., 2009. Microglial VEGF receptor response is an integral chemotactic component in Alzheimer's disease pathology. J Neurosci. 29**,** 3-13.
Sagduyu, K., 2002. Neuropsychopharmacology: The fifth generation of progress. American Journal of Psychiatry. 159**,** 133-145.
Sanabria, E.R., Su, H., Yaari, Y., 2001. Initiation of network bursts by Ca2+-dependent intrinsic bursting in the rat pilocarpine model of temporal lobe epilepsy. J Physiol. 532**,** 205-16.
Santhakumar, V., Aradi, I., Soltesz, I., 2005. Role of mossy fiber sprouting and mossy cell loss in hyperexcitability: a network model of the dentate gyrus incorporating cell types and axonal topography. J Neurophysiol. 93**,** 437-53.
Sappey-Marinier, D., Calabrese, G., Fein, G., Hugg, J.W., Biggins, C., Weiner, M.W., 1992. Effect of photic stimulation on human visual cortex lactate and phosphates using 1H and 31P magnetic resonance spectroscopy. J Cereb Blood Flow Metab. 12**,** 584-92.
Sattler, R., Tymianski, M., 2001. Molecular mechanisms of glutamate receptor-mediated excitotoxic neuronal cell death. Mol Neurobiol. 24**,** 107-29.
Savage, D.D., Rigsbee, L.C., McNamara, J.O., 1985. Knife cuts of entorhinal cortex: effects on development of amygdaloid kindling and seizure-induced decrease of muscarinic cholinergic receptors. J Neurosci. 5**,** 408-13.
Sayyah, M., Javad-Pour, M., Ghazi-Khansari, M., 2003. The bacterial endotoxin lipopolysaccharide enhances seizure susceptibility in mice: involvement of proinflammatory factors: nitric oxide and prostaglandins. Neuroscience. 122**,** 1073-80.
Scharfman, H.E., Schwartzkroin, P.A., 1988. Electrophysiology of morphologically identified mossy cells of the dentate hilus recorded in guinea pig hippocampal slices. J Neurosci. 8**,** 3812-21.
Scharfman, H.E., 1991. Dentate hilar cells with dendrites in the molecular layer have lower thresholds for synaptic activation by perforant path than granule cells. J Neurosci. 11**,** 1660-73.
Scharfman, H.E., 1995. Electrophysiological evidence that dentate hilar mossy cells are excitatory and innervate both granule cells and interneurons. J Neurophysiol. 74**,** 179-94.
Scharfman, H.E., Goodman, J.H., Sollas, A.L., Croll, S.D., 2002. Spontaneous limbic seizures after intrahippocampal infusion of brain-derived neurotrophic factor. Exp Neurol. 174**,** 201-14.

Schilling, M., Strecker, J.K., Ringelstein, E.B., Schabitz, W.R., Kiefer, R., 2009. The role of CC chemokine receptor 2 on microglia activation and blood-borne cell recruitment after transient focal cerebral ischemia in mice. Brain Res. 1289**,** 79-84.
Schlaepfer, D.D., Hauck, C.R., Sieg, D.J., 1999. Signaling through focal adhesion kinase. Prog Biophys Mol Biol. 71**,** 435-78.
Segre, J.A., Bauer, C., Fuchs, E., 1999. Klf4 is a transcription factor required for establishing the barrier function of the skin. Nat Genet. 22**,** 356-60.
Serhan, C.N., Chiang, N., Van Dyke, T.E., 2008. Resolving inflammation: dual anti-inflammatory and pro-resolution lipid mediators. Nat Rev Immunol. 8**,** 349-61.
Shankaran, S.S., Capell, A., Hruscha, A.T., Fellerer, K., Neumann, M., Schmid, B., Haass, C., 2008. Missense mutations in the progranulin gene linked to frontotemporal lobar degeneration with ubiquitin-immunoreactive inclusions reduce progranulin production and secretion. J Biol Chem. 283**,** 1744-53.
Sharma, A.K., Jordan, W.H., Reams, R.Y., Hall, D.G., Snyder, P.W., 2008. Temporal profile of clinical signs and histopathologic changes in an F-344 rat model of kainic acid-induced mesial temporal lobe epilepsy. Toxicol Pathol. 36**,** 932-43.
Sherr, C.J., Roberts, J.M., 1999. CDK inhibitors: positive and negative regulators of G1-phase progression. Genes Dev. 13**,** 1501-12.
Shi, J., Johansson, J., Woodling, N.S., Wang, Q., Montine, T.J., Andreasson, K., 2010. The prostaglandin E2 E-prostanoid 4 receptor exerts anti-inflammatory effects in brain innate immunity. J Immunol. 184**,** 7207-18.
Shie, J.L., Chen, Z.Y., Fu, M., Pestell, R.G., Tseng, C.C., 2000. Gut-enriched Kruppel-like factor represses cyclin D1 promoter activity through Sp1 motif. Nucleic Acids Res. 28**,** 2969-76.
Shields, J.M., Christy, R.J., Yang, V.W., 1996. Identification and characterization of a gene encoding a gut-enriched Kruppel-like factor expressed during growth arrest. J Biol Chem. 271**,** 20009-17.
Shim, J., Lee, H., Park, J., Kim, H., Choi, E.J., 1996. A non-enzymatic p21 protein inhibitor of stress-activated protein kinases. Nature. 381**,** 804-6.
Shin, E.J., Jeong, J.H., Chung, Y.H., Kim, W.K., Ko, K.H., Bach, J.H., Hong, J.S., Yoneda, Y., Kim, H.C., 2011. Role of oxidative stress in epileptic seizures. Neurochem Int. 59**,** 122-37.
Shoyab, M., McDonald, V.L., Byles, C., Todaro, G.J., Plowman, G.D., 1990. Epithelins 1 and 2: isolation and characterization of two cysteine-rich growth-modulating proteins. Proc Natl Acad Sci U S A. 87**,** 7912-6.
Sjogren, M., Folkesson, S., Blennow, K., Tarkowski, E., 2004. Increased intrathecal inflammatory activity in frontotemporal dementia: pathophysiological implications. J Neurol Neurosurg Psychiatry. 75**,** 1107-11.
Sleegers, K., Brouwers, N., Maurer-Stroh, S., van Es, M.A., Van Damme, P., van Vught, P.W., van der Zee, J., Serneels, S., De Pooter, T., Van den Broeck, M., Cruts, M., Schymkowitz, J., De Jonghe, P., Rousseau, F., van den Berg, L.H., Robberecht, W., Van Broeckhoven, C., 2008. Progranulin genetic variability contributes to amyotrophic lateral sclerosis. Neurology. 71**,** 253-9.
Sloviter, R.S., 1987. Decreased hippocampal inhibition and a selective loss of interneurons in experimental epilepsy. Science. 235**,** 73-6.

Sloviter, R.S., 1989. Calcium-binding protein (calbindin-D28k) and parvalbumin immunocytochemistry: localization in the rat hippocampus with specific reference to the selective vulnerability of hippocampal neurons to seizure activity. J Comp Neurol. 280**,** 183-96.

Sloviter, R.S., Sollas, A.L., Barbaro, N.M., Laxer, K.D., 1991. Calcium-binding protein (calbindin-D28K) and parvalbumin immunocytochemistry in the normal and epileptic human hippocampus. J Comp Neurol. 308**,** 381-96.

Sng, J.C., Taniura, H., Yoneda, Y., 2004. A tale of early response genes. Biol Pharm Bull. 27**,** 606-12.

Soriano, F.X., Papadia, S., Hofmann, F., Hardingham, N.R., Bading, H., Hardingham, G.E., 2006. Preconditioning doses of NMDA promote neuroprotection by enhancing neuronal excitability. J Neurosci. 26**,** 4509-18.

Speth, C., Joebstl, B., Barcova, M., Dierich, M.P., 2000. HIV-1 envelope protein gp41 modulates expression of interleukin-10 and chemokine receptors on monocytes, astrocytes and neurones. AIDS. 14**,** 629-36.

Spina, S., Murrell, J.R., Huey, E.D., Wassermann, E.M., Pietrini, P., Baraibar, M.A., Barbeito, A.G., Troncoso, J.C., Vidal, R., Ghetti, B., Grafman, J., 2007. Clinicopathologic features of frontotemporal dementia with progranulin sequence variation. Neurology. 68**,** 820-7.

Stafstrom, C.E., 2005. The role of the subiculum in epilepsy and epileptogenesis. Epilepsy Curr. 5**,** 121-9.

Stringer, J.L., Lothman, E.W., 1992. Bilateral Maximal Dentate Activation Is Critical for the Appearance of an Afterdischarge in the Dentate Gyrus. Neuroscience. 46**,** 309-314.

Sumrejkanchanakij, P., Tamamori-Adachi, M., Matsunaga, Y., Eto, K., Ikeda, M.A., 2003. Role of cyclin D1 cytoplasmic sequestration in the survival of postmitotic neurons. Oncogene. 22**,** 8723-30.

Suzuki, A., Tsutomi, Y., Akahane, K., Araki, T., Miura, M., 1998. Resistance to Fas-mediated apoptosis: activation of caspase 3 is regulated by cell cycle regulator p21WAF1 and IAP gene family ILP. Oncogene. 17**,** 931-9.

Suzuki, A., Stern, S.A., Bozdagi, O., Huntley, G.W., Walker, R.H., Magistretti, P.J., Alberini, C.M., 2011. Astrocyte-neuron lactate transport is required for long-term memory formation. Cell. 144**,** 810-23.

Suzuki, Y., Funakoshi, H., Machide, M., Matsumoto, K., Nakamura, T., 2008. Regulation of cell migration and cytokine production by HGF-like protein (HLP) / macrophage stimulating protein (MSP) in primary microglia. Biomed Res. 29**,** 77-84.

Szczepanik, A.M., Ringheim, G.E., 2003. IL-10 and glucocorticoids inhibit Abeta(1-42)- and lipopolysaccharide-induced pro-inflammatory cytokine and chemokine induction in the central nervous system. J Alzheimers Dis. 5**,** 105-17.

Szydlowska, K., Tymianski, M., 2010. Calcium, ischemia and excitotoxicity. Cell Calcium. 47**,** 122-9.

Tajima, T., Murata, T., Aritake, K., Urade, Y., Hirai, H., Nakamura, M., Ozaki, H., Hori, M., 2008. Lipopolysaccharide induces macrophage migration via prostaglandin D(2) and prostaglandin E(2). J Pharmacol Exp Ther. 326**,** 493-501.

Takahashi, K., Tanabe, K., Ohnuki, M., Narita, M., Ichisaka, T., Tomoda, K., Yamanaka, S., 2007. Induction of pluripotent stem cells from adult human fibroblasts by defined factors. Cell. 131**,** 861-72.

Tang, W., Lu, Y., Tian, Q.Y., Zhang, Y., Guo, F.J., Liu, G.Y., Syed, N.M., Lai, Y., Lin, E.A., Kong, L., Su, J., Yin, F., Ding, A.H., Zanin-Zhorov, A., Dustin, M.L., Tao, J., Craft, J., Yin, Z., Feng, J.Q., Abramson, S.B., Yu, X.P., Liu, C.J., 2011. The growth factor progranulin binds to TNF receptors and is therapeutic against inflammatory arthritis in mice. Science. 332**,** 478-84.

Tapia, L., Milnerwood, A., Guo, A., Mills, F., Yoshida, E., Vasuta, C., Mackenzie, I.R., Raymond, L., Cynader, M., Jia, W., Bamji, S.X., 2011. Progranulin deficiency decreases gross neural connectivity but enhances transmission at individual synapses. J Neurosci. 31**,** 11126-32.

Thompson, W.L., Karpus, W.J., Van Eldik, L.J., 2008. MCP-1-deficient mice show reduced neuroinflammatory responses and increased peripheral inflammatory responses to peripheral endotoxin insult. J Neuroinflammation. 5**,** 35.

Tiamkao, S., Pratipanawatr, T., Jitpimolmard, S., 2011. Abdominal epilepsy: an uncommon of non-convulsive status epilepticus. J Med Assoc Thai. 94**,** 998-1001.

Timsit, S., Rivera, S., Ouaghi, P., Guischard, F., Tremblay, E., Ben-Ari, Y., Khrestchatisky, M., 1999. Increased cyclin D1 in vulnerable neurons in the hippocampus after ischaemia and epilepsy: a modulator of in vivo programmed cell death? Eur J Neurosci. 11**,** 263-78.

Tonjes, A., Fasshauer, M., Kratzsch, J., Stumvoll, M., Bluher, M., 2010. Adipokine pattern in subjects with impaired fasting glucose and impaired glucose tolerance in comparison to normal glucose tolerance and diabetes. PLoS One. 5**,** e13911.

Treinies, I., Paterson, H.F., Hooper, S., Wilson, R., Marshall, C.J., 1999. Activated MEK stimulates expression of AP-1 components independently of phosphatidylinositol 3-kinase (PI3-kinase) but requires a PI3-kinase signal to stimulate DNA synthesis. Mol Cell Biol. 19**,** 321-9.

Tsirka, S.E., Yao, Y., 2010. The C Terminus of Mouse Monocyte Chemoattractant Protein 1 (MCP1) Mediates MCP1 Dimerization while Blocking Its Chemotactic Potency. Journal of Biological Chemistry. 285**,** 31509-31516.

Tureyen, K., Brooks, N., Bowen, K., Svaren, J., Vemuganti, R., 2008. Transcription factor early growth response-1 induction mediates inflammatory gene expression and brain damage following transient focal ischemia. J Neurochem. 105**,** 1313-24.

Turrin, N.P., Rivest, S., 2004. Innate immune reaction in response to seizures: implications for the neuropathology associated with epilepsy. Neurobiol Dis. 16**,** 321-34.

Urrila, A.S., Hakkarainen, A., Heikkinen, S., Vuori, K., Stenberg, D., Hakkinen, A.M., Lundbom, N., Porkka-Heiskanen, T., 2004. Stimulus-induced brain lactate: effects of aging and prolonged wakefulness. J Sleep Res. 13**,** 111-9.

Van Damme, P., Van Hoecke, A., Lambrechts, D., Vanacker, P., Bogaert, E., van Swieten, J., Carmeliet, P., Van Den Bosch, L., Robberecht, W., 2008. Progranulin functions as a neurotrophic factor to regulate neurite outgrowth and enhance neuronal survival. J Cell Biol. 181**,** 37-41.

Van Der Wal, E.A., Gomez-Pinilla, F., Cotman, C.W., 1994. Seizure-associated induction of basic fibroblast growth factor and its receptor in the rat brain. Neuroscience. 60**,** 311-23.

Van der Zee, C.E., Rashid, K., Le, K., Moore, K.A., Stanisz, J., Diamond, J., Racine, R.J., Fahnestock, M., 1995. Intraventricular administration of antibodies to nerve growth factor retards kindling and blocks mossy fiber sprouting in adult rats. J Neurosci. 15**,** 5316-23.

van der Zee, J., Le Ber, I., Maurer-Stroh, S., Engelborghs, S., Gijselinck, I., Camuzat, A., Brouwers, N., Vandenberghe, R., Sleegers, K., Hannequin, D., Dermaut, B., Schymkowitz, J., Campion, D., Santens, P., Martin, J.J., Lacomblez, L., De Pooter, T., Peeters, K., Mattheijssens, M., Vercelletto, M., Van den Broeck, M., Cruts, M., De Deyn, P.P., Rousseau, F., Brice, A., Van Broeckhoven, C., 2007. Mutations other than null mutations producing a pathogenic loss of progranulin in frontotemporal dementia. Hum Mutat. 28**,** 416.

van Eijsden, P., Notenboom, R.G., Wu, O., de Graan, P.N., van Nieuwenhuizen, O., Nicolay, K., Braun, K.P., 2004. In vivo 1H magnetic resonance spectroscopy, T2-weighted and diffusion-weighted MRI during lithium-pilocarpine-induced status epilepticus in the rat. Brain Res. 1030**,** 11-8.

van Gassen, K.L., de Wit, M., Koerkamp, M.J., Rensen, M.G., van Rijen, P.C., Holstege, F.C., Lindhout, D., de Graan, P.N., 2008. Possible role of the innate immunity in temporal lobe epilepsy. Epilepsia. 49**,** 1055-65.

van Swieten, J.C., Heutink, P., 2008. Mutations in progranulin (GRN) within the spectrum of clinical and pathological phenotypes of frontotemporal dementia. Lancet Neurol. 7**,** 965-74.

van Weering, H.R., Boddeke, H.W., Vinet, J., Brouwer, N., de Haas, A.H., van Rooijen, N., Thomsen, A.R., Biber, K.P., 2011. CXCL10/CXCR3 signaling in glia cells differentially affects NMDA-induced cell death in CA and DG neurons of the mouse hippocampus. Hippocampus. 21**,** 220-32.

Vezzani, A., Conti, M., De Luigi, A., Ravizza, T., Moneta, D., Marchesi, F., De Simoni, M.G., 1999. Interleukin-1beta immunoreactivity and microglia are enhanced in the rat hippocampus by focal kainate application: functional evidence for enhancement of electrographic seizures. J Neurosci. 19**,** 5054-65.

Vezzani, A., Moneta, D., Conti, M., Richichi, C., Ravizza, T., De Luigi, A., De Simoni, M.G., Sperk, G., Andell-Jonsson, S., Lundkvist, J., Iverfeldt, K., Bartfai, T., 2000. Powerful anticonvulsant action of IL-1 receptor antagonist on intracerebral injection and astrocytic overexpression in mice. Proc Natl Acad Sci U S A. 97**,** 11534-9.

Vezzani, A., 2005. Inflammation and epilepsy. Epilepsy Curr. 5**,** 1-6.

Viviani, B., Bartesaghi, S., Gardoni, F., Vezzani, A., Behrens, M.M., Bartfai, T., Binaglia, M., Corsini, E., Di Luca, M., Galli, C.L., Marinovich, M., 2003. Interleukin-1beta enhances NMDA receptor-mediated intracellular calcium increase through activation of the Src family of kinases. J Neurosci. 23**,** 8692-700.

Walker, P.D., Carlock, L.R., 1993. Immediate early gene activation during the initial phases of the excitotoxic cascade. J Neurosci Res. 36**,** 588-95.

Wang, S., Cheng, Q., Malik, S., Yang, J., 2000. Interleukin-1beta inhibits gamma-aminobutyric acid type A (GABA(A)) receptor current in cultured hippocampal neurons. J Pharmacol Exp Ther. 292**,** 497-504.

Wang, Y., Qin, Z.H., 2010. Molecular and cellular mechanisms of excitotoxic neuronal death. Apoptosis. 15**,** 1382-402.

Watson, A., Eilers, A., Lallemand, D., Kyriakis, J., Rubin, L.L., Ham, J., 1998. Phosphorylation of c-Jun is necessary for apoptosis induced by survival signal withdrawal in cerebellar granule neurons. J Neurosci. 18**,** 751-62.

Wei, D., Gong, W., Kanai, M., Schlunk, C., Wang, L., Yao, J.C., Wu, T.T., Huang, S., Xie, K., 2005. Drastic down-regulation of Kruppel-like factor 4 expression is critical in human gastric cancer development and progression. Cancer Res. 65**,** 2746-54.

Wei, D., Kanai, M., Huang, S., Xie, K., 2006. Emerging role of KLF4 in human gastrointestinal cancer. Carcinogenesis. 27**,** 23-31.

Weiss, J.H., Hartley, D.M., Koh, J., Choi, D.W., 1990. The calcium channel blocker nifedipine attenuates slow excitatory amino acid neurotoxicity. Science. 247**,** 1474-7.

Wernig, M., Meissner, A., Foreman, R., Brambrink, T., Ku, M., Hochedlinger, K., Bernstein, B.E., Jaenisch, R., 2007. In vitro reprogramming of fibroblasts into a pluripotent ES-cell-like state. Nature. 448**,** 318-24.

Wernig, M., Zhao, J.P., Pruszak, J., Hedlund, E., Fu, D., Soldner, F., Broccoli, V., Constantine-Paton, M., Isacson, O., Jaenisch, R., 2008. Neurons derived from reprogrammed fibroblasts functionally integrate into the fetal brain and improve symptoms of rats with Parkinson's disease. Proc Natl Acad Sci U S A. 105**,** 5856-61.

Wieraszko, A., Seyfried, T.N., 1989. Increased amount of extracellular ATP in stimulated hippocampal slices of seizure prone mice. Neurosci Lett. 106**,** 287-93.

Willaime, S., Vanhoutte, P., Caboche, J., Lemaigre-Dubreuil, Y., Mariani, J., Brugg, B., 2001. Ceramide-induced apoptosis in cortical neurons is mediated by an increase in p38 phosphorylation and not by the decrease in ERK phosphorylation. Eur J Neurosci. 13**,** 2037-46.

Williamson, A., Spencer, D.D., 1994. Electrophysiological characterization of CA2 pyramidal cells from epileptic humans. Hippocampus. 4**,** 226-37.

Willnow, T.E., Petersen, C.M., Nykjaer, A., 2008. VPS10P-domain receptors - regulators of neuronal viability and function. Nat Rev Neurosci. 9**,** 899-909.

Wittner, L., Huberfeld, G., Clemenceau, S., Eross, L., Dezamis, E., Entz, L., Ulbert, I., Baulac, M., Freund, T.F., Magloczky, Z., Miles, R., 2009. The epileptic human hippocampal cornu ammonis 2 region generates spontaneous interictal-like activity in vitro. Brain. 132**,** 3032-46.

Wozny, C., Gabriel, S., Jandova, K., Schulze, K., Heinemann, U., Behr, J., 2005a. Entorhinal cortex entrains epileptiform activity in CA1 in pilocarpine-treated rats. Neurobiol Dis. 19**,** 451-60.

Wozny, C., Knopp, A., Lehmann, T.N., Heinemann, U., Behr, J., 2005b. The subiculum: a potential site of ictogenesis in human temporal lobe epilepsy. Epilepsia. 46 Suppl 5**,** 17-21.

Xia, X., Serrero, G., 1998. Identification of cell surface binding sites for PC-cell-derived growth factor, PCDGF, (epithelin/granulin precursor) on epithelial cells and fibroblasts. Biochem Biophys Res Commun. 245**,** 539-43.

Xia, Z., Dudek, H., Miranti, C.K., Greenberg, M.E., 1996. Calcium influx via the NMDA receptor induces immediate early gene transcription by a MAP kinase/ERK-dependent mechanism. J Neurosci. 16**,** 5425-36.

Xiong, Z.Q., Qian, W., Suzuki, K., McNamara, J.O., 2003. Formation of complement membrane attack complex in mammalian cerebral cortex evokes seizures and neurodegeneration. J Neurosci. 23**,** 955-60.

Xu, B., Michalski, B., Racine, R.J., Fahnestock, M., 2004. The effects of brain-derived neurotrophic factor (BDNF) administration on kindling induction, Trk expression and seizure-related morphological changes. Neuroscience. 126**,** 521-31.

Xu, J.H., Long, L., Tang, Y.C., Zhang, J.T., Hut, H.T., Tang, F.R., 2009. CCR3, CCR2A and macrophage inflammatory protein (MIP)-1a, monocyte chemotactic protein-1 (MCP-1) in the mouse hippocampus during and after pilocarpine-induced status epilepticus (PISE). Neuropathol Appl Neurobiol. 35**,** 496-514.

Yabuuchi, K., Minami, M., Katsumata, S., Satoh, M., 1993. In situ hybridization study of interleukin-1 beta mRNA induced by kainic acid in the rat brain. Brain Res Mol Brain Res. 20**,** 153-61.

Yang, F., Liu, Z.R., Chen, J., Zhang, S.J., Quan, Q.Y., Huang, Y.G., Jiang, W., 2010. Roles of astrocytes and microglia in seizure-induced aberrant neurogenesis in the hippocampus of adult rats. J Neurosci Res. 88**,** 519-29.

Yang, Y., Goldstein, B.G., Chao, H.H., Katz, J.P., 2005. KLF4 and KLF5 regulate proliferation, apoptosis and invasion in esophageal cancer cells. Cancer Biol Ther. 4**,** 1216-21.

Yeo, S.I., Kim, J.E., Ryu, H.J., Seo, C.H., Lee, B.C., Choi, I.G., Kim, D.S., Kang, T.C., 2011. The roles of fractalkine/CX3CR1 system in neuronal death following pilocarpine-induced status epilepticus. J Neuroimmunol. 234**,** 93-102.

Yin, F., Banerjee, R., Thomas, B., Zhou, P., Qian, L., Jia, T., Ma, X., Ma, Y., Iadecola, C., Beal, M.F., Nathan, C., Ding, A., 2010. Exaggerated inflammation, impaired host defense, and neuropathology in progranulin-deficient mice. J Exp Med. 207**,** 117-28.

Yoon, H.S., Chen, X., Yang, V.W., 2003. Kruppel-like factor 4 mediates p53-dependent G1/S cell cycle arrest in response to DNA damage. J Biol Chem. 278**,** 2101-5.

Youn, B.S., Bang, S.I., Kloting, N., Park, J.W., Lee, N., Oh, J.E., Pi, K.B., Lee, T.H., Ruschke, K., Fasshauer, M., Stumvoll, M., Bluher, M., 2009. Serum progranulin concentrations may be associated with macrophage infiltration into omental adipose tissue. Diabetes. 58**,** 627-36.

Young, C.C., Stegen, M., Bernard, R., Muller, M., Bischofberger, J., Veh, R.W., Haas, C.A., Wolfart, J., 2009. Upregulation of inward rectifier K+ (Kir2) channels in dentate gyrus granule cells in temporal lobe epilepsy. J Physiol. 587**,** 4213-33.

Zhang, J., Zhang, D., McQuade, J.S., Behbehani, M., Tsien, J.Z., Xu, M., 2002. c-fos regulates neuronal excitability and survival. Nat Genet. 30**,** 416-20.

Zhang, S.J., Steijaert, M.N., Lau, D., Schutz, G., Delucinge-Vivier, C., Descombes, P., Bading, H., 2007a. Decoding NMDA Receptor Signaling: Identification of Genomic Programs Specifying Neuronal Survival and Death. Neuron. 53**,** 549-62.

Zhang, W., Geiman, D.E., Shields, J.M., Dang, D.T., Mahatan, C.S., Kaestner, K.H., Biggs, J.R., Kraft, A.S., Yang, V.W., 2000. The gut-enriched Kruppel-like factor (Kruppel-like factor 4) mediates the transactivating effect of p53 on the p21WAF1/Cip1 promoter. J Biol Chem. 275**,** 18391-8.

Zhang, Y.J., Xu, Y.F., Dickey, C.A., Buratti, E., Baralle, F., Bailey, R., Pickering-Brown, S., Dickson, D., Petrucelli, L., 2007b. Progranulin mediates caspase-dependent cleavage of TAR DNA binding protein-43. J Neurosci. 27**,** 10530-4.

Zheng, D., Butler, L.S., McNamara, J.O., 1998. Kindling and associated mossy fibre sprouting are not affected in mice deficient of NGFI-A/NGFI-B genes. Neuroscience. 83**,** 251-8.

Zheng, Y., Brady, O.A., Meng, P.S., Mao, Y., Hu, F., 2011. C-terminus of progranulin interacts with the beta-propeller region of sortilin to regulate progranulin trafficking. PLoS One. 6**,** e21023.

Zhou, J., Gao, G., Crabb, J.W., Serrero, G., 1993. Purification of an autocrine growth factor homologous with mouse epithelin precursor from a highly tumorigenic cell line. J Biol Chem. 268**,** 10863-9.

Zhu, J., Nathan, C., Jin, W., Sim, D., Ashcroft, G.S., Wahl, S.M., Lacomis, L., Erdjument-Bromage, H., Tempst, P., Wright, C.D., Ding, A., 2002. Conversion of proepithelin to epithelins: roles of SLPI and elastase in host defense and wound repair. Cell. 111**,** 867-78.

Zhu, S., Tai, C., MacVicar, B.A., Jia, W., Cynader, M.S., 2009. Glutamatergic stimulation triggers rapid Krupple-like factor 4 expression in neurons and the overexpression of KLF4 sensitizes neurons to NMDA-induced caspase-3 activity. Brain Res. 1250**,** 49-62.

Zhu, X., Raina, A.K., Smith, M.A., 1999. Cell cycle events in neurons. Proliferation or death? Am J Pathol. 155**,** 327-9.

Zucchini, S., Buzzi, A., Barbieri, M., Rodi, D., Paradiso, B., Binaschi, A., Coffin, J.D., Marzola, A., Cifelli, P., Belluzzi, O., Simonato, M., 2008. Fgf-2 overexpression increases excitability and seizure susceptibility but decreases seizure-induced cell loss. J Neurosci. 28**,** 13112-24.